

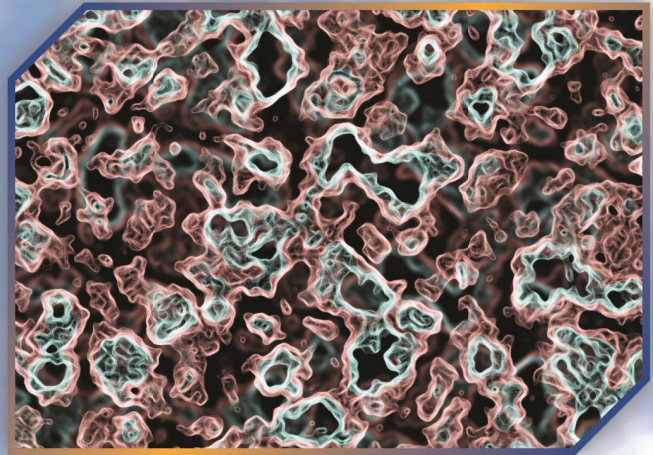
Environmental Research & Technology

YEAR : 2021

VOLUME : 04

ISSUE : 01

e-ISSN: 2636-8498





Environmental Research & Technology

<http://dergipark.gov.tr/ert>



ACADEMIC ADVISORY BOARD

Prof. Dr. Adem Basturk (Yildiz Technical University)

Prof. Dr. Mustafa Ozturk (Yildiz Technical University)

Prof. Dr. Lutfi Akca (Istanbul Technical University)

Prof. Dr. Oktay Tabasaran (Stuttgart University)

Prof. Dr. Ahmet Demir (Yildiz Technical University)

SCIENTIFIC DIRECTOR

Prof. Dr. Ahmet Demir (Yildiz Technical University)

EDITOR IN CHIEF

Prof. Dr. Mehmet Sinan Bilgili (Yildiz Technical University)

ASSISTANT EDITOR

Assoc. Prof. Dr. Hanife Sari Erkan (Yildiz Technical University)

CONTACT

Yildiz Technical University
Environmental Engineering Department, 34220 Esenler
Istanbul – Turkiye
Web: <http://dergipark.gov.tr/ert/>
E-mail: ert@yildiz.edu.tr



Environmental Research & Technology

<http://dergipark.gov.tr/ert>



Co-Editors (Air Pollution)

Prof. Dr. Arslan SARAL (Yildiz Technical University, Turkiye)
Prof. Dr. Mohd Talib LATIF (Universiti Kebangsaan, Malaysia)
Prof. Dr. Nedim VARDAR (Interamerican University of Puerto Rico, Puerto Rico)
Prof. Dr. Sait Cemil SOFUOGLU (Izmir Institute of Technology, Turkiye)
Prof. Dr. Wina GRAUS (Utrecht University, The Netherlands)

Co-Editors (Environmental Engineering and Sustainable Solutions)

Prof. Dr. Bulent Inanc (Istanbul Technical University, Turkiye)
Prof. Dr. Guleda ENGIN (Yildiz Technical University, Turkiye)
Prof. Dr. Hossein KAZEMIAN (The University of Northern British Columbia, Canada)
Prof. Dr. Raffaella POMI (Sapienza University of Rome, Italy)
Prof. Dr. Yilmaz YILDIRIM (Bulent Ecevit University, Turkiye)
Prof. Dr. Zenon HAMKALO (Ivan Franko National University of Lviv, Ukraine)

Co-Editors (Waste Management)

Prof. Dr. Bestami OZKAYA (Yildiz Technical University, Turkiye)
Prof. Dr. Bulent TOPKAYA (Akdeniz University, Turkiye)
Prof. Dr. Kahraman UNLU (Middle East Technical University, Turkiye)
Prof. Dr. Mohamed OSMANI (Loughborough University, United Kingdom)
Prof. Dr. Pin Jing HE (Tongji University, China)

Co-Editors (Water and Wastewater Management)

Prof. Dr. Ayse FILIBELI (Dokuz Eylul University, Turkiye)
Prof. Dr. Baris CALLI (Marmara University, Turkiye)
Prof. Dr. Marina PRISCIANDARO (University of L'Aquila, Italy)
Prof. Dr. Selvam KALIYAMOORTHY (Nagoya University, Japan)
Prof. Dr. Subramanyan VASUDEVAN (Central electrochemical Research Institute, India)



Editorial Board

Prof. Dr. Andjelka MIHAJLOV (University of Novi Sad, Serbia)

Prof. Dr. Artur J. BADYDA (Warsaw University of Technology, Poland)

Prof. Dr. Aysegul PALA (Dokuz Eylul University, Turkiye)

Prof. Dr. Aysen ERDINCLER (Bogazici University, Turkiye)

Prof. Dr. Azize AYOL (Dokuz Eylul University, Turkiye)

Prof. Dr. Bulent KESKINLER (Gebze Technical University, Turkiye)

Prof. Dr. Didem OZCIMEN (Yildiz Technical University, Turkiye)

Prof. Dr. Erwin BINNER (University of Natural Resources and Life Science, Austria)

Prof. Dr. Eyup DEBIK (Yildiz Technical University, Turkiye)

Prof. Dr. F. Dilek SANIN (Middle East Technical University, Turkiye)

Prof. Dr. Gulsum YILMAZ (Istanbul Universtiy Cerrahpasa, Turkiye)

Prof. Dr. Hamdy SEIF (Alexandria University, Egypt)

Prof. Dr. Hanife BUYUKGUNGOR (Ondokuz Mayis University, Turkiye)

Prof. Dr. Ilirjan MALOLLARI (University of Tirana, Albania)

Prof. Dr. Ismail KOYUNCU (Istanbul Technical University, Turkiye)

Prof. Dr. Jaakko PUHAKKA (Tampere University Finland)

Prof. Dr. Lucas Alados ARBOLEDAS (University of Granada, Spain)

Prof. Dr. Mahmoud A. ALAWI (University of Jordan, Jordan)

Prof. Dr. Marcelo Antunes NOLASCO (University of São Paulo, Brazil)

Prof. Dr. Martin KRANERT (University of Stuttgart, Germany)

Prof. Dr. Mehmet Emin AYDIN (Necmettin Erbakan University, Turkiye)



Environmental Research & Technology

<http://dergipark.gov.tr/ert>



- Prof. Dr. Mesut AKGUN (Yildiz Technical University, Turkiye)
- Prof. Dr. Mufide BANAR (Eskisehir Technical University, Turkiye)
- Prof. Dr. Mufit BAHADIR (Technische Universität Braunschweig, Germany)
- Prof. Dr. Mukand S. BABEL (Asian Institute of Technology, Thailand)
- Prof. Dr. Mustafa ODABASI (Dokuz Eylul University, Turkiye)
- Prof. Dr. Mustafa OKUTAN (Yildiz Technical University, Turkiye)
- Prof. Dr. Neslihan DOĞAN SAĞLAMTİMUR (Nigde Omer Halisdemir University)
- Prof. Dr. Nihal BEKTAŞ (Gebze Technical University, Turkiye)
- Prof. Dr. Nurdan Gamze TURAN (Ondokuz Mayıs University, Turkiye)
- Prof. Dr. Omer AKGIRAY (Marmara University, Turkiye)
- Prof. Dr. Osman ARIKAN (Istanbul Technical University, Turkiye)
- Prof. Dr. Osman Nuri AGDAG (Pamukkale University, Turkiye)
- Prof. Dr. Ozer CINAR (Yildiz Technical University, Turkiye)
- Prof. Dr. Pier Paolo MANCA (University of Cagliari, Italy)
- Prof. Dr. Recep BONCUKCUOGLU (Istanbul University Cerrahpasa, Turkiye)
- Prof. Dr. Saim OZDEMIR (Sakarya University, Turkiye)
- Prof. Dr. Sameer AFIFI (Islamic University of Gaza, Palestine)
- Prof. Dr. Serdar AYDIN (Istanbul Universtiy Cerrahpasa, Turkiye)
- Prof. Dr. Timothy O. RANDHIR (University of Massachusetts Amherst, U.S.A.)
- Prof. Dr. Ulku YETIS (Middle East Technical University, Turkiye)
- Prof. Dr. Victor ALCARAZ GONZALEZ (University of Guadalajara, Mexico)
- Prof. Dr. Yaşar NUHOGLU (Yildiz Technical University, Turkiye)



Environmental Research & Technology

<http://dergipark.gov.tr/ert>



TABLE OF CONTENTS

Title	Pages
Research Articles	
Climate change impact assessment under data scarcity by hydrological and hydrodynamic modeling in Izmit Bay/Turkey DOI: https://doi.org/10.35208/ert.777323 <i>Güleda Engin, Ahmet Adiller, Philipp Klug, Meltem Çelen, Frank Herrmann, Heike Bach, Frank Wendland</i>	1-17
Assessment of Yalova University Campus according to LEED V.4 certification system DOI: https://doi.org/10.35208/ert.812339 <i>Hikmet Erbiyik, Tuğçe Çatal, Sinem Durukan, Doğan Güneş Topaloğlu, Ümit Ünver</i>	18-28
Reducing greenhouse gas emissions from solid wastes management in north eastern Nigeria: An integrated solid waste management approach DOI: https://doi.org/10.35208/ert.837071 <i>Richard Mshelia, Abubakar Maiwada Danjuma</i>	29-34
Isotherm, kinetic and thermodynamic studies of methylene blue adsorption using <i>Leucaena leucocephala</i> DOI: https://doi.org/10.35208/ert.810226 <i>Ali Rıza Kul, Adnan Aldemir</i>	35-41
Investigation of the usability of zinc ferrite nanoparticles synthesized by microwave assisted combustion method as photocatalyst for removal of organic dyes from wastewaters DOI: https://doi.org/10.35208/ert.820613 <i>Zeynep Karcıoğlu Karakaş</i>	42-52
A new calculation method of efficiency for gypsum and wastewater hydrocyclones in FGD unit in a power plant DOI: https://doi.org/10.35208/ert.841720 <i>Mehmet Bilen</i>	53-62
Pre-irradiation grafting of acrylic acid and sodium styrene sulfonate on non-woven polyethylene fabric for heavy metal removal DOI: https://doi.org/10.35208/ert.828089 <i>Nazia Rahman, Md. Imran Biswas, Mahbub Kabir, Nirmal Chandra Dafader, Shahnaz Sultana, Md. Nabul Sardar, Farah Tasneem Ahmed, Abdul Halim</i>	63-72

Boron rejection from aqueous solution and wastewater by direct contact membrane distillation DOI: https://doi.org/10.35208/ert.842919 <i>Burcu Tan, Uğur Selengil, Tijen Ennil Bektaş</i>	73-82
Density cleaning for some Turkish lignites DOI: https://doi.org/10.35208/ert.828660 <i>Serdar Yılmaz, Mehmet Bilen</i>	89-96
Effectiveness of fly ash in boron removal from Tuzla (Çanakkale) geothermal fluid DOI: https://doi.org/10.35208/ert.842192 <i>Mehmet Oğuzhan Şahin, Tijen Ennil Bektaş, Deniz Şanlıyüksel Yücel</i>	102-107
Investigation of electricity generation performance of grape marc in membrane-less microbial fuel cell DOI: https://doi.org/10.35208/ert.881517 <i>Banu Taşkan</i>	108-115

Short Communication

Country in transition (Serbia) case: Circular economy starts from waste management DOI: https://doi.org/10.35208/ert.853792 <i>Andjelka Mihajlov, Aleksandra Mladenovic, Filip Jovanovic</i>	83-88
--	-------

Review Articles

Zero waste strategies and Turkey's zero waste project DOI: https://doi.org/10.35208/ert.843106 <i>Burcu Tan</i>	97-101
---	--------



RESEARCH ARTICLE

Climate change impact assessment under data scarcity by hydrological and hydrodynamic modeling in Izmit Bay/Turkey

Guleda Onkal Engin^{1,*} , Ahmet Adiller¹ , Philipp Klug² , Meltem Celen³ , Frank Herrmann⁴ , Heike Bach² , Frank Wendland⁴ 

¹Yildiz Technical University, Department of Environmental Engineering, Esenler, İstanbul, 34220, TURKEY

²VISTA Remote Sensing in Geosciences GmbH, 80333 Munich, GERMANY

³Gebze Technical University, Department of Environmental Engineering, Gebze, Kocaeli, 41400 TURKEY

⁴Forschungszentrum Juelich, Institute of Bio- and Geosciences (IBG), Institute 3: Agrosphere 52425 Juelich, GERMANY

ABSTRACT

To assess climate change impact on the hydrology of Izmit Bay, a coupled model chain using the results of four combinations of Global Climate Models (GCMs) and Regional Climate Models (RCMs) and consisting two hydrological models (mGROWA and PROMET) and one hydrodynamic model (MIKE 3HD) was established. Climate model data of the 4 GCM-RCM combinations were applied to both hydrological models. The resulting 8 streamflow data of the hydrological models were then applied to the MIKE 3HD to assess possible hydrodynamic situations in Izmit Bay. Related model results indicate a range of possible future streamflow regimes suitable for the analysis of climate change impact on Izmit Bay. In order to evaluate the effects of the hydrological changes only on the bay, the bay was considered as closed in terms of hydrodynamics. There is a clear indication that the climate change induced impacts on streamflow may influence the sea level in the Bay to a minor extent. However, climate change induced water exchange processes in the Bay may have a much bigger influence. Hence, it is suggested that further simulations should be run once the hydrologic regime of the Marmara Sea has been assessed in a broader macro-scale study.

Keywords: River discharge; PROMET; m-GROWA; MIKE 3HD

1. INTRODUCTION

The gradual increase in world's population and industrial activities go hand in hand with the needs of the population to jeopardize natural resources. Water is the most important natural resource, as it is essential for human survival and important to many sectors of the economy. Pressures on water resources induced by human activities, e.g. population growth and field irrigation, are aggravated by climate change. According to the Intergovernmental Panel on Climate Change (IPCC), the global average temperature has increased since 1951, while regional precipitation patterns have changed considerably in the last century [1]. Recently, the number of publications and research on climate change impact on hydrological cycle and surface/sub-surface water resources has increased significantly [2-6], indicating that the effects of the climate change vary from one region to another.

Due to the high population density, the concentration of economic activities and the sensitive aquatic ecosystems, coastal regions are most vulnerable to climate change. Izmit Bay, located in the province of Kocaeli in the eastern part of the Marmara Sea in Turkey is not an exception in this regard. Kocaeli has a population of 1.78 million [7] and accommodates the most important petrochemical and automotive industries of Turkey. Therefore, forecasting the impact of climate change on water resources in Izmit Bay and its catchment is important to reveal a situation that might be encountered in the future and in order to derive necessary precaution measures in due time.

Despite the fact that the number of hydrologic models had already grown until the 1990s as indicated in a survey by Singh [8], the application of hydrological models in Turkey is relatively new [9-11]. Only one study considering hydrological modeling was

Corresponding Author: gengin@yildiz.edu.tr (Guleda Onkal Engin)

Received 5 August 2020; Received in revised form 11 January 2021; Accepted 13 January 2021

Available Online 26 January 2021

Doi: <https://doi.org/10.35208/ert.777323>

© Yildiz Technical University, Environmental Engineering Department. All rights reserved.

conducted in the study site so far [12]. The general reason for limited environmental modeling studies in Turkey could be attributed to limited data availability. With regard to assessing climate change phenomena however, modeling studies in Turkey are as common as in other parts of the world [13-16].

General Circulation Models (GCM) are used to forecast climate development on earth using also information on processes in the atmosphere, oceans, vegetation etc. [17]. As the spatial resolution of the GCMs is limited to approx. 110 x 110 km at present, Regional Climate Models (RCMs) are used for regional downscaling of GCMs under consideration of information on regional site conditions, e.g. topography. Whereas so called dynamical RCMs disaggregate the results of GCM down to ca. 7 x 7 km, so called statistical RCMs forecast the impact for meteorological stations. Consequently, even in case the same IPCC emission scenario (SRES, A1B) is used as input, the results of different RCMs display considerable differences for the areas applied, simply because certain processes and feedbacks are modeled differently. In order to reduce the uncertainty of different RCMs in the prediction of possible future hydrologic conditions the application of an ensemble of RCMs is suggested as input in hydrologic models in order to account for different emission scenarios and initial conditions [18].

In this study, the effects of climate changes on Izmit Bay were evaluated using two different hydrological models, namely PROMET [19] and mGROWA [20-22]. Both models were applied for Izmit Bay in order to determine streamflow data for the reference period (REF) 1971-2000 and the future period (FUT) 2041-2070 using the results of the regional climate models applied (ECH-RCA, ECH-REM, ECH-RMO, HCH-RCA) as input. In order to further analyze the effects of climate change induced streamflow variations on sea level variations in the coastal area, Izmit Bay was modeled hydrodynamically using MIKE 3HD model developed by Danish Hydraulic Institute [23]. For this purpose, Izmit Bay was assumed as a closed system in the hydrodynamic model set-up, i.e. without an exchange of water to the open sea, so that the changes in Izmit Bay determined with MIKE 3HD were attributed to changes in the streamflow data exclusively. The related MIKE 3HD simulations should be repeated once the hydrologic regime of the catchments of the Black Sea and the Aegean Sea and the processes in the Sea have been assessed in a broader macro-scale study.

2. MATERIALS AND METHOD

2.1. Study site: The Izmit Bay

The Izmit Bay is located at the eastern part of the Marmara Sea in the Province of Kocaeli of Marmara Region in Turkey (Fig 1). The Bay is about 45 km in length, 1.8 to 9 km in width and has a surface of 261 km². The catchment area of Izmit Bay comprises 2255 km² and is very heterogeneous in terms of soil cover and topography. It comprises a high portion of arable land in the lowland area of the eastern part and a high portion of forests in the northern and southern part,

where the elevation rises up to approximately 1500 m above sea level.

There are about forty rivers and streams having a wide range of discharge values in the basin. Among them, regular flow measurement is carried out only in 5 streams with high discharge values. These are the Tavşanlı stream, Çınarlı stream, Ketenci stream, Kirazdere stream and Yalakdere stream respectively. As it can be seen from Fig 1 Ketenci stream has 3 discharge gauging stations while the others have 1 discharge gauging station. The Kirazdere stream has the highest mean annual flow value, which is about 4.5 m/s.

Formations bearing the groundwater in the basin are alluvials in the coastal lowlands and Triassic limestones. Triassic limestone rock unit mostly outcrop in the North and East sides of the Tavşanlı stream (Fig 1). The discharge of groundwater in the lowland areas is usually into the bay, whereas the discharge from the Triassic limestones is into the springs and rivers. Since all the lowland areas are connected to the coastal line of the Izmit bay, seawater intrusion into the wells is an important problem in the region. High quantity water withdrawal from the wells used by industrial facilities in the northern part of the basin cause this problem to be accelerated. The bay can be divided into three sub-sections due to its narrow openings. Detailed information about sub-sections can be found in Table 1 [24].

Since the 1960s thousands of small manufacturing facilities as well as four-hundred large industrial plants, including the most important petrochemical industries, have been built around the Bay. At present, these facilities constitute 13% of Turkey's industrial production [25]. Izmit Bay has a great importance for the transportation of raw materials and products. As it is also the sink for treated industrial wastewaters, water quality of Izmit Bay has been assessed frequently in some studies [26-29]. In contrast, the hydrology of Izmit Bay has only been determined by Karpuzcu et al. [30] with respect to the mean long-term runoff conditions. In the EU 7th Framework Program project CLIMB, Izmit Bay and its catchment have been chosen as a case study area to analyze the possible impact of climate change on the hydrology of the catchment and the bay.

2.2. Data availability

All the input data needed to run the hydrologic models (see Table 2) was provided by state organizations or derived by satellite images. Meteorological data was provided by Turkish State Meteorological Service. Since the meteorological data in the study area were available for the years 1971-2000, this period was chosen as a reference. Discharge data and information about gauging stations were provided by General Directorate of the State Hydraulic Works. Most of the digital maps (Soil, DEM, Geological boundaries etc.) were provided from the Ministry of Forestry and Water Works, formerly known as the Ministry of Environment and Forestry. Pre-processing and parametrization of these maps for hydrologic modeling was carried out by Karpuzcu et al. [30].

Table 1. Physical properties (characteristics) of Izmit Bay's sub-sections

Section	Length (km)	Width (km)	Max. depth (m)	Surface area (km ²)
East	16	2-5	35	44
Middle	20	3-10	180	166
West	17	3-5.5	1000	100

Table 2. Input data needed to run the hydrologic models PROMET and mGROWA

	Data basis	Data source
Hydrology	Catchment areas, rivers and lakes, hydrographs	General Directorate of state Hydraulic Works (DSI)
Climatic data	Hourly/daily/monthly series of precipitation, temperature, sunshine duration, solar radiation, wind speed, relative humidity, daily precipitation, minimum & maximum temperature as minimum	Turkish State Meteorological Service
Soil data	Available field capacity, field capacity, bulk density, root depth, capillary rise rates, depth to groundwater, influence of perching water soil type and texture as minimum	Derived from soil map of Turkey
Land cover	Land use categories and percentage imperviousness	Derived from Landsat TM satellite images
Hydrogeology	Hydraulic conductivity	Derived from geological map of Turkey
Topography	Hill slope and aspect	SRTM (NASA), (30 m)
Geology	Geology of covering layers	Geological map of Turkey

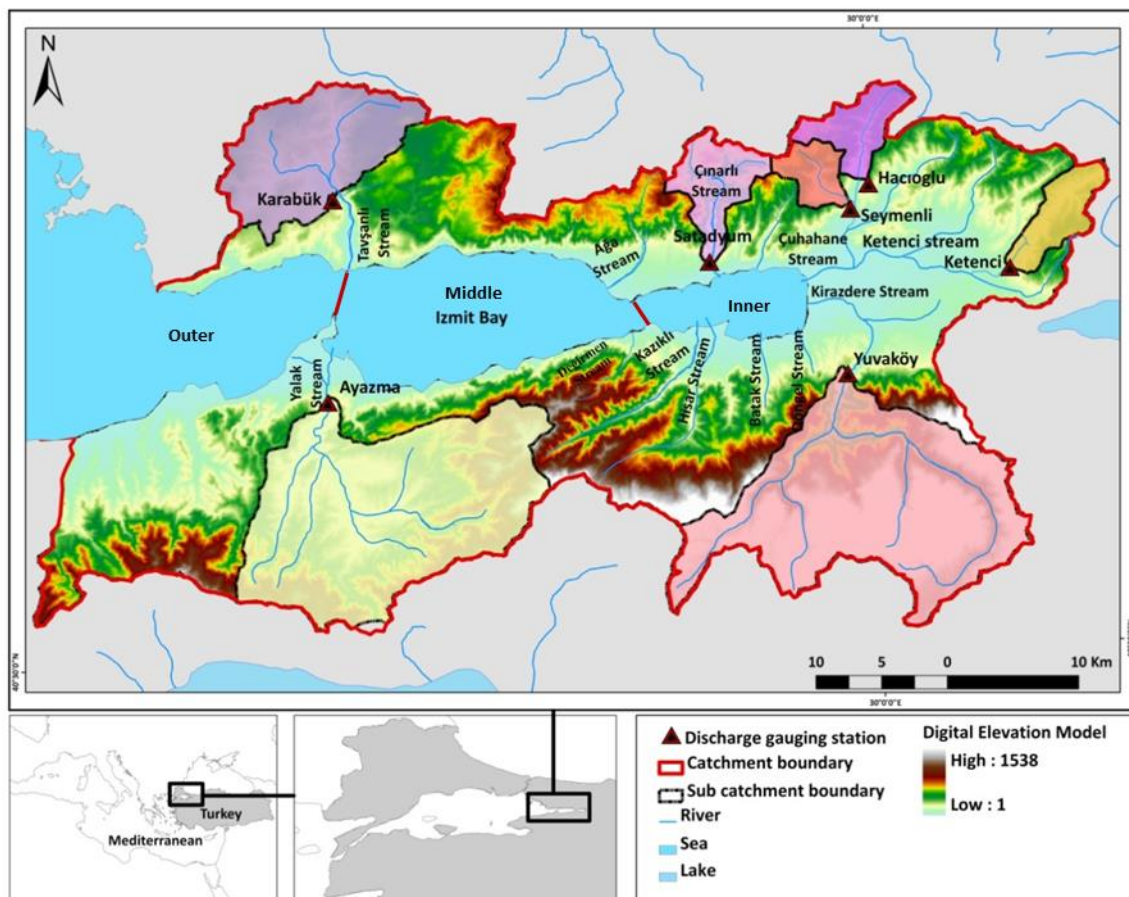


Fig 1. Overview of the sub-catchments in the Izmit Bay catchment and the available gauge stations

For the representation of land use change in the modeling of the Izmit Bay catchment, two land use maps were derived from two Landsat TM satellite images from June 25, 2000 and July 31, 2010. The satellite images have been processed with a VISTA intern software package, including radiometric and atmospheric corrections [31]. The satellite images have been classified with a maximum likelihood approach in 9 classes (estate, industry, rainfall and irrigated cropland, deciduous and coniferous forest, bare areas, mosaic cropland/natural vegetation and water bodies). The land use map derived from the year 2000 acquisition was used for modeling the REF period 1971-2000 whereas the land use map from

2010 was used for the modeling of the FUT period 2041-2070.

One of the important inputs for the hydrodynamic model is the bathymetry of the bay. The bathymetry map was derived by digitization of an analog bathymetry map which was prepared by the Office of Navigation, Hydrography and Oceanography. The bathymetry data of the Bay can be seen in Fig 2. The location of sea level monitoring station (Yalova Mareographic Station) is also presented in Fig 2. The dimensions were selected to be 2D and UTM coordinate system for the map coordinate system. As it can be seen from the bathymetry map the deeper parts of the Bay are below 1120 m.

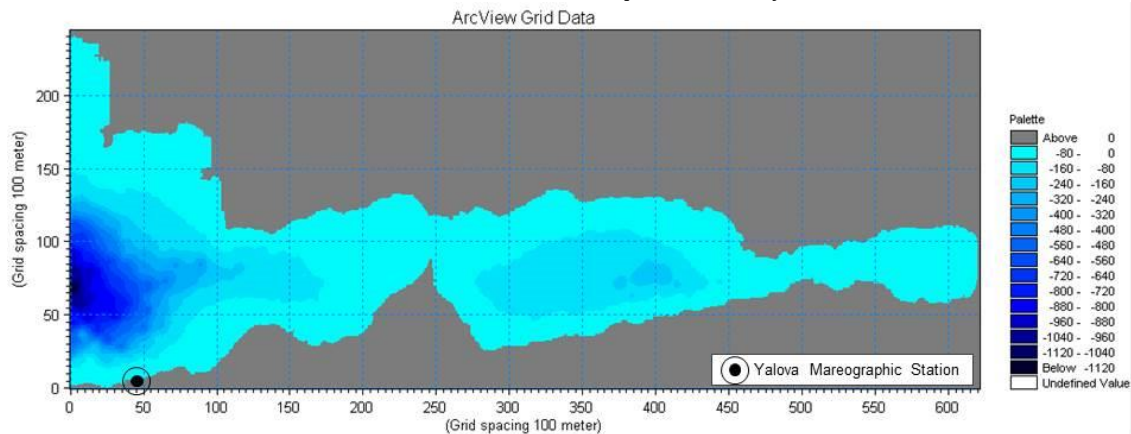


Fig 2. Bathymetry map of the Izmit Bay

2.3. Izmit Bay model chain

To assess the climate change impact on the hydrodynamics of the Izmit Bay, a coupled model chain consisting of four combinations of global (GCM) and regional (RCM) climate models, two hydrological models (HM) and a hydrodynamic model (HDM) are established (Fig 3).

By using a complex auditing method, four combinations of the GCM – RCM models, namely ECH-RCA, ECH-REM, ECH-RMO and HCM-RCA (see Table 3) were selected by Deidda et al. [17] and these models fitted best for the data set. Two periods were selected to be used within the model chain, starting with the years 1971-2000 as the REF period and the years 2041-2070 as the FUT period for climate change impact assessment. The climate data for both periods were bias-corrected and downscaled to a spatial resolution of 1 x 1 km. A detailed description of the auditing, the bias-correction and the downscaling of the climate model outputs can be found in Deidda et al. [17].

The downscaled climate data were then used as input for the two hydrological models, namely PROMET (Mauser and Bach, 2009) and mGROWA [21]. Consequently, an ensemble of 8 GCM-RCM-HM combinations was considered in order to assess climate change impact on Izmit Bay. In this way, 40 simulated streamflow hydrographs at the outlet of the 5 major rivers discharging into the Izmit Bay for the two periods were simulated. The streamflow simulations were carried out with monthly time step. From the ensemble of 8 streamflow model results for

the FUT period, the 4 best performing GCM/RCM couples of the hydrological models were selected as inflow boundary conditions to the hydrodynamic model.

In the following sections, the terrestrial part of the model chain is introduced, starting with a description of the hydrological models PROMET and mGROWA.

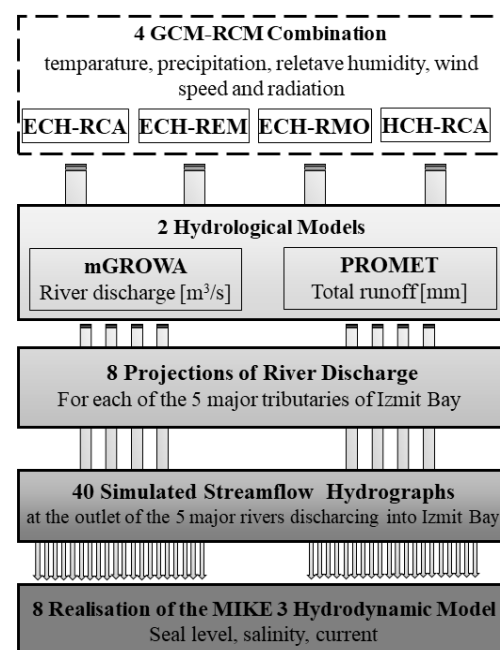


Fig 3. Model chain applied in order to assess the impact of climate change on the hydrodynamics of the Izmit Bay

Table 3. Climate models that have provided climate forcing

Scale	Acronym	Climatological center and model
GCM	ECH	Max Planck Institute for Meteorology, Germany, ECHAM5/MPI OM
GCM	HCH	Hadley Centre for Climate Prediction, Met Office, UK, HadCM3 Model (high sensitivity)
RCM	REM	Max Planck Institute for Meteorology, Hamburg, Germany, REMO Model
RCM	RMO	Royal Netherlands Meteorological Institute (KNMI), Netherlands, RACMO2 Model
RCM	RCA	Swedish Meteorological and Hydrological Institute (SMHI), Sweden, RCA Model

2.4. PROMET model description

The fully distributed, physically based hydrological model PROMET (Processes of Radiation, Mass and Energy Transfer) was developed to study the impact of climate change on the water cycle of large scale, complex watersheds [19]. PROMET was built and tested within the integrative research project GLOWA-Danube [32-33], and has been applied in a variety of studies at different scales from pixel [34] over single fields [35] and smaller regions (100 km²) to a mesoscale catchment (100,000 km²) as well as for numerous locations and climatic conditions in a variety of studies [31, 36-37].

The architecture of PROMET as shown in Fig 4 consists of eight components: meteorology, land surface energy and mass balance, vegetation, snow and ice, soil hydraulic and soil temperature, ground water, channel flow, man-made hydraulic structures.

PROMET strictly follows the principle of conserving mass and energy, using spatial input of topography, land use, soil texture and meteorology for each grid cell. PROMET is not calibrated using historical runoff data to preserve its predictive power. The usual calibration procedures using measured streamflow, simplified process representations, lumped model parameters and the fact that the simultaneous conservation of mass and energy is not guaranteed, makes it difficult and potentially risky to use these approaches to predict future states of regional hydrologic systems under changing boundary conditions with respect to climate. Physical

consistency and predictive power should not be diminished or lost in the model calibration process. Therefore, the values of the model parameters of PROMET are not calibrated using measured discharge. Instead, the literature sources and/or measurements (both in the field and from remote sensing sources) were used. Concerning the channel flow component, each modeled grid cell is hydraulically connected to its hydraulic neighbour within a channel network using a digital elevation model. Flow velocities are considered by the Maskincum-Cunge method [38] modified by Todini [39]. A detailed description of the components of PROMET is given in [19].

The model environment was set up for the Izmit Bay catchment using spatial data derived with remote sensing methods [31]. These data include land use maps for the years 2000 and 2010 derived from LANDSAT imagery, a SRTM DEM and vegetation parameters like LAI and albedo for all land use classes using a look up table inversion of the model SLC [40]. PROMET requires meteorological information on precipitation, air temperature, wind speed, humidity and radiation/cloud cover. This data as well as runoff data for validation purposes were provided from the Turkish state agencies [30]. PROMET was set up for the Izmit Bay with a spatial resolution of 300 x 300 m and a temporal resolution of one hour. A series of tests revealed that there is no significant loss of accuracy in the results when reducing the resolution from 100 m to 300 m, but an enormous increase (9 times) of modeling speed was achieved.

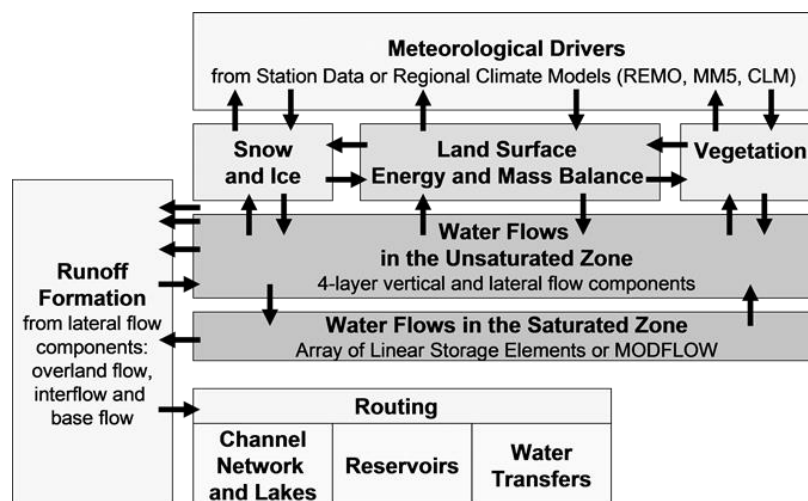


Fig 4. Schematic diagram of the components of PROMET and the interfaces between them. Boxes indicate components and arrows indicate interfaces, through which data is exchanged [19]

2.5. mGROWA model description

The mGROWA model [21] was developed for determining water balance and runoff of large areas (river basins, Federal States etc.). Soil moisture dynamics, capillary rise from groundwater to the root zone, actual evapotranspiration and total runoff generation are calculated in daily steps. Although groundwater recharge and direct runoff (drainage runoff, interflow) are determined in daily steps as well, model results are presented in monthly time steps, as groundwater management is usually based on this temporal aggregation level. For the simulations, a 100x100 m grid was selected. By doing so, the Izmit Bay catchment was sub-divided into 187,972 grid cells for which soil water balance and runoff were determined individually. However, as the individual grid cells are not linked together, lateral flow processes are not considered in mGROWA.

Fig 5 shows the data basis needed to run the mGROWA model and the water balance quantities calculated in two general modeling steps. Precipitation and grass-reference evapotranspiration have to be regionalized (pre-processed) prior to the modeling from the available climatic data sources, i.e. data from climate monitoring stations, weather radars or climate projections. For this purpose, regionalization procedures adapted to the available data sources are selected, according to Kunkel et al, [41] and Marke et al, [42]. The data bases of the Izmit Bay catchment were made available by the Turkish state agencies (State Hydraulic Works and State Meteorological Service). Pre-processing and parametrization of these maps for hydrologic modeling was carried out and described comprehensively in [30].

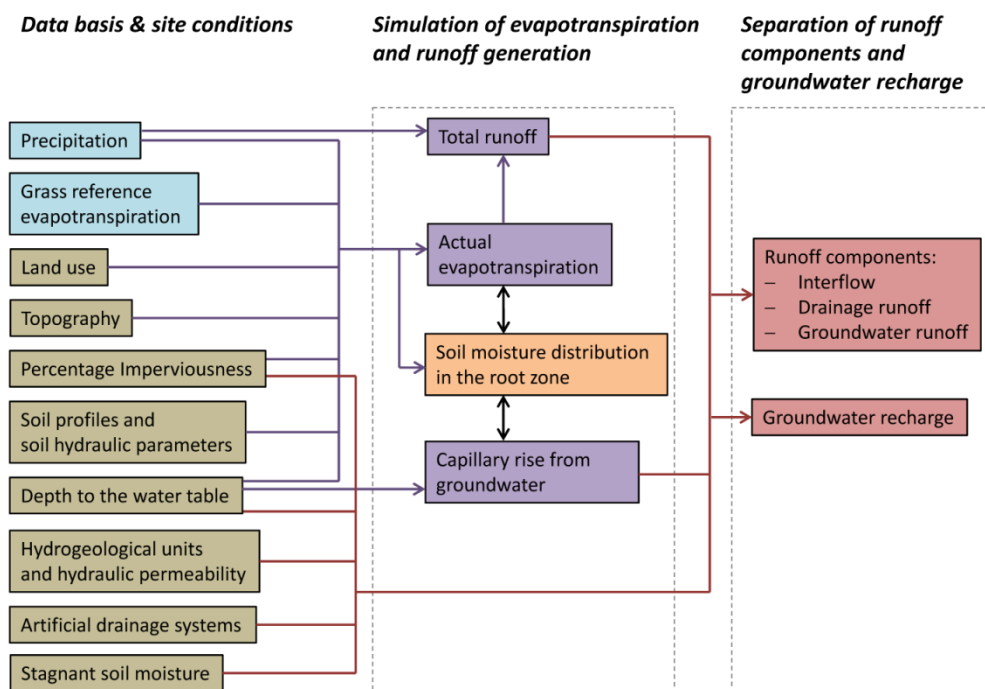


Fig 5. Data basis and general modeling scheme of mGROWA [21]

The spatially and temporally highly distributed simulation of vertical soil moisture dynamics in each grid cell of the study area is the essential part of the first mGROWA simulation step, i.e. for determining actual evapotranspiration and runoff generation. This includes the explicit consideration of the plant available water stored in the root zone which is increased by capillary rise from groundwater in areas where shallow groundwater occurs. The water balance equation and its climatic, runoff and storage terms are the basis for this simulation step (Eq. 1).

$$\frac{ds}{dt} = p + q_{cr} - et_a - q_t \quad (1)$$

In eq. 1 p represents the precipitation level (mm d^{-1}), q_{cr} the capillary rise from groundwater (mm d^{-1}), et_a the actual evapotranspiration (mm d^{-1}), q_t the generated total runoff (mm d^{-1}), s the amount of water stored in a grid cell (mm) and t the time (d). At sites

covered with vegetation s corresponds to the soil water content θ . In urban areas s represents the water stored on impervious surfaces.

In the mGROWA model, special attention has been paid to the calculation of actual evapotranspiration and the associated storage functions (Eq. 2). Grass reference evapotranspiration et_0 (mm d^{-1}) is determined based on the Penman-Monteith-equation [43]; k_{LN} is a land use specific evapotranspiration factor (crop coefficient); $f(\beta, \gamma)$ represents a topography function in order to correct actual evapotranspiration according to hill slope and exposition [44] and $f(s)$ is a storage function which takes the water available for the evapotranspiration processes into account.

$$et_a = et_0 \cdot k_{LN} \cdot f(\beta, \gamma) \cdot f(s) \quad (2)$$

The storage function is defined differently for different site conditions. For land surfaces covered

with vegetation, the function values of $f(s)$ originate from a multi-layer soil water balance model [21,45]. This sub-model simulates the water fluxes in the root zone with respect to the continuity equation but ignores the dependency of percolation on unsaturated hydraulic conductivity. For impervious surfaces in urban areas and free water surfaces, specific storage functions have been implemented in mGROWA, respectively [21].

The mGROWA model has been developed in order to determine runoff generation as well as percolation and groundwater recharge rates respectively for large areas temporally and spatially highly distributed. Same as PROMET, mGROWA is not calibrated using historical runoff data to preserve its predictive power. However, mGROWA does not take into account the simulation of streamflow as PROMET does. In order to benefit from the main features of both models, mGROWA and PROMET have been merged in the model chain. In this way, the total runoff generation in the grid cells calculated with mGROWA was fitted to the time patterns of the hydrographs simulated with PROMET. The main advantage of this procedure was that the balanced total runoff simulated with two different hydrological model concepts could serve as boundary condition for the subsequent model element of the chain. The resulting 8 realizations of streamflow were subsequently used as boundary

conditions for the simulation of the hydrodynamics in the Izmit Bay based on the MIKE 3HD model.

2.6. MIKE 3HD model description

MIKE 3HD [23], is a modeling program which uses hydrological and hydrodynamic properties of water bodies in order to determine a variety of different characteristics of surface water; such as coastal, lake and reservoir hydrodynamics (circulation, water levels, flow rates etc.), coastal and inland flooding, water quality and sediment structure.

The MIKE 3HD module solves a number of different equations including conservation of mass and momentum, salinity and temperature variations. Mass conservation in the two/three dimensional system was expressed using the Reynolds-Average-Navier-Stokes equations, considering the assumptions of Boussinesq and of hydrostatic pressure.

In addition, the system is closed by a turbulence closure scheme. In order to characterize the eddy viscosity different turbulence models (Smagorinsky model, k model, k-ε model, mixed Smagorinsky / k-ε model and a constant eddy viscosity model) are included in the model.

The needed databases given in process chart (Fig 6) can be divided as basic parameters for identifying the system and hydrodynamic parameters.

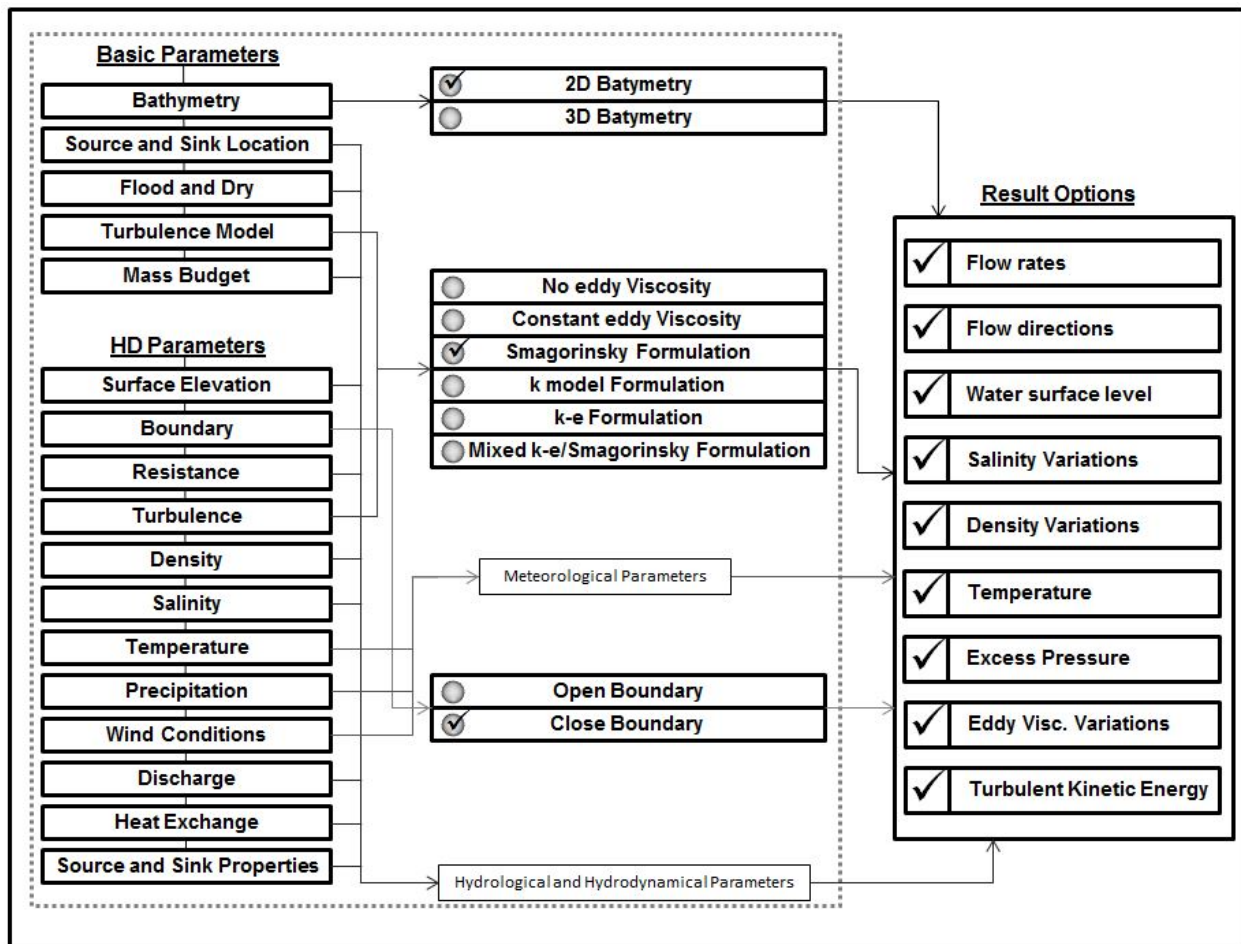


Fig 6. Preferences made during model installation (MIKE 3HD)

Fig 6 shows preferences made during model installation. Accordingly, the model is run in 2D. In the production of the numerical bathymetry map, an analog map provided from the map general command has been used. The resolution of the digital bathymetry map is 100m. The Smagorinsky model was chosen for turbulence calculations, as this model is commonly used.

The bay was considered hydrodynamically closed. However, in terms of meteorological variables, the model is operated as an open system. The results of the climate models (precipitation, temperature) and the data of stations belonging to the meteorological administration (wind speed) were used as meteorological data. In the same way, the model results for the two hydrologic models are used as discharge data and the data of the stations belonging to the state water works are used for the other rivers which are not considered in the hydrological modeling.

3. RESULTS & DISCUSSION

3.1. Model results of the hydrologic models PROMET and mGROWA

The hydrologic models were validated using the available gauging station runoff data for the years 1975-2009 showing good results in both cases. As an example Fig 7 shows the comparison of measured and modeled mean streamflow (MQ) for PROMET for the available discharge stations, revealing a R^2 of 0.8824. Looking on the comparison of measured and modeled MQ for the three discharge station with the highest runoff values, a slight overestimation of streamflow for Karabük and Ayazma as well as a slight underestimation for Yuvaköy can be seen. The mean Nash-Sutcliffe model efficiency coefficient calculated from daily measured and modelled discharge data for all stations was found to be 0.35 and indicates a sufficient model performance. The relevant output of the model within the model chain is streamflow into the bay from five outlets.

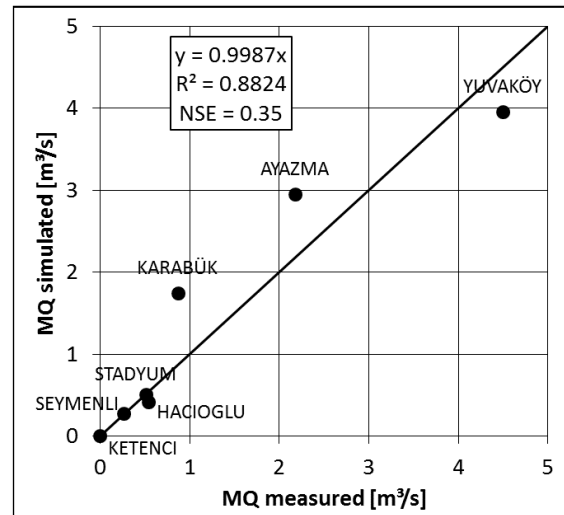


Fig 7. Comparison of measured and PROMET simulated MQ for all discharge stations in the Kocaeli catchment

After validation, PROMET was run for both periods (REF and FUT) with the climate data from the four GCM-RCM combinations to assess the climate change impact on the hydrology of the Izmit Bay catchment. Exemplary results from the PROMET model are shown in Tables 4 and 5.

Table 4 gives an overview on the mean annual values of some important hydrological parameters derived by the PROMET model driven by the four different climate model scenarios. Displayed are the absolute values for both periods REF and FUT.

Table 5 shows the relative changes from REF to FUT with regard to the mean annual values, again for all four climate model combinations. The Tables 4 and 5 show that HCH-RCA, in comparison to the other climate models, predicts the driest conditions for the future with a decrease of 106 mm (-13.1%) in mean annual precipitation and an increase of mean annual temperatures of 3 °C (+23.3%). This leads to a decrease in percolation of water from the lowest modeled soil layer, which indicates a decrease of ground water recharge.

Table 4. Absolute values for the REF and FUT periods for several water balance variables (annual mean) and for all 4 climate models (modeled with PROMET)

PROMET results	ECH-RCA		ECH-REM		ECH-RMO		HCH-RCA	
	REF	FUT	REF	FUT	REF	FUT	REF	FUT
Temperature (°C)	13.1	15.1	13.0	15.0	13.1	14.9	12.9	15.9
ET pot (mm)	980.0	1028.5	920.5	980.3	908.5	954.4	961.0	1067.2
ET act (mm)	384.1	350.4	397.6	358.7	367.0	342.2	379.5	334.5
Percolation (mm)	214.7	206.8	209.4	192.2	219.1	227.0	215.3	168.7
Precipitation (mm)	811.5	788.0	816.5	766.5	799.1	811.1	808.4	702.1
Runoff (mm)	434.0	441.2	424.4	412.8	438.6	476.4	432.5	371.8
Water budget (mm)	427.3	437.6	418.9	407.9	432.2	468.9	428.9	367.6

Table 5. Absolute increase of mean annual temperatures and relative difference from REF to FUT for several water balance variables (annual mean) as well as for all 4 climate models (modeled with PROMET)

PROMET results	ECH-RCA	ECH-REM	ECH-RMO	HCH-RCA
Temperature (°C)	+2.0	+2.0	+1.8	+3.0
ET pot	+4.9%	+6.5%	+5.1%	+11.1%
ET act	-8.8%	-9.8%	-6.7%	-11.9%
Percolation	-3.7%	-8.2%	+3.6%	-21.6%
Precipitation	-2.9%	-6.1%	+1.5%	-13.1%
Runoff	+1.6%	-2.7%	+8.6%	-14.0%
Water budget	+2.4%	-2.6%	+8.5%	-14.3%

The moistest future climate conditions were predicted by using climate data from ECH-RMO with a slight increase of mean annual precipitation. All four climate models show an increase of potential evapotranspiration and a decrease of actual evapotranspiration. The runoff (combination of direct runoff, interflow and baseflow) as well as the water budget (precipitation minus actual evapotranspiration) was simulated to increase slightly for ECH-RCA, to decrease slightly for ECH-REM, to increase for ECH-RMO and to decrease for HCH-RCA.

Fig 8 shows the quotient ET_i as an example for spatially fully distributed output of PROMET. ET_i was calculated by the PROMET modeled monthly mean actual evapotranspiration divided by potential evapotranspiration, as spatial output for the whole Kocaeli catchment for the moistest climate forcing ECH-RMO. ET_i can be regarded as an indicator for drought conditions, since the gap between actual and potential evapotranspiration was high during dry periods and low during periods where enough water was available for the transpiration of plants and the evaporation of surfaces. In Fig 8, the green areas stand for moist conditions whereas the red areas indicate dry conditions. It is visible that there is a predicted increase of ET_i in the months from November to January using ECH-RMO as climate forcing. In June, the climate model scenario shows a decrease of ET_i . Areas which show the most decrease of ET_i comparing REF and FUT were the regions around the coastline due to expanding industry, which was included into the modeling by using two different land use maps for the REF and FUT period.

The simulated streamflow into the bay of both hydrological models was linked to the MIKE 3HD hydrodynamic model, i.e. a total of 8 different possible present and 8 future runoff regimes were used as variable boundary conditions of the Izmit Bay model. The mean streamflow (MQ) differs only slightly between both hydrological models but varies more pronounced when different GCM-RCM combinations drive the hydrological models (see Fig 9). The differences of low water streamflow (LQ) are marginal. In fact, all combinations of the ensemble tend to simulate a seasonal running dry at the end of dry summer half-years in the reference and future

periods, respectively. The variability of high-water streamflow (HQ) is considerably, on the one hand between the two hydrological models and on the other hand between the four GCM-RCM-combinations. However, as the 20th and 70th percentiles (Q0.2, Q0.7) of the flow duration curves show, the intermediate streamflow varies little between both the hydrological models and the GCM-RCM-combinations.

The mGROWA-setup driven with observed climate data is validated using measured streamflow data of the 3 observed river gauges for the years 1975-2009, for which time series was almost complete (Fig 9).

As indicated by the performance criteria $NSE_c = 0.78$ and $PBIAS_c = -3.1\%$, there is a good fit of observed and simulated mean annual total runoff in the selected catchments. Model results presented in Figs 8 for PROMET model are not presented for mGROWA model, because differences in the model results of the two models are insignificant. Instead, direct comparisons of the model results are presented.

Accordingly, Fig 10 shows the comparison of PROMET and mGROWA modeled mean streamflow in (m^3/s) of the 5 major rivers in Izmit Bay for the REF period (1971-2000) and the FUT period (2041-2070). Displayed are the MQs of all four used climate model inputs. It is visible that the modeled MQ is very similar between the two hydrological models for all climate scenarios and rivers.

In the reference period the modeled MQs of the different climate scenarios are not scattered very much, which indicates a very stable performance of all GCM-RCMs. In the FUT period differences in the MQ are visible between the different climatic drivers. The scattering of the MQ is relative to the size of the catchments and therefore bigger for the Kirazdere and Yalakdere rivers, which leads to an increased uncertainty of the climate change impact on the hydrology.

ECH-RMO as climate forcing leads to an increase of modeled mean run-off for all rivers, whereas HCH-RCA is the driest scenario with a relatively huge decrease of modeled MQ. For ECH-RCA and ECH-REM it depends on the river if the MQ will increase or decrease. Using ECH-RCA as climate forcing Kirazdere and Yalakdere will show no or a very small change in

MQ, whereas the use of ECH-REM leads to a decrease of MQ. In the case of Ketenci and Tavşanlı ECH-RCA predicts a slight increase of MQ, whereas ECH-REM

indicates no or only a small decrease of MQ. For Çınarlı the modeled changes in MQ are very small besides a decrease for the dry HCH-RCA scenario.

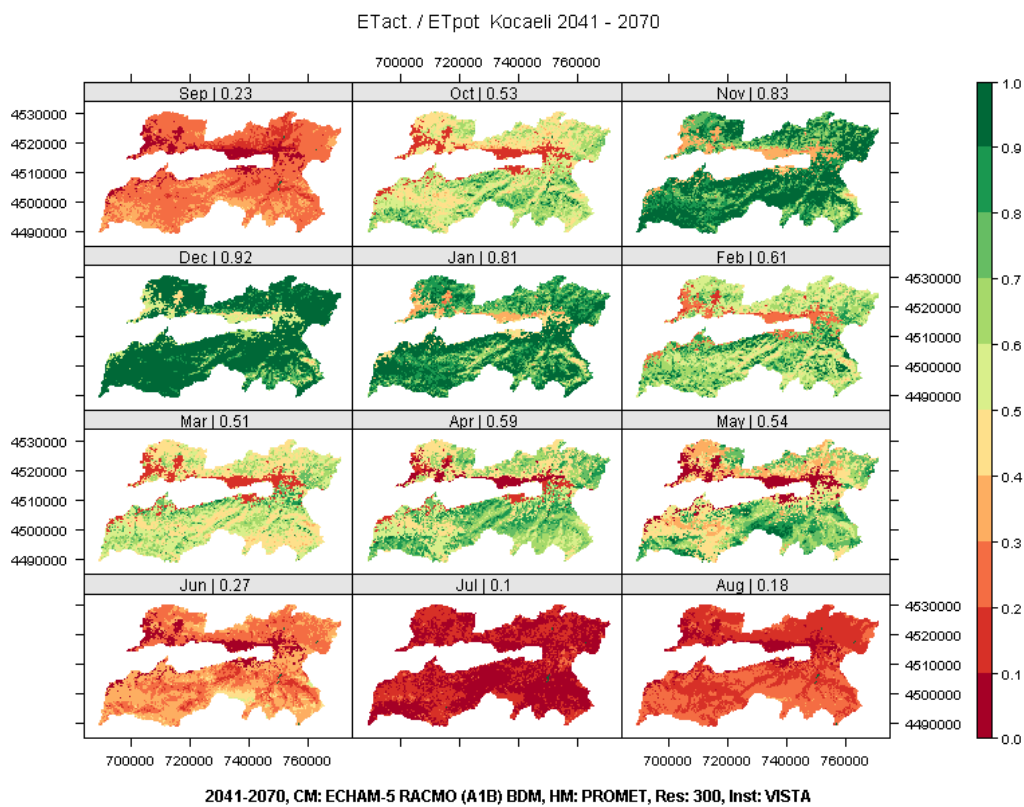
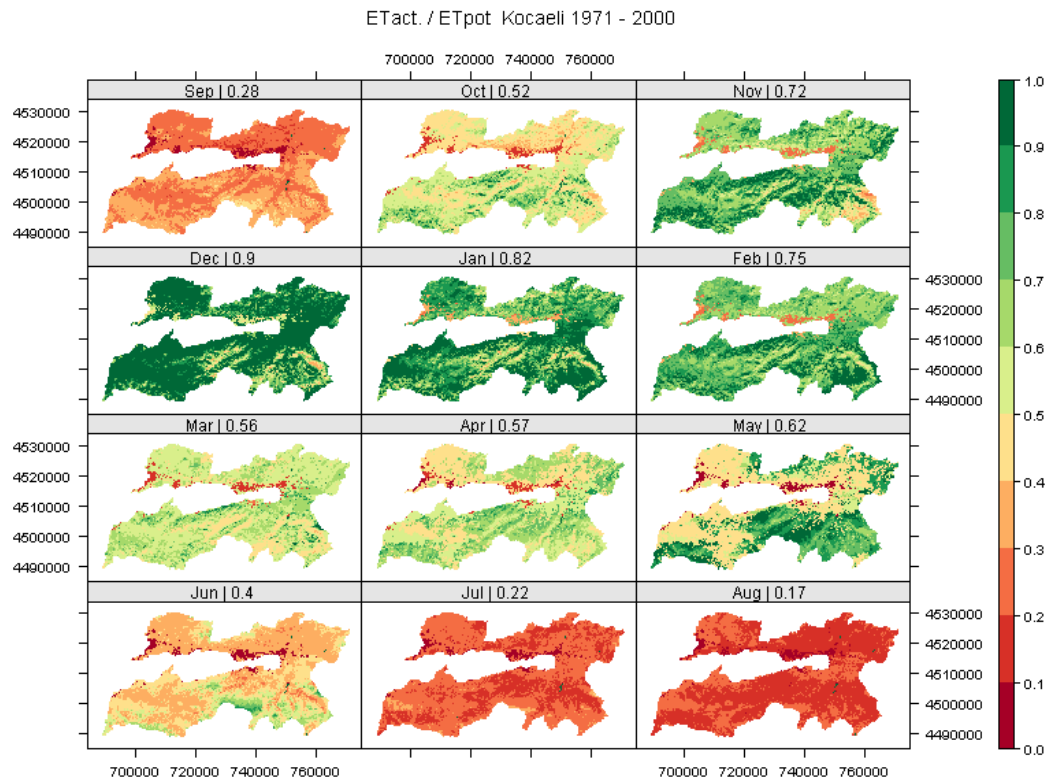


Fig 8. PROMET modeled monthly mean actual evapotranspiration divided by potential evapotranspiration as an indicator for drought conditions. REF period from 1971-2000, FUT period from 2041-2070. 300 m spatial resolution. Climate model forcing is ECH-RCA

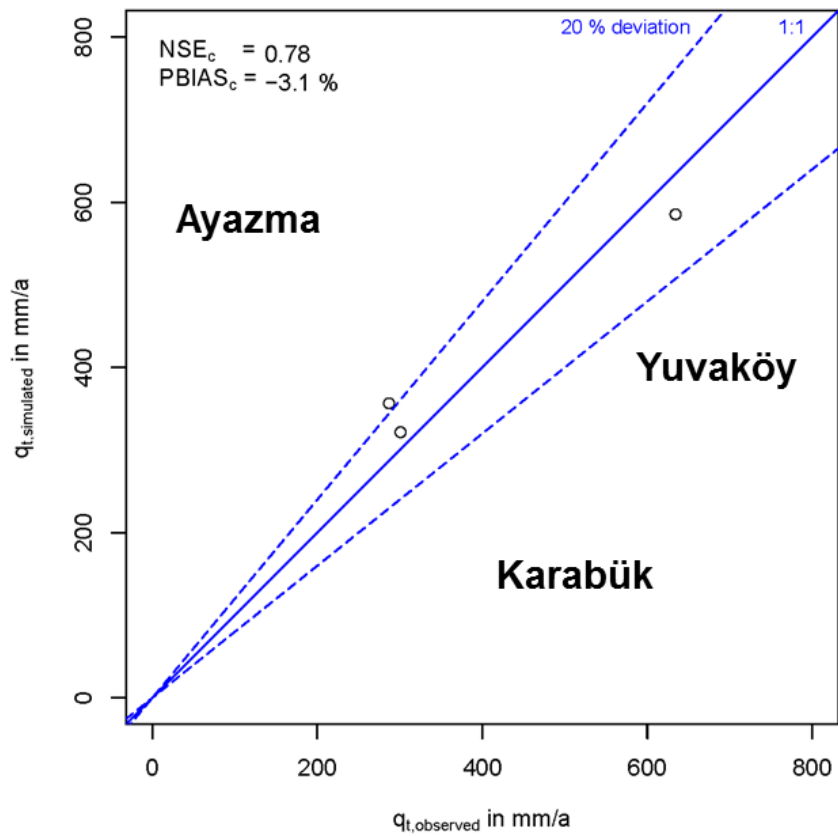


Fig 9. Validation results of the 3 observed river gauges for the years 1975-2009 (mGROWA)

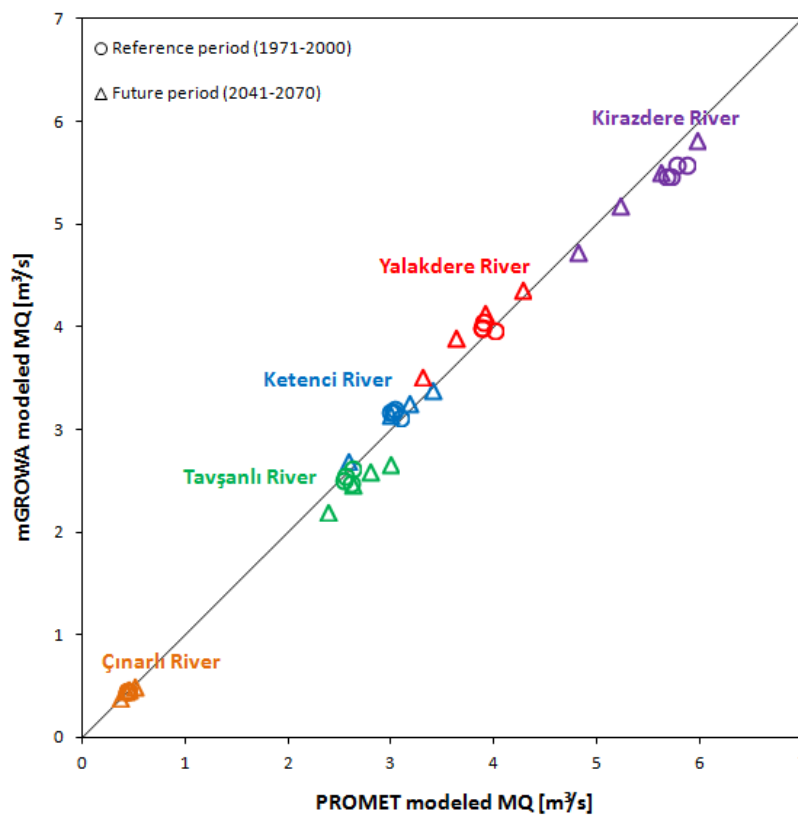


Fig 10. PROMET and mGROWA modeled mean streamflow in m^3/s of the 5 major rivers in Izmit Bay for the reference period (1971-2000) and the future period (2041-2070). Displayed are the MQs of all four used climate model inputs

A selection of raster hydrographs to portray the variety of simulated streamflow in the Kirazdere River is given in Figs 11 to 14. This type of Fig to visualize time-series in a raster form is designed according to suggestions in [46]. The combination ECH-RMO leads to the highest increase of mean streamflow when comparing the REF and FUT periods (Fig 11). In addition, a shift in the frequency and magnitude of the high-water streamflow events is clearly visible. While high-water events are simulated to be relatively equally distributed within the winter half-year of the

REF period, in the FUT period, high-water events occur more often and long-lasting from December to February and decrease in March and April. Low-water events seem to stay unchanged. Fig 12 shows the differences of the raster hydrograph in Fig 11 and the corresponding ECH-RMO - mGROWA hydrograph. While the general time-pattern of streamflow is simulated nearly equal with both models (the reasons are already described above), the differences are explained by the amount of water that was balanced as total runoff using different modeling concepts.

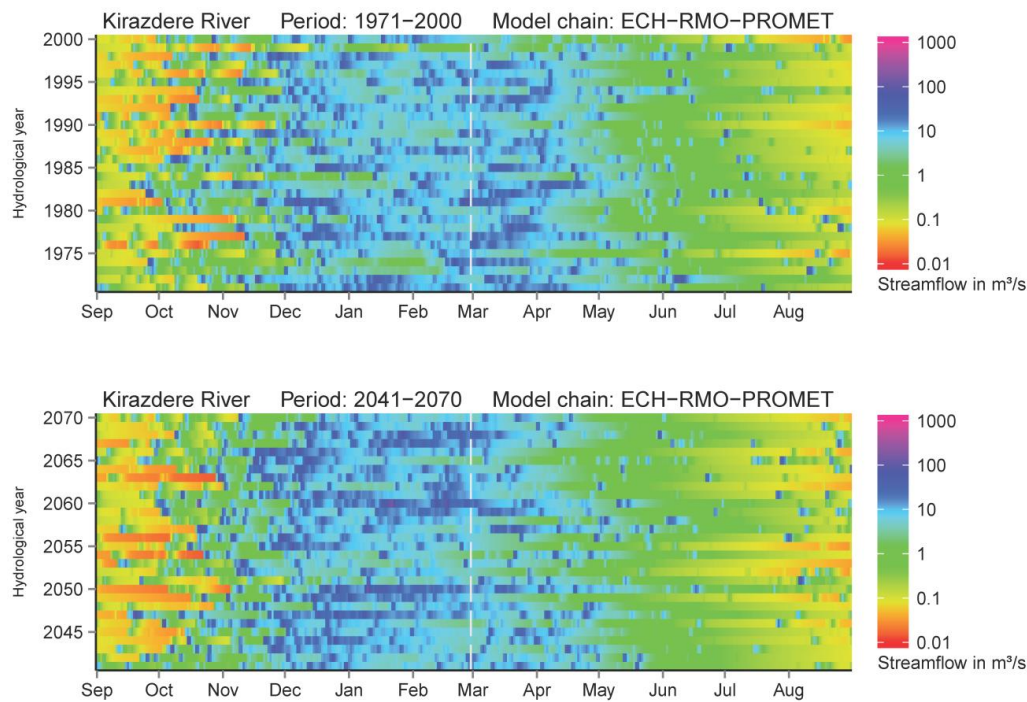


Fig 11. Raster hydrograph for the Kirazdere River simulated with the model chain ECH-RMO-PROMET

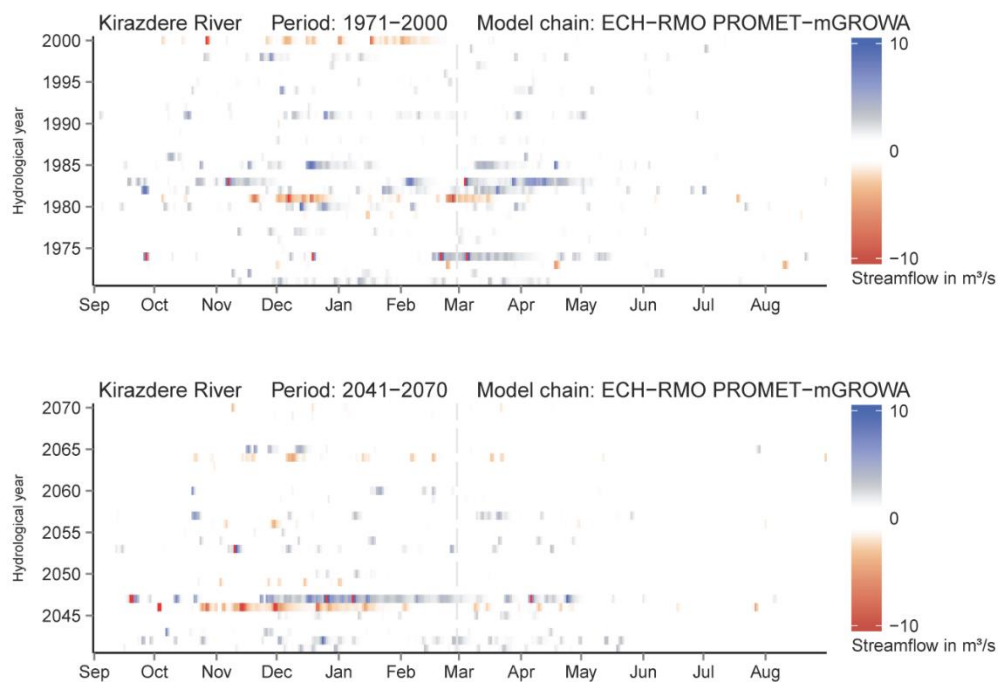


Fig 12. Differences in the raster hydrographs for the Kirazdere River (ECH-RMO PROMET-mGROWA)

In contrast to the combination ECH-RMO, HCH-RCA causes a considerable decline of mean streamflow and duration of high-water phases during winter as well as an extension of low-water phases close to running dry of the river during summer when comparing both periods (Fig 13). In the same way, for the combination HCH-RCA, the differences between streamflow balanced with PROMET and mGROWA are shown in Fig 14. The Kirazdere River has a mountainous headwater with elevations up to 1500 m, whereas in the other catchments elevation reaches up to 700 m only. The slight tendency of the mGROWA model to underestimate observed total runoff in relatively wet mountainous regions becomes visible in Fig 13 where

streamflow is lower in the reference period compared to PROMET. We assume that this slight underestimation is due to the mGROWA input parameter effective field capacity in the root zone derived by using the tabulated pedo-transfer functions in [47] for the main soil groups of the digital soil map of Kocaeli Province 1/25 000.

Finally, it can be noted that the resulting ensemble of 8 inflow boundary conditions comprise a range of possible future streamflow regimes which is suitable for the analysis of climate change impact on the hydrodynamics of the Izmit Bay.

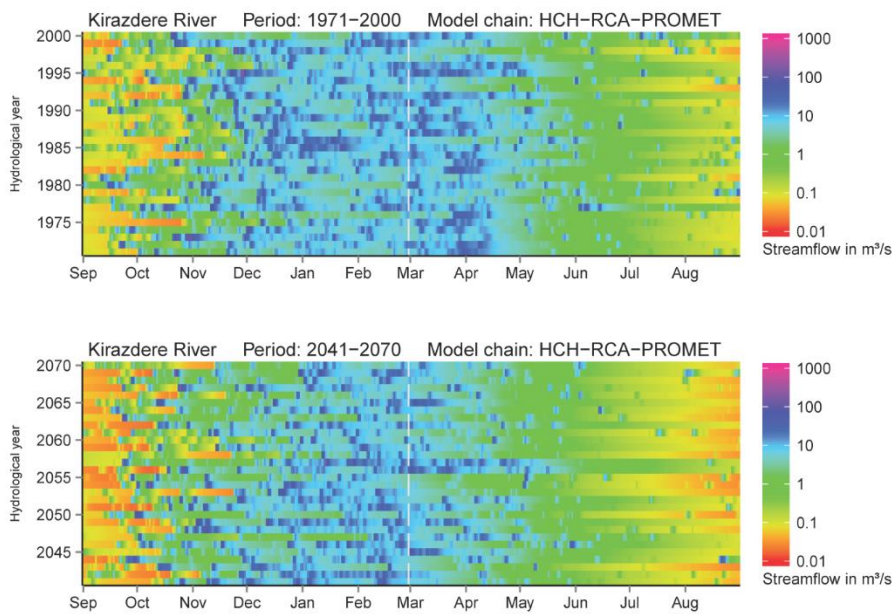


Fig 13. Raster hydrograph for the Kirazdere River simulated with the model chain HCH-RCA-PROMET

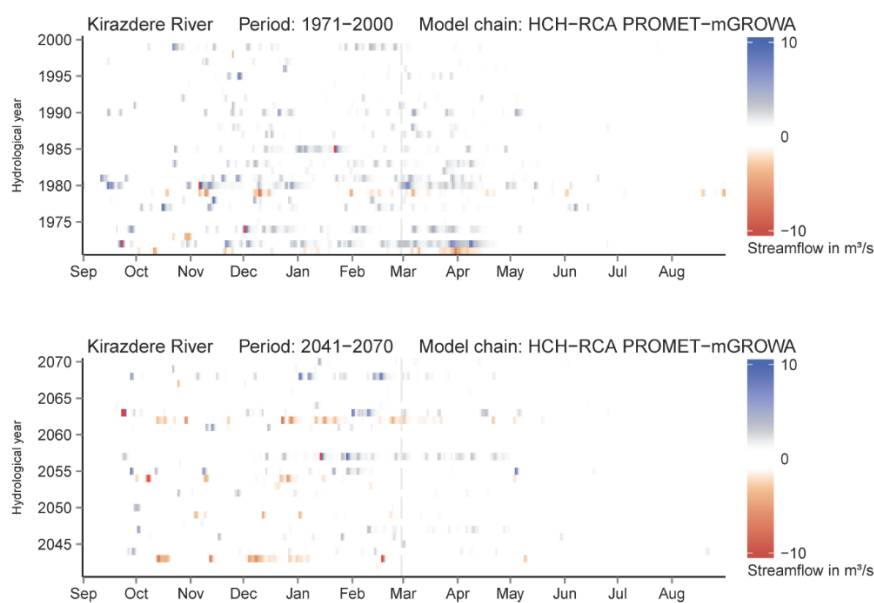


Fig 14. Differences in the raster hydrographs for the Kirazdere River (HCH-RCA PROMET-mGROWA)

3.2. Preliminary results of MIKE 3HD hydrodynamic model

The model setup procedure for Izmit Bay was carried out in two stages. In the first step, the basic parameters, such as the bathymetrical description (provided by the Naval Forces) were introduced to the model. After digitization, a 250 m grid size was set in the model. As it can be seen from the bathymetry map (Fig 2), the boundary was selected so that deeper parts of the Bay (below 1120 m) were included in the modeling. Therefore, it was intended to reflect the depth effect of the Marmara Sea (the deepest point of 1270 m) into the model. The locations of the sources and sinks were also defined during the model establishment. As a secondary step, all the inputs such as wastewater discharges, streams and rivers entering the water body were identified.

When considering the overflow and dry conditions, a minimum water level (here 0.001 m) was selected. The turbulence model was determined using the Smagorinsky formulation [23]. The vertical and horizontal borders of the system were entered into the mass budget system. The sea surface level, boundary conditions, friction coefficient, turbulence and temperature changes, precipitation values and wind were the system parameters for the hydrodynamic information. As mentioned in the previous sections, the streamflow rates were taken from the PROMET and mGROWA model results for the modelled 5 major streams. Precipitation data were taken from the results of the RCMs. Because of lack of data, water temperature and salinity parameters were assumed to be constant (temperature value assumed to be constant at 10 °C). The Smagorinsky coefficient which was used at the turbulence module, was

selected to be $C_s = 0.176$. The sea level data was taken from the Yalova Mareographic Station, which is the only available sea level change monitoring station within the region. The mean value of September was 0.35 m. This mean value was used as an initial sea level value. Consequently, the sea level change was determined as a function of time in the x and y directions.

MIKE 3 HD simulation runs were performed for the Izmit Bay using streamflow data provided by the models PROMET and mGROWA based on climate data from an ensemble of four general GCM and RCM combinations mentioned before, namely the ECH-RCA, ECH-REM, ECH-RMO and HCM-RCA models. In accordance with the hydrologic simulations, MIKE 3HD simulations were carried out for the reference period (1971-2000) and the future period (2041-2070) in order to assess possible variations in sea level. Both modeling periods start on 1st of September and end on 31st of August.

Fig 15 presents the monthly mean sea level change results of MIKE 3HD using PROMET and mGROWA runoff data. The mean values of the reference period indicate that the variations in sea level are more prominent between September and February compared to the other half of the year. This is due to the fact that most precipitation events occur during this period. The variations between the reference period and the future periods are quite significant between September and February, so that the seasonal pattern of precipitation may sustain in the future. Vice versa, the values between February and August show that sea level change is smoother and the predictions for future periods are close to the reference values.

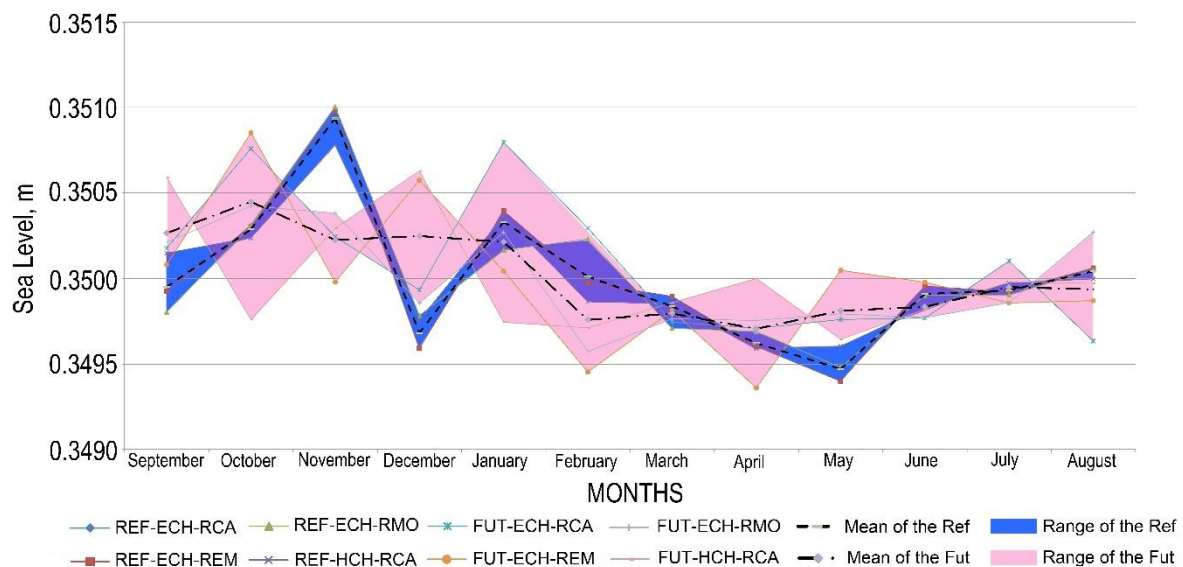


Fig 15. Monthly mean sea level change results of MIKE 3 using PROMET and mGROWA runoff data

The monthly mean sea level change values obtained from the MIKE 3HD simulation runs using river discharge data provided by PROMET and mGROWA models can be found in Table 6. As can be seen, both

PROMET and mGROWA model results are quite comparable to each other and the differences between the two models are negligible.

Table 6. Monthly mean values of the sea level change results using river discharge data provided by the PROMET (VISTA) and mGROWA (FZJ) models

	PROMET REF (m)	mGROWA REF (m)	PROMET FUT. (m)	mGROWA FUT (m)	Mean of the REF (m)	Mean of the FUT (m)
September	0.3499	0.3500	0.3503	0.3502	0.3500	0.3503
October	0.3502	0.3504	0.3503	0.3506	0.3503	0.3504
November	0.3509	0.3510	0.3501	0.3504	0.3509	0.3502
December	0.3494	0.3500	0.3500	0.3505	0.3497	0.3502
January	0.3503	0.3504	0.3502	0.3502	0.3503	0.3502
February	0.3500	0.3500	0.3498	0.3497	0.3500	0.3498
March	0.3501	0.3496	0.3498	0.3498	0.3498	0.3498
April	0.3501	0.3491	0.3497	0.3497	0.3496	0.3497
May	0.3498	0.3491	0.3499	0.3497	0.3495	0.3498
June	0.3500	0.3498	0.3498	0.3499	0.3499	0.3498
July	0.3500	0.3499	0.3499	0.3500	0.3499	0.3499
August	0.3500	0.3501	0.3499	0.3500	0.3500	0.3499

Hence the deviation of the model results from the actual level at the reference sea level gauging station Yalova (0.35m) is negligible. As Izmit Bay is assumed to be a hydro dynamically closed system in the MIKE 3HD model set-up, there is a clear indication that the climate change induced impacts on streamflow may only to a minor extent affect the sea level in the bay. Instead, climate change induced water exchange of the bay with the open sea may probably has a greater influence on sea level changes, if the model domain will be set up as an open system. The related MIKE 3HD simulations should be repeated once the hydrologic regime of the catchments of the Black Sea and the Aegean Sea and the processes in the Sea have been assessed in a broader macro-scale study.

4. CONCLUSIONS

An ensemble of 4 global climate model/regional climate model couples has been applied to drive the hydrological models PROMET and mGROWA. Based on these overall 16 simulation setups which comprise two hydrological periods from 1971-2000 (reference period) and 2041-2070 (future period) respectively, a bandwidth of possible future development paths of the regional streamflow was determined. Due to the global warming predicted in the climate models and the resulting shift of rainfall periods with increasing precipitation during the winter months and decreasing precipitation during the summer months, river streamflow is simulated to increase in winter and the rivers will fall dry more often and longer than in present times during drought periods in summer.

On the other hand, it was shown that the impact of streamflows of the reference and the future period on the sea level changes is low. This indicates that the effects of climate change on terrestrial hydrology will be negligible or not likely to be reflected in the bay. From here, it can be concluded that under the global climate change conditions, the Izmit Bay will be more exposed to the effects of Marmara Sea. This in mind, we conclude the related MIKE 3HD simulations should

be repeated once the hydrologic regime of the catchments of the Black Sea and the Aegean Sea and the processes in the Sea have been assessed in a broader macro-scale study. The latter however was not part of the work packages of the EU 7th Framework Programme project CLIMB.

In a more general sense it can be concluded that the coupling of Global and Regional Climate Models with the hydrologic models PROMET / mGROWA and MIKE 3HD is technically possible. An application for a small bay (here Izmit Bay) however should include discharge data from all catchments (here the Aegean – Mediterranean – Black Sea system) and the related exchange processes with the open seas.

ACKNOWLEDGMENT

This work was supported by the European Union 7th Framework Programme [Grant number 244151].

REFERENCES

- [1]. IPCC, 2014: Climate Change 2014: Synthesis Report. Contribution of Working Groups I, II and III to the Fifth Assessment Report of the Intergovernmental Panel on Climate Change [R.K. Pachauri and L.A. Meyer (eds.)]. IPCC, Geneva, Switzerland, pp. 151.
- [2]. S.N. Gosling, R.G. Taylor, N.W. Arnell and M.C. Todd, "A comparative analysis of projected impacts of climate change on river runoff from global and catchment-scale hydrological models," *Hydrology and Earth System Science*, Vol. 15, pp. 279-294, 2011.
- [3]. A.J. Lamadrid and K.L. MacClune, Climate and Hydrological Modeling in the Hindu-Kush Himalaya Region. Feasibility Report for a Himalayan Climate Change Impact and Adaptation Assessment. International Centre for

- Integrated Mountain Development. Kathmandu, 2010.
- [4]. A. Panagopoulos, G. Arampatzis, E. Tziritis and V. Pinaras, F. Herrmann, R. Kunkel, F. Wendland, "Assessment of climate change impact in the hydrological regime of River Pinios Basin, Central Greece," *Desalination and Water Treatment*, Vol. 57, pp. 2256-2267, 2016.
- [5]. S. Praskievicz and H. Chang, "A review of hydrological modeling of basin-scale climate change and urban development impacts," *Progress in Physical Geography*, Vol. 33, pp. 650-671, 2009.
- [6]. K.M. Strzepek and A.L. Mccluskey. Modeling the Impact of Climate Change on Global Hydrology and Water Availability - Discussion Paper Number 8, 2010.
- [7]. The Turkish Statistical Institute, TUIK, Available: <http://www.tuik.gov.tr>, (accessed 06 July 2017).
- [8]. V.P. Singh, "Computer models of watershed hydrology," *Water Resources Publications*, Colorado, 1995.
- [9]. M. Albek, U. Bakır Ogutveren and E. Albek, "Hydrological modeling of Seydi Suyu watershed (Turkey) with HSPF," *Journal of Hydrology*, Vol. 285, pp. 260-271, 2004.
- [10]. H. Apaydin, A.S. Anli and A. Ozturk. "The temporal transferability of calibrated parameters of a hydrological model," *Ecological Modelling*, Vol. 195, pp. 307-317, 2006.
- [11]. P. Droogers, W.G.M. Bastiaanssen, M. Beyazgul, Y. Kayam, G.W. Kite and H. Murray Rust, "Distributed agro-hydrological modeling of an irrigation system in western Turkey," *Agricultural Water Management*, Vol. 43, pp. 183-202, 2000.
- [12]. F. Keskin, "Hydrological model study in Yuvacik dam basin by using GIS analysis," (Doctoral dissertation). Middle East Technical University, 2007.
- [13]. G. Benito, N.G. Macklin, C. Zielhofer and A.F. Jones, M.J. Machado, "Holocene flooding and climate change in the Mediterranean," *Catena*, Vol. 130, pp. 13-33, 2015.
- [14]. D. Bozkurt and O.L. Sen, "Climate change impacts in the Euphrates-Tigris Basin based on different model and scenario simulations," *Journal of Hydrology*, Vol. 480, pp. 149-161, 2013.
- [15]. A. Erturk, A. Ekdal, M. Gurel, N. Karakaya, C. Guzel and E. Gonenc, "Evaluating the impact of climate change on groundwater resources in a small Mediterranean watershed," *Science of the Total Environment*, Vol. 499, pp. 437-447, 2014.
- [16]. Y. Fujihara, K. Tanaka, T. Watanabe and T. Nagano, T. Kojiri, "Assessing the impacts of climate change on the water resources of the Seyhan River Basin in Turkey: Use of dynamically downscaled data for hydrologic simulations," *Journal of Hydrology*, Vol. 353, pp. 33-48, 2008.
- [17]. R. Deidda, M. Marrocu, G. Caroletti, G. Pusceddu, A. Langousis, V. Lucarini and A. Speranza, "Regional climate models' performance in representing precipitation and temperature over selected Mediterranean areas," *Hydrology and Earth System Sciences*, Vol. 17, pp. 5041-5059, 2013.
- [18]. R. Ludwig, A. Soddu, R. Duttman, N. Baghdadi, S. Benabdallah, R. Deidda and T. Ammerl, "Climate-Induced Changes on the Hydrology of Mediterranean Basins - A Research Concept to Reduce Uncertainty and Quantify Risk," *Fresenius Environmental Bulletin*, Vol. 19 (10a), pp. 2379 - 2384, 2010.
- [19]. W. Mauser and H. Bach, "PROMET - Large scale distributed hydrological modeling to study the impact of climate change on the water flows of mountain watersheds," *Journal of Hydrology*, Vol. 376, pp. 362-377, 2009.
- [20]. L. Ehlers, F. Herrmann, M. Blaschek, F. Wendland and R. Duttman, "Sensitivity of mGROWA-simulated groundwater recharge to changes in soil and land use parameters in a Mediterranean environment and conclusions in view of ensemble-based climate impact simulations," *Science of the Total Environment*, Vol. 543, pp. 937-951, 2015.
- [21]. F. Herrmann, L. Keller, R. Kunkel H. Vereecken and F. Wendland, "Determination of spatially differentiated water balance components including groundwater recharge on the Federal State level - A case study using the mGROWA model in North Rhine-Westphalia (Germany)," *Journal of Hydrology: Regional Studies*, Vol. 4, pp. 294-312, 2015.
- [22]. P. Kreins, M. Henseler, J. Anter, F. Herrmann and F. Wendland, "Quantification of Climate Change Impact on Regional Agricultural Irrigation and Groundwater Demand," *Water Resources Management*, Vol. 29, pp. 3585-3600, 2015.
- [23]. DHI. MIKE 21 MIKE 3 Flow Model FM, Short description of Hydrodynamic Module. DHI Software. Denmark, 2013.
- [24]. Kocaeli Mayorship, Kocaeli Environmental Status Report, 2006, Available: http://cdr.cevre.gov.tr/2010_icdrler/kocaeliicd2010.pdf, (accessed 01 December 2015).
- [25]. Kocaeli Governorship, Turkish Government, Available: <http://www.kocaeli.gov.tr/sanayikenti-kocaeli>, (accessed 06 July 2017).
- [26]. H.A. Ergül, T. Varol and U. Ay, "Investigation of heavy metal pollutants at various depths in the Gulf of Izmit," *Marine Pollution Bulletin*, Vol. 73, pp. 389-393, 2013.
- [27]. E. Morkoç, O.S. Okay, L. Tolun, V. Tufekçi, H. Tufekçi and T. Legoviç, "Towards a clean Izmit Bay," *Environmental International*, Vol. 26, pp. 157-161, 2001.
- [28]. L. Tolun, O.S. Okay, A.F. Gaines, M. Tolay, H. Tufekçi and N. Kiratlı. "The pollution and toxicity of surface sediments in Izmit Bay (Marmara Sea)," Turkey. *Environmental International*, Vol. 26, pp. 163-168, 2001.
- [29]. L. Tolun, O.S. Okay, D. Martens and K.W. Schramm, "Polycyclic aromatic hydrocarbon contamination in coastal sediments of the Izmit

- Bay (Marmara Sea): Case studies before and after the Izmit Earthquake," *Environment International*, Vol. 32, pp. 758-765, 2006.
- [30]. M. Karpuzcu, N. Agiralioğlu, N. Alpaslan, G. Engin, H. Gömann, O. Gunduz and F. Wendland. Integrated Modeling of Nutrients in Selected River Basins of Turkey. Schriften des Forschungszentrums. Jülich, Reihe Energie & Umwelt, Vol. 17, pp. 183, 2008.
- [31]. H. Bach, M. Braun, G. Lampart and W. Mauser, "The use of remote sensing for hydrological parameterisation of Alpine catchments," *Hydrology and Earth System Sciences*, Vol. 7, pp. 862-876, 2003.
- [32]. R. Ludwig, W. Mauser, S. Niemeier, A. Colgan, R. Stolz, H. Escher-Vetter and R. Hennicker, "Web-based modeling of energy, water and matter fluxes to support decision making in mesoscale catchments - the integrative perspective of GLOWA-Danube," *Physics and Chemistry of the Earth*, Vol. 28, pp. 621-634, 2003.
- [33]. W. Mauser and R. Ludwig. A research concept to develop integrative techniques, scenarios and strategies regarding global changes of the water cycle. In: M. Beniston (Ed.), *Climatic Change: Implications for the Hydrological Cycle and for Water Management: Advances in Global Change Research GLOWA-DANUBE*. Kluwer Academic Publishers, Dordrecht and Boston, pp. 171-188, 2002.
- [34]. P. Klug, H. Bach and S. Migdall, Monitoring Soil Infiltration in Semi-Arid Regions with Meteosat and a Coupled Model Approach Using PROMET and SLC. Paper presented at the meeting of ESA Living Planet Symposium, Edinburgh, 2013.
- [35]. H. Bach, W. Verhoef, K. Schneider, "Coupling remote sensing observation models and a growth model for improved retrieval of (geo)biophysical information from optical remote sensing data," *Remote Sensing for Agriculture, Ecosystems and Hydrology*, 4171, 1-11, 2000.
- [36]. R. Ludwig and W. Mauser, "Modeling catchment hydrology within a GIS based SWAT-model framework," *Hydrology and Earth System Science*, Vol. 4(2), pp. 239-249, 2000.
- [37]. U. Strasser and W. Mauser, "Modeling the spatial and temporal variations of the water balance for the Weser catchment 1965-1994," *Journal of Hydrology*, Vol. 254 (1-4), pp. 199-214, 2001.
- [38]. J.A. Cunge, "On the subject of a flood propagation computation method (Muskingum method)," *Journal of Hydraulic Research*, Vol. 7, pp. 205-230, 1969.
- [39]. E. Todini, "A mass conservative and water storage consistent variable parameter Muskingum-Cunge approach," *Hydrology and Earth System Science*, Vol. 4, pp. 1549-1592, 2007.
- [40]. W. Verhoef and H. Bach, "Coupled soil-leaf-canopy and atmosphere radiative transfer modeling to simulate hyperspectral multi-angular surface reflectance and TOA radiance data," *Remote Sensing of Environment*, Vol. 109, pp. 166-182, 2007.
- [41]. R. Kunkel, H. Röhm, J. Elbracht and F. Wendland, "Das CLINT Interpolationsmodell zur Regionalisierung von Klimadaten und WETTREG Klimaprojektionen für Analysen zum regionalen Boden- und Grundwasserhaushalt in Niedersachsen und Bremen. GeoBerichte-Landesamt für Bergbau", *Energie und Geologie*, Vol. 20, pp. 6-31, 2012.
- [42]. T. Marke, W. Mauser, A. Pfeiffer and G. Zängl, "A pragmatic approach for the downscaling and bias correction of regional climate simulations: evaluation in hydrological modeling," *Geoscientific Model Development*, Vol. 4, pp. 759-770, 2011.
- [43]. R.G. Allen, L.S. Pereira, D. Raes and M. Smith, *Crop evapotranspiration - Guidelines for computing crop water requirements*, 1998.
- [44]. R. Kunkel and F. Wendland, "The GROWA98 model for water balance analysis in large river basins - the river Elbe case study," *Journal of Hydrology*, Vol. 259, pp. 152-162, 2002.
- [45]. N. Engel, U. Müller and W. Schäfer, "BOWAB - Ein Mehrschicht-Bodenwasserhaushaltsmodell," *GeoBerichte - Landesamt für Bergbau, Energie und Geologie*, Vol. 20, pp. 85-98, 2012.
- [46]. E. Strandhagen, W.A. Marcus and J.E. Meacham, "Views of the Rivers: Representing Streamflow of the Greater Yellowstone Ecosystem," *Cartographic Perspectives*, Vol. 55, pp. 54-59, 2006.
- [47]. U. Müller and A. Waldeck, *Auswertungsmethoden im Bodenschutz*. Vol 19: Landesamt für Bergbau, Energie und Geologie Niedersachsen, 2011.



RESEARCH ARTICLE

Assessment of Yalova University Campus according to LEED V.4 certification system

Hikmet Erbyık¹, Tuğçe Çatal², Sinem Durukan², Doğan Günes Topaloğlu², Ümit Ünver^{3,*}

¹Yalova University, Engineering Faculty, Department of Industrial Engineering, Yalova, TURKIYE

²Yalova University, Engineering Faculty, Department of Energy Systems Engineering, Yalova, TURKIYE

³Yalova University, Engineering Faculty, Department of Mechanical Engineering, Yalova, TURKIYE

ABSTRACT

In this paper, a detailed literature review on the LEED Certification system is embedded in to green building certification case study. Within the study, information about the parameters of the LEED system and the algorithm that should be applied in order to get full score from the audit were compiled. The conditions of Turkey were taken into account through the study. The study was presented in an analytical order for scientists to easily access information about the LEED Certification system. In addition, the evaluation required to get an appropriate score from the LEED certification system is given with a case study; analysis Yalova University Campus.

Keywords: Green buildings, LEED certificate, LEED V.4, green campus, sustainable buildings

1. INTRODUCTION

The need for technology and industrialization increases with the increasing population of the world. These needs increase energy consumption, while they also increase the amount of carbon dioxide emissions. The increase in energy consumption increases the interest in renewable energy sources. Alternative searches are considered in order to reduce carbon dioxide emission [1]. 30% of the total energy consumption is realized by the building sector. Residential buildings consume quarter of the energy and the remaining is consumed in public and commercial buildings. According to the data between 2010 and 2017, the energy demand of buildings has increased by 20% worldwide [2].

The green building concept is constantly being developed in order to reduce the negative effects buildings on the environment. The most common green building certification systems used in the world are BREEAM (Building Research Establishment Environmental Assessment Method), LEED (Leadership in Energy and Environmental Design), Greenstar and CASBEE (Comprehensive Assessment System for Built Environment Efficiency), SBTOOL (Sustainable Building Tool) and DGNB (Deutsche

Gesellschaft für Nachhaltiges Bauen) [3]. Green building certification systems have been created to benefit the environment by maintaining the buildings consume less energy, generate less construction and demolition waste, and buildings to have improved water efficiency [4].

There is an increase in the number of efforts to construct and develop sustainable buildings around the world. It is seen that green building projects are designed in line with ecology, health and welfare, economy, CO₂, energy, innovation, indoor environmental quality, management, materials, land use, environmental pollution, transportation, waste and water management, renewable technology.

One of the most popular green building certification systems used in the world is the LEED (Leadership in Energy and Environmental Design) certification system. Figure 1 shows the emblem of the LEED Certification system [1].

In this paper, the LEED Certification system was examined, the parameters of the system were introduced and the action plan that should be done in order to get a full score from the system was studied. Research results in people living in Turkey to access more detailed information about LEED and could

Corresponding Author: umit.unver@yalova.edu.tr (Ümit Ünver)

Received 19 October 2020; Recived in revised form 2 January 2021; Accepted 4 January 2021

Available Online 15 January 2021

Doi: <https://doi.org/10.35208/ert.812339>

© Yildiz Technical University, Environmental Engineering Department. All rights reserved.

benefit from the system is targeted to reach potential. This paper is aimed to enable scientists to obtain more detailed information about LEED and reach the potential to benefit from the certificate system.



Fig 1. LEED certification system emblem

2. LEED CERTIFICATION SYSTEM

Extinction possibility of world's fossil fuels that are used for global energy production and human beings' day by day increasing dependency to the energy has affected all industrial sectors as well as construction sector adversely. Construction sector also has been searching new solution methods for this adverse effect. This solution methods were concerned in the past years for finding new energy sources, on the contrary in our day's main concern is to consume our energy by referring and searching energy saving methods. As the result of this searches; green building concept has been initiated by considering; low carbon emission processes, consuming natural resources in energy efficient manner, consideration of user health [5], [6]. Main environmental problems in our days; inefficient and unsuitable use of buildings (consumption of fossil fuels and CO₂ emission), negative trend of waste in energy use, energy losses suffered starting from the feasibility and design stages up to whole stages of production and construction of the buildings and life cycle processes. Because of this, Green Building certification systems are emerged in many countries.

LEED System has been developed by United States of America (USA) Green Buildings Council. Its proliferation has been assured by LEED president of Management Board, Mr Robert K. Watson, between 1995 to 2006 years. LEED Certification System provides knowledge on how to design, construct of a green building and how to manage it and to define the required types of maintenance solutions. As having been internationally recognized green building assessment system, the objective of LEED, to minimize the impacted harms onto environment of the private and state owned buildings in the construction sector and to sustain it by reviewing their life cycle assessment [1].

In order to maintain any building possessing green building features as having LEED certificate; the position of the building, its design, its waste and other pollutant details during the construction and demolition stages, has to be calculated and its productivity aspects have to be monitored. In addition, consideration of healthcare and environmental protection during the life cycle period and usage of natural resources during the construction stages toward affecting positively on human health has to be aimed. The differences between green buildings and classic buildings are given with Figure2.

LEED Certification System consists of various versions as V4, with 8 main credit categories and is distributed to 99 points in TOTAL. Extra 10 points is being taken from 'regional priorities' and 'innovation' categories. In addition to these, another 1 point could also be taken from 're-integrative process' category (this credits is assessed in terms of the maintaining project sustainability). In Table1, LEED system and V4 categories credits points are shown.

LEED point scoring system has certain stages. For any building, in order to obtain LEED green building certificate, it is necessary primarily to comply with the minimum program requirements. In case of the complying these requirements, in order to get certificate mandatory pre-requisites that are not included in the grading system also have to be maintained. For any building, in order to get green building certificate, program main requirements and pre-requisites have to be achieved and the minimum intended objective of 40 points has to be exceeded.

Table 1. LEED system V4 category rating points

LEED Credits	Score
1 Re-integrative process	1
2 Innovation	6
3 Location And Transportation	16
4 Energy and Atmosphere	33
5 Water Efficiency	11
6 Sustainable Sites	10
7 Indoor Environmental Quality	16
8 Materials and Resources	13
9 Regional Priority	4
TOTAL	110

Green Buildings may have 4 different certificate levels. LEED Certificate types are shown in Figure 2.



Fig 2. LEED certificate types

2.1. Advantages and disadvantages of LEED certification system

In a building that has LEED Certificate, in addition to building's compliance of all the legal requirements, it is also assured that the building is designed in comprehensive manner. Thus, more habitable buildings in terms of human health could be achieved by maintaining higher water saving and energy efficiency and less environmental pollution. The advantages of LEED system can be cited as follows;

- Reduces operational cost, maintains increasing asset values,
- Contributes into reduction of amount of wastes that are disposed into fields.
- Maintains energy saving as well as water saving,
- Renders healthier and safer habitable places to the building users.

- Maintains mitigating gas emissions.
- Provides having tax reduction, reconstruction permit, and also other incentives [2].

The disadvantages of LEED system could be cited as follows;

- Higher first investment cost,
- Prolonging the building construction period due to compliance with the mandatory procedures.

2.2. LEED V4 main credits

LEED main credits are consists of 8 headings in total. These headings are cited as follows;

1. Innovation (IN)
2. Location and transportation (LT)
3. Energy and atmosphere (EA)
4. Water Efficiency (WE)
5. Sustainable sites (SS)
6. Indoor environmental quality (EQ)
7. Materials and resources (MR)
8. Regional priority (RP)

Innovation (IN)

It is a category that is placed for encouraging and rewarding the concerned projects in order to exhibit innovative performance. Expectations and scorings under this category are shown in Table 2 [6 – 8].

Table 2. Innovation

No	Score	Credit	Objective
1	5	Innovation	To encourage performing projects having extraordinary or innovative performance features. The more the project having 100 % efficiency, profitability and effectiveness, the more innovative performance features are.
2	1	LEED Accredited Personnel	To encourage the coherence of group that is working for LEED project, furthermore to maintain easing the implementation and certification process.

While making assessments for these credits in Yalova University Campus, it is not possible getting grade from the no.1 and no. 2 credits. In order to get point grade from no. 1 credits, an innovative action should be maintained such as; meting the energy need of the university by utilizing solar power. In order to get point credits from no.2 point, at least 1 person from the university must obtain accredited LEED professional certificate.

Location and transportation (LT).

Expectations and point scorings under this category are shown in Table 3.

Table 3. Location and transportation

No	Score	Credit	Objective
1	between 5 to 9	Place Selection for Local Development	Enhances the development of settlements in urban areas by utilizing existing infrastructure in order to protecting natural resources, to reduce the vehicle traffic in transportation as much as possible, physical activity, walking and outdoor field of interest open air media [8].
2	1	Sensitive Field Protection	Protected areas such as lake, river, natural habitat protection areas, sea, water reservoirs, water resources, sporting areas, agricultural areas, must not be approached nearer than 15 meters and those areas must not be selected as project areas.
3	between 1 to 2	High Priority Field	The project has to be encouraged in such places that require further development and having low development means [9].
4	1	Environmental Density and Usage Diversity	By encouraging the urban areas that have existing infra structure, protecting green fields, habitable fields, and natural resources. To encourage voluntary walking, to increase transportation efficiency, and to reduce the transportation distance by vehicles [10].
5	between 1 and 2	Quality Access to the Mass Transportation	To reduce the vehicle usage as a result of the increasing the usage of transportation areas that having multi selection alternatives, to reduce carbon emissions and greenhouse effect, to mitigate the hazardous aspects onto society health and environment by reducing usage of motor vehicles [11].
6	1	Bicycle Facilities	To reduce vehicle usage by encouraging bicycle usage, to increase physical activity possibilities that affect human health positively. In this regard safer bicycle roads and storing units must be maintained [12].
7	1	To Reduce Car Park Areas	To minimize environmental harms that emerges due to car park activities, field location, automobile addiction and surface rain water.
8	1	Green Vehicles	To aim the usage of alternative fuel consumption vehicles instead of conventional vehicles in order to reduce the pollution [13].

Energy and atmosphere (EA)

It is important in green building design to reduce the energy costs and to increase the energy performance by reducing the energy needs [14]. The most important

and highest point grade providing category is Energy and Atmosphere among the LEED certificate main credits. In fact, buildings are responsible for the largest energy consumption among other sectors [15].

Energy and Atmosphere category, contains different sub-headings such as; the efficient design and construction, follow up of energy usage, usage of renewable energy sources, efficient implementations, efficient devices and illumination systems, energy production in-field or outer-field, and other innovative

strategies [2]. In this category while completing all credits, total 31 point grade can be obtained [16]. All credits and point grading are shown in Table 4. for Energy and Atmosphere.

Table 4. Energy and atmosphere

No	Score	Credit	Objective
1	Prerequisite	Fundamental Commissioning and Verification	It defines the auditing of operating conditions of defined energy consumption systems in buildings and compliance of technical capacity against the standards and technical specifications. The systems that are required to be audited; illumination systems, hot water systems, HVAC systems, renewable energy systems, mechanical, automation systems and electric of the building has been defined in this credits [4, 5, 15].
2	Prerequisite	Minimum Energy Performance	It is aimed to avoid the use of excessive energy, to reduce the potential harms that could be imposed on the environment and economy by considering the energy efficiency for the systems in the building [17]. To define energy performance point grade energy consumptions have to be measured at certain intervals. Energy counters have to be provided in order to measure the total building energy consumption [8, 17, 18].
3	Prerequisite	Building-Level Energy Metering	It is applied for energy management and saving in order to monitor the energy usage in the whole building [17]. The aim is to follow up the energy consumption for certain devices for how much energy is consummated in the building.
4	Prerequisite	Fundamental Refrigerant Management	It is applied to mitigate the harm into ozone layer and to reduce the thickness of ozone layer. If the mechanical coolant systems are used, it provides the usage of systems that do not contain chlorofluorocarbon (CFC) and hydro-chlorofluorocarbon (HCFC), and the products that do not harm the atmosphere [18].
5	6	Enhanced Commissioning	Test and start up systems contain; ventilating systems, heating systems, cooling systems, (HVAC) systems, illumination systems, water supply systems, and renewable energy systems as a whole. Main aim in this credits, to ensure the targeted energy efficiency values at the project commencing period, to be consistent with the resultant measurement values at the project completion period [19].
6	16	Optimize Energy Performance	It is applied for reducing environmental and economic effects due to use of excessive energy in order to increasing energy performance [18]. As per with TS 825 standard, energy consumption amount for building heating must be restricted and overall energy saving must be increased.
7	1	Advance Energy Metering	It is applied for supporting energy management, in order to ensure better energy saving by monitoring building system energy consumption and to catch up better opportunities.
8	2	Grid Harmonization	It is applied for rendering systems as more efficient, in order to maintain energy production and distribution systems more effective and to reduce the greenhouse gas emissions, and to increase the network reliability [7].
9	5	Renewable Energy	It is aimed here to reduce the dependency in the fossil fuel usage and to mitigate the harms on the environment and atmosphere due to the fossil fuel usage by increasing renewable energy usage [20].
10	1	Enhanced Refrigerant Management	It is aimed here, to support the compliance with the Montreal Protocol, to use the suitable fluid in the coolant systems by preventing ozone layer deployment and global warming [18].

It is assessed that only 8 points grade could be taken from credit no#6 from this section for Yalova University. There is not any existing set up for the other headings. Furthermore some point grade could be taken from #No. 7 heading, by integrating SCADA system into electric system. In addition, it might be possible for the University producing its own electricity by PV systems as in [21]. In this regard by utilizing the advantages provided by Ministry of Energy and Natural Resources, self-liquidating investments could be made and total point could also be taken from the No#9 credit point. Finally, coolant gases to be used in air handling unit could be replaced with the environmental friendly gases as per Montreal Protocol, total point could also be taken from #No.10 credit point.

Water efficiency

Reduction of water resources day by day, necessitates the more efficient use of water [22]. There is a category in LEED certification system for water efficiency. To reduce water consumption and re-use waste waters by recycling are also requirements in LEED certificate system. In the LEED certification, usage of water in more efficient manner in indoor and outdoor spaces, usage of more efficient bath tub faucets and toilet tanks are also required by considering the ecologic location of the building. In LEED certificate, water efficiency category consists of 7 credits [23]. In the scope of LEED certificate, while completing all credits, in water efficiency category, 12 credit points can be taken. Credits and credit points for water efficiency category are shown in Table 5.

Unfortunately, Yalova University is not able to score in this regard, due to lacking infra structure facilities in water efficiency. As of start-up of the specially designed rain water collection system operation for Yalova University Engineering Faculty building, under this heading, it is assessed that full point grade of (10) could be taken with the compliance of items 4, 5 and 7 [25]. Furthermore, with the usage of passive systems (non-energy consumption) in cooling towers, point

grade could also be taken from the credit no.#6. Another point grade could also be taken from the credit no.#7, by providing SCADA complied water meters in the campus buildings. In this way, all kinds of water consumption will be able to determined and recorded. In conjunction with starting the record keeping of water meters, further studies could also be initiated toward water regime definition and water consumption reduction.

Table 5. Water efficiency

No	Score	Credit	Objective
1	Prerequisite	Outdoor Water Use Reduction	It is applied for reducing outdoor water consumption reduction. There are some alternatives to reduce the outdoor water consumption. Overall water usage could be made in more efficient manner, such as; the selected plants may need less amount of irrigation water in landscapes. Rain water may be utilized for irrigation, waste water recycling could be made, by a careful selection of the floor coating materials [13].
2	Prerequisite	Indoor Water Use Reduction	Calculating the consumption amount from the water network according to the water users in the building, and planning the use of potable water as %20 or %30 less than the defined standards would help to get a higher score. In addition designing double sanitary water lines from alternative water sources such as drinking water, will help to reduce water consumption [24].
3	Prerequisite	Building-Level Water Metering	Water amount measurements must be made with required measurement equipment's during the construction stages of the building.
4	2	Reduction of outdoor water consumption	In this credit, the aim is to consume recycled grey water or rain water usage instead of potable network water in the irrigation of the plants. In the landscape arrangements due to irrigation efficiency, in case of reducing network potable water by 50% scores 1 point, not to use network potable water scores 2 points.
5	7	Reduction indoor water consumption	Indoor water consumption includes the water consumption inside the building. Selecting the fittings and fixtures from the low water consumption types, such as; selection of low flow rate shower head, provides an effect in water consumption reduction. Among the hot water distribution systems, central circulation cycles could be formed, grey water obtained from recyclable water or rain water, could be designed in order to use these waters for the needs such as toilet flush [13].
6	2	Cooling tower and process water consumption	These systems are utilized for disinfection in air conditioning water supply system, controlling corrosion, and saving in water consumption in cooling tower [19].
7	1	Water metering	This credit, as in line with this study, include installing permanent water meters at least two types or more of the water types such as irrigation, internal plumbing installation equipment, household type hot water, improved hot water, and other process waters [19]. The aim of installing these water meters is to measure water consumption to assist in determining alternative ways of water consumption.

Sustainable lands

Green buildings are environmental friendly structures and aims to minimize the energy consumption. While looking at the case from the sustainability point of view, selection of the land for building construction and land management during the construction stage, are the credits that deserve close care [26]. Sustainable

lands category is related with the effects of the intended building on the project environment and the eco-system. Land greening contains the credits such as, assessing and re-use of rain waters that are falling into project field, access means to the building, heat island effect, reduction of illumination pollution and reduction of overall pollution and wastes relevant to construction [23, 27]. In the LEED system, while complying all credits in the sustainable lands category,

a total of 12 point grades could be taken [28]. All credits and point grades in the sustainable lands category are shown in Table 6.

Since the Yalova University Campus has been designed in such a way not deteriorate the natural structure and to protect the local habitat, can take some points from credit #3, #4, and #5 and;

- i. Due to proper measures are taken with regard to release and discharge of surface

- ii. Due to provision of sufficient green fields and reduction of heat island effect, from credit #7
- iii. Due to provision of suitable illumination design, from credit #8 credit point can be taken.

It is estimated that Yalova University Campus could take 8 credit points out of 12 points from this section.

Table 6. Sustainable sites

No	Score	Credit	Objective
1	Prerequisite	Prevention of Construction Activity Pollutions	It aims to make and implement plans for prevention of construction activity pollutions in project field, any possible decadence in the area during the construction, and the cases such as erosion.
2	Prerequisite	Environmental Site Assessment	Environmental pollution around the construction environment must be controlled and assessed in terms of the human health. In order to define whether environmental pollution is evident or not around the field, first phase Environmental Field Assessment must be made as explained in the ASTM E1527-05 [29].
3	1	Site Assessment	Relevant assessments must be made in order to verify the building sustainability and exploring possible developments for the land. It has to be defined that how these assessments will affect the project after land selection. The assessment must contain the topography, hydrology, climate, flora, fauna, manpower employment, and effects on the human health [1].
4	2	Restore and protect habitat	It aims to protect the natural fields around the land or to repair some parts of the deteriorated fields due to building construction. It aims to impose minimum harm on the land environment due to project [1].
5	1	Open Fields	Open fields must be constructed for social and physical activities in order to maintain direct interaction with the nature. %30 of the total land must be provided as the open fields [28, 29].
6	3	Rain Water management	It is the credit that is used for protecting water balance of the land, controlling the water quality and disposing surface waters [1].
7	2	Reduction of Heat Island Effect	Heat islands are the fields that are warmer to a great extent than the surrounding rural areas due to human activities. The aim of this credit is to reduce the potential harm on the environment into minimum level by reducing heat island effect in the field [7].
8	1	Reduction of Lighting Pollution	This improvement must be made with considering the illumination and light proofing needs. Hence, illumination needs must be met and unnecessary environmental pollution must be avoided [1].
9	1-4	Site Master Plan	This credit includes health projects. In the Health Campus like projects, resting areas must be provided for the patients and visitors. Resting areas must be constructed outside the hospital building.
10	1	Joint Use of Facilities	The aim of this criterion is to provide benefits to the citizens by enabling direct access into open environment and natural fields. While constructing the required fields in this credit, the credit must be met for indoor air quality and outdoor air pollutants concentration strategies [29].

Regional priority

Since the LEED certification is a system of United States of America original, special local regulations has to be taken while being implemented by different countries. A wide scoped extensive study is being done in this regard by USGBC that will enable to achieve the regional integrations. Until the above mentioned study is finalized, this credit is named "Regional Priority" is considered a temporary credits.

Regional priorities are related with the relevant country and location in which the project takes place. For the concerned country that project is implemented, deserved credit points are gained by complying the special geographic priorities and environmental features that are defined by USGBC local councils [13]. 4 credits have been defined in this regard by USGBC regional councils. These credits can be cited as;

optimized energy performance, renewable energy, rain water design, consumption control, and heat island effect, framework. Each credit counts 1 point. While satisfying all credits in this category a total of 4 points can be taken.

Materials and resources (MR)

Effective use of structural materials enables the protection of natural raw materials. Therefore, during the selection of materials, effect on the environment and human health, endurance, economy, and aesthetics have to be taken into consideration [7, 23]. There are various effects of the production and consumption of the structural materials on the global and local environment. There might be some harms imposed on the environment during the extraction, processing, production, and transportation of the materials [30, 31]. One of the underlying credits on the basis of LEED

certification system is re-using of the materials. Possibility of recycling in the materials and use of local materials are the important factors in the evaluation of the materials. Selection of non-local materials causes the environmental pollution and excess energy consumption during their transportation. The review of LEED with regard to materials and resource credits; reveals the aim of minimization of energy consumption, and other adverse effects during the production, processing, transportation, maintenance, and disposal similar issues of the materials that are used during the construction of the buildings. Under

the ‘Materials and Resources’ heading, collection of recyclable materials is considered as pre-requisite. Expectations and relevant point credits under this heading is given with Table 7.

With consideration of this credit, the University Campus may take total points from the credit #3, due to light steel constructions of Energy Systems Engineering Department and Foreign Languages Department buildings, the other buildings may only take 2 credit points. Other buildings may not take credit points from the other issues.

Table 7. Materials and resources

No	Score	Credit	Objective
1	Prerequisite	Collection and storage of recyclable wastes	The aim is to reduce the wastes that are generated by householders, transported into storage areas, and disposed.
2	Prerequisite	Construction and demolition waste management planning.	The aim is to reduce the amount of wastes by recycling that are disposed in the field and in the incineration plants.
3	5	Reduction of the life cycle effects of the building	The aim is to analyse the environmental effects of the products and materials and to ensure their re-use [32].
4	2	Definition and optimization of building products-definition of environmental effects of the products	The aim is, in the Life Cycle Assessment, to maintain the usage of products that have recyclable features, with non-global warming potential, and economic with low cost.
5	2	Definition and optimization of building products-raw material resources	By selecting from ‘Approved Suppliers List’, to be published by raw materials suppliers, at least 20 different products from at least 5 different manufacturers must be procured and used. The raw materials extraction locations, must provide commitments for compliance and obedience to the long term ecologic land use, and minimization of environmental harms that are generated from production processes [33].
6	2	Definition and optimization of building products- material content	The chemicals contained in the products, is recorded into inventory with the defined method for ‘Name and Chemical Service Record No. (CASRN) and the project teams must select the products from ‘Approved Suppliers List’ in order to minimize the usage and harmful effects of the hazardous materials. This credits is used for improvement of life cycle effects of the materials and for encouraging the raw materials manufacturers to produce approved products [3, 34].
7	2	Construction and demolition wastes management	The aim is to reduce the construction and demolition wastes that are disposed in the storage areas and incineration plants, by re-gaining , re-use and recycling of the materials [35].

Indoor places and environmental quality (EQ)

For improving life quality of indoor places, indoor air quality has to be improved, and in order to maintain user health and comfort, low emission content materials have to be used [1, 36]. Providing suitable conditions for the sake human health and comfort in indoor places enhances productivity of humans, prevent stress accumulation, and affects human health in a positive manner. On the other hand, prevention of pollution and controlling indoor air quality is essential in order to improve the indoor places life quality [27]. Basic goal of the indoor places life quality system of LEED certificate is to protect the health and comfort of the house holders. Project equipment, reviews the resultant decisions on the indoor environment that are taken by monitoring indoor air quality, visual, thermal,

acoustic, comfort conditions. In the “Indoor Air Quality” category, there are two mandatory prerequisites that are imposed by LEED. One of them is “minimum indoor air quality performance” and the other one is “tobacco control”. In our days smoking is prohibited in indoor places, hence in the mandatory requirements scope, the requirements of this item have been complied. Expectations and credit points under this heading is given with Table 8 [37].

It is assessed that, about the indoor place quality Yalova University may score 2 points from each of the credits # 4, #5, and #7, may score 1 point from each of the credits #6, #8, #9 and #10, 0 point from credits #1, #11, and #12.

Table 8. Indoor environmental quality

No	Score	Credit	Objective
1	Prerequisite	Minimum indoor air quality	To achieve at least minimum indoor thermal comfort standards to satisfy occupants [38].
2	Prerequisite	Environmental tobacco smoke control	This item is applied for preventing or minimizing the exposure of building inhabitants to tobacco smokes that is received by indoor place surfaces and HVAC distribution systems.
3	Prerequisite	Minimum acoustic performance	Acoustic is accepted as prerequisite mandatory item in school buildings, it pays due care to the reduction of excessive sound severity in line with architectural material selection
4	2	Improved indoor air quality strategies	It is applied for ensuring the comfort, prosperity, and productivity of building house holders by improving indoor place air quality [39, 40].
5	3	Low emission materials	It is aimed for improving air quality, human health and productivity and reducing the chemical pollutants concentrations that might impose harms into environment.
6	1	Indoor air quality management plan in the construction	It is applied for protecting the employees and building house holders by preventing the harmful effects of the pollutants that are generated in the indoor places during the construction period.
7	2	Indoor air quality assessment	It is applied for providing better indoor air quality during the post construction and building occupancy period.
8	1	Thermal Comfort	It is applied for, improving building house holder's productivity, comfort and prosperity by providing better quality thermal comfort.
9	2	Indoor Illumination	It supports the productivity, comfort and prosperity of the building inhabitants in order to provide high quality illumination.
10	3	Daylight	It is applied for providing natural light to the building users and for reducing electric energy to be consumed for illumination.
11	1	Quality scenery	It is applied for providing beautiful scenery to the building inhabitants; it involves the house holder's relations with natural outdoor environment.
12	1	Acoustic performance	It provides, comforted working areas to encourage the prosperity productivity and communication of the house holders by an effective and improved acoustic design [28].

3. ADAPTATION OF LEED V.4 CERTIFICATION SYSTEM INTO YALOVA UNIVERSITY CASE; EVALUATION

In the evaluations, the building has been oriented according to atmospheric conditions such as sun, prevailing wind direction etc. in the design of installation and heat-water insulation systems, sustainable energy approach and ecologic features have been considered. The elements such as the ecologic features that are considered during the project design stage, solid and void volumes that are implemented on the facades, and access features are the important factors that are considered in formation of green buildings [26, 41, 42].

In this study, while assessment credits for the LEED green building are compared with each other, energy, ecology, indoor place environmental quality, environmental pollution and water issues are considered as important credits, on the other hand economy and waste issues are also taken into consideration [43].

The objective of LEED certification system; to reduce energy costs, to reduce carbon emissions, to provide more healthy environments, and to obtain high performance in the key fields of human health and

environment. Among the formed credits in LEED system; aim and requirements, and other requirements that needed for prerequisite and for credit demand are defined. The defined requirements enable the approval of assessed system via development process.

In the LEED certification system, in some cases different alternatives could be offered for different building types under a certain credits. The point grade of some credits may present different values with regard to building types. In some cases sub-headings are shown twice. The first one is prerequisite, the second one is considered as credits. While making selection, the sub-headings of LEED certificate system, is defined by giving references in the tables and figures for point scoring values [18, 43]. In the following section, we have discussed the possible scoring of Yalova University vs LEED credits.

The evaluation process took 6 months. All of the authors have participated in the evaluation process. One of evaluators of this study is International Lead Auditor (Quality environment Safety Energy and Management System). 3 of the auditors are energy system engineers and they have Certificate of LEED Green Building Certificate Systems. The last evaluator is an academician; areas of interest are energy efficiency, green buildings and he is also instructor in Energy Systems Engineering department. But still we cannot add the LEED Accredited Personnel score from

Innovation credit since none of the evaluators have accreditation. The campus scores 54/110 points (Table 9). Details are given as following;

Innovation (6 points)

In order to take full points from this category, at least one academic staff person from Yalova University, must obtain LEED accredited professional certificate and electrical energy needed for the University Campus must be provided from renewable energy sources (e.g Solar Power).

Location and transportation (16 points)

In the existing situation Campus Field takes 12 points out of 16 points. In order to take points from the credit #4, it is recommended that a pedestrian walking road by the sea side must be constructed between Campus and City Centre. By increasing the usage of green vehicles (electrical), encouraging voluntary physical activities by reducing the car park areas, protection of natural living quarters and providing suitable infra structure for bicycle usage, expected credit note could be increased as 3 points.

Energy and atmosphere (31 points)

Yalova University in this category is not able to get credit point from the "optimization of energy performance", "advance level energy measurement", "improved coolant management", "green power", and "carbon foot print" credits. In order to get more points from those credits, campus energy usage must be measured and monitored by SCADA system and alternative ways for better energy saving methods could be defined. On the other hand in order to measure energy consumption in advance level, SCADA system can be utilized. In order to improve energy performance, a general energy modelling for building and relevant simulation study for this modelling could be made. Furthermore, in order to reduce the greenhouse gases emissions, usage of renewable energy sources, e.g. construction of solar power fields over the sea could be provided, Refrigerant agreed in the Montreal Protocol can be used. For reducing the carbon footprint, energy efficient lighting, heating, cooling devices and smart network projects can be utilized.

Water efficiency (12 points)

Yalova University, in this category, has not taken any point from cooling tower water consumption and has taken low point grade from reduction of indoor places water consumption credits. In order to increase the grading of water efficiency category, pump driven passive systems could be used instead of electricity operated fan systems in cooling towers, in irrigation recycled grey water or rain water could be used instead of network potable water in the irrigation. Less water requiring plants could be preferred, water measurement could be provided for each building in order to follow up the water consumption. Higher grade can be achieved from this category, by using grey water that is obtained from recycled water or rain

water. The grey water and rain water can be utilized also in toilet flushes and similar needs.

Sustainable sites (12 points)

In this category, Yalova University has scored 7 points out of 12 points. The Campus has failed to take full point grade from rain water management, reduction of heat island effect, and reduction of illumination pollution. In order to take more point from this category, for reducing the heat island effect for providing shadows, renewable energy sources such as photovoltaics, solar heat collectors could be utilized. In order to increase the intended score, protection of regional habitat, rain water harvest system, covering the roofs with green vegetation could be advised.

Regional priority (4 points)

In this category, Yalova University could score full points due to its natural location. Yalova University's location has the potential to meet all general framework requirements, such as for optimized energy performance, renewable energy, rain water design-amount control and heat island effect. According to Pushkar (2018), by complying with; thermal comfort providing implementations, energy efficient illumination, green vegetation application on the roofs toward preventing heat island effect, and rain water harvest, 4 full score could be taken [45].

Materials and resources (13 points)

Yalova University, in this category, with regard to; life cycle effects reduction of the building, building products definition and optimization- raw materials resources, materials content, and flexible design credits has not been qualified to take any points. In order to increase the expected points from this category, waste materials that could be re-used in other fields, the building materials may have selected from bio-accumulation, having less toxic chemical content, coating materials to be used for internal and external facade of the building. Lead containing materials must not be used, building materials and products of having life cycle assessment info and life cycle assessment labels could be preferred. If the University may present some objective proofs that above specified materials are selected and used in the existing buildings, it may take some points from this section as well.

Indoor places and environmental quality (16 points)

Yalova University in this category, with regard to; thermal comfort, indoor place illumination, day light, and acoustic credits has not been qualified to take any points. In order to take full points from this credit, university may define a strategy for maintaining thermal comfort in winter months, in order to provide thermal comfort. A thermal management system that is connected to SCADA system may be utilized. High quality illumination systems may be preferred. The building design may be made in such a way to utilize the day light for a maximized period, and provide better sound insulation in the classrooms for preventing external noise. University may take some

points from this credit provided that full or partial compliance is made for the above mentioned issues.

Table 9. Evaluation of Yalova University according to LEED V4

LEED Credits	Score	LEED Score
Innovation	0	6
Location and Transportation	12	16
Energy and atmosphere	8	33
Water Efficiency	10	11
Sustainable sites	7	10
Regional priority	4	4
Materials and resources	3	13
Indoor environmental quality	10	16
Total Score	54	110

The certification systems, encourages the use of natural resources in proper and non-harming manner. In Turkey, scaling of all kind of new or existing buildings by LEED or similar certification systems has to be encouraged in order to use natural resources in right places and in suitable manner. Therefore, public institutions has to lead this implementation and to pose a good sample and publishing their annual gains in this regard every year could be useful for industrial encouragement. Besides, if the defined tax for these green buildings is kept fairly lower than the conventional buildings a promotive instrument can be gained as well.

REFERENCES

- [1]. E. Çelik, "Assesment on Green Building Rating Systems and Their Adaptations to Turkey", Graduate School of Science Engineering and Technology, ITU, Istanbul, 2009.
- [2]. Z. F. Uruk and A. K. Külünkoğlu İslamoğlu, "Comparison of Breeam, Leed and DGNB green building certification systems in a standard residence" (in Turkish), *European Journal of Science and Technology*, Issue. 15, pp. 143-154, 2019.
- [3]. C. Kurtay and S. Jahed, "Comparison of design criteria about energy in healthcare building according to BREEAM and LEED certification systems", in *5th International Symposium on Innovative Technologies in Engineering and Science*, 29-30 September 2017, pp. 965-974, 2017.
- [4]. E. Gülşeker, "Evaluation of basic education building in LEED certification system: Konya case" (in Turkish), Graduate School of Science and Engineering, Necmettin Erbakan University, Konya, 2018.
- [5]. G. Utkutuğ, "Examples of architecture and high performance green buildings towards a sustainable future" (In Turkish), In *X. Ulusal Tesisat Mühendisliği Kongresi*, 13-16 April, 2011, pp. 1517-1538.
- [6]. O. Kazancı, "Strategic analysis of green building industry using pestel approach" (In Turkish)", Graduate School of Science and Engineering, Bulent Ecevit University, Zonguldak, 2017.
- [7]. N. C. Arslan, "An approach for design process of green buildings projects: Leed V4 certification process model" (In Turkish), Graduate School of Science Engineering and Technology, ITU, Istanbul, 2015.
- [8]. D. İ. Yılmaz, "Developing a sustainable construction manual for contractor corporations and analyzing the difficulties encountered in Leed applications" (In Turkish), Graduate School of Science Engineering and Technology, ITU, Istanbul, 2014.
- [9]. S. Akca, "A study on measuring the consistency of LEED green building evaluation system criteria at the level of design scales, conceptual leveling and resource use" (In Turkish), Graduate School of Science and Engineering, YTU, Istanbul, 2011.
- [10]. "LEED V4.1 Building design and construction", U.S. Green Building Council, 2020.
- [11]. B. F. Babilolyaei, "Green school design criteria, international LEED assessment certificate and application" (In Turkish), Graduate School Of Natural And Applied Sciences Gazi University, Ankara, 2012.
- [12]. K. S. Kayıhan and S. Tönük, "Elementary School Buildings with the Direction of Sustainability Awareness Construction" (In Turkish), *Politeknik Dergisi*, Vol. 14 (2), pp. 163-171, 2011.
- [13]. K. Çelik, "LEED certification systems and evaluation of their implementation in Turkey" (In Turkish), Institute of Graduate Education IKU, Istanbul, 2016.
- [14]. A. Hamzakadi and F. I. Turkdogan, "Integrated study of building information modeling (BIM) with green buildings for a sustainable environment", *Environmental Research & Technology*, Vol. 2 (1), pp. 46-54, 2019.
- [15]. N. Cambaz, E. G. Taskin, and A. Ruzgar, "Life cycle assessment of an office: Carbon footprint of an office staff", *Environmental Research & Technology*, Vol. 1 (4), pp. 34-39, 2018.
- [16]. G. Selçuk, "Formation of the contract documents of the new construction and major renovation projects projected to get the Leed certificate" (In Turkish), Graduate School of Science Engineering and Technology; ITU; Istanbul, 2010.
- [17]. E. Namlı and M. Yücel, "Energy performance classes prediction of concrete buildings with artificial intelligence models" (In Turkish), *Uludağ University Journal of The Faculty of Engineering*, Vol. 22 (3), pp. 325-346, 2018.
- [18]. A. P. Gürgün, "2009 LEED-NC certified evaluation of the energy and atmosphere of the building loan in Turkey", *Politeknik Dergisi*, Vol. 20 (2), pp. 383-392, 2017.
- [19]. A. Aytekin, "Investigation of an existing building for LEED certificate: credit opportunities and suggestions" (In Turkish), Institute of Pure and Applied Sciences, Marmara University, Istanbul, 2019.
- [20]. İ. H. Orhan and L. G. Kaya, "A review of LEED certificated green buildings and indoor environmental quality" (In Turkish), *Mehmet Akif Ersoy Üniversitesi Fen Bilimleri Enstitüsü Dergisi*, Vol. 28 (1), pp. 18-28, 2016.

- [21]. I. Anyanele, O. Isamotu, and B. Akinde, "Barriers and opportunities to operate photovoltaic systems in commercial buildings in Nigeria", *Environmental Research & Technology*, Vol. 2 (2), pp. 19–25, 2019.
- [22]. N. Dogan-Saglamtimur and F. Ciner, "A guide to theory and practice of drinking water: PURE-H₂O approaches", *Environmental Research & Technology*, Vol. 2 (3), pp. 130–140, 2019.
- [23]. USGBC, "LEED v4- Reference Guide for Building Design And Construction", U.S. Green Building Council. 2013.
- [24]. A. Öztürk, "Analysis of green building certificationsystems" (In Turkish), Energy Institute, Istanbul Technical University, Istanbul, 2015.
- [25]. E. Kucukkaya, A. Kelesoglu, H. Gunaydin, G. A. Kilic, and U. Unver, "Design of a passive rainwater harvesting system with green building approach", *International Journal of Sustainable Energy*, pp. 1–13, 2020.
- [26]. S. B. Erdede and S. Bektaş, "Land management benchmark proposal for a national green building certification system" (In Turkish), In *2nd International Symposium on Innovative Approaches in Scientific Studies* 30 Nov- 2 Dec 2018, Vol. 1, pp. 182–187.
- [27]. D. Zinzade, "An investigation of sustainability formulating the high rise buildings" (In Turkish), Graduate School of Science Engineering and Technology, ITU, Istanbul, 2010.
- [28]. E. Y. Gürez, "The effect of sustainability concept on spacing measurement parameters; Sustainable green hotel illustration" (In Turkish), Institute of Graduate Education IKU, Istanbul, 2019.
- [29]. S. Jahed, "Comparison of design criteria in healthcare building according to international BREEAM and LEED Certification Systems" (In Turkish), Graduate School of Natural and Applied Sciences Gazi University, Ankara, 2018.
- [30]. B. Görgün, "Evaluating Leed and Breaam energy efficiency criteria to form a roadmap for Turkish green building assessment system" (In Turkish), Graduate School of Science Engineering and Technology, ITU, Istanbul, 2012.
- [31]. H. Aksel and İ. Çetiner, "Construction waste management practices on-sites: A case study of Istanbul city", *Environmental Research & Technology*, Vol. 3 (2), pp. 50–63, 2020.
- [32]. B. Kobaş, "Evaluating BREEAM and LEED's building material credits in order to form a roadmap for Turkish green building assessment system" (In Turkish), Graduate School of Science Engineering and Technology, ITU, Istanbul, 2011.
- [33]. G. Akgül, "The assesment of project stakeholders' sustainability perceptions in turkish construction industry" (In Turkish), Graduate School of Science Engineering and Technology, ITU, Istanbul, 2014.
- [34]. G. Y. Işıldar and A. Gökbayrak, "Evaluation of green building criteria according to development level of countries" (In Turkish), *Ömer Halisdemir Üniversitesi Mühendislik Bilimleri Dergisi*, Vol. 7 (1), pp. 46–57, 2018.
- [35]. E. Özdemir, "Selection of building materials and requirements for Turkey in terms of legislation and green building certification" (In Turkish), Graduate School of Science Engineering and Technology, ITU, Istanbul, 2012.
- [36]. Ö. Kaynakli, Ü. Ünver, M. Kiliç, and R. Yamankaradeniz, "Thermal comfort zones according to the steady-state energy balance model" (In Turkish), *Pamukkale Üniveritesi Mühendislik Fakültesi Dergisi*, Vol. 9 (1), pp. 23–30, 2003.
- [37]. H. O. Kaya, "Examination and proposals on Turkish applications of Leed and Breeam as criteria based assessment and certification methods" (In Turkish), Graduate School of Natural and Applied Sciences 9 Eylül University, Izmir, 2012.
- [38]. E. G. Yetkin, "The comparative analysis of LEED, BREEAM and DGNB systems to determine the green building certification systems energy criteria in the scope of existing buildings" (In Turkish), Graduate School of Science Engineering and Technology, ITU, Istanbul, 2014.
- [39]. O. Kaynakli, U. Unver, and M. Kilic, "Evaluating thermal environments for sitting and standing posture", *International Communications in Heat and Mass Transfer*, Vol. 30 (8), pp. 1179–1188, 2003.
- [40]. Y. Ajami, "Evaluation of occupant perception of IEQ in LEED platin certified office buildings: an office sample in Istanbul" (In Turkish), Graduate School of Natural and Applied Sciences, BAU, Istanbul, 2018.
- [41]. S. B. Erdede, B. Erdede, and S. Bektaş, "Evaluation of sustainable green buildings and certification systems" (In Turkish In 5. Uzaktan Algılama - CBS Sempozyumu (UZAL-CBS 2014, 14-17 October pp. 14–17, 2014,
- [42]. M. Anbarcı, Ö. Giran, and İ. H. Demir, "International green building certification systems and building energy efficiency implementation in Turkey" (In Turkish), *NWSA-Engineering Sciences*, 1A0309, Vol. 7 (1), pp. 368–383, 2012.
- [43]. R. Gurbuz and L. Aridag, "The comparison of criteria asla and leed for sustainable landscape design", *Beykent University Journal of Science and Engineering*, Vol. 6 (2), pp. 77–92, 2013.
- [44]. L. O. Uğur and N. Leblebici, "Investigation of the effects of energy and water saving benefits on property value in LEED certified green buildings", *Teknik Dergi*, Vol. 30 (1), pp. 8753–8776, 2019.
- [45]. S. Pushkar, "The effect of regional priority points on the performance of LEED 2009 certified buildings in Turkey, Spain, and Italy", *Sustainability (Switzerland)*, Vol. 10 (10), pp. 1–19, 2018.



RESEARCH ARTICLE

Reducing greenhouse gas emissions from solid wastes management in north eastern Nigeria: An integrated solid waste management approach

Richard Mshelia^{1,*} , Abubakar Danjuma Maiwada² 

¹Department of Mechanical Engineering, Bayero University, Kano, PMB 3011, NIGERIA

²Centre for Renewable Energy Research, Bayero University Kano, PMB 3011 NIGERIA

ABSTRACT

The solid waste management (SWM) sector is responsible for the emission of about 5% of all global greenhouse gas (GHG) emissions. In developing countries where the sector is less organised, the carbon footprint of the sector is much higher, so also is the potential for reducing these emissions. This study assessed the potential for reducing the GHGs emission from the SWM sector in northeastern Nigeria. Based on literature study, it was found that open dumping in dumpsites and unsanitary landfills is a solid waste disposal method in the region. It was estimated that 350,822.80 tonnes of MSW is disposed of in dumpsites annually, and anaerobically decomposes 403373.25 tonnes of carbon dioxide equivalent (tCO_{2e}) into the atmosphere. However, when an integrated solid waste management (ISWM) system, which comprises composting of organic materials, recycling of paper, glass and metals and incineration of garbage, is employed, a reduction in the region's SWM carbon footprint of up to 99.5% is attainable. It was also found that composting is the ISWM element with the highest carbon sink potential, this is because of the high organic matter in the region's wastes. The study suggests public-private partnership so as to be able to reform the SWM sector in the region and make it more sustainable.

Keywords: Carbon footprint, composting, greenhouse gases, incineration, integrated solid waste management, municipal solid waste management

1. INTRODUCTION

Global warming has been on the front burner as the greatest existential threat to humans pre -Covid 19. Its attendant consequences such as loss of biodiversity, floods, drought and submerging of islands are evidence and testament to the threat it poses. The anthropogenic emission of greenhouse gases (GHGs) has been identified as the major contributor to the accelerated warming of the globe [1], [2]. Even though the contribution of the solid waste management (SWM) industry to the global emission of GHGs is just about 5% [3], the potential for further reducing the carbon footprint of the industry is huge, particularly in developing countries where the industry is somewhat informal, less regulated and structured.

The practice of open dumping in unsanitary landfills and open burning is pervasive in developing countries, Nigeria is not an exception [4], this practice has been

found to have higher carbon footprint when compared to other SWM techniques such as composting, incineration with energy recovery and anaerobic digestion [5]. This is because of the large quantities of methane that is emitted from the decomposition of the organic fraction of solid wastes, keeping in mind that methane has a high global warming potential - 28 times more than carbon dioxide [6], this makes these methods of solid waste disposal (SWD) unsustainable thus amplifying the need for a cleaner and more sustainable SWM technique.

Integrated solid waste management (ISWM) is widely seen in the waste management industry as the most sustainable SWM method, researchers see it as the solution to achieving a relatively clean SWM industry [7]-[9]. ISWM is a multidimensional approach to SWM, it is the use of a range of different waste management options rather than a single option [10]. The concept of ISWM emerged from the realisation that technical

Corresponding Author: rbmshelia@gmail.com (Richard Balthe Mshelia)

Received 7 December 2020; Received in revised form 30 December 2020; Accepted 4 January 2021

Available Online 15 January 2021

Doi: <https://doi.org/10.35208/ert.837071>

© Yildiz Technical University, Environmental Engineering Department. All rights reserved.

solutions alone do not adequately address the complex issue of SWM and that a single choice of approach/method for waste management is frequently unsatisfactory, inadequate, and not economical [10]. ISWM approach to waste management encapsulates the hierarchical order of waste management which priorities waste prevention and reduction in quantities of waste generated over the various existing disposal methods. It is not a strict technical approach to waste handling rather a holistic approach to SWM in an integrated manner.

The various waste management techniques that combine to form ISWM are individually known as its elements. Elements that constitute a typical ISWM model in order of importance are: waste prevention; waste reduction/minimization; re-use of materials and products; material recovery from waste streams (recycling); composting to produce manures; incineration with energy recovery; incineration without energy recovery and disposal in landfills [11]. This hierarchical order is based on the 3Rs of SWM (reduce, reuse and recycle) [12].

The northeast geopolitical region of Nigeria comprises six states: Adamawa; Bauchi; Borno; Gombe; Taraba and Yobe. The region lies within longitude 9.9992 and 13.1520 and latitude 11.8846 and 7.9867 [13]–[15]. As at 2016, the region had an estimated population of 26,263,865 [16]. Open dumping of MSW in unsanitary landfills, dumpsites and sometimes occasional open burning is the SWD method practiced across the region [17]. The chain of SWD in the region essentially entails disposing of wastes at designated waste collection points, the state waste collection agencies routinely collecting the waste from these points and disposing them off at unsanitary landfills and dumpsites. The little form of recycling that exists in the SWM chain in the region is the collection of metal scraps by scavengers from the waste collection points or at the dumpsites.

An estimated 350,822.80 tonnes of MSW is generated on an annual basis in the region [17]. Due to similarity in the culture, traditions, vegetation and climate of the region, there is little variation in the composition of the waste generated in the cities of the region. This makes the formulation of a common ISWM model for the entire region possible. This study seeks to assess the potential role of an ISWM system in reducing the GHGs

emission from the SWM sector in North-eastern Nigeria.

2. MATERIALS AND METHODS

To estimate the potential reduction in the quantity of GHGs emission an ISWM approach can bring to the SWM sector in north eastern Nigeria, an extensive literature review was undertaken to first determine the region’s current carbon footprint. The composition of the MSW generated in the region was considered so as to determine the ISWM element most suitable for each category of waste generated in the city. Lifecycle carbon footprint approach was used to estimate the footprint for each of the elements of the ISWM system. Standard lifecycle assessment data for each of these elements was obtained from literature.

The elements considered for the formulation of the ISWM model are recycling, composting, and incineration with energy recovery and landfilling of inert materials. These SWD methods were selected to be the elements of the region’s ISWM system based on the composition of the waste being generated there. The proposed treatment of MSW generated in the region involves composting of organic materials, recycling of glass, papers and metals, incineration of garbage with recovery of electricity and landfilling of inert materials. Even though reduction in waste generation and reuse of materials are essential elements of an ISWM system, they are excluded from this study since the exact GHGs emissions avoided from these elements cannot be ascertained.

To estimate the emission from the region, the following assumptions were made in line with precedence seen in literature:

1. All glass materials are recyclable.
2. All papers are high grade deinked paper.
3. All metals in the region’s MSW are aluminium.
4. The humus obtained from composting is used as a substitute for chemical fertilizer.

Data used for estimating the carbon footprint for each element of the ISWM using the lifecycle assessment (LCA) approach was obtained from literature, and presented in Table 1.

Table 1. ISWM elements and their corresponding LCA carbon footprints

ISWM Element	Carbon Footprint
Recycling of Glass	1.25tCO ₂ eq/tonne of glass [18]
Recycling of Paper	212kgCO ₂ eq/tonne of waste [19]
Recycling of Aluminium	3.05tCO ₂ eq/tonne of Aluminium [20]
Composting of Organic Waste	-690kgC/tonne of Composted Waste [21]
Incineration with electricity recovery	-0.179tCO ₂ eq/tonne of incinerated waste [22]

The framework for the ISWM system is seen in Figure 1, this involves the recycling of recyclable materials, composting of organic materials, incineration of garbage and landfilling of inert materials.

In determining the emission from current practice of open dumping so as to be able to estimate the

reduction in GHGs emissions that the ISWM system brings. IPCC’s waste model shown in equations 1-3 was used [23]. The composition of the waste generated in the region presented in Table 2 was also used for the estimations [17].

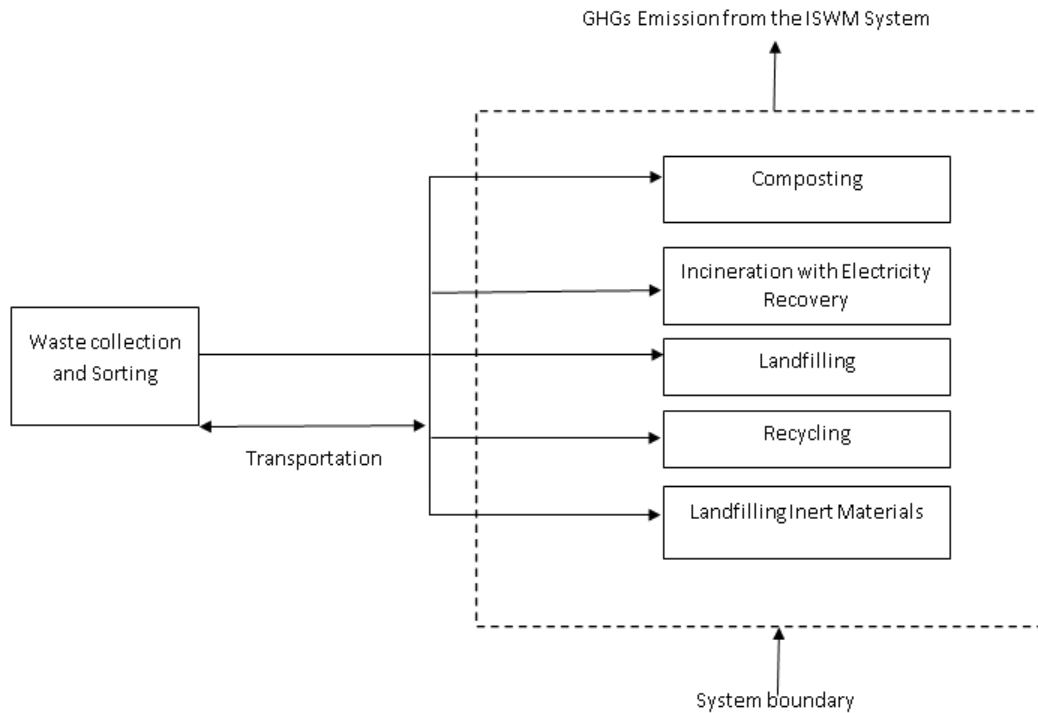


Fig 1. Framework for integrated solid waste management model

Table 2. Composition of municipal solid waste in northeastern Nigeria

Category	% Weight
Food	6.3
Garden Waste	19.0
Plastics	24.4
Paper	8.6
Textiles	2.8
Leather/Rubber	15.3
Glass	4.6
Metal	5.9
Inert Materials	13.2

$$CH_4 \text{ Emissions} = MSW_x \times L_o \times (1 - f_{rec}) \times (1 - OX) \quad (1)$$

Where,

MSW_x = Mass of solid waste sent to landfill in inventory year (metric tonnes)

L_o = Methane generation potential (m^3 /tonne)

f_{rec} = Fraction of methane recovered at the landfill (flared or energy recovery)

OX = Oxidation factor (0.1 for managed sites, 0 for unmanaged sites)

$$L_o = MCF \times DOC \times DOC_F \times F \times \frac{16}{12} \quad (2)$$

Where,

$MCF = 0.6$ for dumpsites and unmanaged landfills

DOC = Fraction of Degradable organic carbon (tonnes C/tonnes waste)

DOC_F = Fraction of DOC that ultimately degrades (0.6).

F = Fraction of methane in landfill gas (0.5)

$\frac{16}{12}$ = Stoichiometric ratio between methane and carbon

$$DOC = (0.15 \times A) + (0.2 \times B) + (0.4 \times C) + (0.43 \times D) + (0.24 \times E) \quad (3)$$

A = Fraction of solid waste that is food

B = Fraction of solid waste that is garden waste and other plant debris

C = Fraction of solid waste that is paper

D = Fraction of solid waste that is wood

E = Fraction of solid waste that is textiles

Global warming Factor of $CH_4 = 28$ [6]

3. RESULTS AND DISCUSSION

It was found that on average, 350,822.80 tonnes of MSW is disposed of at dumpsites and unsanitary landfills in the region. The composition of which includes 21,984.90 tonnes of food wastes; 66,773.27 tonnes of garden and yard wastes; 30,112.29 tonnes of paper wastes; 16,137.85 tonnes of glass; 85,483.82 tonnes of plastics; 9,823.04 tonnes of textile materials; 53,734.36 tonnes of leather and rubber and 46,133.20 tonnes of inert materials. Given this profile of MSW generated and disposed of in dumpsites in the region. It was estimated using IPCC's model that when the waste anaerobically decomposes in these dumpsites and unsanitary landfills, 403,373.25tCO₂e is emitted into the atmosphere on an annual basis. This means for each tonne of MSW disposed of in the region, 1.15tCO₂e

is emitted into the atmosphere from its natural decomposition.

If the proposed ISWM model is implemented, it is expected that the emission of GHGs from the management of MSW in the region will reduce. To ascertain this potential reduction, examining the system based on each element of the ISWM model is the logical thing to do.

It has been established by an earlier research that the food waste generated in the country and the atmospheric condition are suitable for composting [24]. And since open windrow composting is what is to be used as the preferred composting method, little technical know-how is required. For composting as an element of the ISWM model, it was found that when the 88,758.17 tonnes of garden and food wastes disposed of in dumpsites in the region on an annual basis is rather composted in an open windrow and the resultant compost is used in place of inorganic fertilizer, a net reduction of GHGs emission of

61,243.14tCO₂e will be attained annually. For recycling, it was estimated that recycling the 67,065.63 tonnes of metals, glass and papers generated in the region will be responsible for the emission of 90,043.35tCO₂e. With each of the three components (metals, glass and papers) responsible for 63,487.23tCO₂, 20,172.31 tCO₂ and 6,383.81 tCO₂ respectively. It was estimated that when the garbage component of the MSW is incinerated and the electricity generated from it substitutes grid electricity, a reduction in carbon emission of -26,678.38tCO₂ can be attained.

Table 3 shows the net carbon footprint for each of the components of the waste generated in the region. Likewise, Figure 2 graphically shows the carbon footprint of each of the elements of the proposed ISWM model.

Table 3. Carbon footprint for each component of municipal solid waste

MSW Component	Carbon Footprint (tCO ₂ eq/yr)
Recycling of Glass	20,172.31
Recycling of Paper	6,383.81
Recycling of Metals	63,487.23
Composting of Food Waste	-15,169.58
Composting of Yard Waste	-46,073.56
Incineration of Plastics	-15,301.60
Incineration of Textiles	-1,758.32
Incineration of Leather/rubber	-9,618.45
Total	2,121.83

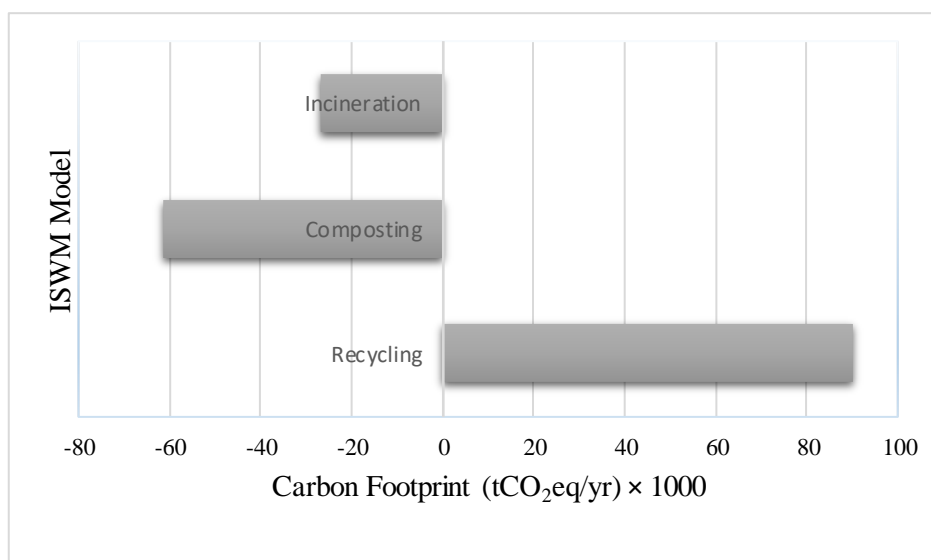


Fig 2. Carbon footprint of each integrated solid waste management element

It can be seen from Figure 2 that in the ISWM model, composting is the largest carbon sink. Giving that 25.3% (88,758.17 tonnes) of the waste disposed of at dumpsites and unsanitary landfills in the region are organic wastes. It is not surprising that a reduction in GHGs emission of such magnitude is attainable from

composting of organic wastes and usage of the compost in place of inorganic fertilizer. It is worthy to mention that the low quantity of food waste in the general volume of waste generated in the region is due to the generic manner of dealing with food waste in Nigeria, that is the feeding of household animals with food remnants/waste instead of trashing, this explains the

low quantity of food waste reaching dumpsites in the region and the country at large [25]. It can be seen recycling has the highest carbon footprint of all the ISWM elements, recycling is usually an energy intensive process even though not as intensive as production from virgin materials [26], [27].

It is estimated that if the proposed ISWM model is implemented in the region, the net GHGs emission from the regions MSW will be only 2,121.83tCO_{2e} as seen in Table 3, this is a reduction of 99.5%. By all standards, attaining a reduction in GHGs emission of up to 99.5% is remarkable. Juxtaposing this result with those of studies done in other places, it can be seen that the potential for reduction in the emission of GHGs in Northeastern Nigeria is remarkable. Maalouf and El-Fadel [28] developed an ISWM model and used data from countries around the world to test it, the researchers found that the potential for reduction in carbon footprint ranges from 24 to 95%. Sandulescu [2] found that implementing a particular ISWM model in Bucharest the capital of Romania would bring about a 5% reduction in the city's GHGs emission from SWM. In the same vein, Sun et al., [29] carried out a comparative study of Japan and China, the researchers found that if the ISWM model they developed is implemented strictly in the two countries, there is a potential for reduction in emission of GHGs from the SWM sector of up to 181.37 million tCO_{2e} and 96.76 million tonnes respectively. It has been noted that the potential for reduction of carbon footprint of the SWM sector is more in developing countries where the sector is somewhat less organised and regulated. This buttresses the point made by Abu Qdais et al., [30] where the researchers stated that "the room for reduction of GHGs is greater in developing countries". Another reason for this aside the less organised nature of the SWM sector in developing countries is the lack of awareness about the need for responsible and climate conscious usage of material and resources among the general populace.

4. CONCLUSIONS

Although it is generally assumed that the contribution of developing economies to global anthropogenic GHGs emission is minute, their rapid population and economic growth is set to make their contribution significant if no action is taken to make resource and material utilisation sustainable in these regions. The SWM sector is one of the key areas in which sustainability needs to be encouraged in developing countries due to the fast growing population and economies in these regions coupled with the adoption of western lifestyle which encourages high consumption and waste generation.

This study examined the possibility of reducing the carbon footprint of the SWM sector of Nigeria's northeastern region by adoption of an ISWM model. Using the LCA approach, it was found that the current annual quantity of MSW disposed of in dumpsites is responsible for the emission of 403,373.25tCO_{2e}. It was estimated that if an ISWM model which constitutes recycling, composting and incineration is implemented in the region, there will be a reduction of 99.5% in the

emission of GHGs from the disposal component of SWM chain in the region.

Composting was found to be the element of the ISWM model with the highest carbon sink, this is because of the high organic matter content of the waste generated in the region. To successfully implement the proposed model or any other advanced SWM scheme, a number of behavioural and structural changes need to be undertaken. One of the steps to achieving such changes is by enlightening the populace about the implications of excessive waste generation and the need for conscious materials usage and consequently reduction in waste generation. Another is the importance of reusing items that can be reused (items like polythene bags) instead of discarding them after single use. Importantly, the need for waste segregation from source (household and businesses), this reduces the cost, energy and consequently the carbon footprint of the SWM chain. For structural changes, proximity principle which advocates for the processing (sorting, recycling, composting, landfilling and/or incineration) of waste as close to its source as possible should be adopted, this will reduce the carbon footprint associated with the transportation leg of the SWM chain.

Overhauling the SWM sector in the region which is largely government dominated is capital intensive, the current economic realities of the country will not allow governments in the region to undertake such audacious project, as such it is suggested that government partners with investors who can make the necessary investment into the system so as to be able to achieve sustainability in the sector.

REFERENCES

- [1]. F. A. Armah, G. T. Yengoh, M. Ung, I. Luginaah, R. Chuenpagdee, and G. Campbell, "The unusual suspects? Perception of underlying causes of anthropogenic climate change in coastal communities in Cambodia and Tanzania," *Journal of Environmental Planning and Management*, Vol. 60 (12) pp. 2150–2173, 2017.
- [2]. E. Sandulescu, "The contribution of waste management to the reduction of greenhouse gas emissions with applications in the city of Bucharest," *Waste Management Resources*, Vol. 1 (22) pp. 413–426, 2004.
- [3]. C. Maria, J. Góis, and A. Leitão, "Challenges and perspectives of greenhouse gases emissions from municipal solid waste management in Angola," *Energy Reports*, Vol. 10, (1) pp. 22–25, 2019.
- [4]. C. C. Ike, C. C. Ezeibe, S. C. Anijiofor, and N. N. Daud, "Solid Waste Management in Nigeria: Problems, Prospects, and Policies," *Journal Solid Waste Technology Management*, Vol. 44 (2), pp. 163–172, 2018.
- [5]. R. B. Mshelia and M. C. Onuigbo, "Simulation of greenhouse gases emission from different solid waste management practices in Gombe, Gombe state, Nigeria," *University of Wah Journal of Science and Technology*, Vol. 4, pp. 9-14, 2020.

- [6]. R. B. Mshelia, I. S. Diso, and T. Y. Jibatswen, "Assessment of greenhouse gases emission sources in a typical Nigerian university campus : case study of Bayero university , Kano new campus," *Bayero Journal of Engineering Technology*, Vol. 15 (2) pp. 30–37, 2020.
- [7]. X. Zeng, Q. Sun, B. Huo, H. Wan, and C. Jing, "Integrated solid waste management under global warming," *Open Waste Management Journal*, Vol. 3 (1) pp. 13–17, 2010.
- [8]. M. S. Al Ansari, "Improving solid waste management in Gulf Co-operation Council States: Developing Integrated Plans to Achieve Reduction in Greenhouse Gases," *Mod. Appl. Sci.*, vol. 6 (2) pp. 60–68, 2012.
- [9]. M. A. Memon, "Integrated solid waste management based on the 3R approach," *Sustainable Solid Waste Management*, Vol. 12, pp. 30–40, 2012.
- [10]. P. Gwom, "Planning for municipal solid waste management: the case of Greater Jos, Nigeria," PhD Thesis, Heriot-Watt University, March 2016.
- [11]. J. Jibril, I. Sipan, and J. Lawal, "3R's critical success factor for integrated solid waste management in higher educational institutions," *OIDA International Journal of Sustainable Development*, Vol. 5 (10) pp. 109–120, 2012.
- [12]. R. Girling, *Rubbish! Dirt on Our Hands and Crises Ahead*. Transworld Publishers Ltd, London, England. 2005.
- [13]. K. A. Salako, "Depth to basement determination using Source Parameter Imaging (SPI) of aeromagnetic data: An application to upper Benue Trough and Borno Basin, Northeast, Nigeria," *Academic Research International*, Vol. 5 (3) pp. 74–86, 2014.
- [14]. M. O. Isikwue and A. Chikezie, "Quality assessment of various sachet water brands marketed in Bauchi metropolis of Nigeria," *International Journal of Advanced Engineering Technology*, Vol. 6, (6) pp. 2489–2495, 2014.
- [15]. G. O. Onogwu, I. A. Audu, and F. O. Igbodor, "Factors influencing agricultural productivity of smallholder farmers in Taraba State, Nigeria," *International Journal of Agricultural Innovation and Research*, vol. 6, no. 1, pp. 114–118, 2017.
- [16]. National Bureau of Statistics, "Population," 2020. Available: [https://nigerianstat.gov.ng/elibrary?queries\[search\]=population](https://nigerianstat.gov.ng/elibrary?queries[search]=population). (Accessed: 01-Jul-2020).
- [17]. R. B. Mshelia, "Evaluation of greenhouse gas emissions from solid waste management practices in state capitals of north eastern Nigeria," *Journal of Engineering Studies and Research*, vol. 26 (4) pp. 40-46, 2020.
- [18]. A. Navarro, R. Puig, and F. P. Palmer, "Product vs corporate carbon footprint: Some methodological issues. A case study and review on the wine sector," *Sci. Total Environ.*, Vol. 581, pp. 722–733, 2017.
- [19]. ASPAPEL, "Contribucion Inicial Del Sector Papelero A La Reduccion De Las Emision CO2En Espana," Madrid, 2003.
- [20]. BSI, "Product Carbon Footprinting for Beginners," 2014. Available: <https://www.bsigroup.com/LocalFiles/en-GB/standards/BSI-sustainability-guide-product-carbon-footprinting-for-beginners-UK-EN.pdf>. (Accessed 28-July, 2020).
- [21]. S. E. Vergara and W. L. Silver, "Greenhouse gas emissions from windrow composting of organic wastes: Patterns and emissions factors," *Environmental Resources Letters*, Vol. 14 (12) p. 124027, 2019.
- [22]. H. Jeswani, R. Smith, and A. Azapagic, "Energy from waste: carbon footprint of incineration and landfill biogas in the UK," *Int. J. Life Cycle Assess.*, Vol. 18 (1), pp. 218–229, 2013.
- [23]. IPCC, IPCC Guidelines for National Greenhouse Gas Inventories. Cambridge University Press, New York, USA. 2006.
- [24]. D. Olukanni and D. Aremu, "Provisional evaluation of composting as priority option for sustainable waste management in South-West Nigeria," *Journal of Pollution*, Vol. 3(3) pp. 417-428, 2017.
- [25]. I. G. Adeyemi and O. K. Adeyemo, "Waste management practices at the Bodija abattoir, Nigeria," *International Journal of Environmental Studies*, vol. 64, no. 1, pp. 71–82, 2007.
- [26]. H. Hao, Q. Qiao, Z. Liu, and F. Zhao, "Impact of recycling on energy consumption and greenhouse gas emissions from electric vehicle production: The China 2025 case," *Resour. Conserv. Recycl.*, Vol. 122, pp. 114–125, 2017.
- [27]. J. Jeswiet and A. Szekeres, "Energy consumption in mining comminution," *Procedia CIRP*, Vol. 48, pp. 140–145, 2016.
- [28]. A. Maalouf and M. El-Fadel, "Carbon footprint of integrated waste management systems with implications of food waste diversion into the wastewater stream," *Resource Conservation and Recycling*, Vol. 133, pp. 263–277, 2018.
- [29]. L. Sun, Z. Li, M. Fujii, Y. Hijioka, and T. Fujita, "Carbon footprint assessment for the waste management sector: A comparative analysis of China and Japan," *Front. Energy*, Vol. 12, (3) pp. 400–410, 2018.
- [30]. H. Abu Qdais, C. Wuensch, C. Dornack, and A. Nassour, "The role of solid waste composting in mitigating climate change in Jordan," *Waste Management Resources*, Vol. 37 (8) pp. 833–842, 2019.



RESEARCH ARTICLE

Isotherm, kinetic and thermodynamic studies of methylene blue adsorption using *Leucaena leucocephala*

Ali Rıza Kul¹ , Adnan Aldemir^{2,*} 

¹Van Yüzüncü Yıl University, Faculty of Science, Chemistry Department, 65080, Van, TURKEY

²Van Yüzüncü Yıl University, Faculty of Engineering, Chemical Engineering Department, 65080, Van, TURKEY

ABSTRACT

In recent years, great focused has been placed on the development of low-cost adsorbents to be used for applications regarding treatment of wastewater. In this study, *Leucaena leucocephala* peel (LLP) was used for adsorption of methylene blue from aqueous solutions. The experiments were conducted at seven concentrations (15, 30, 45, 60, 75, 90, 105 mg L⁻¹) and three temperatures (298, 308, 318 K). The obtained data were applied to adsorption isotherm, kinetic and thermodynamic calculations. The results showed that Freundlich isotherm was more appropriate compared to Langmuir and Temkin isotherms. The kinetic results indicated that the process fitted pseudo second order model with higher R² values compared to pseudo first order and intra-particle diffusion models. Gibbs free energy, enthalpy and entropy values were calculated for 298 K as 2.776 kJ mol⁻¹, 6.262 kJ mol⁻¹ and 11.699 J mol⁻¹, respectively.

Keywords: Adsorption, isotherm, kinetic, *Leucaena leucocephala*, methylene blue, thermodynamic

1. INTRODUCTION

Dyes are used in variety of manufacturing such as textile, plastics, pharmaceutical, paper, printing, rubber, leather, paint, cosmetic, food and pulp [1-3]. Recently, worldwide attention has been brought to the fact that dyes, the toxic effects of which threaten the lives of humans, animals and the environment, are directly discharged into the environment [4]. Various methods have been designed to treat dye wastewater, such as adsorption [5-10], oxidation [11-12], membrane separation [13-14], electrochemical techniques [15-16] and ion exchange [17]. However, none of these methods have been successful in completely removing dyes from wastewater and all have limitations including high cost, secondary pollutant generation and poor removal efficiency. Among the different methods, adsorption has been determined as effective, low-cost and simplest process for wastewater treatment [18-20].

Activated carbon is widely used and it is the most effective adsorbent in the treatment of dyes in wastewater. However, the manufacturing and regeneration costs of activated carbon are high which is remain a major drawback [21-23]. Studies in the

literature have used various low-cost adsorbents such as Barbados shells [24], palm kernel fiber [25], cacti [26], sawdust [27], Eichhorria crassipes roots [28]. But the adsorption capacity of such adsorbents is generally quite low and it has become important to discover more cost effective, eco-friendly, efficient, renewable and abundant materials to be used as adsorbents.

Adsorption onto biochars made from land-plant residues including sawdust, weeds, corn straws, and hickory wood, has been determined as high efficient and eco-friendly option to removal dyes from wastewater [29]. Some studies have evaluated for remove capacity of dye through interactions between the dye molecule and functional groups on the surface of these adsorbents. As most land-plant residues are discarded as waste, their use as low-cost and eco-friendly adsorbents is a promising alternative.

The aim of this study was to investigate dye removal ability of *Leucaena leucocephala* peels (LLP) as a cost effective adsorbent on MB in aqueous solutions containing. MB was selected as the adsorbate as it has been found to adversely affect human health by causing different diseases [30]. Within the scope of

Corresponding Author: adnanaldemir@yyu.edu.tr (Adnan Aldemir)

Received 13 October 2020; Received in revised form 11 January 2021; Accepted 11 January 2021

Available Online 26 January 2021

Doi: <https://doi.org/10.35208/ert.810226>

© Yildiz Technical University, Environmental Engineering Department. All rights reserved.

this research, isotherm, kinetic and thermodynamic studies of the MB adsorption onto LLP was conducted.

2. MATERIALS AND METHOD

2.1. Materials

In this study, methylene blue was used as the adsorbate which formula is $C_{16}H_{18}N_3SCl_3 \cdot 3H_2O$ (MW 319.85 g mol⁻¹). Methylene Blue (MB), sulfuric acid (H₂SO₄) and sodium hydroxide (NaOH) pellets (99 %) were purchased from Merck. The stock solution 1000 mg L⁻¹ by dissolving the exact amount of MB in distilled water. The concentrations of MB solutions used for experiments were prepared by diluting the stock dye solution.

2.2 Adsorbent (*Leucaena leucocephala*) preparation

The *Leucaena leucocephala* peels (LLP), which were used as the adsorbent in the experiments, they were collected from the *Robinia pseudoacacia* trees that were grown on the grounds of Van Yüzüncü Yıl University, Turkey. The collected LLP were washed with distilled water and dried at 75 °C until steady weight was achieved. The dried adsorbent was then ground in a mill and divided into different size groups using a set of sieves. Samples with a particle size between 1.50 mm and 2 mm were used in experiments.

2.3 Adsorption experiments

In the batch experiments, which were carried out in a temperature-controlled water bath, 3 g of adsorbent was treated with 500 mL of the dye solution. The experiments were carried out at seven concentrations (15, 30, 45, 60, 75, 90, 105 mg L⁻¹) and three temperatures (298, 308, 318 K). MB concentration in the dye solution determined over 320 min while the pH was gradually adjusted by adding H₂SO₄ or NaOH

solutions (0.1 M). All these experiments were carried out at pH 5.5. All experiments were performed in triplicate at the same conditions and average values were used to represent for results with all the calculated data. After adsorption experiments, the concentration of MB in the solution was determined with spectrophotometer (PG Instruments, T80 model) at 660 nm wavelength. The MB concentrations were determined with a calibration curve and adsorption capacity of LLP at equilibrium was determined with Eq. (1):

$$q_e = \frac{C_0 - C_e}{m} V \quad (1)$$

where V is solution volume (L), C_0 and C_e are initial and equilibrium concentrations of dye (mg L⁻¹) and m is adsorbent mass (g). The data obtained from experiments were tested by conducting isotherm, kinetic and thermodynamic studies. The amount of adsorption at any time t , q_t (mg g⁻¹), was calculated by Eq. (2):

$$q_t = \frac{C_0 - C_e}{m} V \quad (2)$$

3. RESULTS & DISCUSSION

3.1. Isotherm modelling studies

In the present study, the obtained data were analyzed using Langmuir, Freundlich and Temkin models. The parameters of these models were calculated by linear form of isotherm equations. The amount of MB adsorbed per unit of LLP mass and the equilibrium concentrations in the aqueous solutions for all three temperatures are presented in Fig 1. It was determined that removal efficiency increased with increase in the initial MB concentrations. LLP adsorption capacity of MB concentration ranging from 15 to 105 mg L⁻¹ was determined as 4.785 to 36.235 mg g⁻¹ for 298 K, 5.425 to 39.025 mg g⁻¹ for 308 K and 5.545 to 40.745 mg g⁻¹ for 318 K.

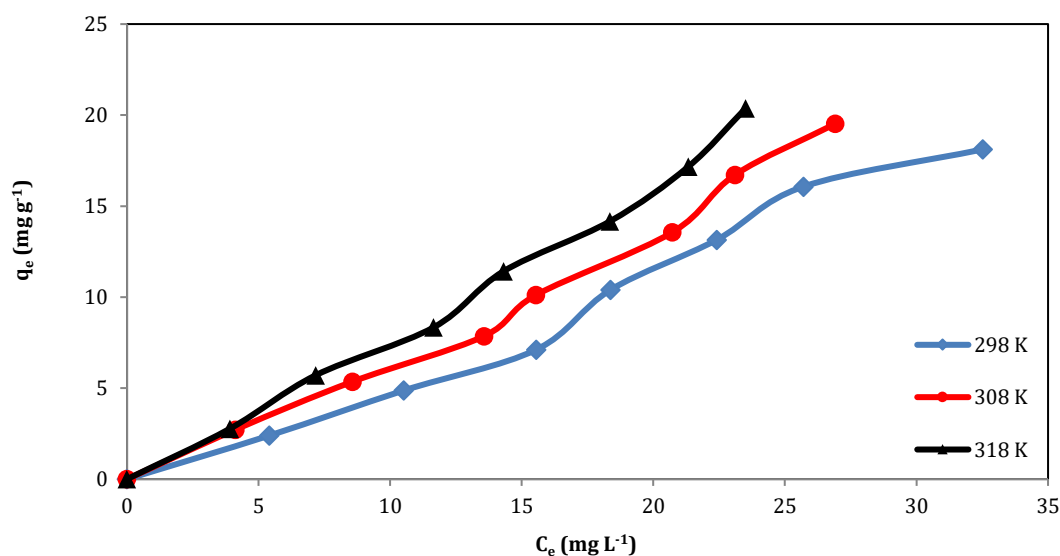


Fig 1. Adsorption isotherms for MB on the LLP at the three temperatures

Langmuir isotherm assumes monolayer coverage of the MB dye onto homogeneous adsorbent surface. Linear representation of Langmuir adsorption isotherm equation is given below:

$$\frac{C_e}{q_e} = \frac{1}{q_m K_L} + \frac{C_e}{q_m} \quad (3)$$

where q_m (mg g⁻¹) is maximum adsorption capacity and K_L (L g⁻¹) is Langmuir constant that can be determined from the plot of C_e/q_e versus C_e . Langmuir isotherm results of the MB adsorption onto LLP for three temperatures are given in Fig 2.

Freundlich isotherm assumes multilayer coverage of MB dye onto the heterogeneous adsorbent surface. Linear representation of Freundlich isotherm equation is presented below:

$$\ln q_e = \ln K_F + \frac{1}{n} \ln C_e \quad (4)$$

where K_F is Freundlich constant and n is heterogeneity factor. K_F and n constants are determined by plotting $\ln q_e$ to $\ln C_e$. Freundlich isotherm results of MB adsorption onto LLP for three temperatures are presented in Fig 3.

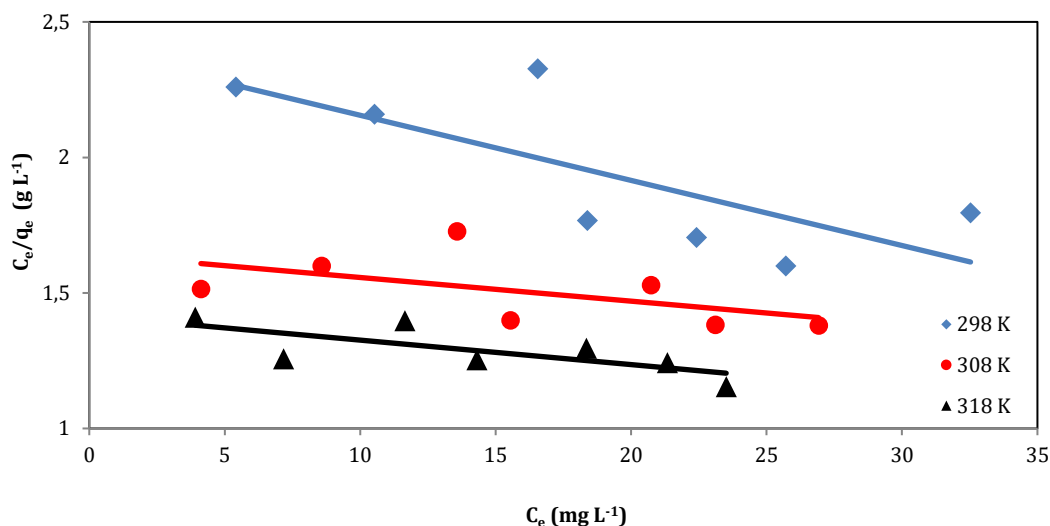


Fig 2. Langmuir adsorption isotherm for MB adsorption onto LLP

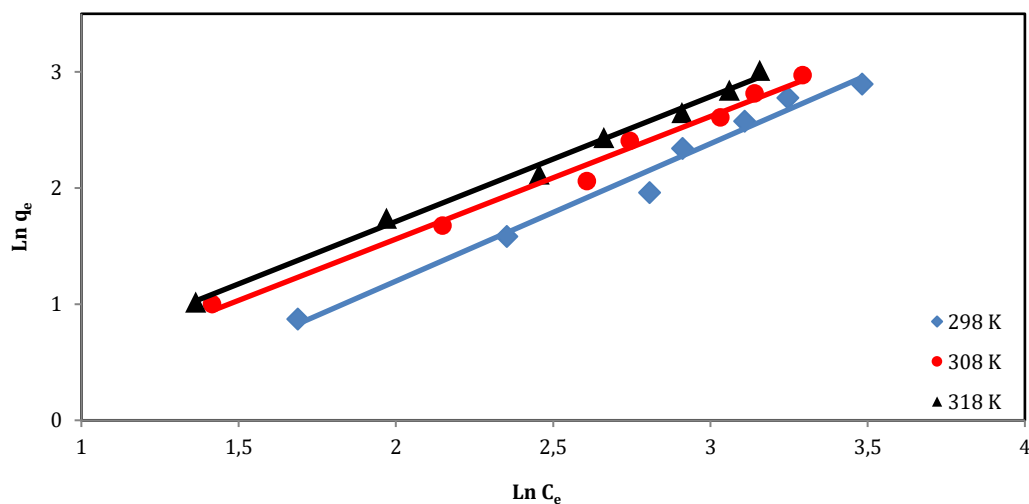


Fig 3. Freundlich adsorption isotherm for MB adsorption onto LLP

Temkin isotherm assumes decrease of adsorption heat in the layer of adsorbents that occurs due to enhancement of surface coverage of adsorbents.

$$q_e = B \ln(K_T C_e) \quad (5)$$

where $B = RT/b_T$, T is absolute temperature (K), R is universal constant (J mol⁻¹ K⁻¹) and K_T is constant (L g⁻¹). It was determined that the increase in isotherm constants increased with increase in temperature of adsorption temperature (B), indicating that adsorption was endothermic. Temkin

isotherm results of the MB adsorption onto LLP for three temperatures are given in Fig 4.

Table 1 clearly shows that three isotherm constants determined in this study are in comparable ranges with the values in previous studies. According to Langmuir isotherm calculations q_m and K_L values were increased with the increase of temperature which signified strong bonding between adsorbate and adsorbent. K_F and n values were increased with the rise of temperature based on the Freundlich isotherm calculations. K_T and b_T values were increased with the

increase of temperature according to Temkin isotherm calculations. R² values of the Freundlich

model were determined to be higher than those of the other models for removal of MB using LLP.

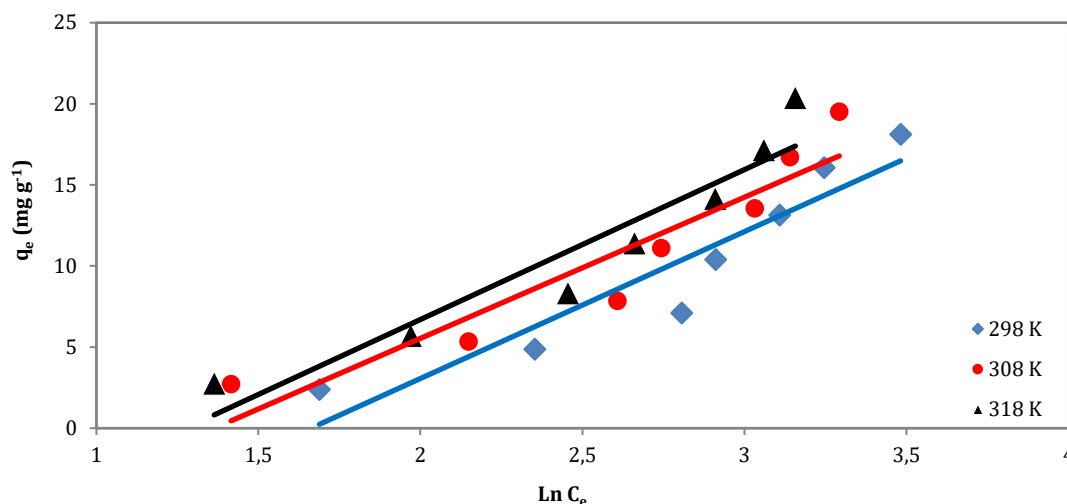


Fig 4. Temkin adsorption isotherm for MB adsorption onto LLP

Table 1. Adsorption isotherm model parameters of MB adsorption onto LLP

Temp K	Langmuir			Freundlich			Temkin		
	K _L (L g ⁻¹)	q _m (mg g ⁻¹)	R ²	n	K _F (L g ⁻¹)	R ²	K _T (L g ⁻¹)	b _T (J mol ⁻¹)	R ²
298	0.0635	41.667	0.5559	0.8451	0.3106	0.9805	0.1898	273.6378	0.8847
308	0.0811	74.943	0.4969	0.9472	0.5763	0.9879	0.2557	284.2975	0.8791
318	0.1002	101.111	0.5241	0.9805	0.6455	0.9947	0.2795	296.1466	0.9032

3.2. Thermodynamic studies

The thermodynamic parameters, Gibbs free energy (ΔG°), enthalpy (ΔH°) and entropy (ΔS°) were significant on the adsorption of MB onto LLP. These parameters were calculated using the equations given below:

$$K_d = C_{Ads}/C_e \tag{6}$$

$$\Delta G^\circ = -RT \ln K_d \tag{7}$$

$$\Delta G^\circ = \Delta H^\circ - T\Delta S^\circ \tag{8}$$

$$\ln K_d = \frac{\Delta S^\circ}{R} - \frac{\Delta H^\circ}{RT} \tag{9}$$

where K_d is the equilibrium constant. The ΔH° and ΔS° parameters were determined from plot natural logarithm of K_d versus $1/T$ given in Fig 5. The thermodynamic parameters of MB adsorption onto LLP are listed in Table 2. The ΔG° values of this removal process were determined as $-1359.6 \text{ J mol}^{-1}$ for 298 K, $-1476.6 \text{ J mol}^{-1}$ for 308 K and $-1593.6 \text{ J mol}^{-1}$ for 318 K. The ΔH° and ΔS° values of removal process of MB onto LLP were found to be $2126.687 \text{ J mol}^{-1}$ and $11.699 \text{ J mol}^{-1} \text{ K}^{-1}$, respectively. The negative ΔG° values were indicated that adsorption was physisorption, which is the showed that feasibility and spontaneous nature of this process. The absolute values of ΔG° were decreased as the temperature

increased, which shows that this separation process was constructive at low temperatures. The positive ΔH° and ΔS° values were demonstrated that process endothermic and the enhanced randomness at the solid-solute interface with affinity of LLP for MB. The low enthalpy values were explained that interaction produces noncovalent bonding between dyes and adsorbents [31].

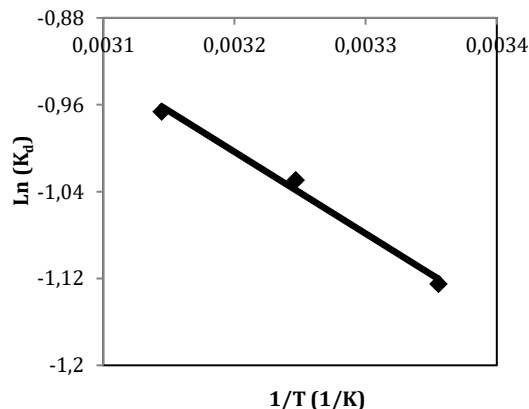


Fig 5. Van't Hoff plot for adsorption of MB onto LLP

Table 2. Thermodynamic parameters of adsorption of MB onto LLP

Temp (K)	ΔG° (kJ mol ⁻¹)	ΔH° (J mol ⁻¹)	ΔS° (J mol ⁻¹ K ⁻¹)	R ²
298	-1.3596			
308	-1.4766	2126.687	11.699	0.9905
318	-1.5936			

Table 3. PFO, PSO and IPD kinetic model parameters of MB adsorption onto LLP

Kinetic Model	Temp (K)	Kinetic coefficients	15 (mg L ⁻¹)	30 (mg L ⁻¹)	45 (mg L ⁻¹)	60 (mg L ⁻¹)	75 (mg L ⁻¹)	90 (mg L ⁻¹)	105 (mg L ⁻¹)	
PFO kinetic model	298	$q_e \text{ exp(mg g}^{-1}\text{)}$	4.785	9.715	14.225	20.815	26.295	32.145	36.235	
		$q_e \text{ exp(mg g}^{-1}\text{)}$	5.425	10.715	15.715	22.225	27.135	33.445	39.025	
		$q_e \text{ exp(mg g}^{-1}\text{)}$	5.545	11.415	16.675	22.845	28.325	34.335	40.745	
	298	$k_1 \text{ (min}^{-1}\text{)}$	0.0251	0.0225	0.0276	0.0335	0.0353	0.0361	0.0379	
		$q_e \text{ cal (mg g}^{-1}\text{)}$	2.5857	7.1821	8.5968	18.610	25.4598	23.6059	28.9277	
		R ²	0.9832	0.9441	0.9437	0.9341	0.9459	0.9269	0.9674	
	308	$k_1 \text{ (min}^{-1}\text{)}$	0.0261	0.0277	0.0286	0.0313	0.0327	0.0345	0.0352	
		$q_e \text{ cal (mg g}^{-1}\text{)}$	2.9544	4.5979	7.9050	11.4489	12.7866	15.9921	23.4062	
		R ²	0.9000	0.9112	0.9188	0.9108	0.8963	0.8786	0.9038	
	318	$k_1 \text{ (min}^{-1}\text{)}$	0.0257	0.0311	0.0322	0.0361	0.0369	0.0384	0.0397	
		$q_e \text{ cal (mg g}^{-1}\text{)}$	2.7442	6.9019	12.8212	12.5585	13.2381	16.7617	23.1478	
		R ²	0.9261	0.9314	0.9398	0.9318	0.9399	0.9226	0.9521	
PSO kinetic model	298	$k_2 \text{ (min}^{-1}\text{)}$	0.0241	0.0074	0.0055	0.0044	0.0034	0.0025	0.0017	
		$q_e \text{ cal (mg g}^{-1}\text{)}$	4.9529	10.5263	14.9700	18.2341	22.2221	33.7837	37.7358	
		R ²	0.9993	0.9961	0.9981	0.9966	0.9894	0.9982	0.9987	
	308	$k_2 \text{ (min}^{-1}\text{)}$	0.0246	0.0101	0.0052	0.0049	0.0042	0.0031	0.0025	
		$q_e \text{ cal (mg g}^{-1}\text{)}$	5.7077	11.1234	16.5016	23.3100	27.2486	34.8432	40.6504	
		R ²	0.9981	0.9997	0.9983	0.9983	0.9988	0.9988	0.9986	
	318	$k_2 \text{ (min}^{-1}\text{)}$	0.0289	0.0106	0.0075	0.0069	0.0051	0.0043	0.0032	
		$q_e \text{ cal (mg g}^{-1}\text{)}$	5.7241	11.8906	17.4825	23.4742	28.9017	35.2112	41.9992	
		R ²	0.9989	0.9988	0.9981	0.9995	0.9998	0.9996	0.9991	
	IPD kinetic model	298	$k_{id} \text{ (mg g}^{-1} \text{ min}^{-0.5}\text{)}$	0.1796	0.5037	0.6501	1.0127	1.2747	1.4049	1.5424
			C (mg g ⁻¹)	2.3385	2.6817	5.3859	6.9283	8.6026	12.9139	15.4132
			R ²	0.6947	0.8259	0.7334	0.7801	0.8143	0.7669	0.7108
308		$k_{id} \text{ (mg g}^{-1} \text{ min}^{-0.5}\text{)}$	0.2272	0.4376	0.7049	0.9644	1.1012	1.3786	1.6116	
		C (mg g ⁻¹)	2.2898	4.8011	6.1241	9.1259	12.2371	14.7973	17.1032	
		R ²	0.7734	0.6985	0.7397	0.7392	0.7084	0.7171	0.7336	
318		$k_{id} \text{ (mg g}^{-1} \text{ min}^{-0.5}\text{)}$	0.1935	0.4715	0.7371	0.8058	0.9135	1.1715	1.5801	
		C (mg g ⁻¹)	2.8841	4.9997	6.5671	12.0673	16.2435	18.7693	19.6741	
		R ²	0.6774	0.7278	0.7547	0.6218	0.5623	0.6083	0.6597	

3.3. Adsorption kinetics studies

In this study, the MB adsorption kinetics were calculated using PFO, PSO and IPD kinetic models. The well-suited model was selected based on the regression coefficient (R²) values. These models were investigated in accordance with the experimental data obtained at varied temperatures and MB concentrations.

The PFO kinetic model is depend on the concentration of solution and solid adsorption capacity.

This model was firstly developed for characterization of liquid-solid adsorption systems depending on adsorption capacity of solid. PFO is applied to study adsorption in liquid-solid systems which have unoccupied adsorptive sites [32]. The PFO kinetic model is given in the equation below:

$$\ln(q_e - q_t) = \ln q_e - k_1 t \quad (10)$$

where k_1 (min^{-1}) is rate constant of PFO kinetic model. To achieve constants with this model, plots were drawn of $\ln(q_e - q_t)$ against t .

The PSO kinetic model, which is explained using bond formation between the adsorptive site and solute molecule [33]. The PSO kinetic model is given in the equation below:

$$\frac{t}{q_t} = \frac{1}{(k_2 q_e^2)} + \frac{t}{q_e} \quad (11)$$

where k_2 ($\text{g mg}^{-1} \text{min}^{-1}$) is rate constant of PSO kinetic model. The values of k_2 and q_e are identified from plot of t/q_t versus t in accordance with Equation (10).

The IPD model equation, which was proposed by Weber and Morris, is obtained by testing the possibility of IPD as the rate limiting step [34]. The IPD kinetic model is given in the equation below:

$$q_t = k_{ipd} t^{0.5} + C \quad (12)$$

where k_{ipd} ($\text{mg g}^{-1} \text{min}^{-1/2}$) is IPD kinetic rate constant and C is boundary thickness. A plot of q_t against $t^{0.5}$ at different MB concentrations gave two phases of linear plot. The PFO, PSO and IPD model parameters are given in Table 3.

The experimental results showed that the R^2 coefficients were close to 1.0 which explained that this process fits the PSO kinetic model. Generally, in most dye adsorption systems the kinetic data is better represented by PSO model. In this study, the experimental and calculated q_e values for 318 K are higher than those for 298 K and 308 K. When the kinetic constants were compared, it was determined that the constant values were closer to both temperatures and concentrations for the PSO model. This result showed that the MG adsorption kinetics onto LLP confirmed the PSO model.

4. CONCLUSIONS

In this study LLP were used as an adsorbent for removal of MB, a widely used dye, from aqueous solutions. Batch experiments were carried out at seven concentrations and three temperatures. LLP adsorption capacity of MB concentration ranging from 15 to 105 mg L^{-1} was determined as 4.785 to 36.235 mg g^{-1} for 298 K, 5.425 to 39.025 mg g^{-1} for 308 K and 5.545 to 40.745 mg g^{-1} for 318 K. In the isotherm model studies, experimental results showed that Freundlich isotherm model was more suitable than the other two isotherms. These isotherm coefficients increased as the temperature increased and R^2 values of Freundlich model were determined to be higher than those of the other two models for removal of MB using LLP. The monolayer adsorption capacity (q_m) of LLP was determined as 41.667 for 298 K, 74.943 for 308 K and 101.111 mg g^{-1} for 318 K. This indicated that process was of an endothermic nature. The experimental data were applied to PFO, PSO and IPD kinetic models. Kinetic studies displayed that adsorption of MB process conformed the PSO model. All kinetic model coefficients increased as the temperature increased and R^2 values of PSO model were higher than the other two models for removal of

MB using LLP. ΔG° values of MB adsorption onto LLP were calculated as $-1359.6 \text{ J mol}^{-1}$ for 298 K, $-1476.6 \text{ J mol}^{-1}$ for 308 K and $-1593.6 \text{ J mol}^{-1}$ for 318 K. ΔH° and ΔS° values of MB adsorption onto LLP were determined to be $2126.687 \text{ J mol}^{-1}$ and $11.699 \text{ J mol}^{-1}$, respectively. The experimental data showed that LLP, which is the waste of *Robinia pseudoacacia* trees, may be an alternative material to removal of dyes from wastewater.

REFERENCES


- [1]. S. Asad, M. A. Amoozegar, A. A. Pourbabae, M. N. Sarbolouki and S. M. M. Dastgheib, "Decolorization of textile azo dyes by newly isolated halophilic and halotolerant bacteria," *Bioresource Technology*, Vol. 98 (11), pp. 2082–2088, 2007.
- [2]. R. L. Singh, P. K. Singh and R. P. Singh, "Enzymatic decolorization and degradation of azo dyes – a review," *International Biodeterioration & Biodegradation*, Vol. 104, pp. 21–31, 2015.
- [3]. C. Srikantan, G. K. Suraishkumar and S. Srivastava, "Effect of light on the kinetics and equilibrium of the textile dye (Reactive red 120) adsorption by helianthus annuus hairy roots," *Bioresource Technology*, Vol. 257, pp. 84–91, 2018.
- [4]. Y. Liu, Y. Liu, R. Qu, C. Ji and C. Sun, "Comparison of adsorption properties for anionic dye by metal organic frameworks with different metal ions," *Colloids and Surfaces A: Physicochemical and Engineering Aspects*, Vol. 586, pp. 1–7, 2020.
- [5]. M. A., Ahmad, N., Ahmad, N. and O. S. Bello, "Modified durian seed as adsorbent for the removal of methyl red dye from aqueous solutions," *Applied Water Science*, Vol. 5, pp. 407–423, 2015.
- [6]. A. A. Spagnoli, D. A. Giannakoudakis and S. Bashkova, "Adsorption of methylene blue on cashew nut shell based carbons activated with zinc chloride: the role of surface and structural parameters," *Journal of Molecular Liquids*, Vol. 229, pp. 465–471, 2017.
- [7]. R. Subramaniam and S. K. Ponnusamy, "Novel adsorbent from agricultural waste (cashew NUT shell) for methylene blue dye removal: optimization by response surface methodology," *Water Resources and Industry*, Vol. 11, pp. 64–70, 2015.
- [8]. M. T. Yagub, T. K. Sen, S. Afroze and H. M. Ang, "Dye and its removal from aqueous solution by adsorption: a review," *Advances Colloid and Interface Science*, Vol. 209, pp. 172–184, 2014.
- [9]. M. Rafatullah, O. Sulaiman, R. Hashim and A. Ahmad, "Adsorption of methylene blue on low-cost adsorbents: a review," *Journal of Hazardous Materials*, Vol. 177(1–3), pp. 70–80, 2010.
- [10]. M. A. M. Salleh, D. K. Mahmoud, W. A. W. A. Karim and A. Idris, "Cationic and anionic dye adsorption by agricultural solid wastes: a comprehensive review," *Desalination*, Vol. 280(1–3), pp.1–13, 2011.

- [11]. Y.-G. Kang, H. Yoon, C.-S. Lee, E.-J. Kim and Y.-S. Chang, "Advanced oxidation and adsorptive bubble separation of dyes using MnO₂-coated Fe₃O₄ nanocomposite," *Water Research*, Vol. 151, pp. 413-422, 2019.
- [12]. A. Muniyasamy, G. Sivaporul, A. Gopinath, R. Lakshmanan, A. Altaee, A. Achary and P. V. Chellam, "Process development for the degradation of textile azo dyes (mono-, di-, poly-) by advanced oxidation process - ozonation: experimental & partial derivative modelling approach," *Journal of Environmental Management*, Vol. 265, pp. 1-10, 2020.
- [13]. Y. Lu, Y. Fang, X. Xiao, S. Qi, C. Huan, Y. Zhan, H. Cheng and G. Xu, "Petal-like molybdenum disulfide loaded nanofibers membrane with super hydrophilic property for dye adsorption," *Colloids and Surfaces A: Physicochemical and Engineering Aspects*, Vol. 553, pp. 210-217, 2018.
- [14]. Y. Ma, P. Qi, J. Ju, Q. Wang, L. Hao, R. Wang and K. Sui, Y. Tan, "Gelatin/alginate composite nanofiber membranes for effective and even adsorption of cationic dyes," *Composites Part B: Engineering*, Vol. 162, pp. 671-677, 2019.
- [15]. L. A. Pereira, A. B. Couto, D. A. L. Almeida and N. G. Ferreira, "Singular properties of boron-doped diamond/carbon fiber composite as anode in Brilliant Green dye electrochemical degradation," *Diamond and Related Materials*, Vol. 103, pp. 1-7, 2020.
- [16]. N. P. Shetti, S. J. Malode, R. S. Malladi, S. L. Nargund, S. S. Shukla and T. M. Aminabhavi, "Electrochemical detection and degradation of textile dye Congo red at graphene oxide modified electrode," *Microchemical Journal*, Vol. 146, pp. 387-392, 2019.
- [17]. J. Joseph, R. C. Radhakrishnan, J. K. Johnson, S. P. Joy and J. Thomas, "Ion-exchange mediated removal of cationic dye-stuffs from water using ammonium phosphomolybdate," *Materials Chemistry and Physics*, Vol. 242, pp. 1-8, 2020.
- [18]. H. N. Bhatti, Y. Safa, S. M. Yakout, O. H. Shair, M. Iqbal and A. Nazir, "Efficient removal of dyes using carboxymethyl cellulose/ alginate/ polyvinyl alcohol/ rice husk composite: Adsorption/desorption, kinetics and recycling studies," *International Journal of Biological Macromolecules*, Vol. 150, pp. 861-870, 2020.
- [19]. C. Puri and G. Sumana, "Highly effective adsorption of crystal violet dye from contaminated water using graphene oxide intercalated montmorillonite nanocomposite," *Applied Clay Science*, Vol. 166, pp. 102-112, 2018.
- [20]. E. Alver, A. Ü. Metin and F. Brouers, "Methylene blue adsorption on magnetic alginate/rice husk bio-composite," *International Journal of Biological Macromolecules*, Vol. 154, pp. 104-113, 2020.
- [21]. F. Dhaouadi, L. Sellaoui, G. L. Dotto, A. Bonilla-Petriciolet, A. Erto and A. B. Lamine, "Adsorption of methylene blue on comminuted raw avocado seeds: Interpretation of the effect of salts via physical monolayer model," *Journal of Molecular Liquids*, Vol. 305, pp. 1-8, 2020.
- [22]. A. H. Jawad, R. Razuan, J. N. Appaturi and L. D. Wilson, "Adsorption and mechanism study for methylene blue dye removal with carbonized watermelon (*Citrullus lanatus*) rind prepared via one-step liquid phase H₂SO₄ activation," *Surfaces and Interfaces*, Vol. 16, pp. 76-84, 2019.
- [23]. D. S. Tong, C. W. Wu, M. O. Adebajo, G. C. Jin, W. H. Yu, S. F. Ji and C. H. Zhou, "Adsorption of methylene blue from aqueous solution onto porous cellulose-derived carbon/montmorillonite nanocomposites," *Applied Clay Science*, Vol. 161, pp. 256-264, 2018.
- [24]. S. Idris, Y. A. Iyaka, M. M. Ndamitso, E. B. Mohammed and M. T. Umar, "Evaluation of kinetic models of copper and lead uptake from dye wastewater by activated pride of barbados shell," *American Journal of Chemistry*, Vol. 1, pp. 47-51, 2012.
- [25]. Y. Ho and A. Ofomaja, "Pseudo-second-order model for lead ion sorption from aqueous solutions onto palm kernel fiber," *Journal of Hazardous Materials*, Vol. 129, pp. 137-142, 2006.
- [26]. F. B. Rebah and S. M. Siddeeg, "Cactus an eco-friendly material for wastewater treatment: a review," *Journal of Materials and Environmental Science*, Vol. 8, pp. 1770-1782, 2017.
- [27]. H. A. Al-Husseiny, "Adsorption of methylene blue dye using low cost adsorbent of sawdust: batch and continues studies," *Journal of University of Babylon*, Vol. 22(2), pp. 296-310, 2014.
- [28]. W. C. Wanyonyi, J. M. Onyari and P. M. Shiundu, "Adsorption of Congo red dye from aqueous solutions using roots of *Eichhornia crassipes*: kinetic and equilibrium studies," *Energy Procedia*, Vol. 50, pp. 862-869, 2014.
- [29]. M. J. Ahmed, P. U. Okoye, E. H. Hummadi and B. H. Hameed, "High-performance porous biochar from the pyrolysis of natural and renewable seaweed (*Gelidium acerosa*) and its application for the adsorption of methylene blue," *Bioresource Technology*, Vol. 278, pp. 159-164, 2019.
- [30]. L. M. Pandey, "Enhanced adsorption capacity of designed bentonite and alginate beads for the effective removal of methylene blue," *Applied Clay Science*, Vol. 169, pp. 102-111, 2019.
- [31]. I. Ghosh, S. Kar, T. Chatterjee, N. Bar and S. K. Das, "Removal of methylene blue from aqueous solution using *Lathyrus sativus* husk: Adsorption study, MPR and ANN modeling," *Process Safety and Environmental Protection*, Vol. 149, pp. 345-361, 2021.
- [32]. S. Langergren and B. K. Svenska, "Zur theorie der sogenannten adsorption gelöster stoffe," *Veternskapsakad Handlingar*, Vol. 24, pp. 1-39, 1898.
- [33]. Y. S. Ho and G. McKay, "Kinetic models for the sorption of dye from aqueous solution by wood," *Process Safety and Environmental Protection*, Vol. 76, pp. 183-191, 1998.
- [34]. W. J. Weber and J. C. Morris, "Kinetics of adsorption on carbon from solution," *Journal of the Sanitary Engineering Division*, Vol. 89, pp. 31-60, 1963.



RESEARCH ARTICLE

Investigation of the usability of zinc ferrite nanoparticles synthesized by microwave assisted combustion method as photocatalyst for removal of organic dyes from wastewaters

Zeynep Karcioğlu Karakaş^{1,*} 

¹ Atatürk University, Engineering Faculty, Environmental Engineering Department, 25240, Erzurum, TURKEY

ABSTRACT

In this study, zinc ferrite nanoparticles, which has an important place among the spinel ferrite structured nanomaterials due to its unique properties, were synthesized by microwave-assisted combustion method and later were used as photocatalysts in the removal of dyestuffs by photocatalytic degradation method from wastewaters of textile industry. In the synthesis studies, it was determined that the microwave effect alone was not sufficient to complete the transformation. Heat treatment application is envisaged to solve this problem and in order to determine the optimum heat treatment temperature, the sample produced by microwave effect were subjected to heat treatment at 300°C, 400°C, 500°C, 600°C, 700°C, 800°C and 900°C, respectively. It has been observed that the heat treatment has a significant effect on the crystal structure of the particles and 700°C has been determined as the optimum heat treatment temperature. The data obtained showed that, under these conditions, the zinc ferrite nanoparticles were successfully synthesized and the powder produced completely consisted of nano-sized particles. Moreover, results showed that the synthesized zinc ferrite nanoparticles has a saturation magnetization value sufficient to separate them from the aqueous medium. Finally, zinc ferrite nanoparticles produced under optimum conditions were used as photocatalysts in the removal of textile dye known as Procion Yellow HE-3G from wastewater by photocatalytic oxidation. In photocatalysis experiments, it was observed that synthesized zinc ferrite nanoparticles provided very high removal efficiencies as photocatalysts and almost all of the dye content in the solution could be removed.

Keywords: Microwave-assisted combustion method, photocatalysis, Procion Yellow HE-3G, zinc ferrite

1. INTRODUCTION

The increase in human population brings about an increase in consumption. As a way of coping with this increase, industrial production has been increasing and diversifying day by day in the modern age. Many different dyestuffs of a wide variety of types are used for various purposes in many industries. When these used dyes are transported to the nature with wastewaters, they can create big environmental problems. It is known that organic dyes can have many negative effects in water. These negative effects have the potential to pose serious threats to human health. In order to prevent against these threats, existing traditional water treatment methods may be insufficient. Therefore, it is highly important to improve the performance of traditional methods or to develop new alternative methods for the treatment of

wastewaters. It is expected that nanotechnology, which produces revolutionary innovations and solutions to solve problems in many different fields, will cause a great change in the field of water treatment technologies. By adapting nanotechnological methods to traditional processes, more innovative, more efficient and more environmentally friendly treatment alternatives can be developed for water treatment [1-3]. Today, scientific studies performed on nanotechnology applications for wastewater treatment focuses on various applications such as nanosensors, nano adsorbents, nanomembranes and nanophotocatalysis. However, the difficulties encountered in most of water treatment studies performed with nanomaterials in the separation of the nanoparticles used to reuse from the aqueous media is an important limiting factor for industrial applications of this

Corresponding Author: kzeynep@atauni.edu.tr (Zeynep Karcioğlu Karakaş)

Received 3 November 2020; Received in revised form 14 January 2021; Accepted 14 January 2021

Available Online 25 January 2021

Doi: <https://doi.org/10.35208/ert.820613>

© Yildiz Technical University, Environmental Engineering Department. All rights reserved.

technologies. Therefore, in many studies, magnetic nanoparticles are more preferred because they can be easily separated by magnetic separation.

Magnetic nanoparticles are used in a wide variety of applications due to their unique structural, electrical and magnetic properties [4-9]. For this reason, there is a significant increase in the number of studies aiming to develop new methods for the synthesis of these particles. Among these studies, in order to increase their industrial use, studies involving lowering process costs, high volume production, simplifying processes and developing more environmentally friendly methods attract more and more attention every day.

Spinel ferrites, an important subgroup of magnetic metal oxide nanoparticles, can exhibit very unusual magnetic properties, depending on the type of metal in their structure, and thus they can be used for many different purposes in industry and technology [10, 11]. Spinel ferrites are defined by the formula MFe_2O_4 . Here, the ions to the M site are Cd^{2+} , Ni^{2+} , Mn^{2+} , Co^{2+} , Zn^{2+} , Cu^{2+} etc. a transition metal ion with +2 charge may come, while this site is expressed as tetrahedral. Fe ion with a +3 charge passes to the octahedral site [12, 13]. Spinel ferrites are known for their strong magnetic properties and are widely used in many different applications where magnetic material is required.

One of the most widely used types of spinel ferrites is zinc ferrites. Zinc ferrites ($ZnFe_2O_4$) are low-cost, non-toxic semiconductor materials with narrow band gap. Zinc ferrite ($ZnFe_2O_4$) nanoparticles, which have industrial use like other spinel ferrites, are also very important materials in the field of biomedical technologies due to their super-magnetic behavior at room temperature and their extraordinary properties such as biological compatibility [11]. Since zinc ferrites do not exhibit toxic properties in terms of human health, they can be used as drug carrier materials in biomedical applications. Moreover, their non-toxicity also provide important advantages when used for environmental purposes such as water and wastewater treatment. Therefore, the development of low cost, environmentally friendly, simple and high efficiency synthesis techniques for the production of zinc ferrites, which is considered as a very important commercial nanomaterial, maintains the importance.

There are many methods suggested in the literature for the synthesis of zinc ferrites. This material has been previously produced by many different researchers using various techniques such as solvothermal synthesis [14], combustion [10], coprecipitation method [15], thermal treatment [16], sol-gel [17], solution combustion method [18], and hydrothermal [19]. Some of these methods require very complex and expensive experimental setups, while others require expensive starting chemicals. Moreover, many of these methods require intensive energy consumption, yet produce a very small amount of product. Moreover, in many of these methods, water is used for the synthesis process, therefore, impurities from water reduce the purity of the products and create wastewater problems at the end of the process. These problems limit the ability to

produce this material on commercial scale. In order to ensure that zinc ferrites can be used in industrial or environmental applications that require extensive use, new methods that will be alternatives to all the above mentioned methods need to be developed.

Accordingly, microwave assisted methods have brought a different dimension to the synthesis of nanomaterials. These techniques allow many different nano-sized materials to be produced simply and in large quantities at a lower cost and environmentally friendly approach. Microwave-assisted methods make it possible to synthesize nanostructures at relatively lower temperatures. Thanks to this technique, the heat required for the reaction is provided by using microwave irradiation instead of conventional methods, and thus the required heat penetrates into the reactive mixture more homogeneously and effectively. Microwave energy is homogeneously distributed not only on the outer surface of the reactive materials, but simultaneously inside the material, thus producing well-crystallized nano-sized powders with smaller particle size and high purity. In addition, this method is a low cost and simple method with uniform particle formation and short reaction times. It is also a suitable method for the preparation of various nanostructured materials with different sizes and shapes. On the other hand, many researchers today focus on combustion method for the synthesis of nanomaterials with small size and different morphology. This method stands out for having the advantages of being low cost, no need for complex devices and being able to work with non-toxic and cheap starting reagents. The most important disadvantage however is that the energy consumption is high as it requires working at high temperatures for long periods. When the combustion method is applied in conjunction with a microwave-assisted heating, heating costs are known to be significantly reduced [20].

Spinel $ZnFe_2O_4$ nanostructures attract more and more attention for environmental applications due to their strong response to visible light, magnetic properties, chemical and thermal stability, biocompatibility and low cost. It provides ease of filtration thanks to its suitability for magnetic separation. Since they are chemically and thermally very stable, they can be reused several times after their first use. [21-23].

It is known that spinel ferrites can be used as adsorbents or photocatalysts for environmental purposes. Zinc ferrite has been used as both an adsorbent and a photocatalyst in many previously published studies. Zn ferrite shows improved photocatalytic behavior and excellent reusability compared to other nano-sized spinel ferrite materials [24]. Spinel zinc ferrites, which are produced in different shapes and sizes by different methods, have been used as photocatalysts in the treatment of wastewater containing various dyes such as methyl orange, methyl red, thymol blue, methylene blue and toxic chemicals such as 4-chlorophenol (4-CP) by photocatalytic oxidation. [4, 21, 25-29].

UV light-driven heterogeneous photocatalytic process is considered to be an effective alternative for the removal of environmental pollutants originating from

organic dyestuffs in wastewaters and has therefore been widely studied by many researchers in the literature. Today, many researchers prefer photocatalytic nanocatalysts to remove the color caused by organic environmental pollutants. Photocatalytic nanocatalysts are widely used for color removal from wastewater due to their high photocatalytic efficiency, low cost and non-toxicity [30, 31].

It is known that the synthesis method of nanoparticles is highly effective on the structural, magnetic, electrical and morphological properties of these materials. Therefore, it is predicted that the synthesis method can be highly influential on the photocatalytic properties of the materials. Accordingly, in this study, zinc ferrite spinel nanomaterials were synthesized by microwave-assisted combustion method, which is considered as an environmental method, and then used as a photocatalyst in the photocatalytic oxidation process of Procion Yellow HE-3G textile dye and its photocatalytic performance was investigated.

2. MATERIALS AND METHOD

2.1. Preparation of materials

In this experimental study, the experimental studies carried out were carried out in two stages. In the first step, the synthesis and characterization of zinc ferrite ($ZnFe_2O_4$) nanoparticles, which have a thermally and chemically stable structure, by microwave-assisted combustion method were investigated. Then, the use of the synthesized particles as photocatalysts in the removal of textile dyes from synthetic wastewaters by photocatalytic degradation process was investigated. In photocatalysis experiments, procion yellow HE-3G, a textile dye from the diazo dyestuffs group and widely used in industry, was used as dye.

In this study, zinc (II) nitrate hexahydrate ($Zn(NO_3)_2 \cdot 6H_2O$), iron (III) nitrate nonahydrate ($Fe(NO_3)_3 \cdot 9H_2O$) and urea ($CO(NH_2)_2$) were used as synthesis reagents. All chemicals used were of analytical grade and were supplied from Sigma-Aldrich (Germany).

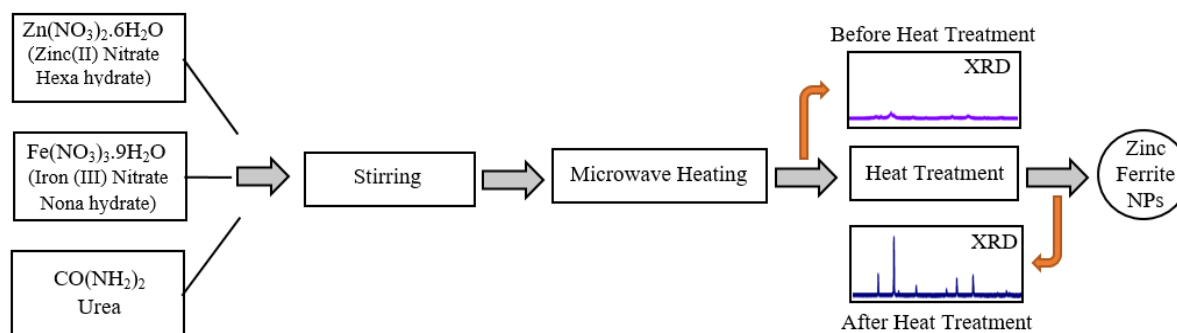


Fig 1. Schematic representation of the experimental procedure applied for synthesis

2.4. Photocatalysis experiments

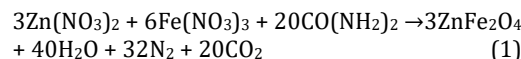
A dye solution containing 100 ppm was prepared for photocatalysis experiments. 100 mL of this solution

2.2. Characterization

In order to determine the structural, morphological and magnetic properties of the synthesized particles, X-Ray Diffraction (XRD), FT-IR, Vibrating Sample Magnetometer (VSM), Scanning Electron Microscope (SEM), and Transmission Electron Microscope (TEM) characterization tests were performed. Bruker D8 Discover model (Germany) XRD system was used for X-ray analysis ($CuK\alpha$, $\lambda = 1.5406 \text{ \AA}$). Vibrating Sample Magnetometer (VSM) measurements performed at room temperature were made by Cryogenic Limited PPMS (UK) system. Perkin Elmer Spectrum Two model system was used for Fourier Transform Infrared Spectroscopy (FT-IR) measurements. The morphological properties of the synthesized zinc ferrite nanoparticles were analyzed with a FEI Talos F200S model Transmission Electron Microscope.

2.3. Synthesis procedure

A mixture consisting of Zinc (II) nitrate hexahydrate, Iron (III) nitrate nonahydrate and urea was prepared for the synthesis of zinc ferrite nanoparticles by microwave assisted combustion method. All reagents were mixed according to stoichiometric proportions in a wide open beaker. The mixture was made homogeneous by using a mechanical mixer. The resulting mixture was placed in a standard microwave oven and it was subjected to microwave irradiation for approximately 5 minutes. The reaction taking place in this process is thought to have taken place as given in Eq. 1.



At the end of the microwave process, a dark brown powder was obtained. Later, the products were subjected to heat treatment in a furnace for the purposes of improving their crystal structure and removing the impurities they contain. Characterization studies were carried out on the final products obtained. The schematic representation of the experimental procedure applied is presented in Fig 1.

was measured and taken into a glass beaker. Then, 2 mL of hydrogen peroxide solution (ww, 0.30%) was added to the solution. A predetermined amount of zinc ferrite was added to the solution as catalyst. The

glass beaker was sealed with aluminum folio to increase the effectiveness of the UV lamp. During the process, the solution was mechanically mixed at a constant stirring speed. At the end of the experiment, catalyst particles were separated magnetically from the mixture. The concentration of the pollutant matter was measured by an UV Spectrophotometer at specific time intervals during the experimental period. Removal efficiencies were calculated with the expression given by Eq. 2.

$$\% \text{ Removal Efficiency} = \frac{C_o - C_e}{C_o} \times 100 \quad (2)$$

Here, C_o (mg L^{-1}) is the initial contaminant concentration and C_e (mg L^{-1}) is the equilibrium concentration at any given time.

3. RESULTS & DISCUSSION

3.1. XRD analysis

XRD analysis was carried out to determine the chemical composition of the samples obtained in the synthesis studies and to characterize their structural properties. The obtained X-ray diffractograms are given comparatively in Fig 2.

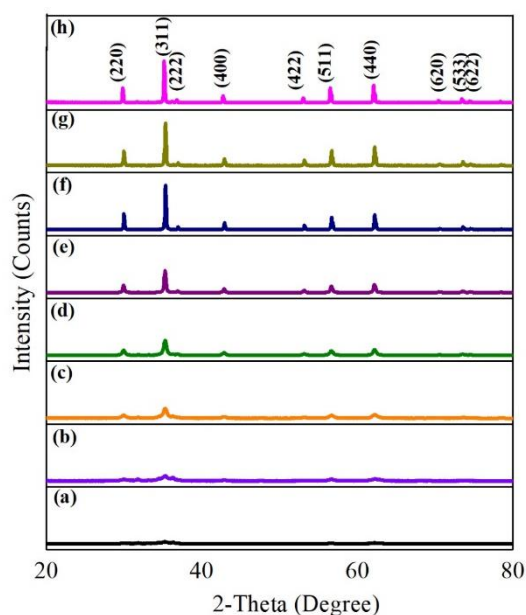


Fig 2. X-Ray diffractograms of zinc ferrite nanoparticles synthesized by microwave-assisted combustion method before and after heat treatment, (a) Precursor, (b) 300°C, (c) 400°C, (d) 500°C, (e) 600°C, (f) 700°C, (g) 800°C, (h) 900°C

The pattern shown as 2a from diffractograms presented in Fig 2, belongs to the precursor sample produced by only microwave effect. The X-ray pattern of this sample shows that the transformation in the sample was not completed. From the X-Ray diffractogram given in Fig 2a, it was determined that the sample produced by applying only microwave was in an amorphous structure. This result has been observed in other similar studies conducted before [20].

It is known that heat treatment has a significantly positive effect on improving the crystal structure of a substance. Accordingly, it was decided to subject the

samples to heat treatment so as to complete their transformation and improve their crystal structure. Accordingly, the solid sample obtained from the microwave system was subjected to heat treatment at temperatures varying between 300°-900°C. For this purpose, the precursor sample was subjected to heat treatment for 4 hours in an muffle furnace at 300°C, 400°C, 500°C, 600°C, 700°C, 800°C and 900°C respectively.

Determining the minimum value of the heat treatment temperature required to complete the conversion is an important parameter in terms of the process economy. From the X-ray diffractograms presented in Fig 2, it is clearly seen that the structure shows a significant change after 500°. Moreover, in the comparison of the diffractogram of the sample prepared with heat treatment applied at 600° with the standard diffraction cards given for ZnFe_2O_4 , it was seen that it is completely compatible with the JCPDS card No 74-2397. It was observed that all reflection peaks given on this card were obtained and the positions of the peaks were correctly also in place [10]. No additional peak of the second phase was observed in the XRD pattern, showing that the as prepared ferrite consisted of single spinel ZnFe_2O_4 phase. In the X-ray diffractograms of samples produced by heat treatment at different temperatures, a peak of 311 crystal planes is observed in the region between $2\theta=36^\circ-38^\circ$. This peak is the major peak in the diffractogram and is specific for spinel oxide structured materials. By using some data of this peak, the crystal sizes of the synthesized samples can be calculated with the Debye-Scherrer equation. The Debye-Scherrer equation is given below as Eq. 3.

$$D = \frac{-0.89\lambda}{\beta \cdot \cos\theta} \quad (3)$$

In this equation; "D" is the crystal size (nm), " β " is the radian value of the half height of the major peak in the x-ray diffractogram (FWHM), " λ " is the wavelength of the X-ray generator used in the XRD system (0.154 nm) and " θ " is the Bragg angle of the dominant peak. The crystal sizes of the samples produced at various temperatures were calculated with the Debye-Scherrer formula and then these values were plotted against the heat treatment temperature. The graphic obtained is presented in Fig 3.

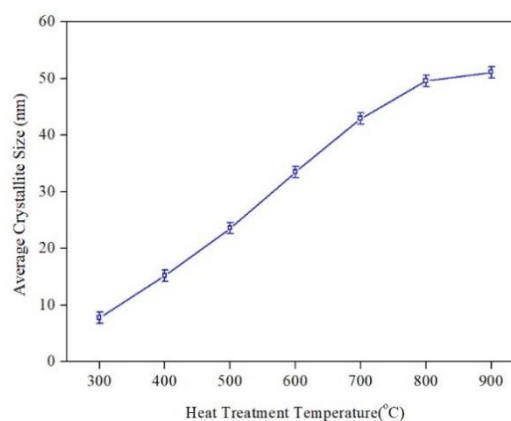


Fig 3. The variations of the average crystallite sizes with increasing heat treatment temperature

According to Fig 3, it is seen that the crystal size of the samples distinctly increases with increasing heat

treatment temperature. It is estimated that this growth originates from sintering occurring with the effect of high temperature. On the other hand, it is known that increasing crystal size may cause a decrease in the surface area. Accordingly, the heat treatment temperature must be optimized to prevent sintering. Accordingly, while the improvement in the crystal structure continues with the increasing temperature, it was determined that the heat treatment applied after 700°C did not cause any change. According to these results, 700°C has been evaluated as the optimum heat treatment temperature for this process.

3.2. FT-IR analysis

Fourier transform infrared spectroscopy is one of the most common analytical techniques used to examine chemical changes and the interactions between reactive substances. Fourier transform infrared spectroscopy analysis was performed on all of the samples obtained in order to evaluate the possible chemical changes originated from the applied heat treatment. FT-IR spectra of the samples were measured between 450 cm^{-1} - 4000 cm^{-1} and obtained spectra are presented comparatively in Fig 4.

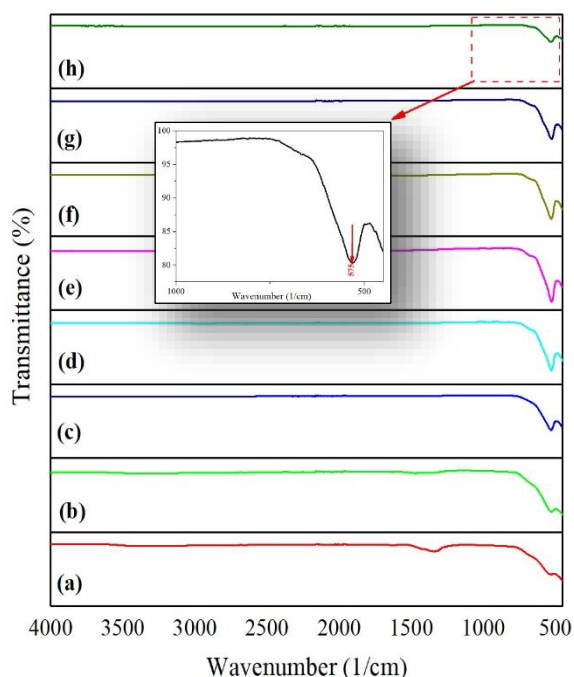


Fig 4. FT-IR spectra of zinc ferrite nanoparticles obtained before and after heat treatment, (a) Precursor samples, (b) 300°C, (c) 400°C, (d) 500°C, (e) 600°C, (f) 700°C, (g) 800°C, (h) 900°C, (i) 1000°C

When the FT-IR spectra given in Fig 4 are examined, a strong absorption band can be observed at 575 cm^{-1} caused by Fe-O tension vibrations [32]. In the FT-IR spectrum of the precursor sample presented in Fig 4a, an absorption band is observed at 1360 cm^{-1} . However, it has been observed that this peak disappears after heat treatments at high temperatures. It was evaluated that this absorption band is due to C-O stretching vibration which is

originating from organic residue emerging with degradation of urea used as fuel [33].

3.3. TEM analysis

Transmission Electron Microscope is an important advanced characterization technique that allows for the microstructure and crystal structures of nanomaterials to be examined. This technique provides simultaneous access to crystallographic and morphological information of nano-sized particles. TEM examination of the ZnFe_2O_4 samples obtained before and after heat treatment was performed and the obtained images are presented in Fig 5.

From the TEM images given Fig 5, it can be seen that the sample, which was not heat treated, consisted of smaller particle size particles, but at the same time they were present in large lumps. It is estimated that this clumping is caused by combustion residual organic materials. After the applied heat treatment, it is thought that the pellets are relatively dispersed, however, it was observed that the average particle size is increased due to the sintering that occurs under the effect of high temperature.

3.4. VSM analysis

Zinc ferrite is a material that is widely used in many different areas due to its strong magnetic properties. It is known that the synthesis method of nanoparticles causes significant changes on magnetic properties. Accordingly, in order to characterize the magnetic properties of zinc ferrite nanoparticles produced by microwave-assisted combustion, Vibrating Sample Magnetometer (VSM) measurements were made in the samples obtained. Hysteresis loops created using the measurement results obtained are presented in Fig 6.

According to the magnetic hysteresis curves given in Fig 6, it is seen that the magnetic properties of the synthesized particles have improved significantly with the increase in the heat treatment temperature in parallel with the results observed in XRD and FTIR analyzes. The similar observations can be seen in some previous studies [20]. These observations show that there is a direct and strong relationship between crystal structure and magnetic properties.

The saturation magnetization value is a characteristic commonly used to evaluate the magnetic properties of ferromagnetic materials. Saturation magnetization defines the maximum magnetization value that a ferromagnetic material can reach. The saturation magnetization value of a sample is determined from magnetic hysteresis loops. In this study, the saturation magnetization values measured at room temperature were determined from hysteresis loops. The variation of saturation magnetization values with increasing heat treatment temperature is presented in Fig 7.

It is clearly seen that the saturation magnetization value increases in parallel with the development of the crystal structure. These results indicate a strong relationship between magnetic properties and crystal structure. The data obtained are compatible with those reported in the literature [20].

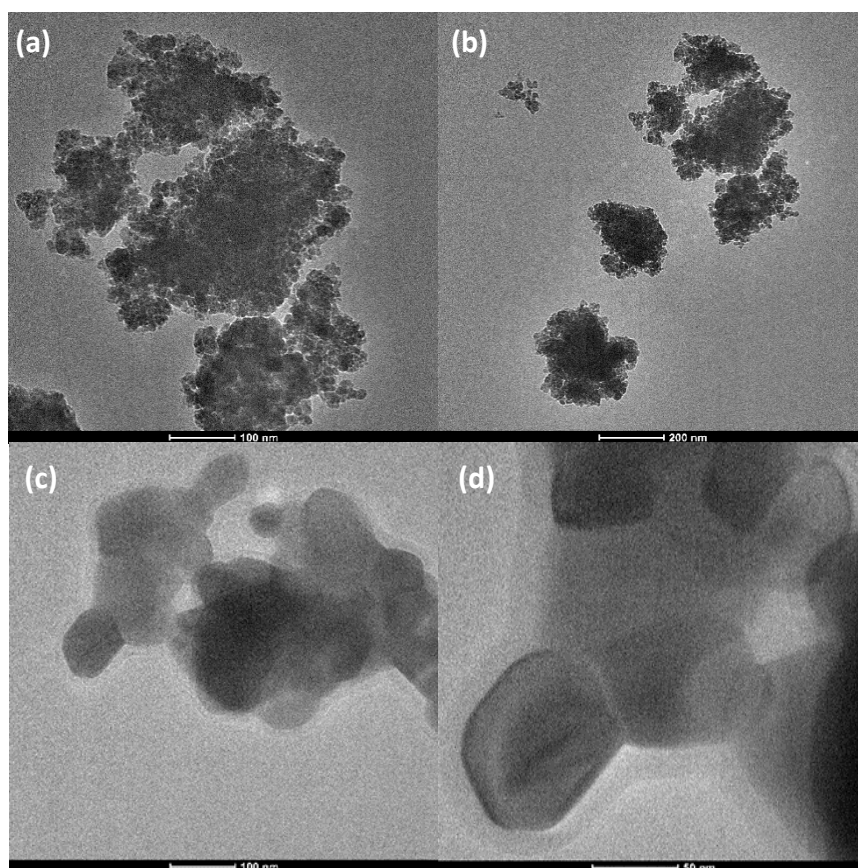


Fig 5. TEM images of ZnFe_2O_4 samples obtained before and after heat treatment; (a-b) sample produced without heat treatment, (c-d) sample produced by heat treatment at 700°C

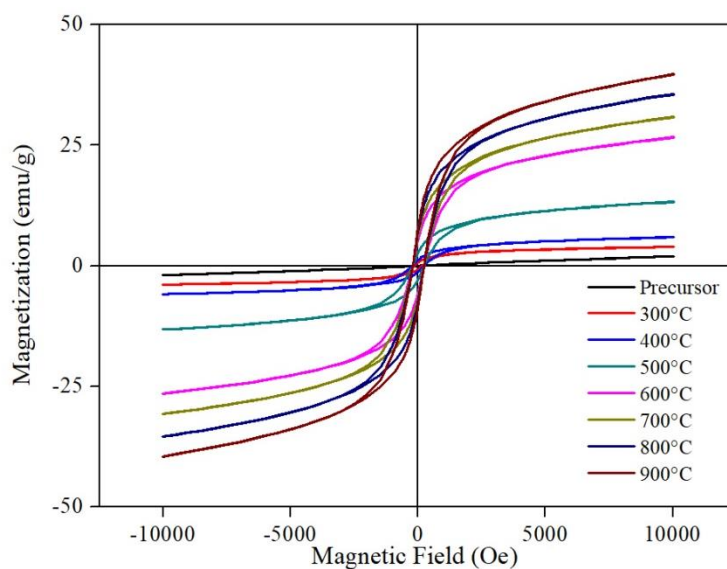


Fig 6. Magnetic hysteresis curves of ZnFe_2O_4 nanoparticles heat treated at different temperatures

One of the most important problems encountered in studies carried out with nanoparticles in an aqueous environment is the separation of the particles used from the environment. It is aimed to separate nanoparticles used as photo-catalysts in the system under study by magnetic separation techniques from the aqueous environment. In some previous studies, it was stated that when the saturation magnetization

value of magnetic nanoparticles is about 20 emu g^{-1} and above, they can be separated from the aqueous environment by applying an external magnetic field [34, 35]. Accordingly, from the particles synthesized in this study, it is seen that the particles subjected to heat treatment at temperatures of 600° and above provide this conditions.

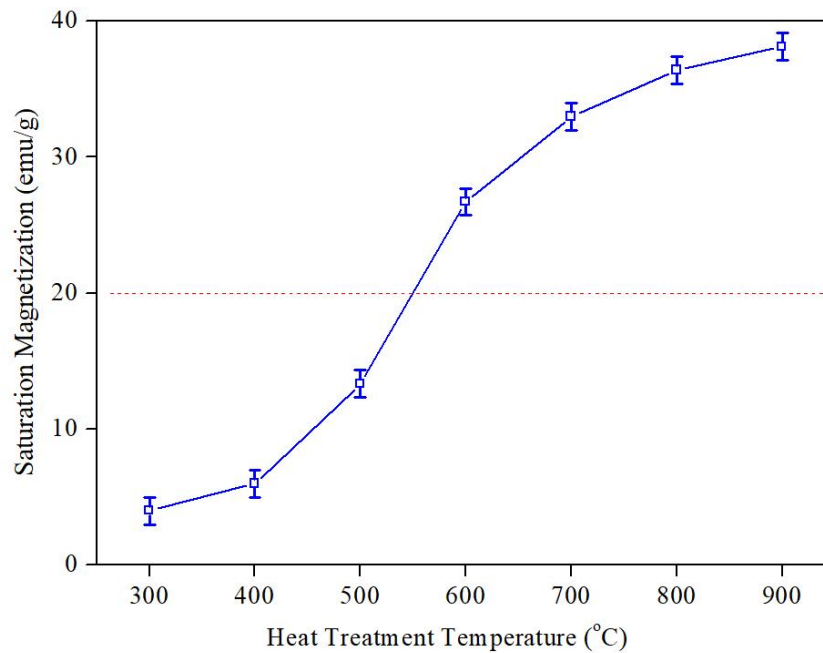


Fig 7. The variation of saturation magnetization values with increasing heat treatment temperature

3.5. The analysis of the surface properties

One of the most important problems encountered in studies conducted with nanoparticles in an aqueous environment is the separation of the particles used from the environment. In the system under this study, it is aimed to separate nanoparticles used as photocatalysts from the aqueous environment by magnetic separation techniques. In some previous studies, it was claimed that when the saturation magnetization value of magnetic nanoparticles is about 20 emu/g and above, they can be separated from the aqueous environment by applying an external magnetic field. The surface areas of nanoparticles are a highly influential characteristic on their catalytic performance. Generally, photocatalysts with larger

surface area are expected to exhibit as more much catalytic performance. Because photocatalysis process starts with the adsorption of the organic pollutant on the catalyst surface.

The Brunauer - Emmett - Teller theory (BET) is a commonly used theory to explain the physical adsorption of gas molecules on a solid surface. The specific surface area of many different types of materials is measured by an analysis technique based on this theory. Surface properties of zinc ferrite nanoparticles were measured with a surface analyzer that performs measurements based on bet theory. The adsorption-desorption isotherms measured at 77 K for the zinc ferrite nanoparticles produced under optimum conditions are given in Fig 8.

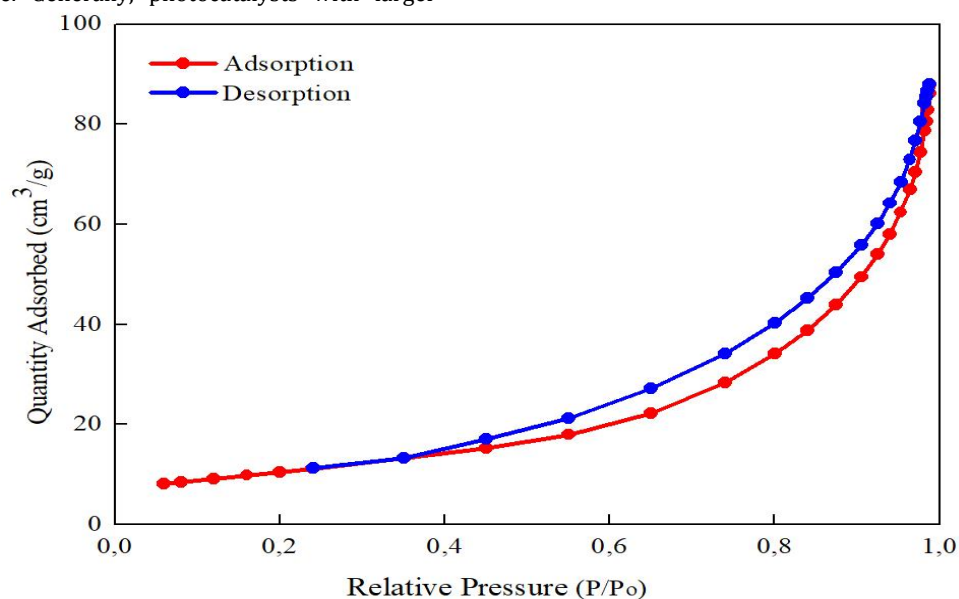


Fig 8. Adsorption-Desorption isotherms of the zinc ferrite nanoparticles prepared in optimum conditions

When the adsorption desorption isotherms presented in Fig 8 are examined, it is seen that the obtained isotherm is substantially similar to the type 3 isotherm according to the IUPAC classification. The classification made by IUPAC for the adsorption hysteresis loops is an approach that is widely accepted by many researchers. The IUPAC classification is an empirical classification of hysteresis loops, based on a previous classification made by de Boer [36-38]. This classification claims that there is a correlation between the shape of the hysteresis loop and the texture (e.g., pore size distribution, pore geometry, and connectivity) of a

mesoporous material [36]. When isotherms presented in Fig 8 are evaluated according to the IUPAC classification, it is seen that the resulting adsorption desorption isotherm has substantial similarities with the Type II isotherm. Type II, is generally used to describe adsorbents whose pore size distribution and pore shape are irregular. Specific surface areas of zinc ferrite nanoparticles synthesized in optimum conditions by microwave-assisted combustion method were calculated with various theories such as BET, Langmuir, t-plot, and single point. The data obtained are presented in Table 1.

Table 1. The various surface properties of the zinc ferrite nanoparticles prepared in optimum conditions

	BET ($\text{m}^2 \text{g}^{-1}$)	Langmuir ($\text{m}^2 \text{g}^{-1}$)	T-Plot ($\text{m}^2 \text{g}^{-1}$)	Single Point ($\text{m}^2 \text{g}^{-1}$)
Surface Area	38.0580	52.5293	37.2451	36.6986

BET surface area of the zinc ferrite nanoparticles subjected to heat treatment at 700°C was determined as approximately $38 \text{ m}^2 \text{g}^{-1}$. This value can be considered to be a very good surface area for a nanoparticle to be used as a photocatalyst.

3.6. Photocatalytic properties

A photocatalyst can be defined as a substance activating with a UV light beam coming onto it. It is

known that zinc ferrite nanoparticles exhibit very good photo-sensitive properties. Accordingly, synthesized zinc ferrite nanoparticles were used as photocatalysts in the process of degradation of procion yellow HE-3G textile dye by photocatalytic oxidation and its effectiveness on removal efficiency was investigated for catalyst dosages of 1 g L^{-1} , 0.5 g L^{-1} , 0.25 g L^{-1} , and 0.01 g L^{-1} , respectively. Absorption spectra obtained from experiment performed for each catalyst dosage are given in Fig 9.

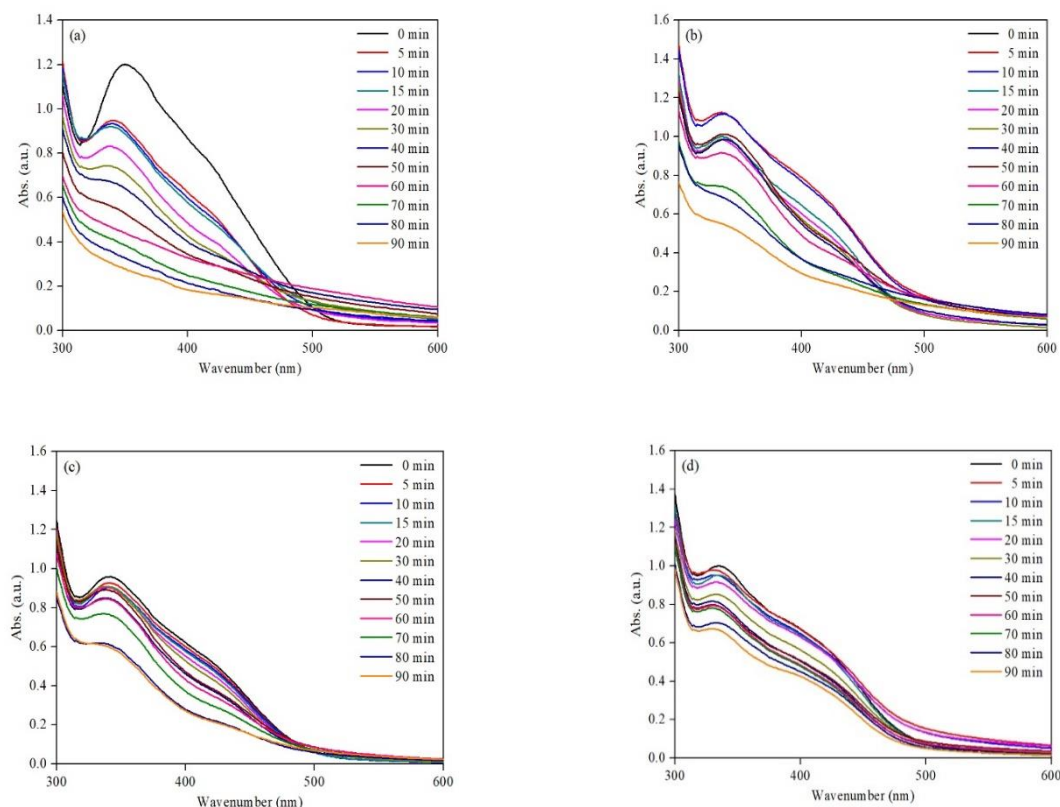


Fig 9. Absorption spectra obtained from experiments performed with different catalyst dosages a) 1 g L^{-1} , b) 0.5 g L^{-1} c) 0.25 g L^{-1} ve d) 0.01 g L^{-1} catalyst dosage

When the absorbance curves given above are examined, it is seen that the removal efficiencies increase significantly with the increasing amount of catalyst as expected. However, results very close to each other were observed in experiments made with 0,25 g L⁻¹ and 0.01 g L⁻¹ catalyst dosages. A graphical figure showing the change in removal efficiency versus time is presented in Fig 10.

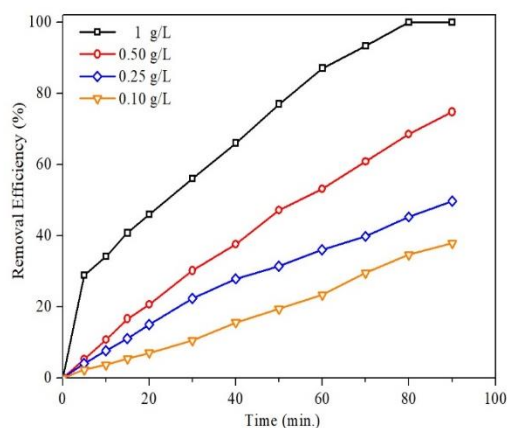


Fig 10. The changes in removal efficiency versus time in experiments performed with various catalyst dosages

The results given in Fig 10 show that the trial performed with a catalyst dosage of 1 g L⁻¹ was clearly much faster than the others. In photocatalysis experiments, a removal efficiency of 100% was achieved at the end of the 80th minute for 1 g L⁻¹ catalyst dosage, while at the end of the 90th minute in experiments made with the 0.5 g L⁻¹, 0.25 g L⁻¹, and 0.01 g L⁻¹ catalyst dosages, respectively removal efficiencies of 74.8, 46.7% and 37.9% were observed. In order to determine whether ZnFe₂O₄ nanoparticles show a photo-catalytic effect during the chemical oxidation process of Procion Yellow HE-3G textile dye, an experiment was conducted by adding only hydrogen peroxide solution and catalyst to the paint solution and covering the surrounding of the beaker with aluminum foil in order to prevent the light exchange with the environment of the system. The absorption spectrum obtained from experiment performed without using any light source is presented in Fig 11.

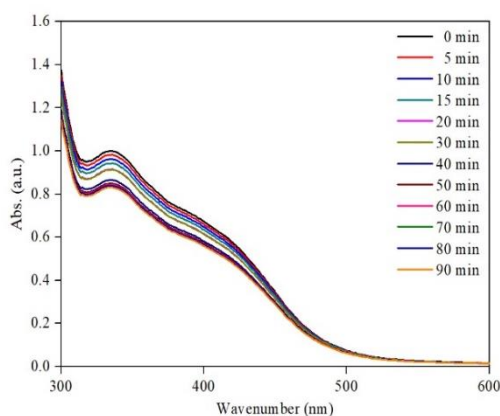


Fig 11. Absorption spectra obtained from the experiment in dark environment without using any light source

When the results given in Fig 11 are examined, it is observed that there is very little removal effect. It is estimated that this removal may have occurred with the adsorption rather than the oxidation. The graph prepared by comparing the results obtained from the experiment without using a UV light source with the results of the experiment carried out with UV irradiation under the same experimental conditions is presented in Fig 12.

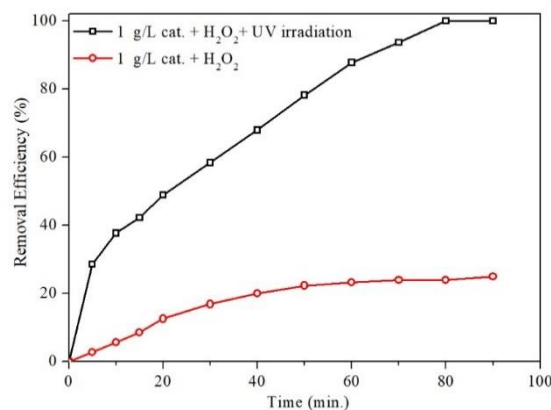


Fig 12. The comparison of the removal efficiency obtained from experiment made with UV effect and the removal efficiency obtained from experiment made without UV irradiation

When the removal efficiencies obtained from the experiments made with and without the UV irradiation are evaluated together, the positive effect of the applied UV irradiation onto removal efficiency can be clearly seen. Accordingly, the obtained results show that the ZnFe₂O₄ nanoparticles used in the process have a photocatalytic effect and this process is a photocatalytic oxidation process.

4. CONCLUSIONS

In this experimental study, zinc ferrite (ZnFe₂O₄) magnetic spinel ferrite nanoparticles were successfully synthesized by microwave-assisted combustion method. Later, the synthesized ZnFe₂O₄ nanoparticles were used as photocatalysts in the process of degradation of Procion Yellow HE-3G textile dye by photocatalytic oxidation. The results obtained from the trials can be summarized as follows.

- The obtained results demonstrated that magnetic ZnFe₂O₄ zinc ferrite nanoparticles can be successfully produced by microwave-assisted combustion method.
- It was determined that zinc ferrite nanoparticles can be produced in a simple, fast and abundantly with the proposed method.
- It has been determined that the synthesized particles have a sufficient level of saturation magnetization to be able to be separated from the aqueous environment.
- The particles produced have demonstrated an effective photocatalytic performance in the process of degrading Procion Yellow H3-EG textile dye by photocatalytic oxidation. The removal efficiency was determined as 100% at the end of

80th minute in experiment made with 1 g L⁻¹ catalyst dosage.

- The results obtained from trials carried out separately in the dark environment and under the influence of UV radiation clearly show that the process takes place photocatalytically.
- As a result, with the proposed synthesis process, zinc ferrite nanoparticles can be synthesized in a simple, fast, environmentally friendly and highly efficient. In addition, synthesized particles have the potential to be used as photocatalysts in dye removal by photocatalytic oxidation process from textile wastewater thanks to their very high photosensitivity.

REFERENCES

- [1]. I. Gehrke, A. Geiser, and A. Somborn-Schulz, "Innovations in nanotechnology for water treatment," *Nanotechnology, Science and Applications*, Vol. 8, pp. 1-17, 2015.
- [2]. K. M. Lee, C. W. Lai, K. S. Ngai and J. C. Juan "Recent Developments of Zinc Oxide Based Photocatalyst in Water Treatment Technology: A Review," *Water Research*, Vol. 88, pp. 428-448 2015.
- [3]. M. Mahendiran, J. J. Mathen, M. Racik, J. Madhavan and M. V. A. Raj "Investigation of structural, optical and electrical properties of transition metal oxide semiconductor CdO/ZnO nanocomposite and its effective role in the removal of water contaminants," *Journal of Physics and Chemistry of Solids*, Vol. 126, pp. 322-334, 2019.
- [4]. R. C. Sripriya, V. A. F. Samson, S. Anand, J. Madhavan and M.V. A. Raj, "Comparative studies of structural, magnetic and photocatalytic degradation on 4-chlorophenol by ZnFe₂O₄ nanostructures prepared via cost effective combustion methods," *Journal of Materials Science: Materials in Electronics*, Vol. 29 (16), pp. 14084-14092, 2018.
- [5]. T. Prakash, G. V. M. Williams, J. Kennedy and S. Rubanov, "High spin-dependent tunneling magnetoresistance in magnetite powders made by arc-discharge," *Journal of Applied Physics*, Vol. 120 (12), 123905, 2016.
- [6]. P. P. Murmu, J. Kennedy, G. V. M. Williams, B. J. Ruck, S. Granville and S. V. Chong, "Observation of magnetism, low resistivity, and magnetoresistance in the near-surface region of Gd implanted ZnO," *Applied Physics Letters*, Vol. 101 (8), 082408, 2012.
- [7]. S. Banik and I. Das, "Large magnetoresistance and relative cooling power in polycrystalline Pr_{0.775}Sr_{0.225}MnO₃ compound," *Journal of Magnetism and Magnetic Materials*, Vol. 460, pp. 234-238, 2018.
- [8]. K. Kaviyarasu, P. P. Murmu, J. Kennedy, F. T. Thema, D. Letsholathebe, L. Kotsedi and M. Maaza, "Structural, optical and magnetic investigation of Gd implanted CeO₂ nanocrystals," *Nuclear Instruments and Methods in Physics Research Section B: Beam Interactions with Materials and Atoms*, Vol. 409, pp.147-152, 2017.
- [9]. T. Prakash, G. V. M. Williams, J. Kennedy and S. Rubanov, "Formation of magnetic nanoparticles by low energy dual implantation of Ni and Fe into SiO₂," *Journal of Alloys and Compounds*, Vol. 667, pp. 255-261, 2016.
- [10]. N. M. Deraz and A. Alarifi, "Microstructure and Magnetic Studies of Zinc Ferrite Nano-Particles," *International Journal of Electrochemistry Science*, Vol. 7, pp. 650-6511, 2012.
- [11]. M. Sertkol, Y. Köseoğlu, A. Baykal, H. Kavas, A. Bozkurt and M. S. Toprak, "Microwave synthesis and characterization of Zn-doped nickel ferrite nanoparticles," *Journal of Alloys and Compounds*, Vol. 486(1-2), pp. 325-329, 2009.
- [12]. A. H. Morr, K. Haneda, "Magnetic structure of small NiFe₂O₄ particles," *Journal of Applied Physics*, Vol. 52 (3), pp. 2496-2498, 1981.
- [13]. N. B. Singh and A. Agarwal, "Preparation, Characterization, Properties and Applications of nano Zinc Ferrite," *Materials Today: Proceedings*, Vol. 5(3), pp.9148-9155. 2018.
- [14]. P. Guo, L. Cui, Y. Wang, M. Lv, B. Wang and X.S. Zhao, "Facile Synthesis of ZnFe₂O₄ Nanoparticles with Tunable Magnetic and Sensing Properties," *Langmuir*, Vol. 29 (28), pp. 8997-9003, 2013.
- [15]. F. Iqbal, M. I. A. Mutalib, M. S. Shaharun, M. Khan and B. Abdullah, "Synthesis of ZnFe₂O₄ Using sol-gel Method: Effect of Different Calcination Parameters," *Procedia Engineering*, Vol. 148, pp. 787-794, 2016.
- [16]. M. G. Naseri, E. B. Saion, M. Hashim, A.H. Shaari and H.A. Ahangar, "Synthesis and characterization of zinc ferrite nanoparticles by a thermal treatment method," *Solid State Communications*, Vol. 151(14-15), pp. 1031-1035, 2011.
- [17]. M. Ebrahimi, R. Raeisi Shahraki, S. A. Seyyed Ebrahimi and S. M. Masoudpanah, "Magnetic Properties of Zinc Ferrite Nanoparticles Synthesized by Coprecipitation Method," *Journal of Superconductivity and Novel Magnetism*, Vol. 27(6), pp. 1587-1592, 2014.
- [18]. S. Sun, X. Yang, Y. Zhang, F. Zhang, J. Ding, J. Bao and C. Gao, "Enhanced photocatalytic activity of sponge-like ZnFe₂O₄ synthesized by solution combustion method," *Progress in Natural Science: Materials International*, Vol. 22(6), pp. 639-643, 2012.
- [19]. J. Zhang, J. M. Song, H. L. Niu, C. J. Mao, S. Y. Zhang and Y. H. Shen, "ZnFe₂O₄ nanoparticles: Synthesis, characterization, and enhanced gas sensing property for acetone," *Sensors and Actuators B: Chemical*, Vol. 221, pp. 55-62, 2015.
- [20]. Z. Karcioğlu Karakaş, R. Boncukcuoğlu, İ. H. Karakaş and M. Ertuğrul, "The effects of heat treatment on the synthesis of nickel ferrite (NiFe₂O₄) nanoparticles using the microwave assisted combustion method," *Journal of Magnetism and Magnetic Materials*, Vol. 374, pp. 298-306, 2015.

- [21]. S. D. Jadhav, P. P. Hankare, R. P. Patil and R. Sasikala, "Effect of sintering on photocatalytic degradation of methyl orange using zinc ferrite," *Materials Letters*, Vol. 65 (2), pp. 371-373, 2011.
- [22]. G. Y. Zhang, Y. Q. Sun, D. Z. Gao and Y. Y. Xu, "Quasi-cube ZnFe₂O₄ nanocrystals: Hydrothermal synthesis and photocatalytic activity with TiO₂ (Degussa P25) as nanocomposite," *Materials Research Bulletin*, Vol. 45 (7), pp. 755-760, 2010.
- [23]. M. Rostami, M. Rahimi-Nasrabadi, M. R. Ganjali, F. Ahmadi, A. F. Shojaei and M. D. Rafiee, "Facile synthesis and characterization of TiO₂-graphene-ZnFe_{2-x}Tb_xO₄ ternary nanohybrids," *Journal of Materials Science*, Vol. 52 (12), pp. 7008-7016, 2017.
- [24]. P. Kharazi, R. Rahimi and M. Rabbani, "Study on porphyrin/ZnFe₂O₄@polythiophene nanocomposite as a novel adsorbent and visible light driven photocatalyst for the removal of methylene blue and methyl orange," *Materials Research Bulletin*, Vol. 103, pp. 133-141, 2018.
- [25]. H. Zhang, R. Hou, Z. L. Lu and X. Duan, "A novel magnetic nanocomposite involving anatase titania coating on silica-modified cobalt ferrite via lower temperature hydrolysis of a water-soluble titania precursor," *Materials Research Bulletin*, Vol. 44(10), pp. 2000-2008, 2009.
- [26]. S. Xu, D. Feng and W. Shangguan, "Preparations and Photocatalytic Properties of Visible-Light-Active Zinc Ferrite-Doped TiO₂ Photocatalyst," *The Journal of Physical Chemistry C*, Vol. 113(6), pp. 2463-2467, 2009.
- [27]. P. P. Hankare, R. P. Patil, A. V. Jadhav, K. M. Garadkar and R. Sasikala, "Enhanced photocatalytic degradation of methyl red and thymol blue using titania-alumina-zinc ferrite nanocomposite," *Applied Catalysis B: Environmental*, Vol. 107 (3-4), pp. 333-339, 2011.
- [28]. R. Jiang, H. Zhu, Y. Fu, S. Jiang, E. Zong and J. Yao, "Photocatalytic Decolorization of Congo Red Wastewater by Magnetic ZnFe₂O₄/Graphene Nanosheets Composite under Simulated Solar Light Irradiation," *Ozone: Science & Engineering*, Vol. 42 (2), pp.174-182, 2020.
- [29]. Y. Fu, X. Wang, "Magnetically Separable ZnFe₂O₄-Graphene Catalyst and its High Photocatalytic Performance under Visible Light Irradiation", *Industrial & Engineering Chemistry Research*, 50 (12), pp. 7210-7218, 2011.
- [30]. C. Tian, Q. Zhang, A. Wu, M. Jiang, Z. Liang, B. Jiang and H. Fu "Cost-effective large-scale synthesis of ZnO photocatalyst with excellent performance for dye photodegradation," *Chemical Communications*, Vol. 48(23), pp. 2858-2860, 2012.
- [31]. M. Mahendiran, J. J. Mathen, K. M. Racik, J. Madhavan and M. V. A. Raj, "Facile synthesis of n-ZnO @ p-CuO nanocomposite for water purification enhanced decolorization of methyl orange," *Journal of Materials Science: Materials in Electronics*, Vol. 30(17), pp. 16099-16109, 2019.
- [32]. Z. Shahnavaaz, F. Lorestani, Y. Alias and P.M. Woi, "Polypyrrole-ZnFe₂O₄ magnetic nanocomposite with core-shell structure for glucose sensing," *Applied Surface Science*, Vol. 317, pp. 622-629, 2014.
- [33]. M. Venkatesh, G. S. Kumar, S. Viji, S. Karthi, and E. K. Girija, "Microwave assisted combustion synthesis and characterization of nickel ferrite nanoplatelets," *Modern Electronic Materials*, Vol. 2 (3), pp. 74-78, 2016.
- [34]. Y. Zhang, M. Yang and X. Huang, "Arsenic (V) removal with a Ce(IV)-doped iron oxide adsorbent," *Chemosphere*, Vol. 51(9), pp. 945-952, 2003.
- [35]. Z. Karcioğlu Karakaş, R. Boncukcuoğlu and İ.H. Karakaş, "Antimony removal from aqueous solutions using magnetic nickel ferrite (NiFe₂O₄) nanoparticles," *Separation Science and Technology*, Vol. 54 (7), pp. 1141-1158, 2018.
- [36]. Z. Allothman, "A Review: Fundamental Aspects of Silicate Mesoporous Materials," *Materials*, Vol. 5, pp. 2874-2902, 2012.
- [37]. K. S. W. Sing, "Reporting physisorption data for gas/solid systems with special reference to the determination of surface area and porosity (Recommendations 1984)," *Pure and Applied Chemistry*, Vol. 57(4), pp. 603, 1985
- [38]. K. S. W. Sing, D. H. Everett, R. A. W. Haul, L. Moscou, R. A. Pierotti, J. Rouquerol and T. Siemieniewska, "Reporting Physisorption Data for Gas/Solid Systems," *Handbook of Heterogeneous Catalysis*, pp. 1217-1230, 2008.



RESEARCH ARTICLE

A new calculation method of efficiency for gypsum and wastewater hydrocyclones in FGD unit in a power plant

Mehmet Bilen^{1,*} 

¹Bülent Ecevit University, Faculty of Engineering, Department of Mining Engineering, İncivez Merkez, Zonguldak, 67100, TURKEY

ABSTRACT

This study was carried on hydrocyclones in the Wet Flue Gas Desulfurization (WFGD) system of a local thermal power plant. In WFGD systems, hydrocyclones are used for classification in terms of PSD of limestone, dewatering the gypsum slurry and recycling the wastewater. Separation efficiencies of hydrocyclones (waste water and gypsum) in power plant were calculated referring to each hydrocyclones' inlet size of D_{25} . Results obtained with Malvern Mastersizer for the samples from each exits of hydroclones were taken into consideration. Separation efficiency for waste water hydrocyclone was calculated as 4.0 % while it was calculated 77.5 % for gypsum hydrocyclone.

Keywords: Wastewater, thermal power plant, particle size distribution, hydrocyclone

1. INTRODUCTION

Power plants are equipped with several sub systems and coal entering to power plant is processed to the final products (ash, byproducts, wastewater and flue gas). In order to decrease the level of SO_2 emission and to purify the wastewater, a technology called Wet Flue Gas Desulphurization (WFGD) is employed. WFGD, due to abovementioned purposes, is one of the most important technology in a power plant in terms of environment. Because of its high efficiency and reliability, WFGD system in the power plants is the most commonly used technology for controlling the emission of SO_2 in the world [1- 4]. Sketch of WFGD system in power plant is provided in Fig 1 [5].

Having more than 100 years history hydrocyclones, mostly employed in WFGD systems of power plants in terms of removing or classifying particles [6], belong to a class of fluid-solid classifying devices that separate dispersed material from a fluid stream. The structure of a hydrocyclone is presented in Fig 2. (Diameter of the hydrocyclone (D), height (H), diameter of the overflow (D_o), thickness of the

overflow (d), diameter of the underflow (D_u), diameter of the inlet (D_i), height of the overflow in cyclone chamber (h), cone angle (θ)) [7].

Separation efficiency or in other words hydrocyclone performance is significantly questioned by many recent researches which includes mostly CFD model approaches recently. Hwang and Chou [8] have employed CFD (computational fluid dynamics) in terms of understanding the separation efficiency differentiation of the designed hydrocyclones. Hwang and Chou [8] have summarized the fact that "design of highly efficient hydrocyclone with CFD is an effective, economical, and timesaving approach". Zhu et al. [9] have conducted a computational study of the flow characteristics and separation efficiency of a mini-hydrocyclone. Cullivan et al. [10, 11] have also employed CFD to simulate fluid velocity, pressure distributions, particle trajectories. Although this wide employment of CFD, there is still this complexity for the performance of a hydrocyclone since it depends on the numerous parameters such as particle size, operating conditions, and geometric structures [8].

Corresponding Author: mehmet.bilen@beun.edu.tr (Mehmet Bilen)

Received 16 December 2020; Received in revised form 12 February 2021; Accepted 20 February 2021

Available Online 26 February 2021

Doi: <https://doi.org/10.35208/ert.841720>

© Yildiz Technical University, Environmental Engineering Department. All rights reserved.

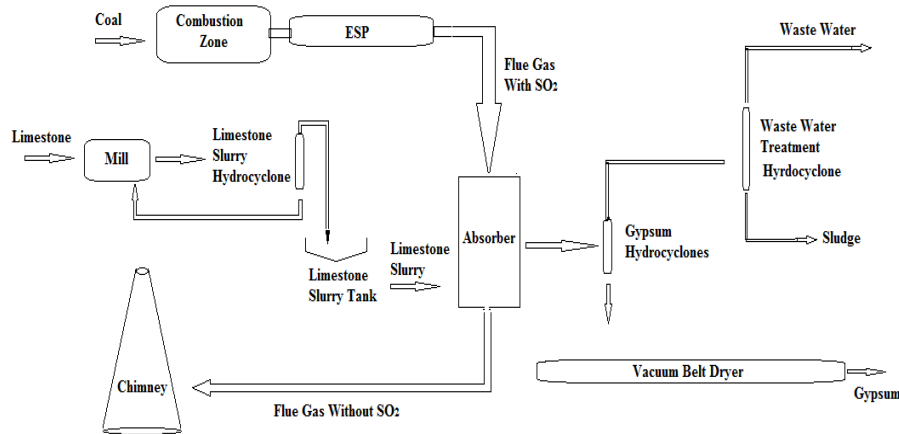


Fig 1. Schematic representation of coal utilizing power plant and final products [5] (Bilen et al.2016)

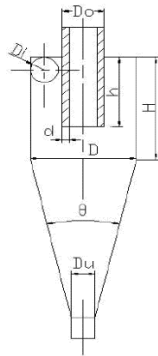


Fig 2. Sketch of hydrocyclone's structure [7]. (Jun et al, 2009)

Separation efficiency is off interest by many researchers [8-15]. In this context, Rocha et al. [12] (2020) have tried to evaluate the role of feed duct changes on hydrocyclone performance, Mousavian and Najafi [13] have investigated the role of geometry. Likewise, Chu et al. [14] have investigated the effect of structural modification on hydrocyclone performance. Boylu et al. [15] have investigated the separation efficiency of Na-bentonite by hydrocyclone. Although CFD approach is useful and reliable method [16] for designing of hydrocyclone, separation efficiency calculation should be based on the real life experimental data evaluation.

In this study, a new calculation method for separation efficiency was proposed. Samples were collected from inlet, upstream and downstream of gypsum and waste water hydrocyclones of a power plant. Collected samples were analyzed in terms of their PSD and a new size parameter of D_{25} was taken into consideration in the order of efficiency calculation.

2. EXPERIMENTAL METHOD

Sieve analysis of the samples from upstreams and downstreams of hydrocyclones in power plant (gypsum and waste water hydrocyclones) a total of 5 samples was done by using Malvern Mastersizer S 2000 with the employment of wet method and PSD of waste water samples was obtained over a range of $0.05 \mu\text{m} - 878.67 \mu\text{m}$. Obscuration of the Mastersizer

experiments was kept between 12% and 18%, mostly about 15%. Prepared waste water samples of lower and upper exits of hydrocyclone of power plant were analyzed and size distribution parameters (D_{10} , D_{25} , D_{50} , D_{90} , D_{32} , D_{43}) for each were obtained. Size parameters and their descriptions are as the following.

D_{10} (μm): sieve opening which 10 % of particles passing through

D_{25} (μm): sieve opening which 25 % of particles passing through

D_{50} (μm): sieve opening which 50 % of particles passing through

D_{90} (μm): sieve opening which 90 % of particles passing through

D_{32} (μm): volume / surface mean (Sauter Mean)

Sauter mean is defined as the diameter of a sphere that has the same volume/surface ratio as a particle of interest.

$$D_{32} = \frac{\sum_1^n D_i^3 v_i}{\sum_1^n D_i^2 v_i} \quad (1)$$

D_{43} (μm): the mean diameter over volume (DeBrouckere Mean)

$$D_{43} = \frac{\sum_1^n D_i^4 v_i}{\sum_1^n D_i^3 v_i} \quad (2)$$

If we assign 3 spheres with diameters 1, 2, 3 units, the calculation of Sauter and De-Brouckere means of these spheres is exemplified as in the following equations (Eq. (3) and Eq. (4)).

$$D_{32} = \frac{1+8+27}{1+2+3} = 2.57 \mu\text{m} \quad (3)$$

$$D_{43} = \frac{1+16+81}{1+8+27} = 2.72 \mu\text{m} \quad (4)$$

2.1 Separation efficiency of hydrocyclones

The particle size distribution of the samples from 3 hydrocyclones in the power plant was measured by Malvern Mastersizer. In this context, a typical plot of

particle size distribution of sand particles from the study of Dwari et al. [17] is provided in Fig 3.

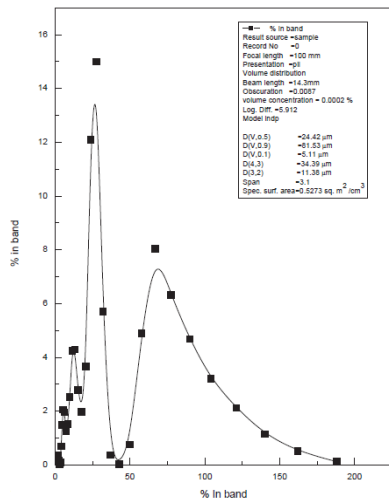


Fig 3. A typical plot of particle size distribution (Malvern particle size analysis for sand inlet sample at 27.6 kN/m² inlet slurry pressure) [17].

Knowing the particle size inlet and overflow, the efficiency of separation can be calculated by Eq. (5).

$$\eta = \frac{\text{Wt \% of particle at inlet} - \text{Wt \% of particle at overflow}}{\text{Wt \% of particle at inlet}} \times 100 \quad (5)$$

Dwari et al. [17] summarized the effect of particle size, velocity of flow, pressure drop on separation efficiency and their finding are represented in Fig 4.

Hydrocyclone studied by Dwari et al. [17] gave very little separation efficiency for the particles below 60 µm. It should be modified to increase the separation efficiency for the particles in range 10-50 µm. In terms of installation angle, Jun et al [7] claimed that it has little effect on classification performance in power plants. Accordingly, changing the installation angle and reducing the installation height is a good way to enhance the production capacity of hydrocyclones. Other than installation angle, particle size there are more parameters affecting hydrocyclone performance as pointed out in the study of Jun et al [7]. For example size of the hydrocyclone is also important and larger the size of hydrocyclone is the lower the separation performance. Regarding to cone angle, total separation efficiency decreases with the cone angle increasing. Last but not the least, increasing the underflow tube length will enhance production capacity at the same time reduce the cut size and increase the separation efficiency [7].

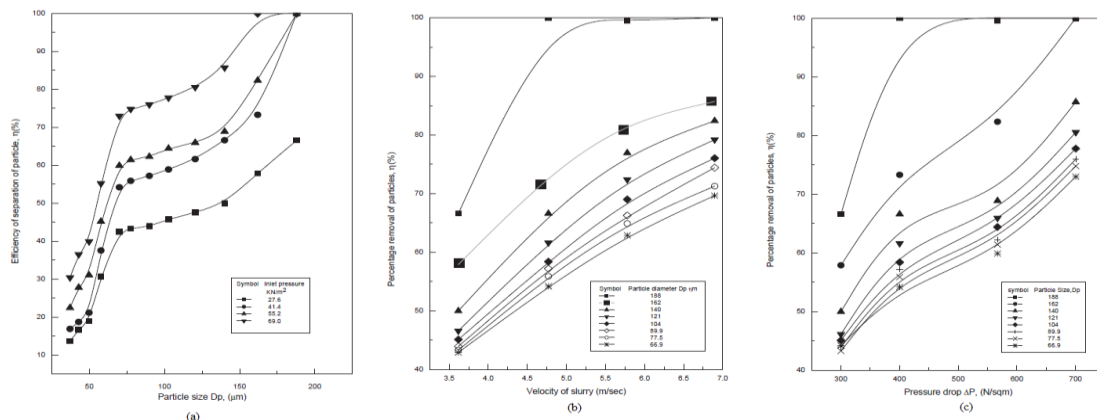


Fig 4. Observations of Dwari et al [17] on parameters affecting the efficiency of separation of particles for sand and fly ash (a) effect of particle size (b) effect of velocity of flow (c) effect of pressure drop

3. RESULTS & DISCUSSION

Separation efficiency of gypsum and waste water hydrocyclone was calculated in terms of Eq. (5). In order to do this calculation, inlet and overflow weight percentages at specific size should be known. For gypsum and waste water hydrocyclone Wt% are provided in Table 1. Malvern Mastersizer analysis results are presented in Fig 5-7 and tabulated in Table 3 for waste water hydrocyclone. For gypsum hydrocyclone, results are presented in Fig 8-10 and tabulated in Table 4, respectively.

The values in Table 1 are raw data of Malvern Mastersizer analysis result. Referring to the values in Table 1, overflow and downstream percentages can be calculated. This calculation is carried out with the basis of x (%) is overflow and y (%) is downstream for gypsum hydrocyclone and k (%) is overflow and z (%) is downstream for waste water hydrocyclone. That is why;

$$x+y=100(\%) \text{ for gypsum hydrocyclone} \quad (6)$$

$$k+z=100(\%) \text{ for waste water hydrocyclone.} \quad (7)$$

Mass balance equations at inlet size of D₂₅ can be written as;

$$26.50*x (\%) + 16.41*y (\%) = 25.86*100 (\%) \text{ for gypsum hydrocyclone,} \quad (8)$$

$$92.61*k (\%) + 20.17*z (\%) = 24.47*100 (\%) \text{ for waste water hydrocyclone.} \quad (9)$$

From Eq. (6)-(9), x is 93.65 (%), y is 6.35 (%), k is 5.94 (%) and z is 94.06 (%), respectively. Having calculated the overflow and downstream ratios for each hydrocyclone, real cumulative undersize percentages at inlet D₂₅ size are provided in Table 2.

Table 1. Wt% (for the inlet D25 size) for gypsum and waste water hydrocyclones without considering overflow and downstream ratios (Refer to Table 3 and Table 4)

Hydrocyclone	Wt% (for the inlet D25 size)		
	Inlet	Overflow	Downstream
Gypsum Hydrocyclone	24.47	92.61	20.17
Wastewater hydrocyclone	25.86	26.50	16.41

Table 2. Wt% (for the inlet D25 size) for gypsum and waste water hydrocyclones with considering overflow and downstream ratios.

Hydrocyclone	Wt% (for the inlet D25 size)		
	Inlet	Overflow	Downstream
Gypsum Hydrocyclone	24.47	5.50	18.97
Waste water hydrocyclone	25.86	24.82	1.04

Replacing the values of inlet and overflow in the Eq. (5) separation efficiencies were calculated as 77.5 % for gypsum hydrocyclone and 4.0 % for waste water hydrocyclone respectively.

Obtained D₂₅ sizes (inlet) are 0.6707 μm (See Table 3) for waste water hydrocyclone and 12.2096 μm (See

Table 4) for gypsum hydrocyclone, respectively. Waste water hydrocyclone has low separation efficiency. This is because coarser particles are fed to gypsum hydrocyclone and finer purification is done with waste water hydrocyclone. This is also supported in the study of Dwari et al. [17] claiming that separation efficiency is very little for fine particles. Separation efficiency of a hydrocyclone is one of the most crucial issue in terms of its design and operation. Yu and Fu [18] have investigated the separation performance of an 8 mm mini hydrocyclone and its application for the treatment of rice starch wastewater. Yu and Fu [18] have summarized the attempts to enhance the separation performance of hydrocyclones. For example, Fu et al. [19] have tried to optimize structural parameters such as cylinder diameter [18]. In addition, researchers have investigated vortex finder structure and size [20,21], inlet dimensions [22], cyclone height [23], underflow pipe diameter [24], and cut size [25] proportional to cylinder diameter roles on separation efficiency [18]. Although these abovementioned researchers have contributed significantly, a correct calculation of separation efficiency is most of the time is unheeded. Each research should initially focus on the correct calculation of the separation efficiency since any efficiency improvement can better be observed later on. Findings of this study would be significant in terms of correct calculation methodology of a hydrocyclone separation efficiencies.

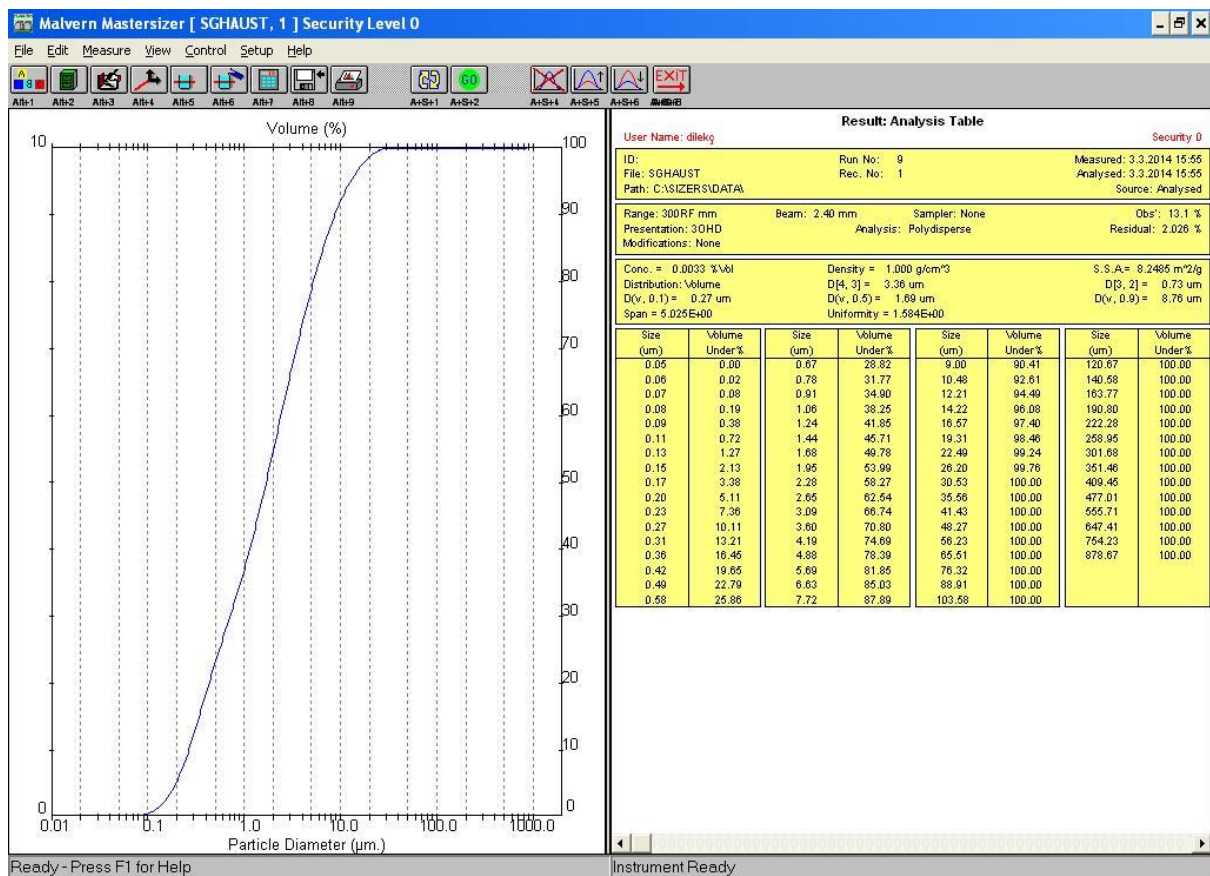


Fig 5. PSD of feed for wastewater hydrocyclone

Table 3. PSD of feed downstream and overflow of wastewater hydrocyclone

Size, μm	Feed			Downstream			Overflow		
	Amount (%)	Cumulative oversize (%)	Cumulative Undersize (%)	Amount (%)	Cumulative oversize (%)	Cumulative Undersize (%)	Amount (%)	Cumulative oversize (%)	Cumulative Undersize (%)
SIZES*	*RESULT*	$\Sigma (+)$ (%)	$\Sigma (-)$ (%)	*RESULT*	$\Sigma (+)$ (%)	$\Sigma (-)$ (%)	*RESULT*	$\Sigma (+)$ (%)	$\Sigma (-)$ (%)
.0582	0.0225	100.00		0.01183	100.00		0.01139	100.00	
.0679	0.05548	99.98	0.02	0.03267	99.99	0.01	0.0298	99.99	0.01
.0791	0.10814	99.92	0.08	0.06688	99.96	0.04	0.06258	99.96	0.04
.0921	0.19493	99.81	0.19	0.1231	99.89	0.11	0.12292	99.90	0.10
.1073	0.33596	99.62	0.38	0.21344	99.77	0.23	0.2322	99.77	0.23
.125	0.55231	99.28	0.72	0.35058	99.55	0.45	0.41792	99.54	0.46
.1456	0.85763	98.73	1.27	0.54284	99.20	0.80	0.70553	99.12	0.88
.1697	1.25399	97.87	2.13	0.79192	98.66	1.34	1.11088	98.42	1.58
.1977	1.7288	96.62	3.38	1.09084	97.87	2.13	1.63276	97.31	2.69
.2303	2.2498	94.89	5.11	1.42014	96.78	3.22	2.24289	95.67	4.33
.2683	2.74683	92.64	7.36	1.73611	95.36	4.64	2.85822	93.43	6.57
.3125	3.1033	89.89	10.11	1.96569	93.62	6.38	3.32238	90.57	9.43
.3641	3.23748	86.79	13.21	2.05701	91.65	8.35	3.51229	87.25	12.75
.4242	3.20554	83.55	16.45	2.04368	89.60	10.40	3.48914	83.74	16.26
.4941	3.1381	80.35	19.65	2.00595	87.55	12.45	3.41904	80.25	19.75
.5757	3.06474	77.21	22.79	1.96022	85.55	14.45	3.33437	76.83	23.17
.6707	2.96115	74.14	25.86	1.88836	83.59	16.41	3.19556	73.50	26.50
.7813	2.95621	71.18	28.82	1.86837	81.70	18.30	3.1667	70.30	29.70
.9103	3.13166	68.23	31.77	1.94126	79.83	20.17	3.34941	67.13	32.87
.0604	3.34608	65.10	34.90	2.03532	77.89	22.11	3.5851	63.78	36.22
.2354	3.59684	61.75	38.25	2.1483	75.85	24.15	3.88012	60.20	39.80
.4393	3.86003	58.15	41.85	2.27225	73.71	26.29	4.21187	56.32	43.68
.6767	4.07305	54.29	45.71	2.38252	71.43	28.57	4.49458	52.11	47.89
.9534	4.20667	50.22	49.78	2.47065	69.05	30.95	4.6786	47.61	52.39
.2757	4.2782	46.01	53.99	2.55088	66.58	33.42	4.7841	42.93	57.07
.6512	4.27343	41.73	58.27	2.62489	64.03	35.97	4.78712	38.15	61.85
.0887	4.19634	37.46	62.54	2.70202	61.40	38.60	4.69218	33.36	66.64
.5983	4.06161	33.26	66.74	2.79323	58.70	41.30	4.54249	28.67	71.33
.192	3.89304	29.20	70.80	2.91264	55.91	44.09	4.25232	24.13	75.87
.8837	3.70186	25.31	74.69	3.06551	53.00	47.00	3.91787	19.88	80.12
.6895	3.45887	21.61	78.39	3.25386	49.93	50.07	3.53662	15.96	84.04
.6283	3.1757	18.15	81.85	3.46693	46.68	53.32	3.09453	12.42	87.58
.7219	2.85974	14.97	85.03	3.69702	43.21	56.79	2.60753	9.33	90.67
.996	2.52804	12.11	87.89	3.93469	39.51	60.49	2.10518	6.72	93.28
0.4804	2.19515	9.59	90.41	4.16458	35.58	64.42	1.61949	4.61	95.39
2.2096	1.88086	7.39	92.61	4.37607	31.41	68.59	1.19187	2.99	97.01
4.2242	1.59212	5.51	94.49	4.50483	27.04	72.96	0.84535	1.80	98.20
6.5712	1.3226	3.92	96.08	4.50398	22.53	77.47	0.58219	0.96	99.04
9.3055	1.05308	2.60	97.40	4.32327	18.03	81.97	0.31904	0.37	99.63
2.4909	0.78356	1.54	98.46	3.93241	13.71	86.29	0.05589	0.06	99.94
6.2019	0.51404	0.76	99.24	3.34194	9.77	90.23	0	0.00	100.00
0.5252	0.24453	0.24	99.76	2.61091	6.43	93.57	0	0.00	100.00
5.5618	0	0.00	100.00	1.91278	3.82	96.18	0	0.00	100.00
1.4295	0	0.00	100.00	1.25531	1.91	98.09	0	0.00	100.00
8.2654	0	0.00	100.00	0.6523	0.65	99.35	0	0.00	100.00
6.2292	0	0.00	100.00	0	0.00	100.00	0	0.00	100.00
5.507	0	0.00	100.00	0	0.00	100.00	0	0.00	100.00
6.3157	0	0.00	100.00	0	0.00	100.00	0	0.00	100.00
8.9077	0	0.00	100.00	0	0.00	100.00	0	0.00	100.00
03.5775	0	0.00	100.00	0	0.00	100.00	0	0.00	100.00
20.6678	0	0.00	100.00	0	0.00	100.00	0	0.00	100.00
40.578	0	0.00	100.00	0	0.00	100.00	0	0.00	100.00
63.7733	0	0.00	100.00	0	0.00	100.00	0	0.00	100.00
90.7959	0	0.00	100.00	0	0.00	100.00	0	0.00	100.00
22.2773	0	0.00	100.00	0	0.00	100.00	0	0.00	100.00
58.953	0	0.00	100.00	0	0.00	100.00	0	0.00	100.00
01.6802	0	0.00	100.00	0	0.00	100.00	0	0.00	100.00
51.4575	0	0.00	100.00	0	0.00	100.00	0	0.00	100.00
09.4479	0	0.00	100.00	0	0.00	100.00	0	0.00	100.00
77.0068	0	0.00	100.00	0	0.00	100.00	0	0.00	100.00
55.713	0	0.00	100.00	0	0.00	100.00	0	0.00	100.00
47.4056	0	0.00	100.00	0	0.00	100.00	0	0.00	100.00
54.2275	0	0.00	100.00	0	0.00	100.00	0	0.00	100.00
78.675	0	0.00	100.00	0	0.00	100.00	0	0.00	100.00

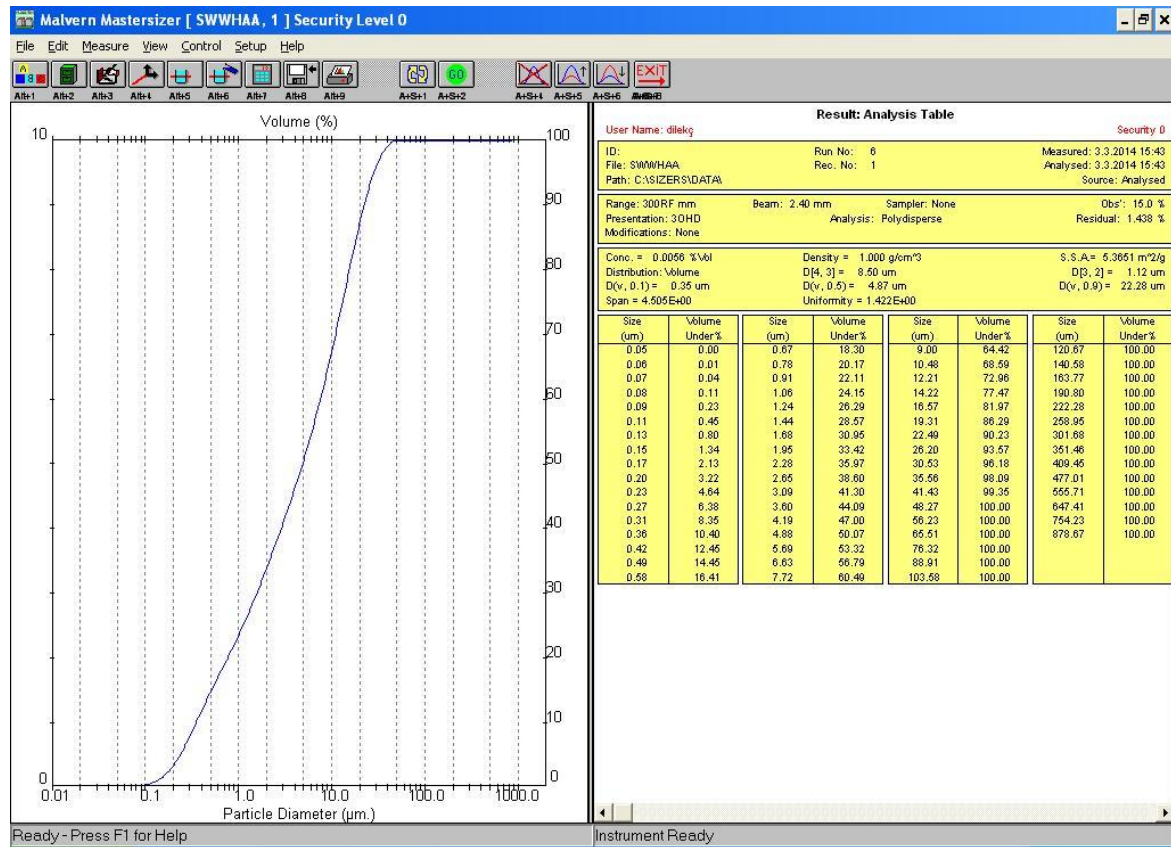


Fig 6. PSD of overflow for wastewater hydrocyclone

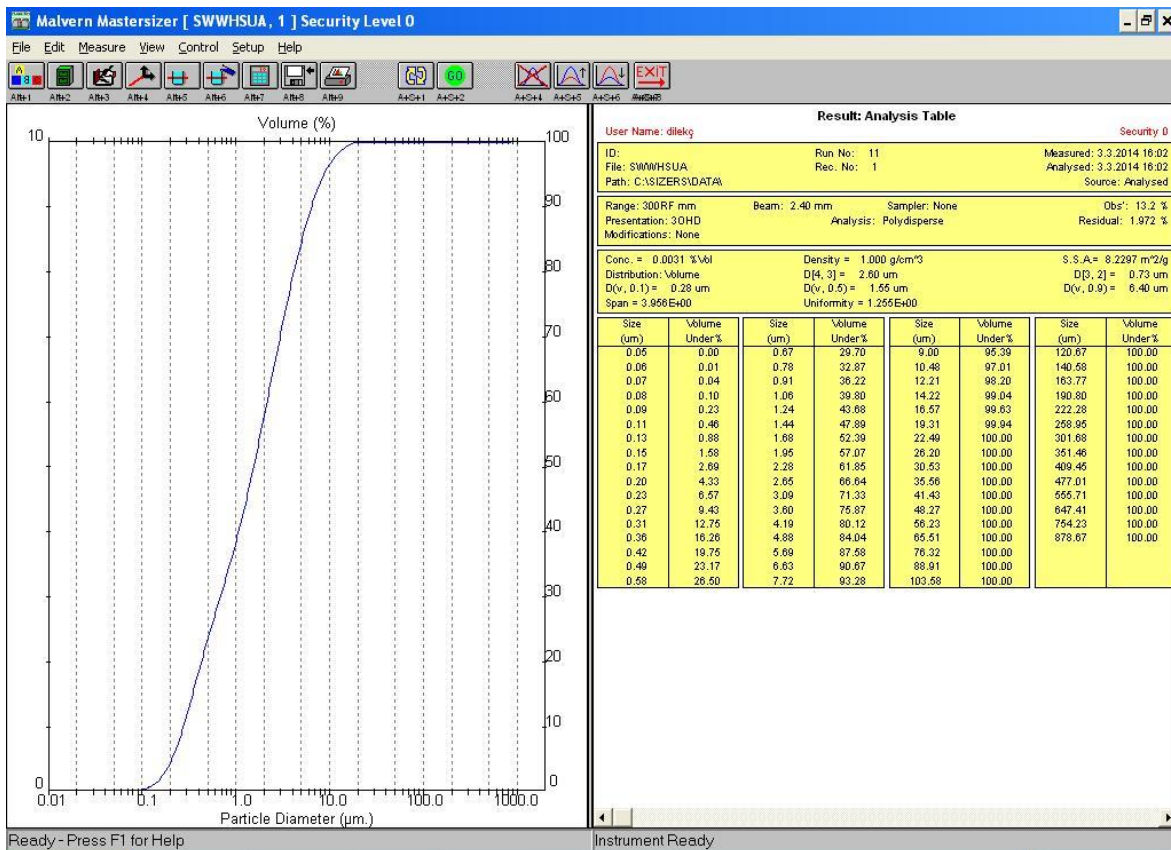


Fig 7. PSD of downstream of wastewater hydrocyclone

Table 4. PSD of feed overflow and downstream of gypsum hydrocyclone

Size, μm	Feed			Downstream			Overflow		
	Amount (%)	Cumulative oversize (%)	Cumulative Undersize (%)	Amount (%)	Cumulative oversize (%)	Cumulative Undersize (%)	Amount (%)	Cumulative oversize (%)	Cumulative Undersize (%)
<i>*SIZES*</i>	<i>*RESULT*</i>	$\Sigma (+)$ (%)	$\Sigma (-)$ (%)	<i>*RESULT*</i>	$\Sigma (+)$ (%)	$\Sigma (-)$ (%)	<i>*RESULT*</i>	$\Sigma (+)$ (%)	$\Sigma (-)$ (%)
0.0582	0.00009	100.00		0.00011	100.00		0.0225	100.00	
0.0679	0.00029	100.00	0.00	0.00033	100.00	0.00	0.05548	99.98	0.02
0.0791	0.00081	100.00	0.00	0.00086	100.00	0.00	0.10814	99.92	0.08
0.0921	0.00218	100.00	0.00	0.00216	100.00	0.00	0.19493	99.81	0.19
0.1073	0.00584	100.00	0.00	0.0054	100.00	0.00	0.33596	99.62	0.38
0.125	0.01509	99.99	0.01	0.01299	99.99	0.01	0.55231	99.28	0.72
0.1456	0.03604	99.98	0.02	0.02918	99.98	0.02	0.85763	98.73	1.27
0.1697	0.07826	99.94	0.06	0.06028	99.95	0.05	1.25399	97.87	2.13
0.1977	0.15407	99.86	0.14	0.11428	99.89	0.11	1.7288	96.62	3.38
0.2303	0.27491	99.71	0.29	0.19872	99.77	0.23	2.2498	94.89	5.11
0.2683	0.43812	99.43	0.57	0.31227	99.58	0.42	2.74683	92.64	7.36
0.3125	0.60424	98.99	1.01	0.43021	99.26	0.74	3.1033	89.89	10.11
0.3641	0.71657	98.39	1.61	0.51612	98.83	1.17	3.23748	86.79	13.21
0.4242	0.7742	97.67	2.33	0.56835	98.32	1.68	3.20554	83.55	16.45
0.4941	0.82854	96.90	3.10	0.61985	97.75	2.25	3.1381	80.35	19.65
0.5757	0.88268	96.07	3.93	0.6703	97.13	2.87	3.06474	77.21	22.79
0.6707	0.89612	95.19	4.81	0.68687	96.46	3.54	2.96115	74.14	25.86
0.7813	0.92615	94.29	5.71	0.7061	95.77	4.23	2.95621	71.18	28.82
0.9103	0.94498	93.37	6.63	0.69228	95.07	4.93	3.13166	68.23	31.77
1.0604	0.97399	92.42	7.58	0.6817	94.37	5.63	3.34608	65.10	34.90
1.2354	1.01031	91.45	8.55	0.66923	93.69	6.31	3.59684	61.75	38.25
1.4393	1.04895	90.44	9.56	0.65514	93.02	6.98	3.86003	58.15	41.85
1.6767	1.06633	89.39	10.61	0.6362	92.37	7.63	4.07305	54.29	45.71
1.9534	1.06704	88.32	11.68	0.62545	91.73	8.27	4.20667	50.22	49.78
2.2757	1.08609	87.25	12.75	0.64502	91.11	8.89	4.2782	46.01	53.99
2.6512	1.11587	86.17	13.83	0.6882	90.46	9.54	4.27343	41.73	58.27
3.0887	1.14576	85.05	14.95	0.74472	89.77	10.23	4.19634	37.46	62.54
3.5983	1.16477	83.91	16.09	0.80082	89.03	10.97	4.06161	33.26	66.74
4.192	1.16767	82.74	17.26	0.84991	88.23	11.77	3.89304	29.20	70.80
4.8837	1.15186	81.57	18.43	0.89251	87.38	12.62	3.70186	25.31	74.69
5.6895	1.1259	80.42	19.58	0.94209	86.48	13.52	3.45887	21.61	78.39
6.6283	0.80059	79.30	20.70	1.02531	85.54	14.46	3.1757	18.15	81.85
7.7219	0.8181	78.50	21.50	1.19071	84.52	15.48	2.85974	14.97	85.03
8.996	0.94013	77.68	22.32	1.49668	83.33	16.67	2.52804	12.11	87.89
10.4804	1.20961	76.74	23.26	1.9949	81.83	18.17	2.19515	9.59	90.41
12.2096	1.69033	75.53	24.47	2.72773	79.83	20.17	1.88086	7.39	92.61
14.2242	2.44522	73.84	26.16	3.71456	77.11	22.89	1.59212	5.51	94.49
16.5712	3.50906	71.39	28.61	4.92738	73.39	26.61	1.3226	3.92	96.08
19.3055	4.8579	67.88	32.12	6.28451	68.47	31.53	1.05308	2.60	97.40
22.4909	6.37249	63.03	36.97	7.65612	62.18	37.82	0.78356	1.54	98.46
26.2019	7.85091	56.65	43.35	8.91463	54.52	45.48	0.51404	0.76	99.24
30.5252	9.1117	48.80	51.20	9.99977	45.61	54.39	0.24453	0.24	99.76
35.5618	10.10905	39.69	60.31	9.7558	35.61	64.39	0	0.00	100.00
41.4295	9.38766	29.58	70.42	8.6601	25.85	74.15	0	0.00	100.00
48.2654	7.78204	20.19	79.81	6.94389	17.19	82.81	0	0.00	100.00
56.2292	5.71574	12.41	87.59	4.97958	10.25	89.75	0	0.00	100.00
65.507	3.63587	6.70	93.30	3.09902	5.27	94.73	0	0.00	100.00
76.3157	1.94854	3.06	96.94	1.58944	2.17	97.83	0	0.00	100.00
88.9077	0.84013	1.11	98.89	0.58222	0.58	99.42	0	0.00	100.00
103.5775	0.2712	0.27	99.73	0	0.00	100.00	0	0.00	100.00
120.6678	0	0.00	100.00	0	0.00	100.00	0	0.00	100.00
140.578	0	0.00	100.00	0	0.00	100.00	0	0.00	100.00
163.7733	0	0.00	100.00	0	0.00	100.00	0	0.00	100.00
190.7959	0	0.00	100.00	0	0.00	100.00	0	0.00	100.00
222.2773	0	0.00	100.00	0	0.00	100.00	0	0.00	100.00
258.953	0	0.00	100.00	0	0.00	100.00	0	0.00	100.00
301.6802	0	0.00	100.00	0	0.00	100.00	0	0.00	100.00
351.4575	0	0.00	100.00	0	0.00	100.00	0	0.00	100.00
409.4479	0	0.00	100.00	0	0.00	100.00	0	0.00	100.00
477.0068	0	0.00	100.00	0	0.00	100.00	0	0.00	100.00
555.713	0	0.00	100.00	0	0.00	100.00	0	0.00	100.00
647.4056	0	0.00	100.00	0	0.00	100.00	0	0.00	100.00
754.2275	0	0.00	100.00	0	0.00	100.00	0	0.00	100.00
878.675	0	0.00	100.00	0	0.00	100.00	0	0.00	100.00

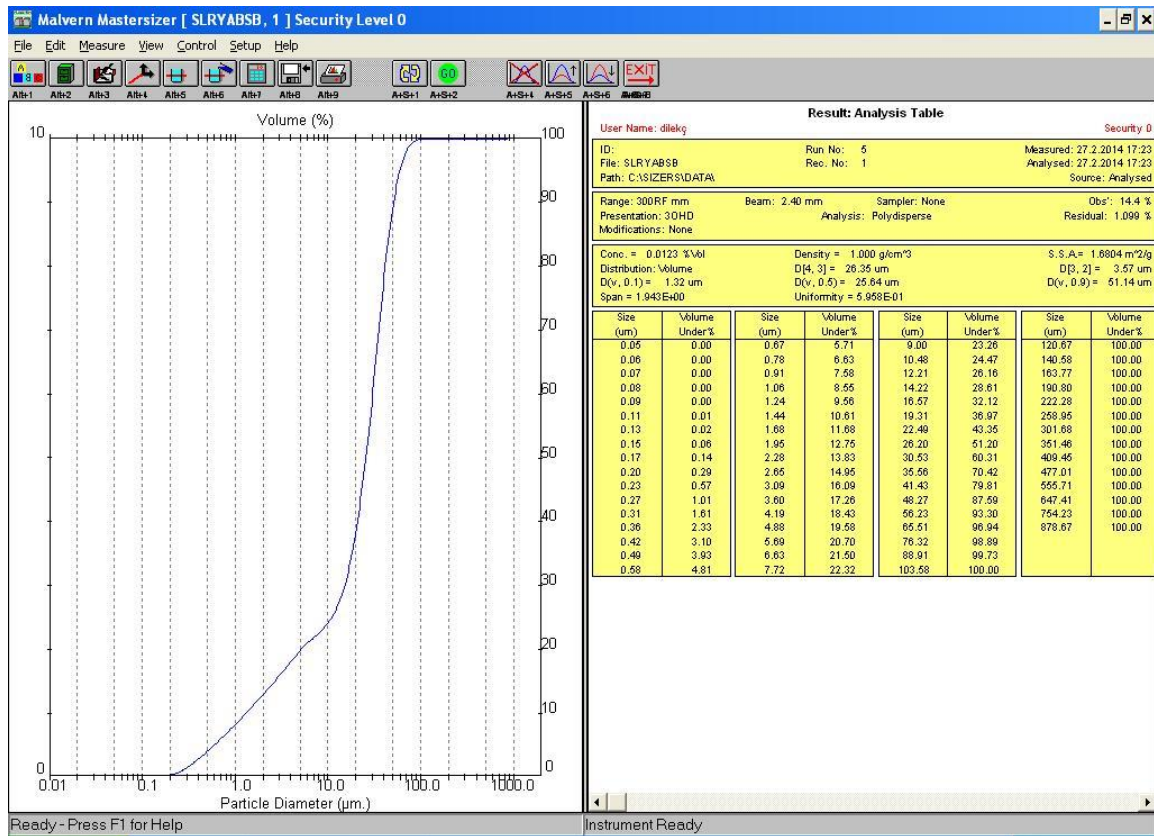


Fig 8. PSD of feed to gypsum hydrocyclone

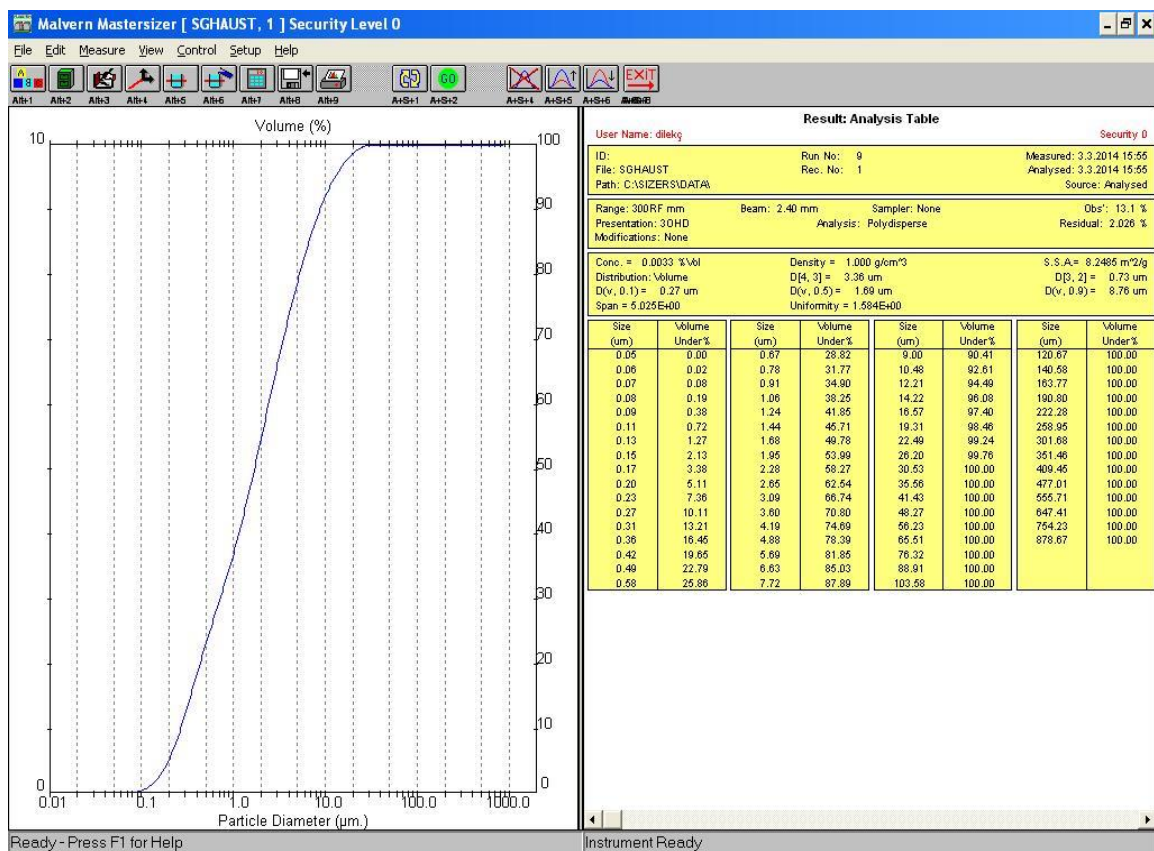


Fig 9. PSD of overflow for gypsum hydrocyclone

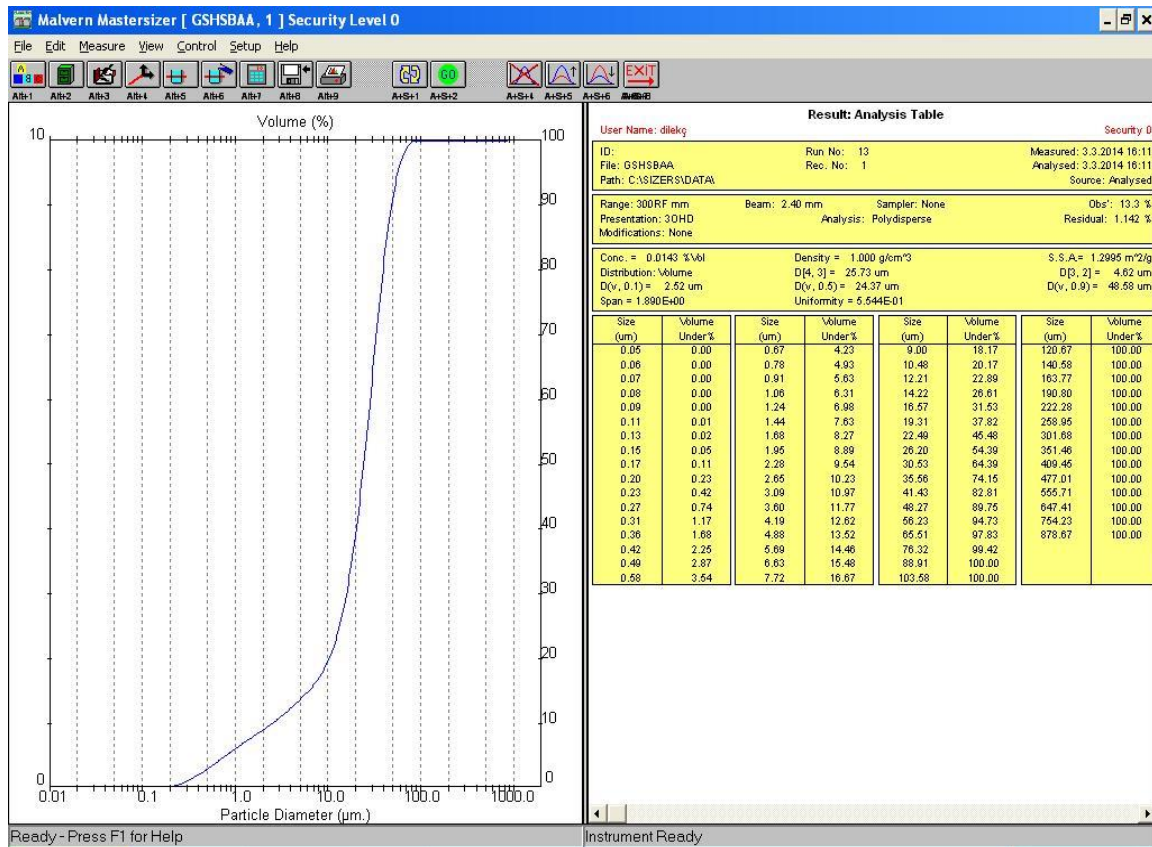


Fig 10. PSD of downstream for gypsum hydrocyclone

4. CONCLUSIONS

In this study, separation efficiencies of gypsum and waste water hydrocyclones in WFGD system in a power plant were calculated. In order to carry out separation efficiency calculation, raw data of particle size analysis carried out with Malvern Mastersizer for each sample (a total of 5) was employed. Respective percentages of overflow and downstream for each hydrocyclone were obtained from this raw data. Separation efficiency for gypsum hydrocyclone was calculated as 77.5 % while it was calculated as 4.0 % for waste water hydrocyclone. Based on the results obtained, it can be emphasized that more analysis on each hydrocyclone especially on waste water hydrocyclone should be carried out. Referring to the study of Dwari et al., [17] separation efficiency is very little for the particles below 60 µm. Although low separation efficiency for fine particles might be understandable, there is a strong requirement of possible increase in terms of environment. This study would be very helpful for future studies on waste water purification systems in power plants and separation efficiency on hydrocyclones.

REFERENCES

[1]. Y. Zhong, X. Gao, W. Huo, Z. Luo, M. Ni and K. K. Cen, "A model for performance optimization of wet flue gas desulfurization systems of power plants," *Fuel Processing Technology*, Vol. 89 (11), pp.1025-1032, 2008.

[2]. P. S. Nolan, K. E. Redinger, G. T. Amrhein and G. A. Kudlac, "Demonstration of additive use for enhanced mercury emissions control in wet FGD systems," *Fuel Processing Technology*, Vol. 85 (6-7), pp. 587-600, 2004

[3]. H. G. Nygaard, S. Kiil, J. E. Johnsson, J. N. Jensen, J. Hansen, F. Fogh and K. D. Johansen, "Full-scale measurements of SO₂ gas phase concentrations and slurry compositions in a wet flue gas desulphurisation spray absorber," *Fuel*, Vol. 83 (9), pp. 1151-1164, 2004.

[4]. D. S. Jin, B. R. Deshwal, Y. S. Park and H. Y. Lee, "Simultaneous removal of SO₂ and NO by wet scrubbing using aqueous chlorine dioxide solution," *Journal of Hazardous Materials*, Vol. 135 (1-3), pp. 412-417, 2006.

[5]. M. Bilen, S. Kizgut and I. Toroglu, "Wastewater treatment with hydrocyclones in power plants," In: *EWMS Eurasia Waste Management Symposium*, Istanbul Turkey, 2016.

[6]. C. Y. Hsu, S. J. Wu and R. M. Wu, "Particle Separation and tracks in a hydrocyclone," *Tamkang Journal of Science and Engineering*, Vol.14 (1), pp. 65-70, 2011.









[7]. H. Jun, A. Lian-suo and W. Zhi-quan, "Study on Application and Operation Optimization of Hydrocyclone for Solid-liquid Separation in Power Plant," In: *Proceedings of the World Congress on Engineering and Computer Science Vol 1*, WCECS 2009, San Francisco, USA, October 20-22, 2009.

- [8]. K.J. Hwang and S.P. Chou, "Designing vortex finder structure for improving the particle separation efficiency of a hydrocyclone," *Separation and Purification Technology*, Vol. 172, pp. 76-84, 2017.
- [9]. G. Zhu, J.L. Liow and A. Neely, "Computational study of the flow characteristics and separation efficiency in a mini-hydrocyclone," *Chemical Engineering Research and Design*, Vol. 90 (12), pp. 2135-2147, 2012.
- [10]. J.C. Cullivan, R. A. Williams, C.R. Cross, "Understanding the hydrocyclone separator through computational fluid dynamics," *Transactions of the Institution of Chemical Engineers: Part A*, Vol.81, pp. 455-466, 2003.
- [11]. J.C. Cullivan, R. A. Williams, T. Dyakowski and C.R. Cross, "New understanding of a hydrocyclone flow field and separation mechanism from computational fluid dynamics," *Minerals Engineering*, Vol. 17, pp. 651-660, 2004.
- [12]. C.A.O. Rocha, G. Ullmann, D.O. Silva and L.G.M. Vieira, "Effect of changes in the feed duct on hydrocyclone performance", *Powder Technology*, Vol. 374, pp. 283-289, 2020.
- [13]. S. M. Mousavian and A.F. Najafi, "Influence of geometry on separation efficiency in a hydrocyclone", *Archieve of Applied Mechanics*, Vol. 79, pp. 1033-1050, 2009.
- [14]. L.Y. Chu, W.M. Chen and X.Z. Lee, "Effect of structural modification on hydrocyclone performance", *Separation and Purification Technology*, Vol. 21 (1-2), pp.71-86, 2000.
- [15]. F. Boylu, K. Çinku, F. Esenli and M.S. Çelik, "The separation efficiency of Na-bentonite by hydrocyclone and characterization of hydrocyclone products," *International Journal of Mineral Processing*, Vol.94 (3-4), pp. 196-202, 2010.
- [16]. A.F. Nowakowski, J.C. Cullivan, R.A. Williams and T. Dyakowski, "Application of CFD to modeling of the flow in hydrocyclones. Is this a realizable option or still a research challenge," *Minerals Engineering*, Vol. 17, pp. 661-669, 2004.
- [17]. R. K. Dwari, M. N. Biswas and B. C. Meikap, "Performance characteristics for particles of sand FCC and fly ash in a novel hydrocyclone," *Chemical Engineering Science*, Vol. 59 (3), pp. 671-684, 2004.
- [18]. J. Yu and J. Fu, "Separation performance of an 8 mm mini hydrocyclone and its application to the treatment of rice starch wastewater," *Separation Science and Technology*, Vol. 55 (2), pp. 313-320, 2020.
- [19]. P.B. Fu, F. Wang, X.J. Yang, L. Ma, X. Cui, H.L. Wang, "Inlet particle sorting cyclone for the enhancement of PM2.5 separation", *Environmental Science & Technology*, Vol. 51 (3), pp. 1587-1594, 2017.
- [20]. I. Karagoz, A. Avci, A. Surmen and O Sendogan, "Design and performance evaluation of a new cyclone separator", *Journal of Aerosol Science*, Vol. 59, pp.57-64, 2013.
- [21]. L.G.M. Vieira and M.A.S. Barrozo, "Effect of vortex finder diameter on the performance of a novel hydrocyclone separator", *Minerals Engineering*, Vol. 57, pp. 50-56, 2014.
- [22]. K. Elsayed, and C. Lacor, "The effect of cyclone inlet dimensions on the flow pattern and performance," *Applied Mathematical Modelling*, Vol.35 (4), pp.1952-1968, 2011.
- [23]. J.X. Yang, G.G. Sun and C.Z. Gao, "Effect of the inlet dimensions on the maximum efficiency cyclone height," *Separation and Purification Technology*, Vol.105, pp. 15-23, 2013.
- [24]. L. Ni, J.Y. Tian and J.N. Zhao, "Experimental study of the effect of underflow pipe diameter on separation performance of a novel de-foulant hydrocyclone with continuous underflow and reflux function", *Separation and Purification Technology*, Vol. 171, pp. 270-279, 2016.
- [25]. L. Ji, S. Kuang, Z. Qi, Y. Wang, J. Chen and A. Yu, "Computation analysis and optimization of hydrocyclone size to mitigate adverse effect of particle density," *Separation and Purification Technology*, Vol.174, pp.251-263, 2017.



RESEARCH ARTICLE

Pre-irradiation grafting of acrylic acid and sodium styrene sulfonate on non-woven polyethylene fabric for heavy metal removal

Nazia Rahman^{1,*} , Md. Imran Biswas² , Mahbub Kabir² , Nirmal Chandra Dafader¹ , Shahnaz Sultana¹ , Md. Nabul Sardar¹ , Farah Tasneem Ahmed¹ , Abdul Halim¹ 

¹Nuclear and Radiation Chemistry Division, Institute of Nuclear Science and Technology, Atomic Energy Research Establishment, Bangladesh Atomic Energy Commission, G. P. O. Box-3787, Dhaka, BANGLADESH

²Department of Chemistry, Jahangirnagar University, Savar, Dhaka-1342, BANGLADESH

ABSTRACT

In present study acrylic acid (AAc) and sodium styrene sulfonate (SSS) were grafted onto non-woven polyethylene fabric using pre-irradiation method and the grafted adsorbent is employed for Cr(III) and Pb(II) adsorption. After irradiation of the non-woven polyethylene fabrics with 50 kGy radiation dose the grafting reaction was carried out at 80° C with monomer solution consisted of 30% AAc, 10% SSS and 4% NaCl in water. A high graft yield of 270% was achieved. Fourier Transform Infrared, Scanning Electron Microscopy and Thermo-gravimetric Analysis were used to analyze the adsorbent. Pb (II) and Cr (III) adsorption from synthetic aqueous solution was attempted by the grafted adsorbent. Adsorption study was accomplished by changing the contact time, pH and initial metal ion concentration. Contact time 48 h and initial metal concentration 1000 ppm were found optimum for all the metal ions studied. pH 6.2 and 5 was observed best for Pb (II) and Cr(III) adsorption respectively. Kinetic adsorption data fitted better with pseudo-second-order equation than pseudo-first-order. Good correlation of experimental data with Langmuir isotherm model suggested monolayer adsorption. Langmuir equation showed that the maximum adsorption capacity for Pb (II) was 38.46 mg g⁻¹ and Cr (III) was 111.11 mg g⁻¹. Experiment on desorption of metal ions and reuse of the adsorbent depicted good results. Adsorbent also showed efficient adsorption of Cr(III) from real waste water. From all the findings it can be expected that the AAc-SSS grafted PE fabric can successfully eliminate Cr(III) and Pb(II) from industrial waste water.

Keywords: Heavy metal, acrylic acid, sodium styrene sulfonate, adsorption, wastewater

1. INTRODUCTION

Environmental contamination arise from discharge of toxic heavy metals in industrial wastewater is a severe global crisis we are experiencing these days. Environmental purity is now a days the major concern [1-2]. Heavy metals commonly generate from metal mineral treating, leather tanning, metallurgical process, glass manufacture, mining action, metal plating, and battery production etc. [3]. Compact structure and harmfulness made the heavy metals are different from other metals. Another alarming matter about heavy metal is their non- biodegradability. They are also unaffected by bacterial breakdown. Natural environment and human health suffer a humongous

danger due to the presence of these heavy metals in water. Because heavy metals have tendency to form complexes with organic matters that can be fatal at little quantities too. Noxious nature of heavy metals, their perseverance in environment and bioaccumulation extremely disturbs the food sequence [4]. After entering into the food chain heavy metals can influence various harmful biochemical reactions and after certain period they can also gather inside living organisms. Therefore, eliminating heavy metals from industrial effluent before their discharge into water stream has given utmost priority in different countries recently.

Harmful heavy metals that are usually inspected are Lead, Copper, Nickel, Cadmium, Mercury and Chromium. Among these, Lead and Chromium are the

Corresponding Author: naziabaec@gmail.com (Nazia Rahman)

Received 19 November 2020; Received in revised form 18 February 2021; Accepted 12 March 2021

Available Online 23 March 2021

Doi: <https://doi.org/10.35208/ert.828089>

© Yildiz Technical University, Environmental Engineering Department. All rights reserved.

groundwater pollutants that are generally discharged from different industries. Leather industry that is one of the major industries in Bangladesh also generates effluents containing large amount of Chromium. 90% of the tanneries in Bangladesh use chrome tanning method. However, in the course of the chrome tanning method, 40% unemployed chromium salts are commonly discharged in the final effluents initiating a serious hazard to the environment. Various interpretations showed that average amount of chromium produced in the effluent of chrome tanning process varies between 2000 to 5000 mg L⁻¹. Composite effluents generated from a tannery can comprise 100-250 mg L⁻¹ of chromium. Most of these effluents are discharged into the nearby water bodies without proper pre-treatment which leads to severe environment pollution. At present most of the tannery uses chromium (III) salts as a tanning agent which does not possess as much threat as chromium (VI) at low concentration. But recent studies revealed that under certain legend conditions, Cr (III) can be toxic at higher concentration [5]. Lead is also found in leather waste water. High level of Lead exposure can cause anemia, weakness, and damage of kidney and brain. Very high Lead exposure can be deadly. Low level of lead exposure may harm different biochemical procedures and psychological activities [6].

Recent technologies applied for heavy metal removal are chemical precipitation, complex-formation, oxidation-reduction, evaporation, electro-deposition and the liquid-liquid surface extraction, membrane separation, reverse osmosis, and adsorption. Most of these techniques are expensive and also unsuccessful when the concentration of heavy metal cation is low. Adsorption is considered as the most effective, cheap, convenient and widely used method for the removal of hazardous heavy metals from wastewater [7-8]. A good number of researches have been conducted on the elimination of toxic metals or dyes using adsorption process [9-15].

Recently, elimination of heavy metal from aqueous solution using graft polymers has become a new approach [16-26]. High value of adsorption capacity of the adsorbent and ability to reuse reduces the probability of secondary pollution. Graft polymer is formed by covalent bonding of monomers with appropriate functionality onto the parent polymer chain. The achievement of graft polymerization is that it allows combination of various functions of the grafted monomer to the parent polymer without affecting the mechanical properties of the parent polymer [27-28]. Radiation-induced grafting is more suitable than other methods for example plasma treatment, oxidation of polymers, decomposition of chemical initiators etc., due to the high penetration ability of ionization radiation into the polymer matrix that induces quick and regular formation of radicals [29].

The trunk polymer utilized to prepare metal adsorbent in present study is non-woven polyethylene. Numerous researches have reported elimination of toxic heavy metal ions by monomer grafted polyethylene (PE) [30-34]. In present study the preparation of a new adsorbent based on non-woven PE fabric were attempted by radiation grafting

technique using binary monomers acrylic acid (AAc) and sodium styrene sulfonate (SSS). The prepared adsorbent is also investigated for adsorption of Pb(II) and Cr(III) from synthetic aqueous solution. The grafted fabric was analyzed by Fourier Transform Infrared (FTIR), Scanning Electron Microscopy (SEM) and Thermo-gravimetric Analysis (TGA). Adsorption capacity of the adsorbent for Cr(III) and Pb(II) was investigated under different environments by changing the contact time, pH and initial metal ion concentration. The kinetics and isotherm of Pb(II) and Cr(III) adsorption were investigated using established models.

2. MATERIALS AND METHOD

2.1. Reagents and materials

The trunk polymer used for making grafted adsorbent was non-woven polyethylene (PE) fabric collected from Kurashiki Textile Manufacturing Co. Ltd. Acrylic acid and sodium styrene sulfonate procured from Sigma Aldrich (USA) were utilized as monomers to graft onto PE. NaOH, NaCl, and HCl were supplied by Merck, Germany. Pb(NO₃)₂ and Cr(NO₃)₃·9H₂O (Merck, Germany) were used in the adsorption experiments.

2.2. Preparation of the adsorbent

The non-woven PE films were subjected to gamma ray irradiation at 50 kGy radiation dose at an ambient temperature. The Cobalt-60 gamma source utilized was a Panoramic Irradiator of 90 kCi Batch Type supplied by BRIT, India. The irradiator activity was 50 kCi and the dose rate used was 13 kGy h⁻¹. The irradiated PE films were stored at dry-ice condition until next use. The monomer solution consisted of 30 % AAc, 10 % SSS and 4 % NaCl in distilled H₂O were bubbled with argon gas to eliminate dissolved oxygen. The de-aerated monomer solution was poured into glass bottle containing irradiated PE films. After the glass bottle was fulfilled with monomer solution, it was securely closed with a lid to escape invasion of oxygen from the air into the monomer solution. Subsequently the grafting reaction was conducted in a water bath at temperature 80°C for 4 h. After that, the grafted PE fabric was washed properly to remove remaining monomer and homopolymer. The degree of grafting was determined by the following formula:

$$\text{Degree of grafting (\%)} = \frac{W_1 - W_0}{W_0} \times 100 \quad (1)$$

Where, W₁ is the dry weight of the grafted PE film and W₀ is the dry weight of the pristine PE film.

The grafted PE films were treated with 1M NaOH at room temperature for 20 minutes. The NaOH treatment is done to ionize the functional groups of the grafted film to improve the metal adsorption.

2.3. Metal ion adsorption by the adsorbent form synthetic wastewater

0.1 g of the adsorbent was dipped in the 50 mL aqueous solutions of Lead (II), and Chromium (III)

separately at 25°C. The adsorption studies were repeated at various times of contact, pH and initial metal ion concentrations. HCl and NaOH solutions were used to adjust the pH of the solutions. Atomic Absorption Spectroscopy were utilized to detect metal ion concentration in the solutions before and after dipping of adsorbent. Using the following formula adsorption capacity of the adsorbent was calculated,

$$Q_0 = \frac{C_1 - C_2}{W} \times V \quad (2)$$

Here,

Q_0 = Adsorption capacity of the adsorbent (mg g^{-1})

W = Mass of dry adsorbent (g)

V = Volume of Metal ion solution (L)

C_1 = Initial concentration of metal ions (mg L^{-1})

C_2 = Final concentration of metal ions after adsorption (mg L^{-1})

2.4. Desorption of metals ions and reuse of adsorbent

Pb(II) and Cr(III) were desorbed from the adsorbent by treatment with 2 M HCl and 2M NaOH respectively for 24 hours. The formula used to calculate desorption percentage is given below:

$$\text{Percentage of desorption} = \frac{\text{Desorbed ions (mg)}}{\text{Adsorbed ions (mg)}} \times 100 \quad (3)$$

After desorption of the metal ions, the adsorbent was reused for metal ion adsorption.

2.5. Adsorption of Cr from real wastewater

Two types of waste water were collected from savar tannery industrial estate. The preliminary properties of the waste waters were as follows: (1) Waste water before treatment (raw waste water): Colour: Deep blue, Odour: Pungent, pH: 7.76, EC: 8.98 mS cm^{-1} (2) Waste water after treatment by conventional (precipitation) method: Color: Light yellow, Odor: No bad odor, pH: 8.2, EC: 1. mS cm^{-1} . The waste waters were digested and then used for adsorption of Cr by the prepared adsorbent. Initial Cr concentration of waste water before treatment (raw waste water) was 1200 mg L^{-1} and initial Cr concentration of waste water after treatment by conventional method was 4 mg L^{-1} .

3. RESULTS AND DISCUSSION

3.1. Preparation and characterization of adsorbent

We have grafted acrylic acid (AAc) and sodium styrene sulfonate (SSS) onto non-woven polyethylene fabric by pre-irradiation method using gamma rays from Co-60 source at room temperature (25°C). At first the non-woven PE polymer backbone was subjected to gamma irradiation to form primary free radicals. Then, the monomer solution was added to the irradiated polymer for grafting. In the reaction graft growing chain and termination reaction was occurred. Finally the graft copolymer was produced. In pre-irradiation technique, monomer is not irradiated directly and formation of homo polymer is relatively lower than simultaneous irradiation technique. A simplified mechanism of grafting is shown in Fig 1. 30 % AAc, 10 % SSS and 4 % NaCl in water was selected as the optimum composition of monomer solution for grafting. The radiation dose applied was 50 kGy. The graft yield achieved under this condition was 270 %. The grafted fabric was analyzed using Fourier Transform Infrared (FTIR), Scanning Electron Microscopy (SEM) and Thermo-gravimetric Analysis (TGA).

3.1.1. FTIR analysis of prepared adsorbent

The IR spectra of PE fabric and grafted PE fabric is shown in Fig 2. The distinctive features of the IR spectra of PE films are due to its C-H stretching and bending vibration. Strong peaks for C-H asymmetric and symmetric stretching were detected at 2910 and 2845 cm^{-1} respectively with weak C-H bending vibration at 1463 cm^{-1} . In grafted PE film, absorption band at 2917, 2848 and 1456 cm^{-1} corresponds to C-H asymmetric and symmetric stretching and C-H bending vibration. A strong absorption band is found at 1738 cm^{-1} that denotes C=O group of acrylic acid. Peak at 1565 and 1370 cm^{-1} results from COO⁻ and CH group of sodium acrylate [35]. Peaks at 1212 and 1010 cm^{-1} could be assigned to the SO₃⁻ group antisymmetric and symmetric vibrational adsorption peaks, respectively [36]. Strong absorption bands of C=O (carboxylic acid) and S=O (sulfonate) group indicates the grafting AAc and SSS on in PE film respectively. The presence of peak for COO⁻ group of sodium acrylate indicates the modification of acid group that increases the metal adsorption.

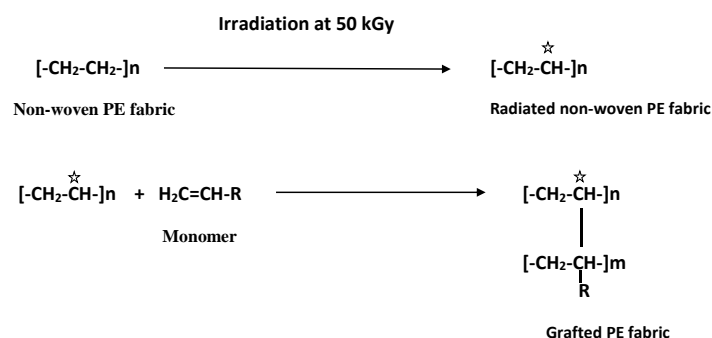


Fig 1. Simplified grafting mechanism

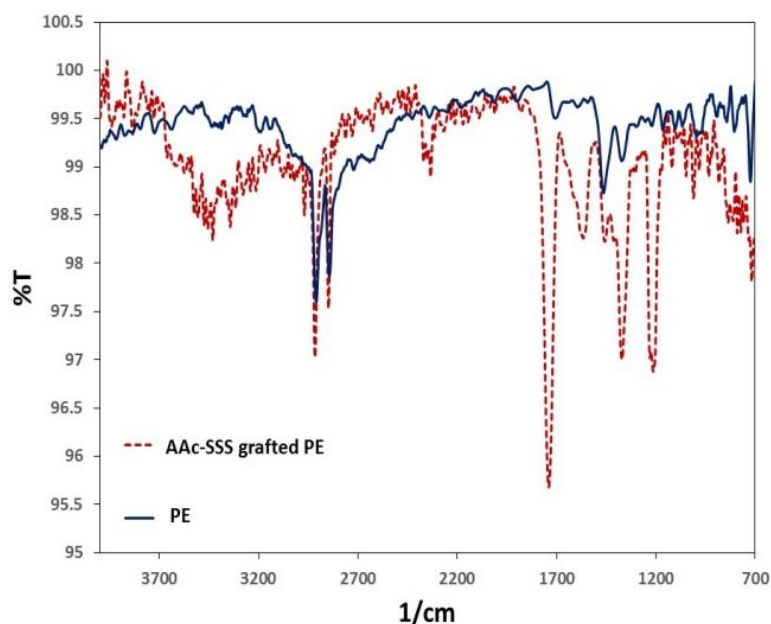


Fig 2. FTIR spectra of PE and grafted Aac-SSS grafted PE

3.1.2. SEM analysis of the adsorbent

Scanning Electron microscopy of nonwoven PE, AAC and SSS grafted PE were analyzed by SEM to relate the physical characteristic of nonwoven PE, AAC and SSS grafted PE. The SEM images of non-woven PE are shown in Fig 3(a), (c) and the SEM image of AAC-SSS grafted PE are shown in Fig 3 (b) and (d). The SEM images of the nonwoven PE fabrics depict transformation of the physical appearance after grafting with AAC and SSS. It seems that a layer of grafted chains covered the surface of PE. The coverage of the surface of polymer with grafted chain is observed in previous study [37]. The grafted surface looks more closely netted due to the grafted chains that represent physical indications of the grafting.

3.1.3. TGA analysis of the adsorbent

The thermo-gravimetric analysis (TGA) thermo-grams for PE fabric and AAC/SSS-PE adsorbent are shown in Fig 4. The weight loss of grafted PE is higher than original PE upto 400°C and after 400°C the weight loss of grafted PE is lower than original PE. The original PE film shows thermal stability up to 200°C and above 200°C it starts to decompose. It shows a three decomposition steps, i.e., 200°C– 255°C, 255°C–499°C and above 499°C. There are six weight loss steps in the TGA curve for AAC/SSS-PE fabric adsorbent. The first weight loss appearing in the temperature range 26°C–129°C is easily understood to be due to the loss of moisture absorbed from air. The weight loss stages at 129°C–222°C, 222°C–376°C, 376–427°C, 427–481°C and above 481°C originated from degradation of grafted chain and degradation of PE.

3.2. Metal ions adsorption by the prepared grafted adsorbent using synthetic wastewater

3.2.1. Variation of metal ion adsorption with change of pH

pH is a key factor to influence the adsorption of metal ions on an adsorbent. The configuration of functional groups present on surface of the adsorbent alters with pH change and this factor affects the adsorption capacity. Fig 5 shows the variation of adsorption capacity of Cr(III) and Pb(II) with the pH variant. pH 6.2 and 5 were optimum for Pb(II), and Cr(III) respectively. Fig 5(b) shows acceleration of the adsorption capacity with the rise of pH from 3 to 5. When the pH is low, large amount of hydrogen ions occupy the surface of the adsorbent and it resists the progression of positively charged metal ions to the functional groups on the adsorbent surface. Again when the pH raised (higher than 5 for Cr(III) and higher than 6.2 for Pb(II)) precipitates of hydroxides of Pb(II) and Cr(III) were produced and as a result the adsorption capacity decreased.

3.2.2. Change of adsorption capacity of the adsorbent with variation of metal ion concentration

Fig 6 shows how the initial concentration of metal ion affects the adsorption capacity of the adsorbent. The figure presents that with the acceleration of initial concentration of metal ions the adsorption capability raises and it reaches the equilibrium value at a high concentration of metal ions. The main cause behind this result is that the reaction sites on the surface of the adsorbent becomes saturated at the certain higher concentration. When the reaction sites are occupied there remains no sites accessible for additional adsorption of metal ions.

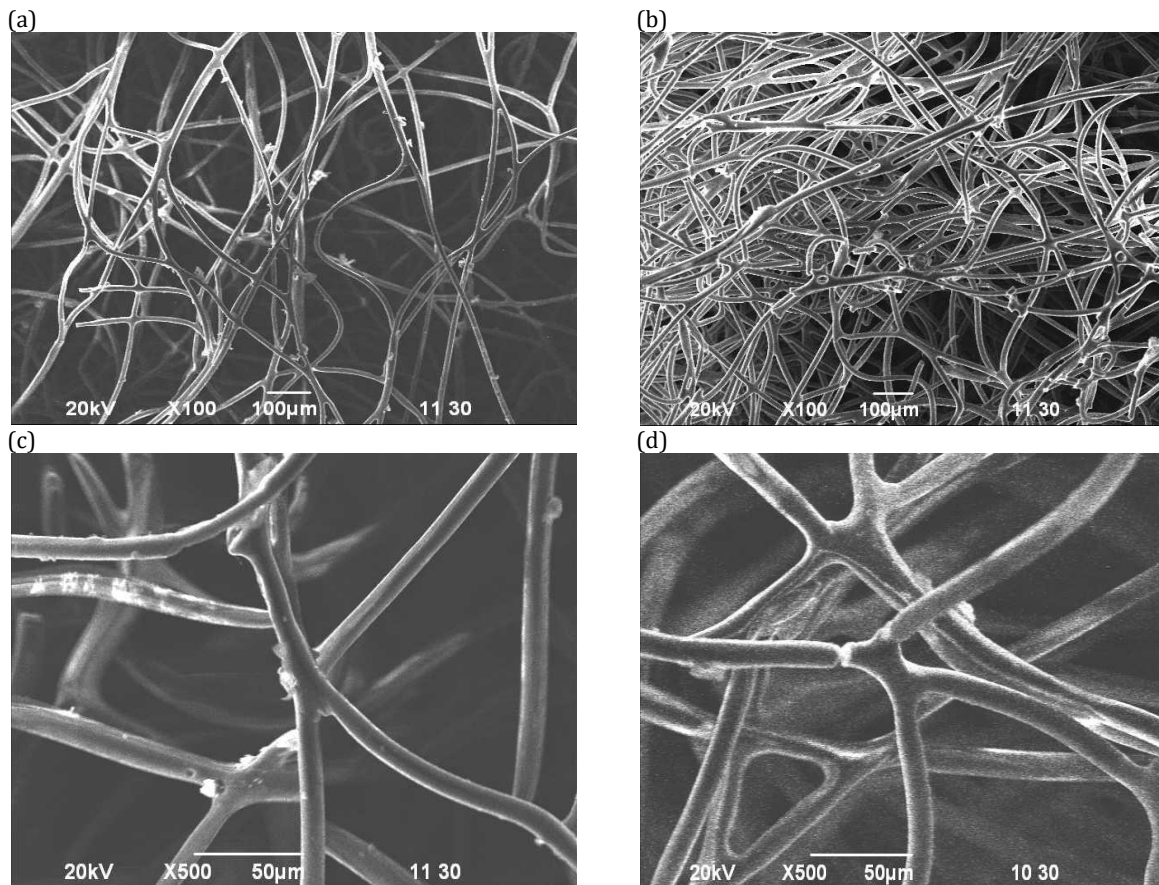


Fig 3. SEM image of non woven PE (a) before grafting (magnification X100) (b) after grafting (magnification X100) (c) before grafting (magnification X500) (d) after grafting (magnification X500)

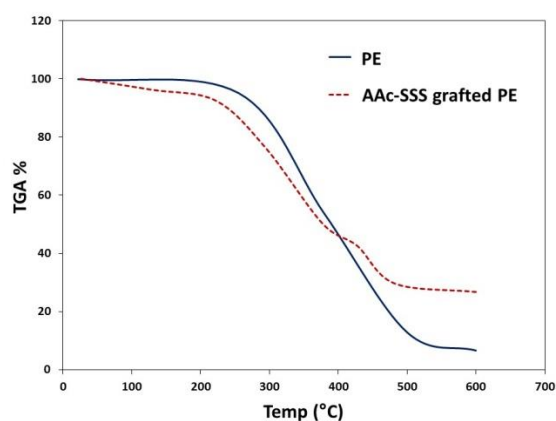


Fig 4. TGA thermogram of non woven PE fabrics and grafted PE fabrics

For realize metal ion adsorption, Langmuir isotherm model were utilized. The equation is as follows:

$$\frac{C_e}{Q_e} = \frac{C_e}{Q_0 + 1} \quad (4)$$

Here,

C_e = Concentration at equilibrium (mg L^{-1})

Q_0 = Monolayer saturation adsorption capacity (mg g^{-1})

Q_e = Capacity of adsorption at equilibrium

b = Langmuir adsorption constant (L mg^{-1}).

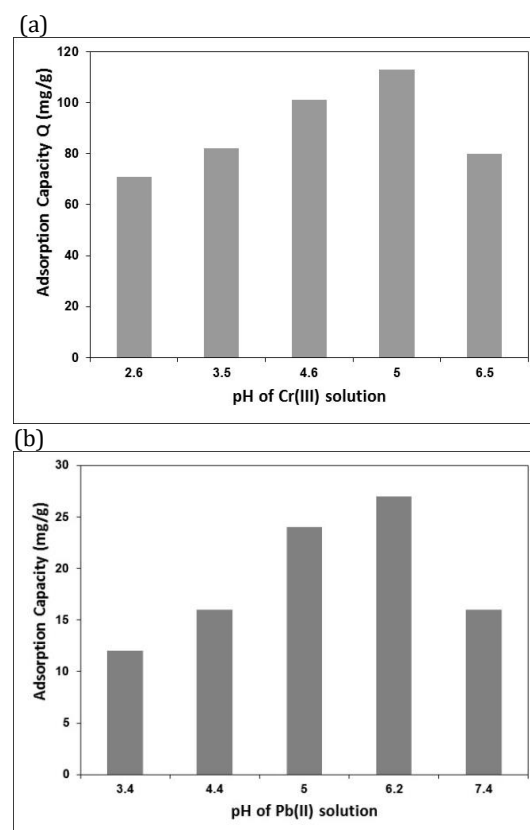


Fig. 5. Adsorption variation of (a) Chromium (III) and (b) Lead(II) due to pH change

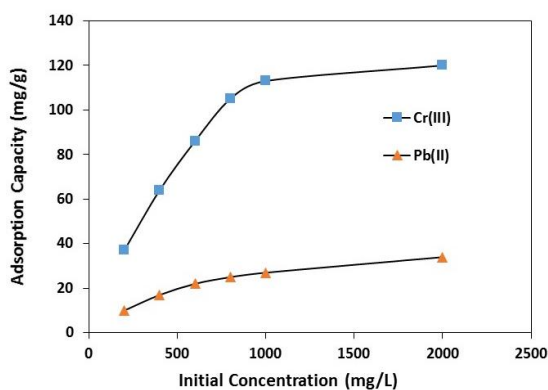


Fig 6. Adsorption capability variation with starting concentration of metal ions

Fig 7 and 8 represents two diagrams obtained by plotting C_e/Q_e against C_e with the data presented in Fig 6. The linearity of C_e/Q_e vs C_e plot demonstrated that the Langmuir adsorption isotherm is obeyed by the adsorption process. Using Langmuir equation, adsorption capacity of monolayer saturation for the Cr(III) and Pb(II) adsorption by the prepared adsorbent was measured as 166.66 and 45.25 (mg g^{-1}) respectively.

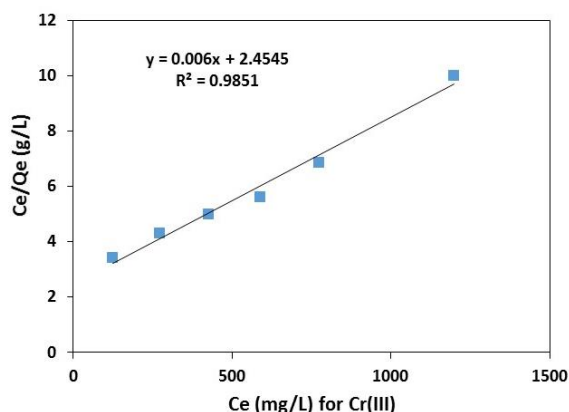


Fig 7. Chromium(III) adsorption Isotherm (Langmuir) plot

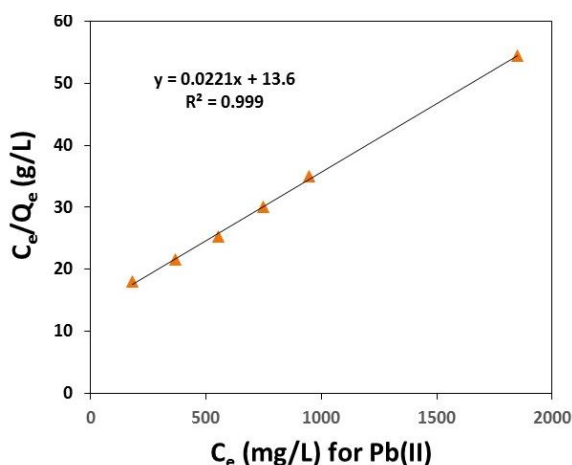


Fig 8. Lead(II) adsorption Isotherm (Langmuir) plot

3.2.3. Change of adsorption capability with contact time

The change of adsorption of Pb (II) and Cr(III) by the adsorbent with change of contact time were studied (Fig 9). 1000 ppm Cr(III) solution with pH 5 and 1000 ppm Pb(II) with pH 6.2 were used in this study. From Fig 4 it can be understood that at the beginning the adsorption rate of Pb(II) and Cr(III) is very fast, then gradually it slows down to reach the equilibrium. After 48 hours the equilibrium adsorption of 113.27 mg g^{-1} and 27 mg g^{-1} was achieved for Cr(II) and Pb(II) metal ions respectively.

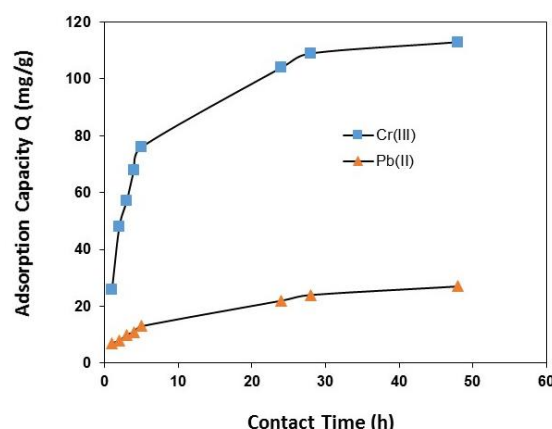


Fig 9. Capacity of adsorption of against standing time

Cr(III) and Pb(II) adsorption were analyzed using pseudo 1st and pseudo 2nd order kinetic model. The pseudo 1st and pseudo 2nd order models [38-39] are described by the following equations

$$\log Q_e - Q_t = \log Q_e - \frac{k_1}{2.303} t \tag{5}$$

$$\frac{t}{Q_t} = \frac{1}{k_2 Q_e^2} + \frac{t}{Q_e} \tag{6}$$

Here,

Q_t = Adsorption capacity at any time (mg g^{-1})

Q_e = Adsorption capacity at equilibrium (mg g^{-1})

k_1 = 1st order rate constant (h^{-1})

k_2 = 2nd order rate constant ($\text{g h}^{-1} \text{mg}^{-1}$)

From the graph of $\log (Q_e - Q_t)$ vs. t , pseudo 1st order rate constant have been determined (Fig 10). The values of k_1 , Q_e , R^2 (correlation coefficient) for both Pb(II) and Cr(III) were presented in Table 1. Results show that the experimental Q_e value and Q_e value measured from the 1st order kinetic model are different from each other. Again from the graph of t/Q_t against t , pseudo 2nd order rate constants have been determined (Fig 11). The values of k_2 , Q_e , R^2 are presented in Table 1. Results show that the experimental Q_e value and the Q_e value measured from the 2nd order kinetic model matches with each other. Therefore, the pseudo 2nd order kinetic model is the best model to interpret Pb(II) and Cr(III) adsorption. As the adsorption follows pseudo 2nd order model the adsorption process might have controlled by the intra-particle diffusion [40].

Moreover it suggests that chelating interaction plays

the lead role in the metal adsorption [41].

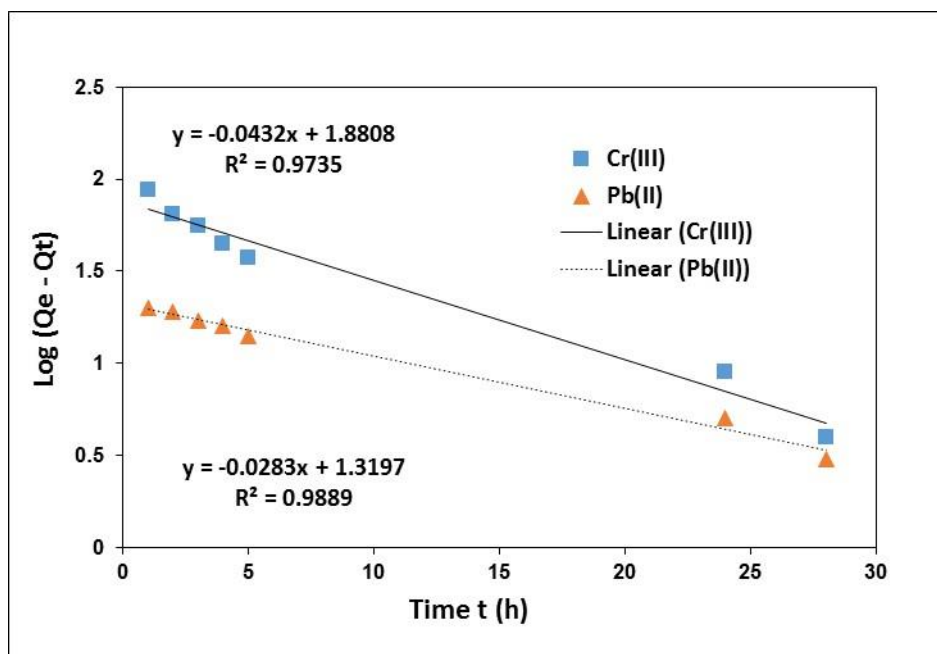


Fig. 10. Pseudo 1st order graph for Lead(II) and Chromium(III) adsorption

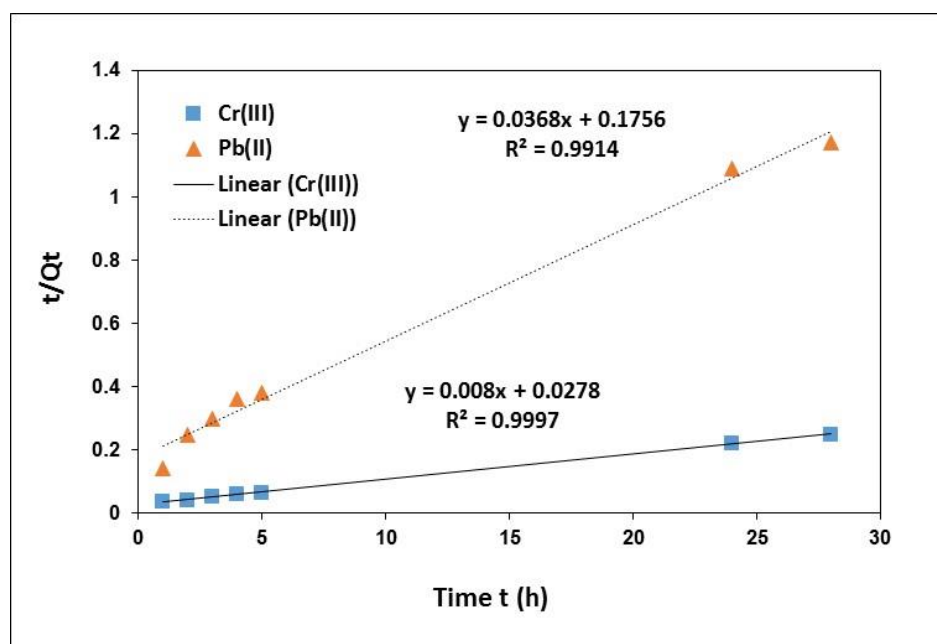


Fig. 11. Pseudo 2nd order graph for Lead(II) and Chromium(III) adsorption

The adsorbent we fabricated exhibited superior metal ion adsorption capacity than other existing adsorbents. Table 2 demonstrates a comparison between present adsorbent with others.

3.2.4. Reuse and desorption

When the adsorption process revealed successful result, the desorption of Pb(II) and Cr(III) was attempted using 2M HCl and 2M NaOH solution

respectively. It took 24 hours to reach desorption equilibrium. The percentage of desorption reached 99 for Pb(II) but 70 % for Cr(III). The Pb(II) and Cr(III) adsorption were tried up to five successive cycles but the successive use of the adsorbent indicated that the sorption capacity not changed noticeably. In addition up to five successive cycles the adsorbent remains usable although there is some degradation of the polymer. The results suggest that the adsorbent can be renewed and used persistently preserving identical efficiency.

Table 1. Determination of rate constants for metal ions adsorption by the grafted adsorbent

Ions of Metal	Qe (experimental) (mg g ⁻¹)	Pseudo (1st-order)			Pseudo (2nd-order)		
		Qe (theor.) (mg g ⁻¹)	k1 (h ⁻¹)	R ²	Qe (theor.) (mg g ⁻¹)	k ₂ (h g ⁻¹ mg ⁻¹)	R ²
Chromium(III)	113	76	0.09	0.97	125.62	0.0023	0.99
Lead(II)	27	21	0.07	0.99	27.19	0.0078	0.99

Table 2. Lead(II) and Chromium (III) uptake capacity of adsorbent compared with other adsorbents

Adsorbent	Uptake Capability of Pb(II) (mg g ⁻¹)	Uptake Capability of Cr(III) (mg g ⁻¹)
AAC-SSS grafted PE (current study)	45	166
Rice husk [42]	11.62	-
Silica Ceramic[43]	2.7	-
Activated carbon from <i>Phoenix dactylifera</i> . L [44]	9.91	-
Activated carbon from Eichhornia[45]	16.61	-
Lignin [46]	-	17.97
Coal [47]	-	2.5-2.6
Chitosan flakes [48]	-	138
Passion-fruit shell biomass [49]	-	27.93

3.3. Adsorption of Cr from real wastewater

Two types of waste water were collected from savar tannery industrial estate: (1) Waste water before treatment (raw waste water) and (2) Waste water after treatment by conventional (precipitation) method. The waste waters were digested and then used for adsorption of Cr by the prepared adsorbent. Initial Cr concentration of waste water before treatment (raw waste water) was 1200 mg L⁻¹ and using this water Cr adsorption capacity of the adsorbent was found to be 65 mg g⁻¹ at pH 2.5. Initial Cr concentration of waste water after treatment by conventional (precipitation) method was 4 mg L⁻¹ and using this water Cr adsorption capacity of the adsorbent was found to be 0.4 mg g⁻¹. The success of present work will encourage us to conduct a study on a real waste water that may be more practical than synthetic one.

4. CONCLUSION

In present study AAC-SSS grafted PE adsorbent were fabricated effectively by the pre-irradiation technique. The adsorbent was investigated by FTIR, TGA and SEM. The prepared adsorbent was investigated to adsorb Pb(II) and Cr(III) ions from aqueous solution. Metal ion adsorption took 48 hours to attain the equilibrium value. pH 6.2 and 5 was observed best for Pb (II) and Cr(III) adsorption respectively. The prospect of the adsorbent for Cr(III) and Pb(II)

adsorption was presented by the maximum adsorption capacity of 113 and 27 (mg g⁻¹) respectively. Investigation of kinetic data depicted better correlation with the pseudo 2nd order kinetics. Again inspection of adsorption isotherm revealed fitting with Langmuir isotherm model. Desorption of metal ions and recycling of the adsorbent were also conducted with success. Furthermore the adsorbent showed promising result in Cr(III) adsorption from real waste water.

ACKNOWLEDGMENTS

The authors are pleased to acknowledge IAEA for technical support to carry out the research. Authors also would like to convey special thanks to the Gamma Source Division of Institute of Food and Radiation Biology, Atomic Energy Research Establishment.

REFERENCES

- [1]. S. Zhai, H. Xiao, Y. Shu, and Z. Zhao, "Counter measures of heavy metal pollution," *Chinese Journal of Geochemistry*, Vol. 32(4), pp. 446-450, 2013.
- [2]. N. Seko, M. Tamada, and F. Yoshii F, "Current status of adsorbent for metal ions with radiation grafting and crosslinking techniques," *Nuclear Instruments and Methods in Physics Research Section B*, Vol. 236, pp.21-29, 2005.

- [3]. M. M. Marjub, N. Rahman, N.C. Dafader, F.S. Tuhen, S. Sultana, and F.T. Ahmed, "Acrylic acid-chitosan blend hydrogel: a novel polymer adsorbent for adsorption of lead(II) and copper(II) ions from wastewater," *Journal of Polymer Engineering*, Vol. 39(10), pp. 883–891, 2019.
- [4]. F. M. D'Itri, in W. P. Cunningham, T. H. Cooper, E. Gorham and M. T. Hepworth (Eds.) *Heavy metals and heavy metal poisoning in Environmental Encyclopedia* (Second edition), Gale Research, Detroit, pp. 511-513, 1998.
- [5]. H. Shrivastava and B.U. Nair, "Protein Degradation by Peroxide Catalyzed by Chromium (III): Role of Coordinated Ligand," *Biochemical and Biophysical Research Communications*, Vol. 270 (3), pp. 749-754, 2000.
- [6]. S. Tong S, Y.E. von Schirnding and T. Prapamontol T, "Environmental lead exposure: a public health problem of global dimensions," *Bulletin of World Health Organization*, Vol. 78 (9), pp. 1068-1077, 2000.
- [7]. S. Madala, S.K. Nadavala, S. Vudagandla, V.M. Boddu and K. Abburi, "Equilibrium, kinetics and thermodynamics of Cadmium (II) biosorption on to composite chitosan biosorbent," *Arabian Journal of Chemistry*, Vol. 10, pp. S1883–S1893, 2017.
- [8]. J. Peric, M. Trgo and N.V. Medvidovic, "Removal of zinc, copper and lead by natural zeolite—a comparison of adsorption isotherms," *Water Research*, Vol. 38, pp. 1893–1899, 2004.
- [9]. D. Balarak, Y. Mahdavi, E. Bazrafshan, A.H. Mahvi and Y. Esfandiyari, "Adsorption of fluoride from aqueous solutions by carbon nano- tubes: determination of equilibrium, kinetic, and thermodynamic parameters," *Fluoride*, Vol. 49 (1), pp. 71–83, 2016.
- [10]. E. Bazrafshan, A.A. Zarei and F.K. Mostafapour, "Biosorption of cadmium from aqueous solutions by *Trichoderma* fungus: kinetic, thermodynamic, and equilibrium study," *Desalination and Water Treatment*, Vol. 57 (31), pp. 14598–14608, 2016.
- [11]. E. Bazrafshan, F. KordMostafapour, S. Rahdar and A.H. Mahvi, "Equilibrium and thermodynamics studies for decolorization of re- active black 5 (RB5) by adsorption onto MWCNTs," *Desalination and Water Treatment*, Vol. 54 (8), pp. 2241–2251, 2015.
- [12]. E. Bazrafshan, M. Ahmadabadi and A.H. Mahvi, "Reactive Red-120 removal by activated carbon obtained from cumin herb wastes," *Fresenius Environmental Bulletin*, Vol. 22 (2a), pp. 584–590, 2013.
- [13]. E. Bazrafshan, P. Amirian, and A.H. Mahvi, and A. Ansari-Moghaddam, "Application of adsorption process for phenolic compounds removal from aqueous environments: a systematic review," *Global NEST Journal*, Vol. 18 (1), pp. 146–63, 2016.
- [14]. E. Bazrafshan, F. KordMostafapour and A.H. Mahvi, "Phenol removal from aqueous solutions using pistachio-nut shell ash as a low cost adsorbent," *Fresenius Environmental Bulletin*, Vol. 21 (10), pp. 2962–2968, 2012.
- [15]. E. Bazrafshan, D. Balarak, A.H. Panahi, H. Kamani and A.H. Mahvi, "Fluoride removal from aqueous solutions by cupric oxide nanoparticles," *Fluoride*, Vol. 49 (3), pp. 233–44, 2016.
- [16]. R. Coşkun and C. Soykan, "Lead(II) adsorption from aqueous solution by poly(ethylene terephthalate)-g-acrylamide fibers," *Journal of Polymer Research*, Vol. 13, pp. 1–8, 2006.
- [17]. H. Bağ, A.R. Türker, R. Coşkun, M. Saçak and M. Yiğitoğlu, "Determination of zinc, cadmium, cobalt and nickel by flame atomic absorption spectrometry after preconcentration by polyethylene terephthalate/ fibers grafted with methacrylic acid," *Spectrochimica Acta Part B: Atomic Spectroscopy*, Vol. 55, pp. 1101–8, 2000.
- [18]. O. Bozkaya, M. Yiğitoğlu and M. Arslan, "Investigation on selective adsorption of Hg(II) ions using 4-vinyl pyridine grafted poly(ethylene terephthalate) fiber," *Journal of Applied Polymer Science*, Vol. 124, pp. 1256–64, 2012.
- [19]. R. Coşkun, C. Soykan, and M. Saçak, "Adsorption of copper(II), nickel(II) and cobalt(II) ions from aqueous solution by methacrylic acid/ acrylamide monomer mixture grafted poly(ethylene terephthalate) fiber," *Separation and Purification Technology*, Vol. 49, pp. 107–114, 2006.
- [20]. R. Coşkun, C. Soykan and M. Saçak, "Removal of some heavy metal ions from aqueous solution by adsorption using poly(ethylene terephthalate)-g-itaconic acid/acrylamide fiber," *Reactive and Functional Polymers*, Vol. 66, pp. 599–608, 2006.
- [21]. M. Arslan, "Preparation and use of amine-functionalized glycidyl methacrylate-g-poly(ethylene terephthalate) fibers for removal of chromium(VI) from aqueous solution," *Fibers and Polymers*, Vol. 11, pp. 325– 330, 2010.
- [22]. M. Yiğitoğlu and M. Arslan, "Adsorption of hexavalent chromium from aqueous solutions using 4-vinyl pyridine grafted poly(ethylene terephthalate) fibers," *Polymer Bulletin*, Vol. 55, pp. 259–268, 2005.
- [23]. M. Yiğitoğlu and M. Arslan, "Selective removal of Cr(VI) ions from aqueous solutions including Cr(VI), Cu(II) and Cd(II) ions by 4- vinyl pyridine/2-hydroxyethylmethacrylate monomer mixture grafted poly(ethylene terephthalate) fiber," *Journal of Hazardous Materials*, Vol. 166, pp. 435–444, 2009.
- [24]. M. Karakısla, "The adsorption of Cu(II) ion from aqueous solution upon acrylic acid grafted poly(ethylene terephthalate) fibers," *Journal of Applied Polymer Science*, Vol. 87, pp. 1216–1220, 2003.
- [25]. H. Hamada, A. Razik and ER Kenawy, "Synthesis, characterization, and amidoximation of diaminomaleodinitrile-functionalized polyethylene terephthalate grafts for collecting heavy metals from waste water," *Journal of Applied Polymer Science*, Vol. 125, pp. 1136–1145, 2012.

- [26]. X. Ping, M. Wangn, X. Ge, "Radiation induced graft copolymerization of n-butyl acrylate onto poly(ethylene terephthalate) (PET) films and thermal properties of the obtained graft copolymer," *Radiation Physics and Chemistry*, Vol. 80, pp. 632-637, 2011.
- [27]. L. Hsieh, Y.M. Shinawatra and M.D. Castillo, "Postirradiation polymerization of vinyl monomers on poly(ethylene terephthalate)," *Journal of Applied Polymer Science*, Vol. 31, pp. 509-519, 1986.
- [28]. E.M. Abdel-Bary, A.A. Sarhan and H.H. Abdel-Razik, "Effect of graft co-polymerization of 2-hydroxyethyl methacrylate on the properties of polyester fibers and fabric," *Journal of Applied Polymer Science*, Vol. 35, pp. 439-448, 1986.
- [29]. M.M. Nasef, "Gamma radiation-induced graft copolymerization of styrene onto poly(ethylene terephthalate) films," *Journal of Applied Polymer Science*, Vol. 77, pp. 1003-1012, 2000.
- [30]. N. Rahman, M.S. Hossen, A.R. Miah, M.M. Marjub, N.C. Dafader, S. Shahnaz, M.F. Alam, "Removal of Cu(II), Pb(II) and Cr(VI) ions from aqueous solution using amidoximated non-woven polyethylene-g-acrylonitrile fabric," *Journal of Environmental Health Science&Engineering*, Vol. 17, pp. 183-194, 2019.
- [31]. E.A. Hegazy, H. Kamal, N. Maziad and A.M. Dessouki, "Membranes prepared by radiation grafting of binary monomers for adsorption of heavy metals from industrial wastes," *Nuclear Instruments and Methods in Physics Research Section B*, Vol. 151, pp. 386-392, 1999.
- [32]. E.A. Hegazy, H. Kamal, N.A. Khalifa and G.H.A. Mahmoud, "Separation and extraction of some heavy and toxic metal ions from their wastes by grafted membranes," *Journal of Applied Polymer Science*, Vol. 81, pp. 849-860, 2001.
- [33]. E.A. Hegazy, H.A. Abd El-Rehim, A.M.I. Ali, H.G. Nowier and H.F. Aly, "Characterization and application of radiation grafted membranes in treatment of intermediate active waste," *Nuclear Instruments and Methods in Physics Research Section B*, Vol. 151, pp. 393-398, 1999.
- [34]. H.A. Abd El-Rehim, E.A. Hegazy, and A.E. Ali, "Selective removal of some heavy metal ions from aqueous solution using treated polyethylene-g-styrene/maleic anhydride membranes," *Reactive and Functional Polymers*, Vol. 43, pp. 105-116, 2000.
- [35]. W.R. Fairheller, J.R. Katon and J.E. Katon, "The vibrational spectra of acrylic acid and sodium acrylate," *Spectrochimica Acta*, Vol. 23A, pp. 2225-2232, 1967.
- [36]. C. González-Blanco, L.J. Rodríguez and M.M. Velázquez, "Effect of the Addition of Water-Soluble Polymers on the Structure of Aerosol OT Water-in-Oil Microemulsions: A Fourier Transform Infrared Spectroscopy Study," *Langmuir*, Vol. 13, pp.1938-1945, 1997.
- [37]. X. Lv, H. Li, Z. Zhang, H. Chang, L. Jiang, and H. Liu, "UV Grafting Modification of Polyethylene Separator for Liion Battery," *Physics Procedia*, Vol. 25, pp. 227-232, 2012.
- [38]. Y.S. Ho, "Review of second-order models for adsorption systems," *Journal of Hazardous Materials*, Vol. 136 (3), pp. 681-689, 2006.
- [39]. C. Namasivayam and D.J.S.E. Arasi, "Removal of congo red from wastewater by adsorption onto waste red mud," *Chemosphere*, Vol. 34 (2), pp. 401-417, 1997.
- [40]. S. Rengaraj, J.W. Yeon, Y. Kim, Y. Jung, Y.K. Ha, and W.H. Kim, "Adsorption characteristics of Cu(II) onto ion exchange resins 252H and 1500H: kinetics, isotherms and error analysis," *Journal of Hazardous Materials*, Vol. 143(1-2), pp. 469-477, 2007.
- [41]. Y. Li, Q.Y. Yue and B.Y. Gao, "Adsorption kinetics and desorption of Cu(II) and Zn(II) from aqueous solution onto humic acid," *Journal of Hazardous Materials*, Vol. 178(1-3), pp. 455-461, 2010.
- [42]. M.G.A Vieira, A.F.A. Neto, M.G.C. Silva and C.N. Carneiro, "Adsorption of lead and copper ions from aqueous effluents on rice husk ash in dynamic equilibrium," *Brazilian Journal of Chemical Engineering*, Vol. 31 (2), pp 519 - 529, 2014.
- [43]. M. Salim and Y. Munekage, "Lead Removal from Aqueous Solution Using Silica Ceramic: Adsorption Kinetics and Equilibrium Studies," *International Journal of Chemistry*, Vol. 1 (1), pp. 23-30, 2009.
- [44]. N. Chaouch, M.R. Ouahrani and S.E. Laouini, "Adsorption of Lead (II) from aqueous solutions onto activated carbon prepared from Algerian dates stones of *Phoenix dactylifera*. L(Ghars variety) by H₃PO₄ activation," *Oriental Journal of Chemistry*, Vol. 30(3), pp. 1317-1322, 2014.
- [45]. P. Shekinah, K. Kadirvelu, P. Kanmani, P. Senthilkumar and V. Subburam, "Adsorption of lead(II) from aqueous solution by activated carbon prepared from Eichhornia," *Journal of Chemical Technology and Biotechnology*, Vol. 77(4), pp. 458-464, 2002.
- [46]. Y. Wu, S. Zhang, X. Guo and H. Huang, "Adsorption of chromium(III) on lignin," *Bioresource Technology*, Vol. 99, pp. 7709-7715, 2008.
- [47]. J. Anwar, U. Shafique, M. Salman, W.U. Zaman, S. Anwar and J.M. Anzano, "Removal of chromium (III) by using coal as adsorbent," *Journal of Hazardous Materials*, Vol. 171, pp.797-801, 2009.
- [48]. L. Pietrelli, I. Francolini, A. Piozzi, M. Sighicelli, I. Silvestro and M. Vocciantè, "Chromium(III) Removal from Wastewater by Chitosan Flakes," *Applied Sciences*, Vol. 10 (6), pp. 1925, 2020. doi:10.3390/app10061925.
- [49]. G. Campos-Flores, J. Gurreonero-Fernández and R. Vejarano R, "Passion-fruit shell biomass as adsorbent material to remove chromium III from contaminated aqueous mediums", IOP Conf. Series: Materials Science and Engineering 620, 2019, 012110 IOP Publishing doi:10.1088/1757-899X/620/1/01211.



RESEARCH ARTICLE

Boron rejection from aqueous solution and wastewater by direct contact membrane distillation

Burcu Tan^{1,*}, Uğur Selengil², Tijen Ennil Bektaş³¹Çanakkale Onsekiz Mart University, Chemistry Department, 17100 Çanakkale, TURKEY²Eskişehir Osmangazi University Chemical Engineering Department, 26480 Eskişehir, TURKEY³Çanakkale Onsekiz Mart University, Chemical Engineering Department, 17100 Çanakkale, TURKEY

ABSTRACT

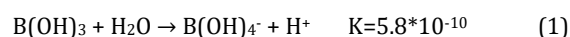
Boron is widely used in various areas of modern technology. Due to the environmental problems arising during the production and use, the studies on the removal and recovery of boron from wastewater have been increased recently. Membrane distillation (MD) system is smaller in size with respect to other common distillation systems and needs lower operating temperatures. In addition, the equipment costs are reduced and the safety of the process increases since it operates at lower pressures. Moreover, the membrane distillation process can remove pollutants from water without using chemicals. In this study, boron rejection from aqueous solutions and wastewater was investigated by using direct contact membrane distillation (DCMD) system where both surfaces of a porous hydrophobic membrane were in contact with liquid streams. The effects of various parameters (pH, feed concentration, feed temperature, etc.) on boron rejection were investigated and the highest boron rejection was found to be 50 % when pH=10 at 50 °C and with feeding by a pump of 54 rpm. According to the test results of wastewater from Kirka Borax treatment plants, the mean distillate fluxes were found as 13, 16 and 14 L m⁻² h⁻¹ at the feed temperatures of 30, 40 and 50 °C, respectively. The boron removal percentages were found to be 47, 64 and 48 % at 30, 40 and 50 °C, respectively. It was observed in the XRD spectra that the crystals in wastewater mainly consist of Na₂B(OH)₄Cl and Mg₂B₂O₅ structures.

Keywords: Boron, membrane distillation, recovery, rejection, wastewater

1. INTRODUCTION

Various environmental problems arise during the production of boron minerals, compounds and derivatives and as a result of the use of boron in many industrial areas. Although a boron product can replace another boron product in some cases, there is not another substitute that can provide the same quality and affordability as boron compounds. As the use of boron compounds becomes widespread, it also brings environmental problems. In the Water Pollution Control Regulation in Turkey, the boron level limitation is 0.3-1 mg L⁻¹ for the water that can be used as irrigation water while the boron level limit in drinking water is given as 0.5 mg L⁻¹. The limit value for boron is given as 500 mg L⁻¹ in discharge standards of mining industry wastewater [1].

Boron is normally present as boric acid and borax ions in water. Boric acid is a very weak monobasic acid with a special structure. It does not give protons in aqueous solution but it receives electrons and holds OH⁻ ions (Eq. 1).



During the formation of boric acid, the B³⁺ cations draw oxygen and as a result of this attraction the O-H bonds are broken and BO₃³⁻ anions are formed. The radius of the B³⁺ cation is very small (0.23 Å) and therefore it is not found free in nature. The compounds of boron with oxygen are abundant due to the great attraction to oxygen. Boron formation varies depending on the pH of the water. B(OH)₃ is dominant in acidic waters (pH <6) [2]. Tetra-penta-hexa and other polyborates are found in natural and alkaline waters. The dissolution of alkali metallic borates is

Corresponding Author: burcu.tan88@gmail.com (Burcu Tan)

Received 18 December 2020; Received in revised form 11 January 2021; Accepted 11 January 2021

Available Online 25 January 2021

Doi: <https://doi.org/10.35208/ert.842919>

© Yildiz Technical University, Environmental Engineering Department. All rights reserved.

This paper has been presented at EurAsia Waste Management Symposium 2020, Istanbul, Turkey

faster in the solutions with medium pH values in comparison with other solutions and the dissolution rate of borates generally increases as temperature increases. Boric acid dissolves more quickly in hot water with respect to cold water.

Eti Mining Operations General Directorate Kirka Boron Plant has 930.000 tons year⁻¹ production capacity. The products produced in this establishment are tincal, boraxpentahydrate, anhydrous borax and calcined tincal. In this plant, the water used in the first washing of the boron mineral taken from the quarries and the waters coming from the other processes are sent to the settling pools and kept in these pools. There are 7 settling pools. The waste ponds cover much more area than the plants. There are a drainage channel surrounding the plant and a secondary water collection pond connected to it so that the ponds do not overflow and damage the agricultural lands due to rainfall. The collected water is delivered to the waste ponds by a pump. A total of approximately 400,000 tons year⁻¹ of waste is generated in the Eti Maden Kirka Boron Plants. These wastes cause environmental problems and they also have some content of boron minerals of high strategic importance.

The direct contact membrane distillation (DCMD) method for boron removal from water and wastewater is a relatively new technology that is an alternative to conventional separation methods. In DCMD, evaporation occurs at the feed-membrane interface and condensation occurs at the distillate-membrane interface. The hot feed solution and the cold distillate solution are in direct contact with the surfaces of the membrane in the feed and distillate regions, respectively. The steam formed on the feed side is carried from the membrane to the distillate side due to the pressure difference. The feed does not enter into the membrane due to the hydrophobic characteristic of the membrane. Only the gas phase formations can enter into the membrane pores. The DCMD is the most commonly used membrane

distillation (MD) configuration because it is suitable for laboratory trials. The main disadvantage of this method is that the heat loss by conduction is high. In the DCMD method, the temperature of the feed solution is below the boiling point. The feed and distillate pressures are close to atmospheric pressure. For all membrane distillation types, the distillate flux is calculated by measuring the condensed flow collected on the distillate side of the membrane. DCMD is suitable for water applications in which the feed solution contains non-volatile components such as salts, colloids, proteins, etc.. This method is also used in some applications such as desalination, reuse of water, food processing and pharmaceuticals [3-5].

The advantages of membrane distillation separation over other conventional separation methods are as follows:

- 1) It requires lower operating temperatures (feed: 30-80 °C, distillate: 15-30 °C) and lower steam pressures with respect to the other distillation processes.
- 2) Lower operating pressures are used with respect to the pressure-driven membrane processes such as reverse osmosis. This is because high pressure is needed to overcome the osmotic pressure for concentrated solutions in reverse osmosis. Furthermore, a more efficient treatment for high concentration solutions or wastewater can be achieved with DCMD.
- 3) 100% (theoretical) retention of non-volatile solutes can be achieved.
- 4) It consumes less energy compared to the multi-stage vacuum evaporation method.
- 5) There is reduced chemical interaction between the membrane and the process solution [3].

There are many studies in the literature that remove boron from low concentration wastewater, groundwater or aqueous solutions (Table 1).

Table 1. Literature studies using the membrane distillation method

Membran Type	Flux	Results	Reference
PTFE	40 kg m ⁻² s ⁻¹	DCMD; 2 M NaCl feed, T _b =55 °C T _s =15 °C salt removal (>99.8%)	[6]
PP	650 L m ⁻² d ⁻¹	DCMD; tap water, feed ve distillate T _b =353 ve T _s =293 K, removal >75%	[7]
SMM(PS)M1	2.45.10 ⁻⁶ m s ⁻¹	DCMD; T _b =50 °C, T _s =40 °C, feed solution is 0.5 M NaCl, salt removal: 99.9 %	[8]
PVDF	10.5 kg m ⁻² s ⁻¹	DCMD; feed: hot boric acid solution, T _b =50 °C T _s =40 °C boron removal (>99.8%)	[9]
PVDF	7.5 kg m ⁻² s ⁻¹	DCMD; feed: super saline solution T _b =59 °C, T _s =20 °C	[10]
PVDF	20 kg m ⁻² s ⁻¹	DCMD; feed: 4.5 M NaCl T _b =60 °C T _s =20 °C	[11]
PP	16 L m ⁻² h ⁻¹	DCMD; feed: boron mine wastewater T _b =40 °C T _s =20 °C, boron removal (%64)	This work

In this study, the effectiveness of the DCMD method on the removal of boron from the high concentration wastewater of the factory extracting boron mine was investigated. In this study, the efficiency of boron uptake from aqueous solution and actual wastewater using direct contact membrane distillation method

was investigated under various conditions. In the experiments carried out for this purpose, the concentrated feed solution taken from the waste water of the Kirka Borax Plant was crystallized and the obtained solid products were characterized.

2. MATERIALS AND METHOD

After the membrane distillation system was installed, the membrane (polypropylene, MD020TP 2N, Microdyn-Nadir GmbH, Germany, containing 40 capillary tubes with a pore diameter of 0.2 μm) was activated before proceeding to preliminary trials. The activation involves washing for 1 hour with distilled water followed by washing with 50% by volume isopropanol aqueous solution for 1 hour.

First, pure water passes through the activated membrane to obtain a regular flux. The flow rates were adjusted using a peristaltic pump. The rpm value of the pump is called flow rate in this study. The feed

and distillate currents were passed through the membrane module according to the countercurrent principle. The effects of the initial pH, feed temperature, feed boron concentration and feed flow rate on performance were investigated while the distillate temperature was kept constant at 20 $^{\circ}\text{C}$. Furthermore, at the end of each experiment, a cleaning process was applied to prevent the contamination of the membrane. Pure water, 1% by mass NaOH aqueous solution, and 1% by mass $\text{C}_6\text{H}_8\text{O}_7$ aqueous solution were passed through the membrane consequently in the cleaning process. Each step was performed at 30 $^{\circ}\text{C}$ for 30 minutes. The experimental setup is shown in Fig 1.

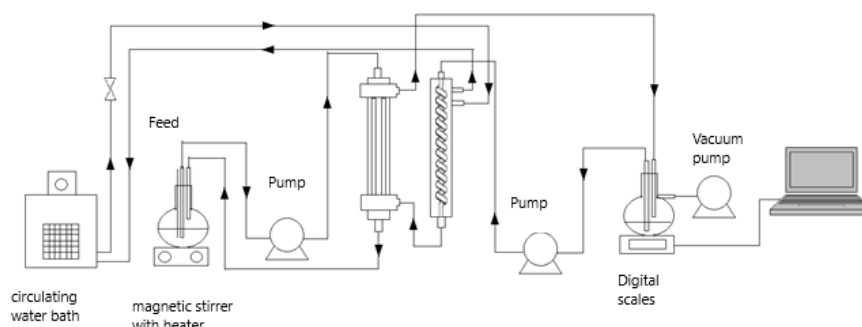


Fig 1. Schematic representation of the experimental system

The distillate stream was continuously weighed on the precision balance and the obtained value was transferred to the computer every 30 seconds. The flux and percentage of the boron retention were calculated from Equations 1 and 2 given below.

$$\text{Flux}(J) = \Delta W(\text{kg}) / [A(\text{m}^2) * \Delta t(\text{h})] \quad (1)$$

$$\text{Boron retention \%} = [(C_f - C_d) / C_f] * 100 \quad (2)$$

Here, ΔW is the amount of distillate measured at certain time intervals, A is the membrane surface area (0.0889 m^2), Δt is the time at which the amount of distillate is recorded, C_f is the boron concentration in the feed and C_d is the distillate boron concentration.

3. RESULTS & DISCUSSION

3.1. Effect of initial pH

In the experiments performed for examining the effect of initial pH on boron retention, the solution with a boron concentration of 100 mg L^{-1} was adjusted to different initial pH values (2, 4, 6, 8, 10 and 12) and passed through the membrane. The pH values of boron solutions were adjusted using NaOH and HCl solutions at different concentrations and measured with a pH meter. The feed temperature was 50 $^{\circ}\text{C}$, the flow rate was 54 rpm, the distillate temperature was 20 $^{\circ}\text{C}$ and the flow rate was 24 rpm. The collected distillate was automatically weighed on a precision scale and the results were transferred to the computer over a period of time. The fluxes were determined. The membrane was cleaned at the end of each experiment. As can be seen in Fig. 2 and Fig. 3, the distillate flux changed between 6 and 9 $\text{L m}^{-2} \text{h}^{-1}$

between the pH values of 2 and 12. The boron retention reached 25% at low pH and 50% at high pH.

3.2. Effect of feed temperature

In the experiments carried out for examining the effect of feed temperature on boron retention, the solution at a boron concentration of 100 mg L^{-1} was adjusted to different temperatures (30, 40, 50 and 60 $^{\circ}\text{C}$) and passed through the membrane. The feeding pH was kept constant at 10, the flow rate was 54 rpm, distillate temperature was 20 $^{\circ}\text{C}$ and flow rate was 24 rpm. The collected distillate was automatically weighed on a precision scale and the results were transferred to the computer over a period of time. The fluxes were calculated. At the end of each experiment, the membrane was cleaned. Fig 4 shows the variation of the distillate flux with feed temperature. The highest distillate flux (7.5 $\text{L m}^{-2} \text{h}^{-1}$) and boron uptake (50% uptake) were obtained at 50 $^{\circ}\text{C}$.

3.3. Effect of feed concentration

In the experiments for examining the effect of feed concentration on boron uptake, the solution was passed through the membrane at different concentrations (50, 100, 250, 500, 750 and 1000 mg L^{-1}). The feeding pH was 10, temperature was 50 $^{\circ}\text{C}$, flow rate was 54 rpm, distillate temperature was 20 $^{\circ}\text{C}$ and flow rate was 24 rpm. The collected distillate was automatically weighed on a precision scale and the results were transferred to the computer over a period of time. The fluxes were calculated. The membrane was cleaned at the end of each experiment. Fig. 5 shows the variation of the distillate flux with

feed concentration. The fluxes ranged between 5 and 7 L m⁻² h⁻¹ while the highest boron uptake was found

to be 52% at a concentration of 100 mg L⁻¹.

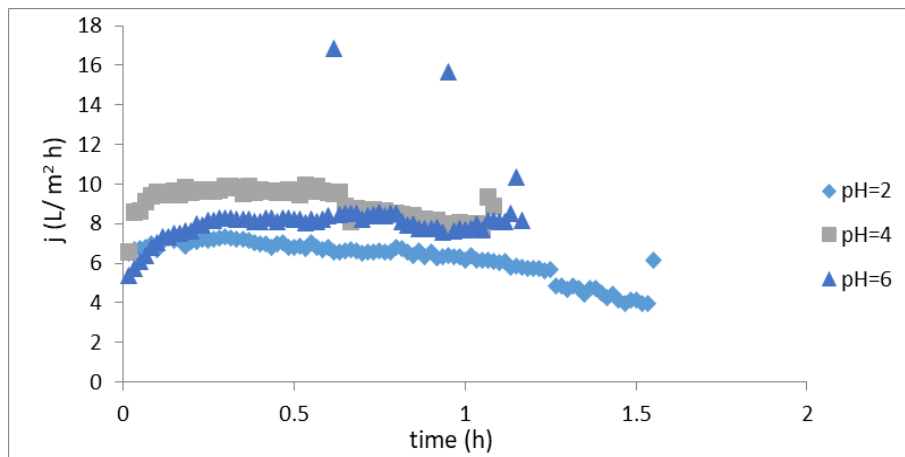


Fig 2. Variation of distillate flux with feed pH

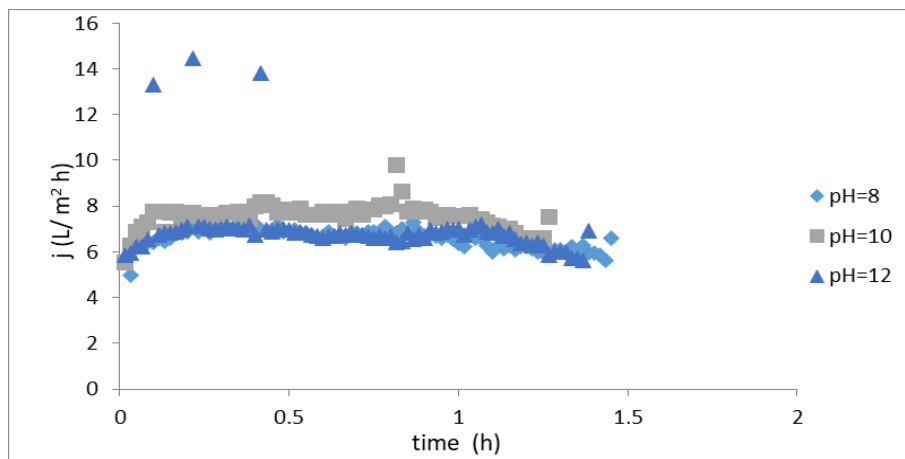


Fig 3. Variation of distillate flux with feed pH

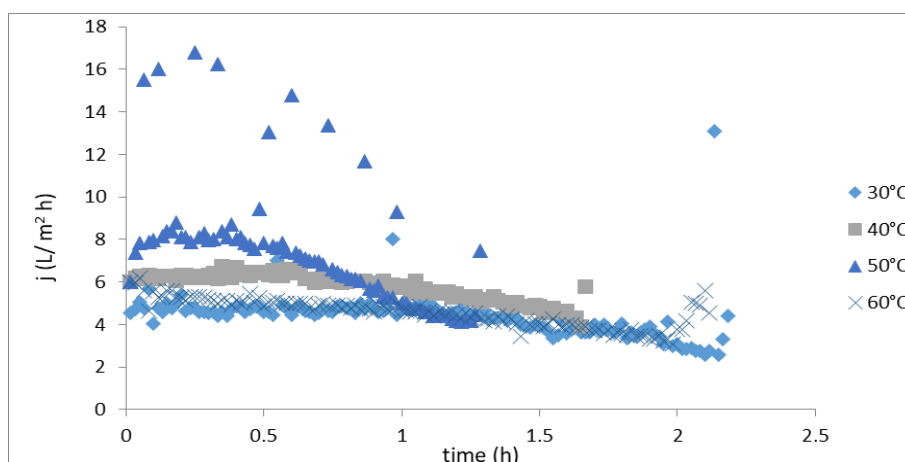


Fig 4. Variation of distillate flux with feed temperature

3.4. Effect of feed flow rate

In the experiments carried out to investigate the effect of feed flow rate on boron retention, a 100 mg L⁻¹ solution was passed through the membrane at different flow rates (54, 75 and 90 rpm). The feeding pH was 10, distillate temperature was 20 °C and flow rate was 24 rpm. The collected distillate was

automatically weighed on a precision scale and the results were transferred to the computer over a period of time. The fluxes were calculated. The membrane was cleaned at the end of each experiment. Fig 6 shows the variation of the distillate flux with feed flow rate. The fluxes ranged between 7 and 9 L m⁻² h⁻¹ while the highest boron retention was 50% at 54 rpm.

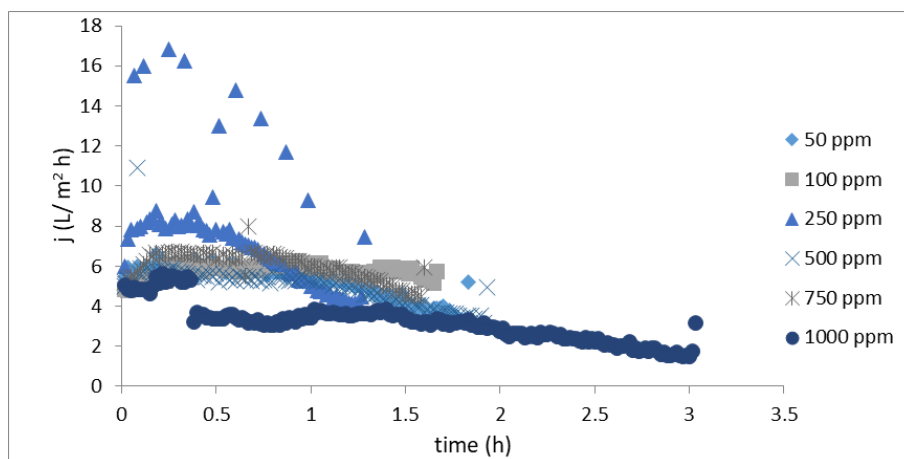


Fig 5. Variation of distillate flux with feed concentration

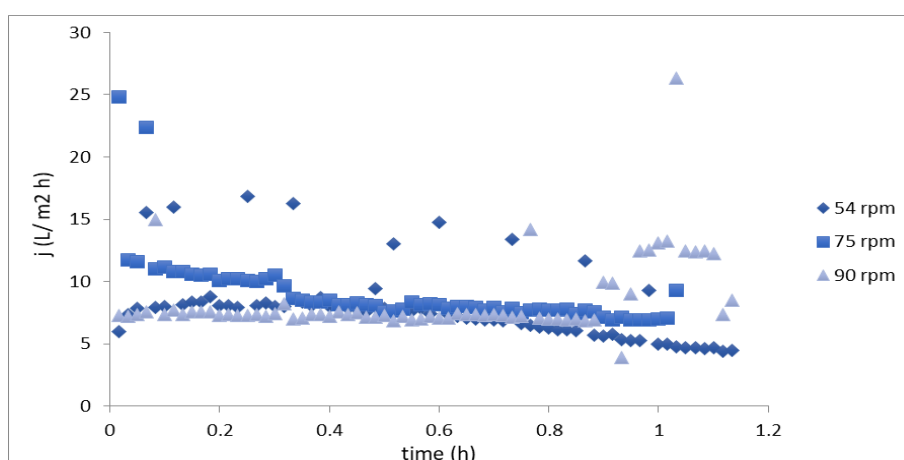


Fig 6. Variation of distillate flux with feed flow rate

3.5. Wastewater experiments

Boron is one of the most used elements in the world due to its superior properties. It is especially important to develop boron removal and recovery techniques from wastewater. The boron contained in the concentrate stream can be recovered as boron crystals by crystallization or evaporation methods. Boron crystals recovered from wastewater can be used in the nuclear field, defense industry, jet and rocket fuel, soap, detergent, solder, photography, textile dyes, glass fiber and paper industry. In this study, boron recovery studies were carried out by removing the water in the concentrated feed stream by evaporation and obtaining boron crystals. First, the wastewater from Eti Kirka Boron Plant was analyzed and the results are given in Table 2. The very high boron concentration of Eti Kirka Boron Plant wastewater is not suitable for the membrane system. A pretreatment was carried out in order to deliver the wastewater sample containing a high amount of boron to the membrane system. Precipitation experiments were carried out using calcium hydroxide. In experimental studies, 500 mL of raw wastewater was taken into beakers. Different amounts of calcium hydroxide (10 and 25g) were added to these samples and mixed for different times (2 and 4 hours) and at different temperatures (80 and 90°C) at 250 rpm and then left to settle. After the precipitation, the samples were filtered and the boron analysis of the clear part was made. Boron removal increased to 85.7% in 90 °C and 2 hours

mixing time. The boron concentration in the waste water sample taken from Kirka boron plant was reduced from 3800 ppm to 500 ppm by pre-precipitation using Ca(OH)₂. After that, DCMD experiments were started. The feed system (wastewater) flow rate was 54 rpm and distillate flow rate was 24 rpm. The wastewater was heated to 30, 40 and 50 °C to observe the changes in the distillate flux (Fig 7). According to Fig 7, the average distillate fluxes for 30, 40 and 50 °C feed temperatures were found to be 13, 16 and 14 L m⁻² h⁻¹, respectively. With increasing temperatures, the boron removal percentages are 47%, 64% and 48%, respectively. At the end of the experiment, the XRD and SEM analyzes of the obtained crystals were performed (Fig 8-13). The SEM analyzes of the contaminated membranes (Fig 14) were also performed.

Table 2. Characterization of wastewater

pH=9.79	
Analysis Type	Amount
Boron analysis (mg L ⁻¹)	3800
Sulphate analysis (mg L ⁻¹)	900
Suspended solid (mg L ⁻¹)	243
COD (mg L ⁻¹)	600

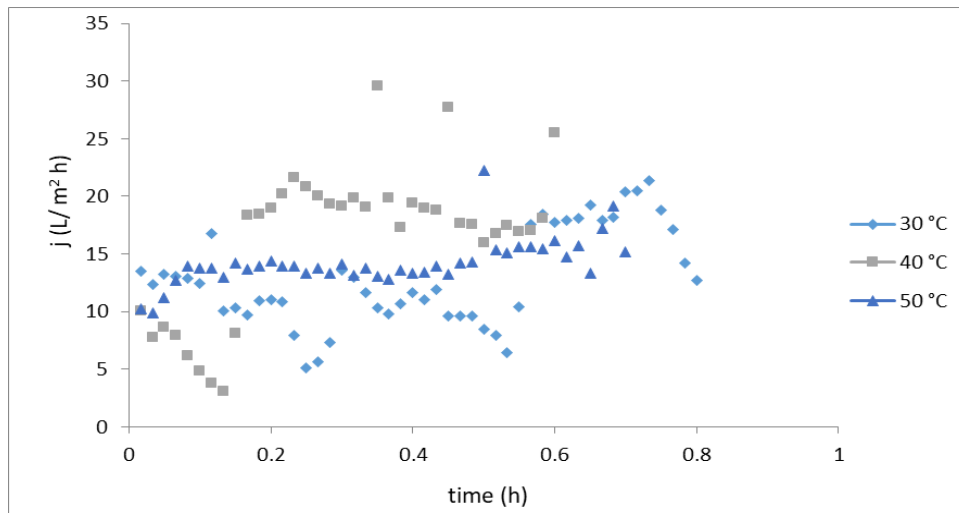


Fig 7. Variation of distillate flux versus time for wastewater

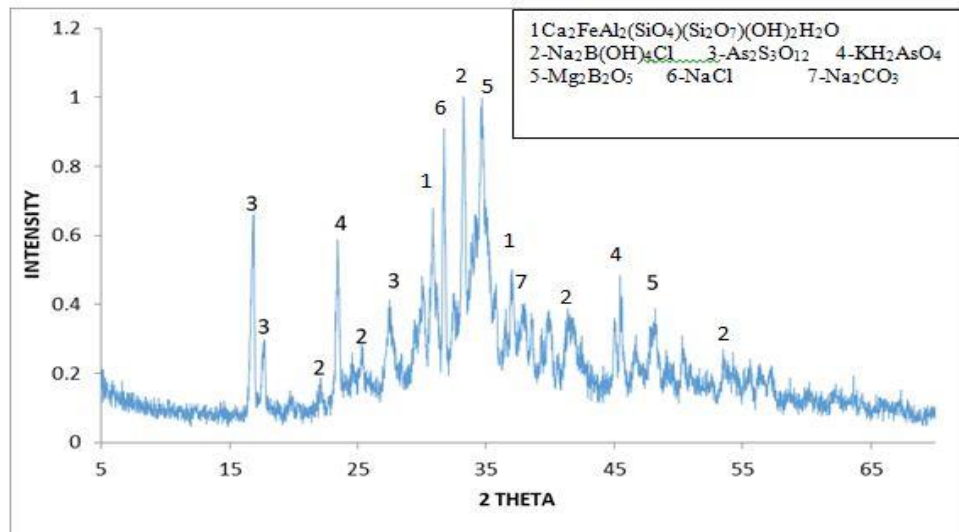


Fig 8. XRD of the crystals obtained from wastewater at 30 °C

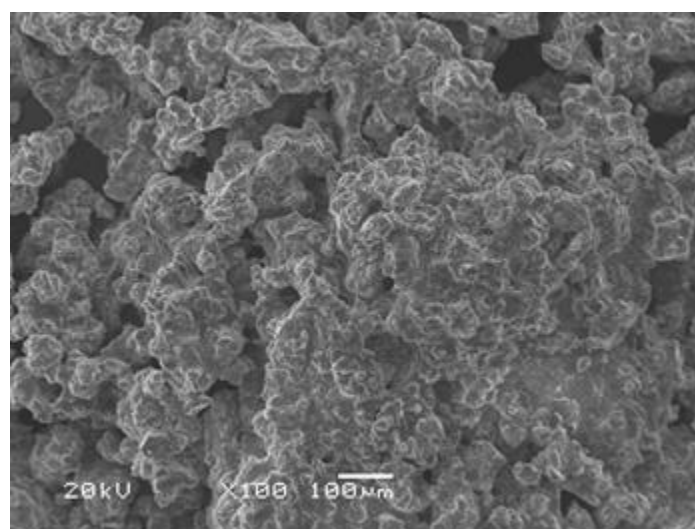


Fig 9. SEM image of the crystals obtained from wastewater at 30 °C

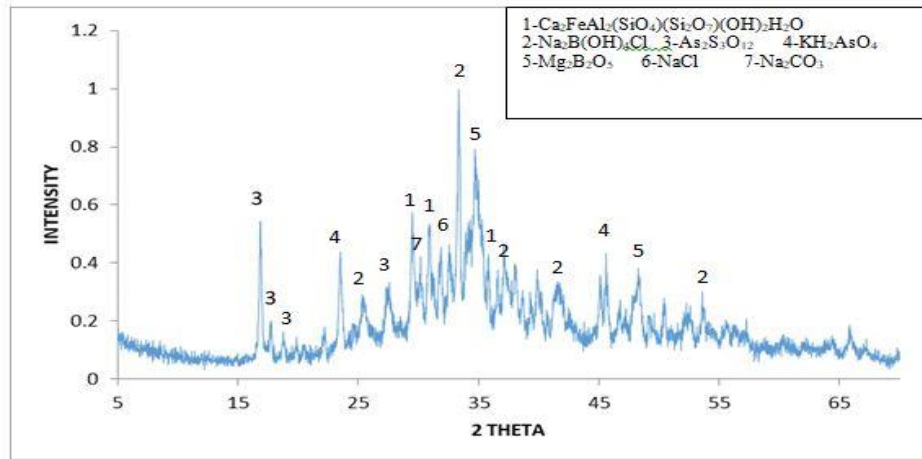


Fig 10. XRD of the crystals obtained from wastewater at 40 °C

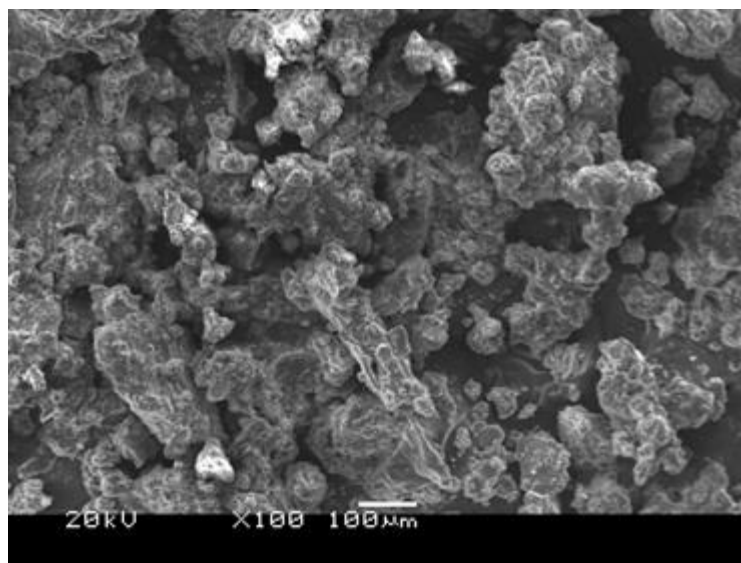


Fig 11. SEM image of the crystals obtained from wastewater at 40 °C

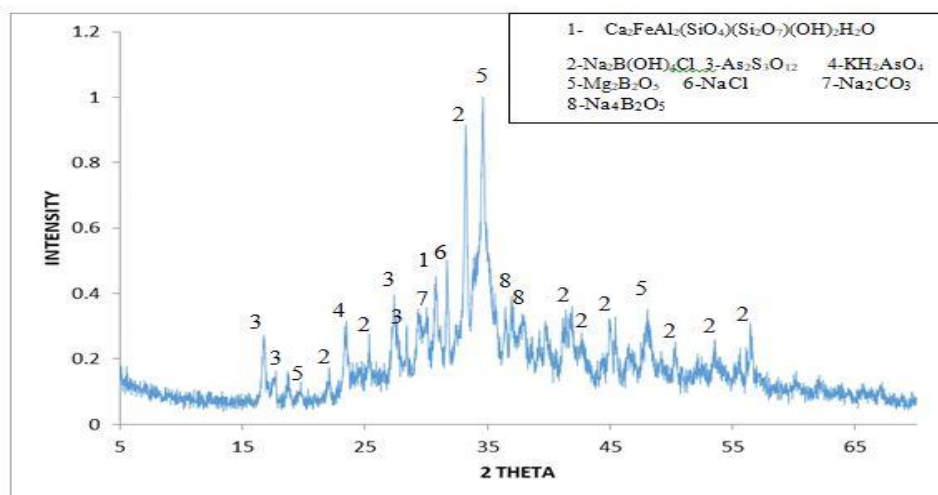


Fig 12. XRD of the crystals obtained from wastewater at 50 °C

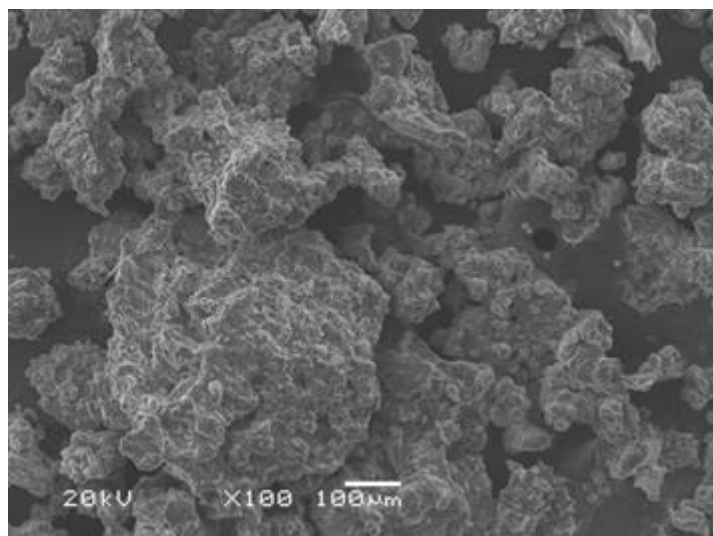


Fig 13. SEM image of the crystals obtained from wastewater at 50 °C

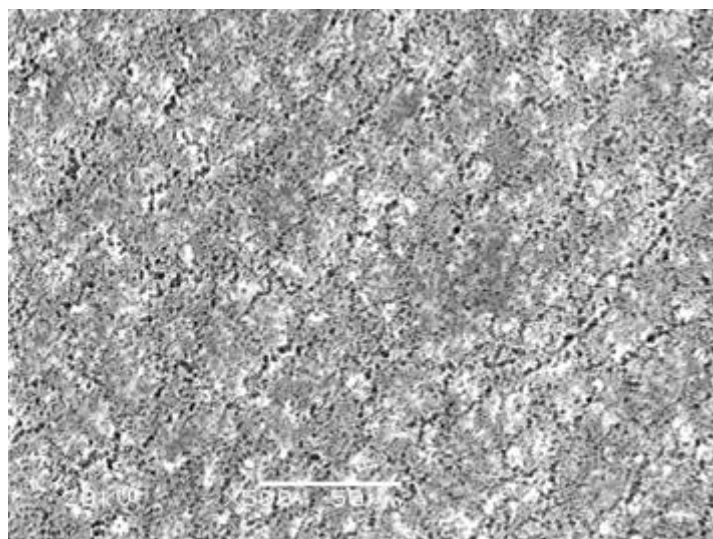


Fig 14. SEM image of the used membrane at the end of the MD experiments using wastewater

4. CONCLUSIONS

Boron is present as boric acid in water below pH=9. In waters above pH=9, borate anions are in the form of $B(OH)_4^-$. The hydrated larger diameter borates at higher pH values are better retained by the membrane in comparison with boric acid at lower pH's. The highest boron removal was found to be 50% at pH=10.

The highest distillate flux ($7.5 \text{ L m}^{-2} \text{ h}^{-1}$) and boron removal (50% removal) were obtained at 50 °C. Usually, there is a linear relationship between the temperature difference of the feed and the distillate and the flux. The greater the temperature difference between the two solutions which come into contact with the two separate surfaces of the membrane, the greater the difference in water vapor pressure which is the driving force for mass transfer. On the other hand, as the temperature rise increases the rate of evaporation, the formation of concentration polarization is also accelerated. Therefore, in the membrane distillation process, it is necessary to

determine the optimum conditions for the temperature and flow rate of the feed solution.

The highest boron removal rate was found to be 52% at 100 mg L^{-1} concentration. Increased concentration of feed solution reduces water vapor pressure and drive power. Thus, the increase in concentration leads to a decrease in distillate flux and boron removal.

In the membrane distillation process, the distillate flux is also related to the flow rate. The shear forces at high flow rates prevent particles from accumulating on the membrane surface. Thus, fouling formation on the membrane surface is reduced. However, in the experiments where the flow rate was examined, the flow rate could not be reached to very high values according to the data obtained in the preliminary studies. The fluxes ranged between 7 and $9 \text{ L m}^{-2} \text{ h}^{-1}$ while the highest boron removal was 50% at 54 rpm. The effect of high flow rates could not be investigated due to the very rapid tearing of the hose.

The optimum pH value was found as 10 in the study. Therefore, the pH (9.8) of the wastewater of Kirka Boron Plant was not changed. For wastewater

experiments, the optimum flow rate found in the previous experiments was used. Therefore, only the temperature of the feed could be studied for wastewater. According to the test results, the average distillate fluxes for the feed temperatures of 30, 40 and 50 °C were found to be 13, 16 and 14 L m⁻² h⁻¹, respectively. Boron removal percentages are 47, 64 and 48%, respectively, with the increasing temperatures.

The feed solution was crystallized at different temperatures. The SEM images of the obtained crystals are not very different from each other. In SEM images of crystals, amorphous layered, plate-like structures have been observed. Boron element is generally found in nature as borate salts or boric acid. Metals such as sodium, calcium, magnesium are found in the structure of boron minerals. In XRD shots, the crystals mostly contain Na₂B(OH)₄Cl and Mg₂B₂O₅ structures although the peak intensities are different. Due to the use of real wastewater, various organic and inorganic contaminants were found in wastewater. Therefore, different compounds other than boron were observed in XRD results.

At the end of the experiments with wastewater, crystals were deposited on the membrane according to the SEM image of the membrane used. Therefore, membrane cleaning was performed at the end of each experiment. Higher boron removal efficiency can be

achieved when this method is applied to waters containing lower concentrations of boron such as geothermal waters.

Along with the capital costs (system investment, auxiliary equipment investment, installation fees, security and control system, etc.) of an MD setup, thermal (energy required for both heating the aqueous feed solution and cooling the permeable aqueous solution or condensate) and electrical (required for operating circulation pumps, vacuum pumps or compressors) energy consumption, energy cost, capacity, feed water quality, optimum flow conditions, long term MD performance, fouling and membrane life, facility life, operation and maintenance (O&M), depreciation, annual operating costs should be considered. The capital cost depends on the capacity and design of the MD system. Fig 15. shows the percentage contribution of different cost elements to capital and O&M expenses for the proposed MD plant in the base case and waste heat integration case. Thermal energy accounts for the largest share of O & M for the base case. Electricity and membrane replacement are the biggest contributors to O&M for waste heat integration situation.

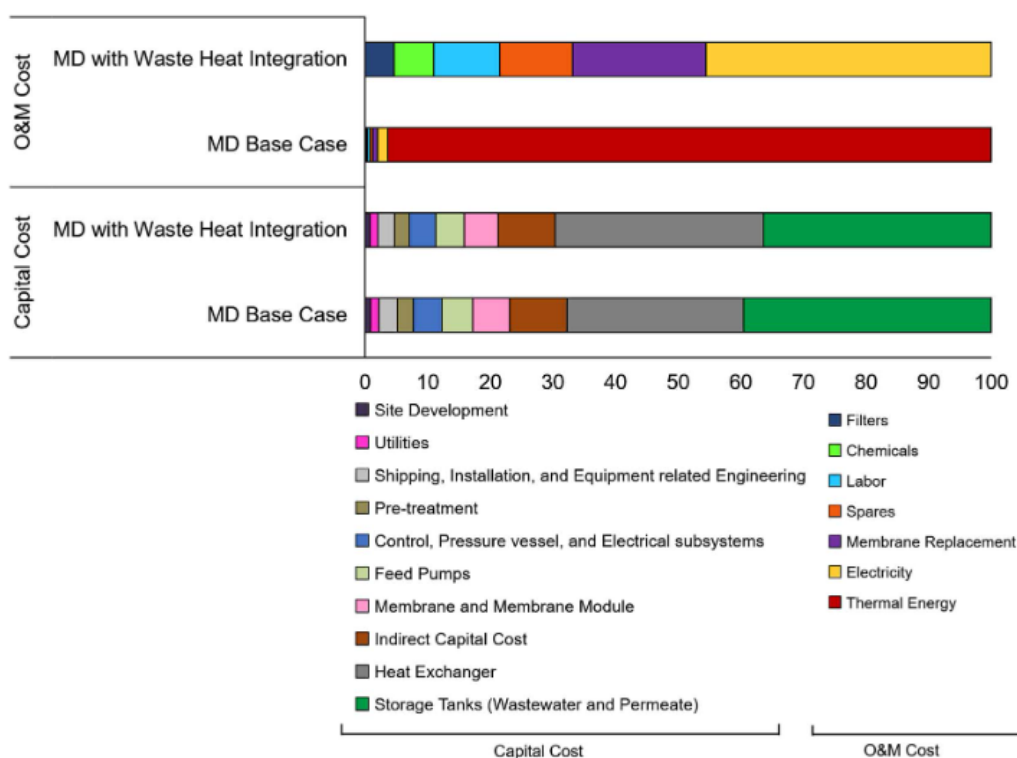


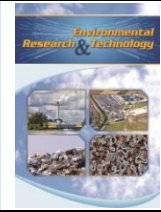
Fig 15. Fractional contribution of capital and O & M costs by various cost elements for base case and MD with waste heat integration scenarios [12]

ACKNOWLEDGMENT

This study was supported by the Scientific Research Projects Commission of Eskişehir Osmangazi University within the framework of the project "201115040". We would also like to thank Prof. Dr. Neşe Öztürk for her valuable ideas and the Eti Kırka Borax Plants for providing wastewater.

REFERENCES

- [1]. Official Gazette, Regulation on Water Pollution Control, No 25687, 31 December 2004.
- [2]. V. Kochkodan, N.B. Darwish and N. Hilal, "The chemistry of boron in water, boron separation processes," Elsevier 1st ed., pp. 35-62, 2015.
- [3]. M. Khayet, T. Matsuura, "Pervaporation and vacuum membrane distillation process: modeling and experiments," *AIChE Journal*, Vol. 50(8), pp. 1697-1712, 2004.
- [4]. A. Alkudhri, N. Darwish and N. Hilal, "Membrane distillation: A comprehensive review," *Desalination*, Vol. 287, pp. 2-18, 2012.
- [5]. P. Onsekizoğlu, "Effects of osmotic distillation and membrane distillation applications on product quality in apple juice production," Doctorate Thesis, Hacettepe University, Ankara, 2010.
- [6]. L. Li, Y. Guan, F. Cheng and Y. Liu, "Treatment of high salinity brines by direct contact membrane distillation: effect of membrane characteristics and salinity," *Chemosphere*, Vol. 140, pp. 143-149, 2015.
- [7]. M. Gryta, "Water purification by membrane distillation process," *Separation Science and Technology*, Vol 41, pp. 1789-1798, 2006.
- [8]. M. Qtaishat, M. Khayet and T. Matsuura, "Novel porous composite hydrophobic/hydrophilic polysulfone membranes for desalination by direct contact membrane distillation," *Journal of Membrane Science*, Vol. 329, pp. 1-2, 193-200, 2009.
- [9]. D. Hou, J. Wang, X. Sun, Z. Luan, C. Zhao and X. Ren, "Boron removal from aqueous solution by direct contact membrane distillation," *Journal of Hazardous Materials*, Vol. 177 pp. 613-619, 2010.
- [10]. R. Bouchrit, "Direct contact membrane distillation: capability to treat hyper-saline solution," *Desalination*, Vol. 376, pp. 117-129, 2015.
- [11]. C. M. Tun, J. T. Fane and M.R. Sheikholeslami, "Membrane distillation crystallization of concentrated salts-flux and crystal formation," *Journal of Membrane Science*, Vol. 257, pp. 144-155, 2005.
- [12]. S. Tavakkoli, O. R. Lokare, R. D. Vidic and V. Khanna, "A techno-economic assessment of membrane distillation for treatment of Marcellus shale produced water," *Desalination*, Vol. 416, pp. 24-34, 2017.



SHORT COMMUNICATION

Country in transition (Serbia) case: Circular economy starts from waste management

Andjelka Mihajlov^{1,*} , Aleksandra Mladenovic¹ , Filip Jovanovic¹ 

¹Environmental Ambassadors for Sustainable Development, Belgrade, SERBIA

ABSTRACT

This paper presents research on the circular economy performance in Serbia. The introduction of a circular economy in the field of waste management is only the first step; the concept of circular economy goes beyond waste management in scope and content. In this paper, the authors emphasize this complexity, starting from the set of available definitions, encompassing the global level, the EU level, as well as the level of Serbia, as a representative country with an economy in transition. An analysis is provided of the concept of circular economy with the targets of the Sustainable Development Goals.

Keywords: Case Study, circular economy, participant science, policy, production and consumption, waste management, sustainable development goals

1. INTRODUCTION

Circular economy is a scenario for societies to transition away from unsustainable linear economies that ultimately deplete finite resources [1, 2]; it is a continual, long-term transition process. There are three key approaches to promoting resource efficiency: 1) extended producer responsibility systems; 2) green public procurement and 3) business partnerships along the value chain.

The methodology used for this analysis is desk review (it is conducted as a compilation of available information with some data availability limitations in practice).

2. THE DEFINITION AND UNDERSTANDING OF THE CIRCULAR ECONOMY CONCEPT

There are more than 100 [3] possible definitions of the circular economy and many different understandings of the concept persist [4,5,6]. The authors' compilation of the meaning of circular economy is presented in Table 1. In addition, numerous consultancy reports have been published.

Table 1. – Circular economy meaning; authors' compilation table

Action areas	Circular economy		
	Priority sectors	Some enablers	Key drivers
production	plastics	innovative	legislation
consumption	food waste	business models	green taxation
waste management	critical raw materials	eco-design	business drivers
secondary raw materials	construction and demolition	extending the product lifetime through reuse and repair	commodity prices raw material shocks
innovation, investigation and monitoring	biomass bio-based products	waste management	

2.1. Circular economy processes

The circular economy is a concept and a process [7]; it is a long-term undertaking that benefits future generations: economic growth with environmental quality and social equity [8].

Corresponding Author: office@ambassadors-env.com (Andjelka Mihajlov)

Received 4 January 2021; Received in revised form 4 March 2021; Accepted 5 March 2021

Available Online 23 March 2021

Doi: <https://doi.org/10.35208/ert.853792>

© Yildiz Technical University, Environmental Engineering Department. All rights reserved.

This paper has been presented at EurAsia Waste Management Symposium 2020, Istanbul, Turkey

The global level and the sustainable development goals

At the global level, the circular economy is increasingly being seen as a shift to a more resource-efficient system [9]. In 2019, the final UNEP [10] resolution invites Member States to achieve sustainable consumption and production, including circular economy, and to consider the outcomes of the GEO-6 report [11] and the Global Resources Outlook 2019 [12]. The 2019 World Resources Forum was centered on the transition to the circular economy, among other perspectives through the lenses of cities and regions, food and bio-based materials and the industry 4.0 [13].

In terms of direction, the links between the Circular Economy and Sustainable Development Goals [14] agendas are obvious. However, the term “circular economy” does not appear in the 2030 Agenda for Sustainable Development, where the Sustainable Development Goals (SDG) and associated targets are set forth. Of course, this does not mean that there is no concept of circular economy in the content of SDGs targets [16], and the quantitative presentation is given in Table 2.

The outcome of the analysis is that as much as the circular economy can help in achieving many SDG targets, the Sustainable Development Goals can also help to promote circular economy practices.

2.2. The European Union level

According to the European Environment Agency report [17] published in October 2019, circular economy initiatives in Europe are still at early stages and they would benefit from more investments in upscaling promising innovations and monitoring progress towards circularity. In 2015, the European Commission [18] presented its Circular Economy Package, which strived for improved cost-efficiency, better balance of current accounts, increased self-sufficiency, new jobs and climate targets. The number of initiatives to implement the concept of circular economy is growing over time [19]. In May 2018, the new EU-wide rules became: 1) adopted for waste management and recycling, 2) proposed for single-use plastic products and 3) proposed for water reuse. The European Commission’s new Circular Economy Action Plan was adopted in 2020 [20, 21]. It introduces legislative and non-legislative measures targeting areas where action at the EU level brings real added value.

2.3. The Country-in-transition level: waste management – the Serbian case

The majority of the generated municipal waste is placed into landfills (about 2 mil. tons in 2019). According to the National Waste Management Strategy from 2003 and 2010, the closure and reclamation of landfills is envisaged, along with the construction of 29 regional sanitary landfills with recyclable waste separation centers and transfer stations. So far, nine regional sanitary landfills are in

place (plus two regional landfills which are under construction), as well as the City of Belgrade “Vinca” landfill with a waste-to-energy facility (construction started in 2020). Centers for separate collection of waste exist in several towns. Also, in certain towns there are facilities for the separation of recyclable waste. There exist 137 non-compliant municipal landfills (operated by public utility companies), a number of illegal (non-controlled) dumpsites (for about 20% of the generated municipal waste). It is noted that there are more than 2000 such sites of different sizes. There is no waste incineration plant. There are no facilities for the treatment of organic municipal waste. Two out of three cement plants substitute fossil fuels with some specific waste streams (at an average rate of about 20%) to recover energy and to obtain raw materials for the production of cement. Waste separation at the municipal level is not sufficiently developed; only certain towns and cities possess infrastructure and some facilities for the separation of recyclable waste. As far as recycling is concerned, there are some registered facilities for the recycling of metal, plastic, PET, etc. The potential for material recycling is 72% for paper and cardboard, 35% for metal, 25% for plastic, 22% for glass and 20% for wood. Also, there are options for some specific waste recycling [30]. The main challenges of an integrated waste management system in the Republic of Serbia include: - appropriate infrastructure for municipal and hazardous waste, - capacities and coverage for basic services, like collection, transport and appropriate waste disposal. It should be noted that an improvement of the data collection system is needed and foreseen.

2.4. The Country-in-transition level: circular economy – the Serbian case

Circular economy in Serbia is in an early stage. This conclusion is based on separate research within the ENV.net project in developing a qualitative citizen science tool; this citizen science tool is developed by the Environmental Ambassadors for Sustainable Development and Ebart media archive, Belgrade (Table 3). Citizen science [21] (or participative science) is public participation and collaboration in scientific research to increase scientific knowledge; the authors developed this citizen, participant science tool considering that journalists/the media represent citizens (with common interests) and also that surveys are crowdsourcing tools (the core power of citizen science).

As a UN member state and EU membership candidate, Serbia is already committed to the circular economy concept [22]. However, no integrated approach is in place yet and the environmental policy framework needs to be reinforced in key economic and sectoral policies. Valuable data are available in the EU Serbia Progress/Annual Reports [23]. In addition, some relevant data are available in the OECD report on Environmental Policy in South East Europe [24-26]. The mapping of the “state of the art” of the Circular Economy in Serbia [27] entails the identification of what is present.

Table 2. Relationship between the circular economy concept and the 169 Sustainable Development Goals targets

Overall relationship of circular economy practices and the 169 targets of the SDGs (between brackets is the number of relevant SDG targets)	
Direct contribution of circular economy practices to achieve target (21)	SDG 6 – Clean Water and Sanitation (4) SDG 7 – Affordable and Clean Energy (3) SDG 12 – Sustainable Consumption and Production (3) SDG 15 – Life on Land (3) SDG 8 – Economic Growth and Decent Work (2) SDG 9 – Industry, Innovation and Infrastructure (2) SDG 2 – Zero Hunger (1) SDG 3 – Good Health and Well-being (1) SDG 11 – Sustainable Cities and Communities (1) SDG 14 – Life below Water (1)
Indirect contribution of circular economy practices to achieve target, e.g. via other SDGs (28)	SDG 12 – Sustainable Consumption and Production (5) SDG 1 – No Poverty (4) SDG 2 – Zero Hunger (3) SDG 8 – Economic Growth and Decent Work (3) SDG 11 – Sustainable Cities and Communities (3) SDG 15 – Life on Land (3) SDG 14 – Life below Water (2) SDG 6 – Clean Water and Sanitation (1) SDG 7 – Affordable and Clean Energy (1) SDG 10 – Reduced Inequalities (1) SDG 13 – Climate Action (1) SDG 16 – Peace and Justice, Institutions (1)
Achieving target will contribute toward circular economy (52)	SDG 17 – Partnership for the Goals (9) SDG 9 – Industry, Innovation and Infrastructure (6) SDG 16 – Peace and Justice, Institutions (6) SDG 4 – Quality Education (5) SDG 8 – Economic Growth and Decent Work (4) SDG 10 – Reduced Inequalities (4) SDG 2 – Zero Hunger (3) SDG 11 – Sustainable Cities and Communities (3) SDG 13 – Climate Action (3) SDG 14 – Life below Water (3) SDG 5 – Gender Equality (2) SDG 12 – Sustainable Consumption and Production (2) SDG 1 – No Poverty (1) SDG 15 – Life on Land (1)
No link or weak link (35)	SDG 3 – Good Health and Well-being (11) SDG 5 – Gender Equality (6) SDG 16 – Peace, Justice and Institutions (5) SDG 10 – Reduced Inequalities (4) SDG 4 – Quality Education (3) SDG 11 – Sustainable Cities and Communities (2) SDG 1 – No Poverty (1) SDG 8 – Economic Growth and Decent Work (1) SDG 14 – Life below Water (1) SDG 15 – Life on Land (1)

In 2020, an Ex-ante analysis of the effects of (future) circular economy policy was finished, and the Serbian Ministry of Environmental Protection, supported by UNDP, published “A Roadmap for circular economy in Serbia” [29].

In 2020, Serbia adopted the New Industrial Policy Strategy 2021-2030; as a horizontal industrial policy, this strategy addresses, among others, the issue of the circular economy [29].

Table 3. Journalists/the media representing citizens' interests in circular economy and waste

Number of articles with the terms "circular economy" and "waste" in written media in Serbia									
2011	2012	2013	2014	2015	2016	2017	2018	2019	2020
0	2	3	5	18	20	21	40	80	80
3169	2648	2040	1878	1673	1243	1421	1416	1559	1258

Although Serbia has possessed Waste Management Strategies since 2003, in line with the EU acquis, an updated/new public policy document for waste management is expected in 2020/2021, as well as a new/updated Law on Waste Management, in line with the EU acquis regarding circular economy and waste.

3. DISCUSSION

The concept of circular economy goes beyond policy for waste management in scope and in content. In Serbia, as presented in Table 3, citizens are much more concerned and informed about waste issues than about the possibilities and meaning of circular economy.

In practice, waste management contributes to circular economy through its elements: overall recycling rates, recycling rates for specific waste streams, as well as waste generation [28]. However, in order to come closer to the real meaning of circular economy (Table 1), it is also important to consider other elements of circular economy: production and consumption (self-sufficiency for raw materials, green public procurement), secondary raw materials (contribution of recycled materials to raw material demand, trade in recyclable raw materials) and competitiveness and innovation (private investments, jobs and gross value added, patents).

To understand circular economy beyond waste management, in countries with economies in transition it is particularly important to know how to bridge identified gaps [1, 31] and not believe that circular economy can be accomplished with interventions only in the waste sector. Waste management should be taken only as an important, possibly first step in building the circular economy process (what should be considered as the initial important step is the planned updated/new public policy document for waste management, as well as a new/updated Law on Waste Management, in line with the EU acquis regarding circular economy and waste in Serbia).

4. CONCLUDING REMARKS

Addressing the circular economy only through waste management issues shows that the circular economy concept is still at an early stage. It should also be noted that circular economy issues in the accession process to the EU are not only a subject of the Chapter on Environment and Climate Change; the circular economy is relevant to all sectors of the economy.

Sustainability in risk management needs to be mainstreamed and long-term thinking fostered (environmental and climate risks are not always adequately considered by the financial sector; social factors can also have concrete consequences for financial institutions, including legal risks etc.).

Some possible ways forward, through the exercising of legally prescribed procedures (in Serbia, but also applicable to other countries with transitional economies/developing countries) include:

- Prepare the appropriate public policy paper for the circular economy which provides guidelines for action; apply an integrated approach

- Foster the circular economy process by strengthening and monitoring the effectiveness of multi-stakeholder coalitions

- Update/adapt the adequate waste management policy paper

- Adapt Agenda 2030 to the implementation of the circular economy concept

- Prepare new appropriate legislation in all sectors of the economy

- Assure stricter enforcement of the environmental policy framework in key economic and sectoral policies (such as a proper implementation of the strategic impact assessment, environmental impact assessment, industrial directives, investment tools)

- Accelerate awareness raising and dissemination of knowledge around circular economy topics, including focusing on educating young people

- Assure means of financing from all sources (often financing unsustainable resource management models).

ACKNOWLEDGMENTS

This research analysis was supported by the EU-funded project ENV.Net Factoring the Environmental Portfolio for WB and Turkey in the EU Policy Agenda, as well as the Serbian Ministry of Environmental Protection.

REFERENCES

- [1]. [Online source]. Available: https://circulareconomy.europa.eu/platform/sites/default/files/circularity_gap_report_2019.pdf (Accessed 2 January 2021).
- [2]. A.Mihajlov., et al, "Scoping the future trends in natural resources availability using selected indicators as measures of progress: the links

- with interests and values”, Conference: 7th Congress Of Environmental Management - X Convención Internacional Sobre Medio Ambiente Y Desarrollo, CD Proceedings (ISBN 978-959-300-073-4), paper GA-002At: Havana, Cuba, 2015.
- [3]. J. Kirchherr, D. Reike and Marko Hekkert, “Conceptualizing the circular economy: An analysis of 114 definitions,” *Resources, Conservation and Recycling*, Vol.127, pp. 221-232, 2017.
- [4]. M. Geissdoerfer, P. Savaget, N.M.P. Bocken and E. JanHultink “The circular economy – a new sustainability paradigm,” *Journal of Cleaner Production*, Vol. 143, pp. 757-768, 2017.
- [5]. N. van Buren, M. Demmers, R. Van der Heijden and F. Witlox “Towards a circular economy: the role of Dutch logistics industries and governments,” *Sustainability*, Vol. 8(7), pp. 647, 2016.
- [6]. J. Potting, M.P. Hekkert, E. Worrell and A. Hanemaaijer, “Circular Economy: Measuring Innovation in the Product Chain” (2017) Available: <http://www.pbl.nl/sites/default/files/cms/publicaties/pbl-2016-circular-economy-measuring-innovation-in-product-chains-2544.pdf> (Accessed 2 January 2021).
- [7]. A. Mihajlov., “Circular Economy Concept: is the loop closed?” Plenary at PIMB Conference – Circular economy – chance for sustainable development, Zrenjanin, Serbia, April 2019.
- [8]. Concepts also supposed to operationalize sustainable development for businesses are the green economy and green growth concepts (UNEP, 2011; OECD, 2016)
- [9]. EMF “Growth Within: A Circular Economy Vision for a Competitive Europe” Ellen MacArthur Foundation, 2015. Available: <https://www.ellenmacarthurfoundation.org/assets/downloads/publications/EllenMacArthurFoundationGrowthWithinJuly15.pdf>. (Accessed 2 January 2021).
- [10]. UNEP/EA.4/L.2 (UNEA 2019), Available: <https://wedocs.unep.org/handle/20.500.11822/28512> (Accessed 2 January 2021).
- [11]. GEO-6 Report. Available: <https://www.unenvironment.org/resources/global-environment-outlook-6> (Accessed 2 January 2021).
- [12]. Global Resources Outlook 2019. Available: <https://www.resourcepanel.org/reports/global-resources-outlook> (Accessed 2 January 2021).
- [13]. See for example S. Rajput and S. Prakash Singh, “Connecting circular economy and industry 4.0,” *International Journal of Information Management*, Vol. 49, pp. 98-113, 2019.
- [14]. [Online source] Available: https://www.un.org/ga/search/view_doc.asp?symbol=A/RES/70/1&Lang=E (Accessed 2 January 2021).
- [15]. P. Schroeder, K. Anggraeni, and U. Weber, “The Relevance of Circular Economy Practices to the Sustainable Development Goals,” *Journal of Industrial Ecology*, Vol. 23 (1), pp. 77-95, 2018.
- [16]. [Online source] Available: <https://www.eea.europa.eu/publications/circular-economy-in-europe-insights> (Accessed 2 January 2021).
- [17]. [Online source] Available: https://ec.europa.eu/environment/circular-economy/index_en.htm (Accessed XX January 2021).
- [18]. F.Preston, J.Lehne and L.Wellesley, “An Inclusive Circular Economy: Priorities for Developing Countries”, Chatham House - The Royal Institute of International Affairs, May 2019.
- [19]. [Online source] Available: <https://ieep.eu/publications/an-analysis-of-the-new-eu-circular-economy-action-plan> (Accessed 2 January 2021).
- [20]. M. Pantzar. and T. Suljada, “Delivering a circular economy within the planet’s boundaries: An analysis of the new EU Circular Economy Action Plan”. Institute for European Environmental Policy (IEEP) and Stockholm Environment Institute (SEI): Brussels and Stockholm, 2020.
- [21]. [Online source] Available: <https://www.nationalgeographic.org/encyclopedia/citizen-science/> (Accessed 2 January 2021).
- [22]. A. Mihajlov., “Sustainable Development Goals Implementation - EU Accession interface in the context of the Western Balkan more efficient and coherent Sustainable Development Pathways” , Conference: Humboldt-Kolleg “Sustainable Development and Climate Change: Connecting Research, Education, Policy and Practice,” In the Book of Abstracts. Available: <http://www.humboldt-serbia.ac.rs/kolleg2018/pics/Humbolt-2018.pdf> (Accessed 2 January 2021).
- [23]. [Online source] Available: <http://www.mei.gov.rs/eng/documents/eu-documents/annual-progress-reports-of-the-european-commission-for-serbia> (Accessed 2 January 2021).
- [24]. [Online source] Available: https://www.oecd-ilibrary.org/development/competitiveness-in-south-east-europe/environmental-policy-in-south-east-europe_9789264298576-18-en (Accessed 2 January 2021).
- [25]. [Online source] Available: http://www.sepa.gov.rs/download/publikacije/MoreFromLess_MaterialResourceEfficiencyEurope.pdf; <https://www.eea.europa.eu/publications/more-from-less> (Accessed 2 January 2021).
- [26]. [Online source] Available: http://www.undp.org/content/dam/serbia/Publications%20and%20reports/English/UNDP_SRB_Study_on_Achievements_and_Perspectives_towards_a_Green_Economy_and_Sustainable_Growth_in_Serbia.pdf (Accessed 2 January 2021).
- [27]. A. Mihajlov, A.Mladenović and F.Jovanović, “Circular Economy in Serbia: The Process Started”, Belgrade: Environmental Ambassadors

- for Sustainable Development, 2019; Available: <http://ambassadors-env.com/en/circular-economy-in-serbia/> (Accessed 2 January 2021).
- [28]. EC: COM(2018)29 final. Available: <https://ec.europa.eu/environment/circular-economy/pdf/monitoring-framework.pdf> (Accessed 2 January 2021).
- [29]. 2020 Spotlight Report on Circular Economy in Serbia. Available: <http://ambassadors-env.com/en/files/Spotlight.pdf> (Accessed 2 January 2021).
- [30]. Guidelines on Circular Economy for the countries of the Western Balkans and Turkey, EEB, Institute for the Circular Economy, 2020, pp.27-30. Available: https://mk0eeborgicuyptuf7e.kinstacdn.com/wp-content/uploads/2021/01/guideline-WBT_INCIEN_final.pdf (Accessed 2 January 2021).
- [31]. A.Mihajlov, H.Stevanovic-Carapina, "Rethinking waste management within the resource-efficient concept", *Environmental Engineering and Management Journal*, Vol. 14 (2), pp. 2973-2978, 201



RESEARCH ARTICLE

Density cleaning for some Turkish lignites

Serdar Yılmaz¹ , Mehmet Bilen^{1,*} 

¹Bülent Ecevit University, Faculty of Engineering, Department of Mining Engineering, İncivez Merkez, Zonguldak, 67100, TURKEY

ABSTRACT

In the scope of this study, in order to determine the floatability characteristics of lignites, 5 samples were collected from various lignite reserves of Turkey namely Dursunbey, Çayırhan, Iğın, Ermenek, and Gürmin-Merzifon. Collected samples were analyzed in terms of float and sink analysis. As regards to float and sink analysis, the original samples were floated and sunk in 2 different $ZnCl_2$ solutions of densities 1.40 and 1.60 g cm^{-3} . Proximate analysis of each original sample for the corresponding lignite was carried out in the beginning of this study. In terms of proximate analysis performed, Dursunbey lignite sample has the lowest ash content of 24.86 % while Gürmin Merzifon lignite sample has the highest ash content of 45.02 %, respectively. Accordingly, 5 float and sink analysis graphic obtained and they would help one to understand and easily figure out the optimum medium density for cleaning.

Keywords: Turkish lignites, coal washability, float and sink, density cleaning, coal preparation

1. INTRODUCTION

Washability test for coals is carried out with float and sink analysis and the data obtained is used to understand which separation medium is optimum for coal cleaning. Coal preparation plants are cleaning the run of mine coals with density medium. More clearly, a solution with magnetites (due to its easy recyclability) is prepared and coal samples are faced with that specific solution. Some amount of coal and lower density materials are floating over the solution while other shales and high density materials are tend to sink. Although this method is environmentally disadvantageous and economically not feasible, it has been widely used in coal preparation plants in the world. Recent technologies are focusing on dry separation of coal and shale, but still this traditional method of cleaning is better in terms of efficiency and capacity.

Lignite reserves are widely present in Turkey and they constitute the major portion. In the study of Çakal et al [1], chemical and physical properties of some lignites were investigated. Çakal et al. [1] have studied 4 different lignite coal samples and they determined the ash contents between 18.6 % and 37.5 %. Sulfur content of lignites are also important in

terms of their utilization as fuel to power plants. Referring back to Çakal et al. [1] study, sulfur contents of the studied samples varies between 1.4 % and 4.4 %. As in the study of İnaner and Nakoman [2], Çan lignites were studied and their ash and sulfur content was determined as 29.67 % and 3% (as received basis) respectively. Same authors have provided a figure of hard coal and lignite deposits of Turkey and it is provided in Fig 1.

The tabulated regional reserve distribution and average chemical properties of Turkish lignites are provided in Table 1 (Adopted from the study of İnaner and Nakoman [3]).

Referring to the Table 1, Turkish lignites have the average of 21% ash content and 2.1% sulfur content, respectively. Moisture content is also high and it is between 20% and 50%. Turkish lignites are mostly utilized as fuel to power plants. There are mostly power plants located nearby these deposits. However referring back to the Table 1, lignites have lower calorific values than steam coals. The boilers of the power plants are designed with respect to coals with specific calorific value. In order to have the designed calorific specification, there should be coal preparation plants. These coal preparation plants utilize the run of mine coal and products are clean

Corresponding Author: mehmet.bilen@beun.edu.tr (Mehmet Bilen)

Received 20 November 2020; Received in revised form 12 February 2021; Accepted 20 February 2021

Available Online 26 February 2021

Doi: <https://doi.org/10.35208/ert.828660>

© Yildiz Technical University, Environmental Engineering Department. All rights reserved.

coals with higher calorific values and lower ash and sulfur content. Depending on the nature of the coals, density cleaning is sometimes hard. In this context, washability of the coal should have been investigated beforehand in order to have optimum usage of chemicals and optimum product properties. Ozbas et

al. [4] have investigated the effect of cleaning process on combustion characteristics of lignites in their study and they have summarized this fact: "reducing the ash and sulfur content by washing has become a compulsory process to obtain an environmentally friendly product".

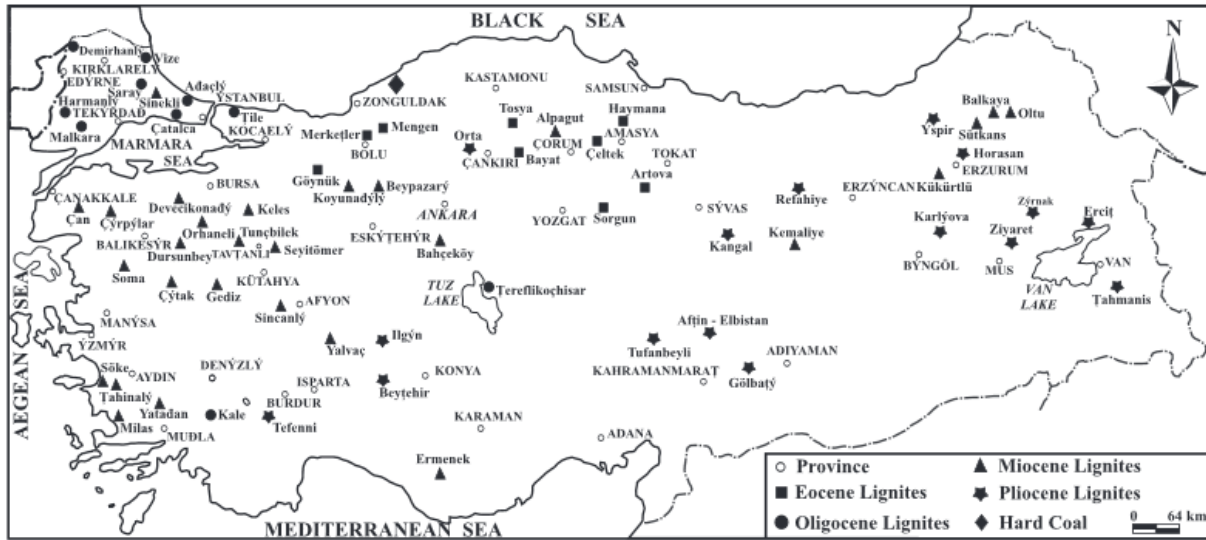


Fig 1. Hardcoal and lignite deposits of Turkey [3]

Table 1. Regional reserve distributions and average chemical properties of Turkish lignites [3]

REGIONS	AGE	RESERVE (109 tonnes)	MOISTURE (%)	S (%)	ASH (%)	CALORIFI C VALUE (kcal kg ⁻¹)
NORTH -WEST ANATOLIA REGION (Kütahya-Balıkesir- Bursa-Manisa-Çanakkale)	Miocene	2	20	1.7	20	3500
SOUTH - MIDDLE - ANATOLIA REGION (Adana- Kahramanmaraş)	Pliocene	4	50	2.0	20	1200
CENTER ANATOLIA REGION (Ankara-Çorum) (Konya-Çankırı- Sivas)(Yozgat)	Miocene Pliocene Eocene	1.45	30	3.2	25	3000
SOUTH WEST ANATOLIA REGION (Aydın-Muğla- Denizli-Isparta-Afyon) (Burdur)	Miocene Pliocene	0.9	30	2.0	20	2500
THRACE REGION (Tekirdağ-Edirne- Kırklareli-Istanbul)	Oli- gocene	0.4	30	3.0	20	2500
EAST ANATOLIA REGION (Bingöl-Erzincan-Van) (Erzurum)	Pliocene Miocene	0.2	20	1.2	20	3000
TOTAL		8.25	36.5	2.1	21	2240

Sivrikaya [5] has studied a low rank lignite and the author has applied dense medium, gravity-based and floatation techniques to evaluate the its cleaning potential. Aktas et al. [6] have studied centrifugal float and sink separation of fine Turkish coals in dense media and they have summarized the dependency of the float fraction grade on the “dense medium density”, “degree of liberation” and the “amount of submicron particles” in the coal samples. However either float and sink characterization of coal samples or the floatability in general depends strongly on the hydrophobicity of the coal samples and as stated by Sivrikaya [5] hydrophobicity changes with rank, petrographic composition and degree of oxidation [7, 8-11]. High ash content along with low carbon content, high content of polar groups (hydroxyl, carboxyl, carbonyl) are considered as the main reasons for the low floatability and hydrophilic nature of lignites [5, 11- 13].

Washability characteristics of coals are tested with float & sink tests. Based on the float and sink test results of a specific coal, extent of the washing conditions are determined [14, 15]. In addition to washability tests, Atesok et al. [16] have employed Reichert spiral to understand the cleaning characteristics of bituminous and lignitic coals. According to Aksoy et al. [17], in terms of lignite fines cleaning, physical processing methods are widely employed since they have lower costs and easier to employ. In order to employ the physical methods, corresponding requirements of each physical separation agent should be understood and this can be realized with washability characterization. However, there are some obstacle for physical separation and the major limiting factor for gravity separation is regarded as its dependency on particle size of coal [17]. So, determination of washability characteristics of lignites and understanding the physical separation requirements beforehand should include the consideration of particle size. Although fine coal cleaning is off great importance by many researchers [18-23], still the washability characterization of lignites has significance in terms of ash and sulfur reduction which are crucial in terms of the processes of further utilization. In addition to the abovementioned, Hacifazlioglu and Toroglu [24] have investigated the optimum design and operating parameters of slime coal cleaning in a pilot scale Jameson cell. Coal cleaning in terms of environmental and economical point of view has great significance. Assessment of cleaning requirements & conditions along with any possible improvements could only be understood with washability characteristics.

In this study washability characteristics of 5 different lignite samples was investigated and this was carried out with the help of float and sink analysis tests. In this context, results are not only tabulated but also corresponding graphical demonstrations of float and sink curves were provided. Based on the tabulated data and considering the corresponding plots of float and sink experiments, density requirement of the cleaning process could be estimated. Not only density of the medium of separation could be understood but also the corresponding ash content of the product at the end of cleaning/washing would be clear with the help of this study.

2. MATERIALS AND METHOD

Coal washability properties are determined by the evaluation of the float and sink test results. Float and sink analysis is carried out on a solution (at a density previously determined) and coal particles either float over or sink in this solution. More clearly, when a coal sample faced with high density medium, particles with lower density tends to float while particles with higher density tends to sink.

Float and sink analysis on the studied samples was carried out with the 1.40 and 1.60 g cm⁻³ solutions. These abovementioned solutions were prepared with ZnCl₂.

3. RESULTS & DISCUSSION

Ash content of run of mine coal samples and their density cleaned fractions were tabulated in Table 2. The most significant decrease in ash content is observed for Gürmin-Merzifon lignite sample while the lowest decrease is observed on Ilgın sample.

Table 2. Ash content of run of mine coals and 1.60 gr cm⁻³ cleaned coals

Sample	Ash Content (%) (as received)	Ash Content (%) (cleaned with 1.60 gr cm ⁻³ medium)
Dursunbey	24.05	16.49
Çayırhan	26.29	17.06
Ilgın	28.52	26.38
Ermenek	23.50	17.55
Gürmin- Merzifon	45.34	23.33

In this study, sieve analysis was carried out for the samples investigated. In order to evaluate the size orientation, samples are only crushed with primary crusher (jaw crusher). In this case, a quick understanding of the float and sink tendency of the samples was addressed and size dependency of washability characteristics was not considered in detail. Tabulated float and sink analysis results (Table 3-7) and float and sink analysis graphs (Fig 2-6) are provided.

Considering float and sink graph (Fig 2) and tabulated data of float and sink experiment (Table 3) for Dursunbey lignite sample, run of mine coal has 24.05% ash content. Fraction of 34.51% for this original sample (Dursunbey lignite) floats at 1.40 g cm⁻³ medium and ash content of this corresponding float is 7.96 %. Original sample has the weight percentage of 38.46 (%) which has the density of +1.40-1.60 gr cm⁻³, and ash content of this abovementioned fraction (middling) is 24.14 %. If Dursunbey lignite (run of mine) is floated at 1.60 g cm⁻³ density solution, 72.97% of it would be collected as float fraction and it would have 16.49 % ash content.

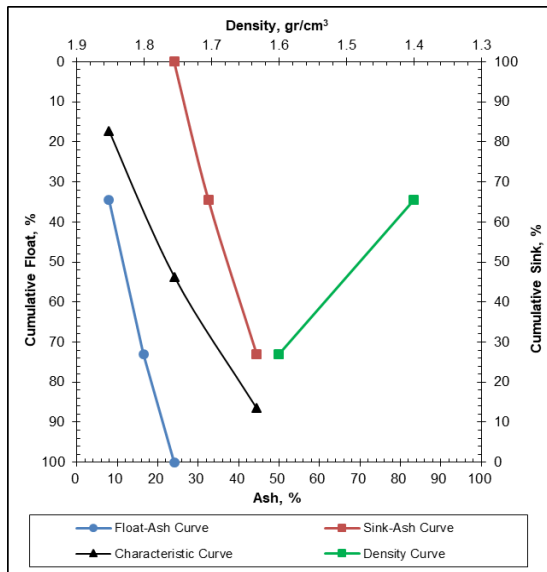


Fig 2. Float and sink graph for Dursunbey lignite sample

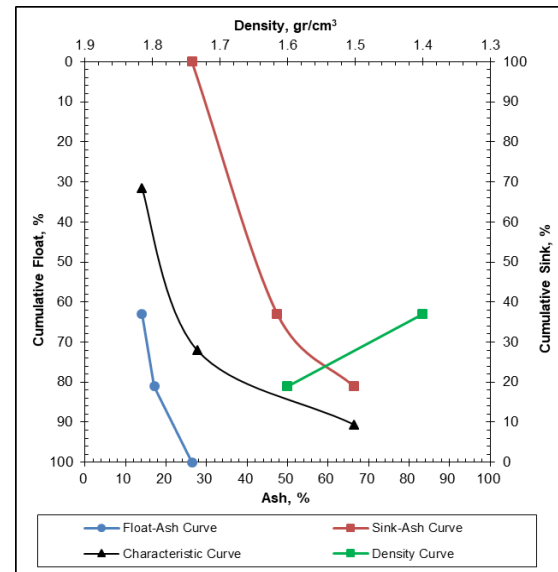


Fig 3. Float and sink graph for Çayırhan lignite sample

Table 3. Float and sink analysis results for Dursunbey lignite sample

Density gr cm ⁻³	Float		Cumulative Float			Cumulative Sink			
	%Amount	%Ash	Content	%Amount	Content	%Ash	%Amount	Content	%Ash
-1.40	34.51	7.96	274.70	34.51	274.70	7.96	100.00	2404.61	24.05
+1.40 - 1.60	38.46	24.14	928.42	72.97	1203.12	16.49	65.49	2129.91	32.52
+1.60	27.03	44.45	1201.48	100.00	2404.61	24.05	27.03	1201.48	44.45
Total	100.00	24.05	2404.61						

Table 4. Float and sink analysis results for Çayırhan lignite sample

Density gr cm ⁻³	Float		Cumulative Float			Cumulative Sink			
	%Amount	%Ash	Content	%Amount	Content	%Ash	%Amount	Content	%Ash
-1.40	62.98	14.02	882.98	62.98	882.98	14.02	99.77	2628.69	26.35
+1.40 - 1.60	17.97	27.71	497.95	80.95	1380.93	17.06	36.79	1745.71	47.45
+1.60	18.82	66.30	1247.77	99.77	2628.69	26.35	18.82	1247.77	66.30
Total	100.00	26.29	2628.69						

As regards to tabulated data (Table 4) and corresponding float and sink graph (Fig 3), Çayırhan lignite sample, which has originally has 26.29 % ash content, can rather be cleaned with 1.40 g cm⁻³ solution. The float fraction of 63.02 % has been collected at the end of 1.40 g cm⁻³ float and sink experiment and corresponding ash content of this collected fraction is 14.02%. A total amount of 81.06% can be collected as float and the ash content would be 17.07 % considering the 1.60 g cm⁻³ cumulative float. The fraction collected as sink for the 1.60 g cm⁻³ (+1.60 g cm⁻³) solution is 18.94 %, which is a little bit more than the middling (+1.40-1.60 g cm⁻³) i.e. 18.04%, and their ash contents are 66.30 % (sink 1.60) and 27.71 % (middling), respectively. It can be claimed that high percentage of float fraction can be collected with only 1.40 g cm⁻³ as an initial evaluation.

In terms of the Ilgin sample, amount of the float fraction (1.40 g cm⁻³) is 78.45 % and ash content of the corresponding is 21.63 %. Referring to tabulated data (Table 5) and graphical representation (Fig 4) of float and sink experiment, Ilgin sample has 28.52 % ash content originally and cumulative float of 1.60 g cm⁻³ has the ash content of 26.38 %. The negligible difference between ash contents for cumulative float of 1.60 g cm⁻³ and original (abovementioned, 26.38 % and 28.52 % respectively) is actually because of the high mass fraction collected as cumulative float, i.e. 94.20 %. In this case, there would be no meaning for the 1.60 g cm⁻³ density cleaning for Ilgin sample, rather it should be cleaned with 1.40 g cm⁻³ solution. Still, 1.40 g cm⁻³ solution did not contribute much since the ash percentage was 28.52 (%) in the beginning and after this test (1.40 g cm⁻³ float and sink) it only decreased to 21.63 %, which can be

interpreted as Ilgin sample does not favor density medium separation.

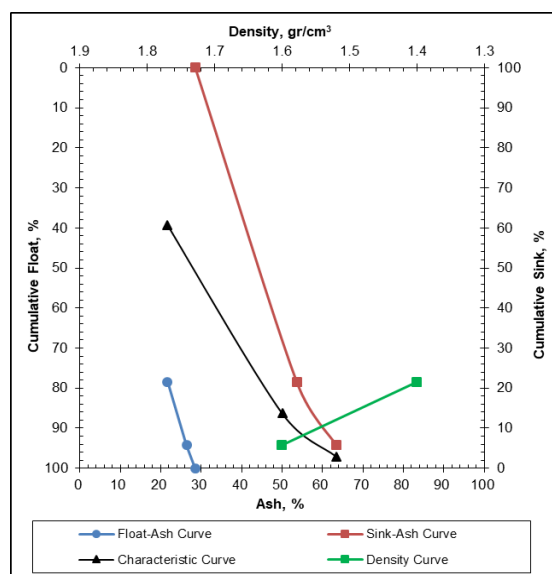


Fig 4. Float and sink graph for Ilgin lignite sample

In terms of the Ilgin sample, amount of the float fraction (1.40 g cm⁻³) is 78.45 % and ash content of the corresponding is 21.63 %. Referring to tabulated data (Table 5) and graphical representation (Fig 4) of float and sink experiment, Ilgin sample has 28.52 % ash content originally and cumulative float of 1.60 g cm⁻³ has the ash content of 26.38 %. The negligible difference between ash contents for cumulative float of 1.60 g cm⁻³ and original (abovementioned, 26.38 % and 28.52 % respectively) is actually because of the high mass fraction collected as cumulative float, i.e. 94.20 %. In this case, there would be no meaning for the 1.60 g cm⁻³ density cleaning for Ilgin sample, rather it should be cleaned with 1.40 g cm⁻³ solution. Still, 1.40 g cm⁻³ solution did not contribute much

since the ash percentage was 28.52 (%) in the beginning and after this test (1.40 g cm⁻³ float and sink) it only decreased to 21.63 %, which can be interpreted as Ilgin sample does not favor density medium separation.

As regards to float and sink graphical representation (Fig 5) and the tabulated data (Table 6), Ermenek lignites which has a 23.51 % ash content (run of mine) can be cleaned with density separation. In terms of float fraction for 1.40 g cm⁻³, ash content of 13.36 % can be obtained at an amount of almost one third (33.59 %) of the total mass. Cumulative float fraction of 1.60 g cm⁻³ on the other hand resulted as an amount of 81.43% with an ash content of 17.85 %. Middling in this case (for Ermenek lignite) is resulted as the highest amount out of the lignite samples investigated, i.e. it has 47.84 % mass fraction for the fraction of +1.40-1.60 g cm⁻³. Higher the amount of the middling fraction is not actually desired in terms of float and sink tests and it can be attributed as the limitation of the floatability of the corresponding sample. Further evaluations as regards to higher amounts of middling can be associated with the less liberation of particles at the specific size orientation tested. In the scope of this study, float and sink analysis was not performed on the samples which are sieve analyzed or size classified. Rather, in order to have an idea about the size orientation of the samples, they were objected to primary crushing. So, initial assessment of lack of the liberation for Ermenek sample can be made in this case considering its high amount of middling. Size reduction would be claimed to contribute float and sink separation of each sample investigated, but the most contribution of size reduction would be observed for Ermenek sample. In order to understand the possibility of density separation of a sample, size distribution should also be questioned.

Table 5. Float and sink analysis results for Ilgin lignite sample

Density gr/cm ³	Float		Cumulative Float			Cumulative Sink			
	%Amount	%Ash	Content	%Amount	Content	%Ash	%Amount	Content	%Ash
-1.40	78.45	21.63	1696.87	78.45	1696.87	21.63	100.00	2852.29	28.52
+1.40 -1.60	15.75	50.02	787.82	94.20	2484.69	26.38	21.55	1155.42	53.62
+1.60	5.80	63.38	367.60	100.00	2852.29	28.52	5.80	367.60	63.38
Total	100.00	28.52	2852.29						

Table 6. Float and sink analysis results for Ermenek lignite sample

Density gr/cm ³	Float		Cumulative Float			Cumulative Sink			
	%Amount	%Ash	Content	%Amount	Content	%Ash	%Amount	Content	%Ash
-1.40	33.59	13.36	448.76	33.59	448.76	13.36	100.00	2350.52	23.51
+1.40-1.60	47.84	21.00	1004.64	81.43	1453.40	17.85	66.41	1901.76	28.64
+1.60	18.57	48.31	897.12	100.00	2350.52	23.51	18.57	897.12	48.31
Total	100.00	23.50	2350.52						

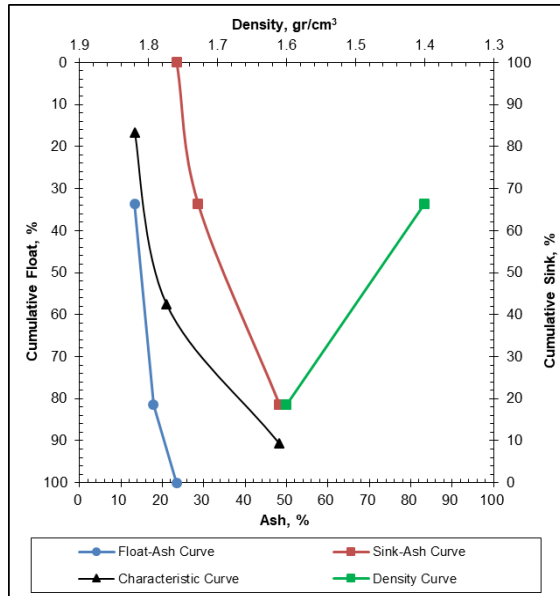


Fig 5. Float and sink graph for Ermenek lignite sample

As it is presented in Fig 6, and as it is tabulated in Table 7, Gürmin Merzifon lignite sample has the highest ash content (45.34 %) among the samples studied and corresponding amount of sink fraction of 1.60 g cm⁻³ is also the highest, i.e. 75.00 %. Although this abovementioned high amount of sink fraction for 1.60 g cm⁻³ can be regarded as not desired for a coal sample to be utilized further, still it can be interpreted as an achievement of the density separation of the specific sample. To be better clear in this context, Gürmin Merzifon lignite sample was observed to be successfully cleaned with density medium. Removal of this 75.00 % of high ash containing fraction would lead a production of clean fraction which has a ash content of 21.47 % (See Cumulative float of 1.60 g cm⁻³). Employment of 1.40 g cm⁻³ density in terms of float and sink test resulted as an amount of 9.89 % with an ash content of 11.00 %. Although the amount of the corresponding float fraction (1.60 g cm⁻³) varies for each of the samples investigated in the scope of this study, clean fraction of Gürmin-Merzifon lignite sample has almost half of the original (run of mine) ash content.

Table 7. Float and sink analysis results for Gürmin Merzifon lignite sample

Density gr/cm ³	Float			Cumulative Float			Cumulative Sink		
	%Amount	%Ash	Content	%Amount	Content	%Ash	%Amount	Content	%Ash
-1.40	6.63	11.00	72.93	6.63	72.93	11.00	98.00	4534.19	46.27
+1.40-1.60	16.37	28.33	463.76	23.00	536.69	23.33	91.37	4461.26	48.83
+1.60	75.00	53.30	3997.50	98.00	4534.19	46.27	75.00	3997.50	53.30
Total	100.00	45.34	4534.19						

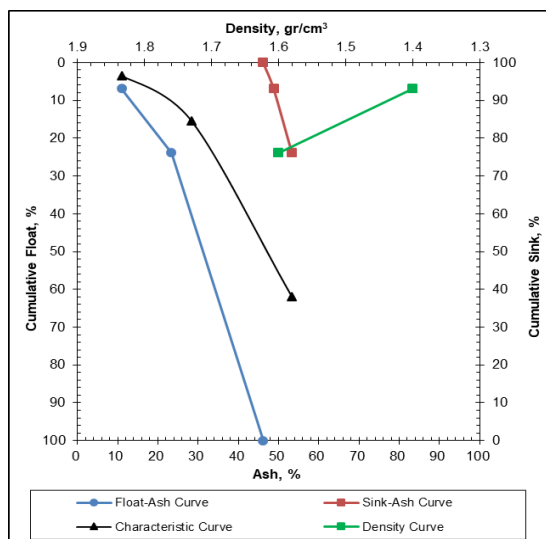


Fig 6. Float and sink graph for Gürmin-Merzifon lignite sample.

In order to evaluate the availability of each coal samples for the density separation, corresponding decrease of ash contents (original to float) can be revisited. In this context of abovementioned, highest rate of ash content decrease was observed with Gürmin-Merzifon sample, i.e. it was originally with an

ash content of 45.34 % and 1.60 g cm⁻³ float fraction has 21.47% ash content, respectively. Accordingly lowest rate of ash content decrease was observed with Ilgın lignite sample and it does not favor density separation. However in this context, combustible recoveries of the each lignites were considered in order to have a correct comparison. Combustible recovery values (%) were tabulated in Table 8 along with ash and amount percentages respectively for -1.40 g cm⁻³ and -1.60 g cm⁻³ for each lignites studied.

Referring to Table 8, combustible recoveries of Ilgın and Çayırhan samples are the highest ones and Gürmin Merzifon sample has the lowest combustible recovery for both fraction, i.e. -1.40 and -1.60 g cm⁻³, respectively. Lignite utilization in terms of thermal energy production purposes would question the combustible recovery. Density cleaning increases the combustible recovery percentage and float fraction of 1.60 g cm⁻³ has the higher combustible recoveries. Ilgın lignite sample has the highest combustible recoveries while Gürmin Merzifon has the lowest. Based on this finding abovementioned, density cleaning should be employed for Ilgın samples as regards to have higher combustible recoveries and combustion efficiency but it might not as much considered as for Gürmin-Merzifon sample. Increase in the density resulted in an increase in combustible recoveries, but higher density of mediums require

more chemicals involvement and that means higher pollution potential for environment.

Float and sink tests are employed mostly in order to understand the cleaning requirements of the run of mine coals. Further utilization of coal always requires lower ash content and lower amount of sulfur. Initial cleaning of coals in the course of coal preparation

plants are rather easier and cheaper. However, not every coal has the same characteristics in terms of their washability tendency. Prior to cleaning at a specific density in coal preparation plants, float and sink tests were carried out in order to have initial idea about the product amount and ash content.

Table 8. Combustible recoveries of the studied lignites

Coal sample	-1.40 g cm ⁻³			-1.60 g cm ⁻³		
	%Amount	%Ash	% Combustible Recovery	%Amount	%Ash	% Combustible Recovery
Dursunbey	34.51	7.96	41.62	72.97	16.49	80.23
Çayırhan	63.02	14.02	73.61	81.06	17.07	88.51
İlgin	78.45	21.63	86.01	94.20	26.38	97.02
Ermenek	33.59	13.36	38.05	81.43	17.85	87.44
Gürmin-Merzifon	9.89	11.00	16.10	25.00	21.47	35.92

4. CONCLUSIONS

In this study, 5 different lignite samples were collected and analyzed in terms of their washability characteristics. Washability of lignites is important since Turkish lignites have respectively high ash content (>20 %). Coal preparation plants clean coals with some specific high density mediums. High density mediums are prepared with some chemicals or recyclable minerals such as magnetites. However still optimization for the density of the medium should be realized since the more the usage of density making chemicals the more pollution to environment and the more the economic loss is. Although recent technologies try to develop systems with less or no usage of water/chemicals, there are still issues like capacity and efficiency which are not overcome yet.

In this study, some characteristics data have been evaluated for some of Turkish lignites. One could easily decide either use of 1.40 or 1.60 g cm⁻³ or in between (-1.60+1.40) solution to reach the desired amount of clean coal with desired ash content. Considering only low ash content should not mean that lignites with high sulfur content are acceptable. Coal preparation plants operators or field engineers should not only question ash content but also sulfur content as regards to density separation characteristics.

In addition to the ash content comparison based on the results obtained (Dursunbey lignite sample has the lowest ash content of 24.86 % while Gürmin Merzifon lignite sample has the highest ash content of 45.02 %), combustible recoveries of each lignite and each separation density (1.40 g cm⁻³, 1.60 g cm⁻³) has been tabulated in this context. It was observed that İlgin lignite sample has the highest combustible recoveries while Gürmin Merzifon has the lowest.

Lignite deposits in Turkey is widely encountered and utilization of these lignites should better carefully considered in terms of environmental and economic reasons. With further studies about characterization of lignite utilization would help to have more developed technologies in this field.

REFERENCES

- [1]. G. Ö. Cakal, H. Yücel and A. Gürüz, "Physical and chemical properties of selected Turkish lignites and their pyrolysis and gasification rates determined by thermogravimetric analysis," *Journal of Analytical and Applied Pyrolysis*, Vol. 80 (1), pp.262-268, 2007.
- [2]. H. İnaner and E. Nakoman, "Properties of the Çanakkale-Çan Lignite Deposit (Northwestern Turkey)," *Geologica Belgica*, Vol. 7 (3-4), pp.273-278, 2004.
- [3]. H. İnaner and E. Nakoman, "Resources, Quality and Economic Importance of Solid Fossil Fuels in Turkey," *Geologica Belgica*, Vol. 7 (3-4), pp.245-250, 2004.
- [4]. K. E. Ozbas, C. Hicyilmaz, M. V. Kök and S. Bilgen, "Effect of cleaning process on combustion characteristics of lignite," *Fuel Processing Technology*, Vol. 64 (1-3), pp.211-220, 2000.
- [5]. O. Sivrikaya, "Cleaning study of a low-rank lignite with DMS, Reichert spiral and flotation," *Fuel*, Vol. 119, pp.211-220, 2000.
- [6]. Z. Aktas, F. Karacan and A. Olcay, "Effect of cleaning process on combustion characteristics of lignite Centrifugal float-sink separation of fine Turkish coals in dense media," *Fuel Processing Technology*, Vol. 55 (3), pp.235-250, 1998.
- [7]. F. F. Aplan "Floatation" M.C. Fuerstenaue (Ed.), *AM Guadin memorial volume*, AIME 1976.
- [8]. F. F. Aplan and B.J. Arnold "Coal preparation" Section 3, *flotation AIME*, Colorado, 1991.
- [9]. D. J. Brown "Coal Floatation" D.W. Fuerstenaue (Ed.), *Frot flotation: 50th anniversary volume*, AIME, New York, 1962.
- [10]. N.T. Moxon, C.N. Benesly, R. Keast-Jones and S.K. Nicol, "Insoluble oils in coal flotation: the effects of surface spreading and pore penetration," *International Journal of Mineral Processing*, Vol. 21, 1997.
- [11]. Y. Cebeci, "The investigation of floatability improvement of Yozgat Ayırdam lignite using

- various collectors," *Fuel*, Vol. 81, pp.281-289, 2002.
- [12]. M. Misra, S. Kumar and F. Chatterje "Flotability and dielectric characterization of the Intrinsic moisture of coal of different ranks," *Coal Prepr*, Vol. 9, 1991.
- [13]. W. Pawlak, A. Turak, J. Janiak, Y. Briker and B. Ignasiak "Oil agglomeration of low-rank coals and development of methods for recovery of oil from agglomerates. In: *11th Annual EPRI contractor's conference on clean liquid and solid fuels*, vol. 20, pp.1-20, California, 1986.
- [14]. Y. Cebeci and N. Aslan "Using float-sink data in simple equations to predict sulfur contents," *Fuel Processing Technology*, Vol. 76, pp.231-239, 2002.
- [15]. G. Tozsin, C. Acar and O. Sivrikaya "Evaluation of a Turkish Lignite Coal Cleaning by Conventional and Enhanced Gravity Separation Techniques," *International Journal of Coal Preparation and Utilization*, Vol. 38 (3), pp.135-148, 2018.
- [16]. G. Atesok, I. Yildirim and M.S. Celik "Applicability of the Reichert spiral for cleaning bituminous and lignitic coals: a pilot scale study," *International Journal of Mineral Processing*, Vol. 40 (1-2), pp.33-44, 1993.
- [17]. D.O. Aksoy, P. Aydar, Y. Toptaş, A. Çabuk and S. Koca, H. Koca "Physical and physicochemical cleaning of lignite and the effect of cleaning on biodesulfurization" *Fuel*, Vol. 132, pp.158-164, 2014.
- [18]. R. Q. Honaker, D. Wang and K. Ho, "Application of the Falcon concentrator for fine coal cleaning" *Minerals Engineering*, Vol. 13 (4), pp.415-427, 2000.
- [19]. R.Q. Honaker, N. Singh and B. Govindarajan, "Application of dense-medium in an enhanced gravity separator for fine coal cleaning", *Minerals Engineering*, Vol.13 (4), pp.415-427, 2000.
- [20]. T. Uslu, E. Sahinoglu and M. Yavuz "Desulphurization and deashing of oxidized fine coal by Knelson concentrator," *Fuel Processing Technology*, Vol. 132, pp.94-100, 2012.
- [21]. E. Sahinoglu "Cleaning of high pyritic sulfur fine coal via flotation," *Advanced Powder Technology*, Vol. 29 (7), pp. 1703-1712, 2018.
- [22]. F. Rubiera, S.T. Hall and C.L. Shah, "Sulfur removal by fine coal cleaning processes," *Fuel*, Vol.76 (13), pp.1187-1194, 1997.
- [23]. G. Cheng, Y. Cao, C. Zhang, Z. Jiang, Y. Yu and M. K. Mohanty "Application of novel flotation systems to fine coal cleaning," *International Journal of Coal Preparation and Utilization*, Vol.40 (1), pp.24-36, 2020.
- [24]. H. Hacifazlioglu and I. Toroglu "Optimization of design and operating parameters in a pilot scale Jameson cell for slime coal cleaning," *Fuel Processing Technology*, Vol.7 (88), pp.731-736, 2007.



REVIEW ARTICLE

Zero waste strategies and Turkey's zero waste project

Burcu Tan^{1,*}

¹Çanakkale Onsekiz Mart University, Chemistry Department, 17100, Çanakkale, TURKEY

ABSTRACT

The amount of waste in the world continues to increase in the framework of the population, increase in purchasing power and technological developments since the past years and this increase necessitates the need for sustainable and integrated management of waste. The disposal of waste without being used in the recycling and recovery process causes serious resource losses, both materially and energy.

The "zero waste" movement has recently gained importance as an alternative to the dominant "take-use-waste" production model and as a viable approach to climate change. Zero waste is a change of perspective. It requires think again about what we traditionally regarded as garbage and instead addressing all materials as valuable resources. Zero waste takes into account the entire material management system, from extraction of natural resources to product design, production and distribution, product use and reuse, recycling, composting, energy recovery and disposal. This paper discusses a variety of zero waste strategy implementations and Turkey's Zero Waste Project.

Keywords: Industrial waste, Turkey's zero waste project, zero waste strategy

1. INTRODUCTION

The result of human activities since the Industrial Revolution is a Earth warming effect resulting from carbon dioxide emissions and increased by emissions of other greenhouse gases. In this context, the challenge today is how to survive on Earth in an unprecedented scenario of economic development with increasing energy demand and global warming processes. Scientists warn that if they do not make significant changes to keep global temperature increases below 1.5 °C, the results will be disastrous. Decarbonisation of the energy sector while meeting the rapidly increasing demand for power, especially in the developing world, is probably the most important challenge facing the global energy system in the next 20 years [1].

Non-renewable resources are running out as a result of excessive consumption. The constant depletion of natural finite resources by the urban population leads to an uncertain future [2].

2. PRINCIPLES OF ZERO WASTE

The Zero Waste International Alliance (ZWIA) has published some principles and practical steps that cover the whole world from the city to the countryside and are applied in these places. The main principles of these publications are presented under the following headings.

2.1. Adopt the zero waste definition

In line with the sustainable development goal, a zero waste definition has been developed. In present, according to Zero Waste International Alliance, "Zero Waste is the conservation of all resources by means of responsible production, consumption, reuse, and recovery of products, packaging, and materials without burning and with no discharges to land, water, or air that threaten the environment or human health".

Corresponding Author: burcu.tan88@gmail.com (Burcu TAN)

Received 13 October 2020; Received in revised form 14 February 2021; Accepted 14 February 2021

Available Online 26 February 2021

Doi: <https://doi.org/10.35208/ert.843106>

© Yildiz Technical University, Environmental Engineering Department. All rights reserved.

This paper has been presented at EurAsia Waste Management Symposium 2020, Istanbul, Turkey

2.2. Establish benchmarks

Having a detailed timetable is essential for setting criteria, monitoring the process and evaluating the successes achieved.

2.3. Engage the whole community

In communities where Zero Waste is targeted, everyone has an individual role. Naturally, every person produces waste. What if everybody takes responsibility for the zero waste target? In such a case, the process to Zero Waste will become more quickly. All organizations (government organizations, non-governmental organizations, business and grassroots movements) and individuals everywhere should adopt the Zero Waste application first and then make it a target. With sustainable policies and implemented programs, society and businesses should be supported and deposit-return service could be provided.

2.4. Demand decision makers manage resources not waste

Waste disposal is mostly carried out through the use of landfills and incinerators. But these methods are not sustainable options. Landfilling is still low cost and can be applied to all types of waste, while it is the source of greenhouse gases. From climate change angle, incineration is the better choice for converting waste into energy [3].

2.5. Perform zero waste assessments

It is important to make evaluations in order to control the current waste management system implemented by the local government.

2.6. Enact extended producer responsibilities rules

This rule leads manufacturers to redesign the product so that the product is less toxic and can be easily reused or recycled after use. In the redesign phase, it forces them to use financial incentives. As a result, the used product is evaluated in an environmentally friendly way. Therefore, it can reduce the amount of waste disposed in landfills [4].

2.7. Expand Zero Waste infrastructures

In order for the Zero Waste program to be implemented and sustainable, a wide infrastructure should be possessed in subjects such as reuse, recycling and composting. Businesses and producers should be encouraged to ensure that the Zero Waste program is sustainable and to collect and process waste materials, take back and recycle worn products. With this incentive, popularizing social re-use can be achieved by supporting non-governmental organizations.

2.8. Challenge businesses to lead the way to Zero Waste

Zero Waste focused businesses have been established all over the world and have brought positive effects on the environment in managing resources and materials. Businesses that have adopted the Zero Waste target reduce the costs of managing resources and waste of their businesses. Therefore, it has also increased operating efficiency. Zero Waste businesses should be supported locally, and businesses should be encouraged to implement this program. In this context, economic incentive funds can be used. Resource managers need to be trained to use the Zero Waste approach and develop the program. Zero Waste is a strategy. To achieve Zero Waste, cultural exchange and organization are required. To create green jobs, it must create programs to educate businesses and visitors about the new rules and programs [3].

3. EXAMPLES OF ZERO WASTE CONCEPT IN SELECTED COUNTRIES

3.1. Singapore application

Singapore is a country that has limited land and natural resources for urban planning and development, and its population is constantly on the rise. For this reason, an integrated and long-term approach has been adopted in waste management. In Singapore, the amount of waste disposed has increased 7 times in the last 50 years, from 1,200 tons/day in 1970 to 8,284 tons/day in 2015. Per capita household waste amount was approximately 0.86 kg / person.day in 2015 [5]. If it continues in this way, the life of the Semakau Landfill is predicted to be about 35 years, and it becomes necessary to build an additional incineration plant every 7 to 10 years. With the Zero Waste Master Plan launched in Singapore, it aims to reduce the amount of incinerated waste sent to Semakau by 30%. It is aimed to increase the recycling rate of Singapore from 60% since 2012 to 70% by 2030. The government determines the domestic recycling rate of 22% in 2018 to 30% by 2030, while the non-domestic recycling rate is; It is aimed to increase from 74% to 81% [6]. Waste management in Singapore has traditionally been undertaken by the Singapore Ministry of the Environment (ENV). The law on solid waste management in Singapore is the Environmental Pollution Control Act (EPCA), which came into force in April 1999, and is a consolidation of existing legislation on air, water and waste control, including Environmental Public Health (EPHA).

3.2. Germany application

The most important legislation affecting waste management in Germany is the "Waste Prevention and Disposal Law", which was adopted in 1972 and significantly revised in 1986 to bring Germany into compliance with the current European Economic Community (EEC) legislation. The law imposes important obligations to reduce the amount of waste generated and to recover and recycle waste. In

addition, the law contains specific provisions on the management of waste containing toxic substances. In accordance with the "Waste Prevention and Disposal Law":

- Setting targets for the reduction, recovery and reuse of non-toxic wastes based on technical feasibility, cost and availability of markets;
- To publish guidelines for the environmentally friendly disposal of waste;
- Regulating the volume and conditions for the application of wastes to agricultural lands;
- Regulating the labeling and recycling of products that can produce toxic waste is among the duties of the government.

The law also gives the government the power to ban the sale of products containing toxic substances. The law defines the concept of "waste" as "... the materials that the producer wants to dispose of or, in particular, what is necessary for the protection of the environment and proper management for the public interest". In the Avoidance and Disposal Law, "waste management" defines "the recovery or production of waste as material or energy (reuse and recovery of waste), waste storage and the necessary collection, transportation, treatment and storage process" [7].

3.3. Indonesia application

When you talk about Zero Waste communities in Indonesia, three cities come to mind: Bandung, Cimahi and Soreang. These cities, which are struggling to manage their waste, have become leaders in Zero Waste program implementation in recent years. Zero Waste Project in Indonesia is carried out by Yayasan Pengembangan Biosains dan Bioteknologi (YPBB). YPBB found that Bandung, the third largest city in Indonesia, 2.5 million people living in the city generate approximately 1.500-1.600 tons of waste each day. Bandung's local government has already allocated 137 billion IDR for annual waste transportation. More than half of resident waste or 63% is organic waste. Recyclable materials come in second at 23% while the rest of 14% are remnant waste. This means that Bandung City can reduce the amount of resident waste brought to landfills by up to 86% and reduce waste collection, transportation and storage filling costs by \$ 17.1 million (19 billion IDR) per year. Subsequently, potential savings can be employed in recruiting more waste workers and in developing more collections, decentralized recycling and the development of composting facilities. The recycling of 950 kg of wastes have provided in the project carried out by YBBB per day. Within the scope of this project has provided savings 63 million IDR (4,300 USD). YPBB is supposed to which can save up more by working with the government on zero waste [8].

4. TURKEY'S ZERO WASTE MANAGEMENT

There is a "Zero Waste" project initiated by the Ministry of Environment and Urbanization in 2017. The project basically aims to prevent waste and to use

resources more efficiently. public institutions/ organizations in the project, educational institutions, shopping malls, hospitals, rest facilities and the implementation of fun-in large businesses and aims to move all applications in Turkey in 2023.

4.1. Types of waste

Wastes are handled in four main groups in practice.

Household waste: The definition of household waste in the Environmental Law; It is defined as "solid wastes from places such as residences, industry, workplaces, picnic areas that are not included in the scope of hazardous and hazardous waste" (Government gazette 09.08.1983, no 2872).

Medical waste: The concept of medical waste is expressed as "cutting-piercing wastes, pathological wastes and infectious wastes" in the Environmental Law. Since medical wastes are more dangerous than other wastes, their inspections are more stringent.

Industrial waste: Industrial wastes are wastes that are harmful to the environment and human health resulting from industrial activities. Industrial wastes can be classified as hazardous and non-hazardous wastes. It is the Waste Management Regulation (Government gazette 02.04.2015, no 29314), which is the most up-to-date and under the main legislation regarding industrial wastes.

Special waste: Waste oils, batteries, used tires and batteries that do not disappear from nature for a long time are listed within the scope of special waste. At the same time, agricultural solid wastes, corporate and industrial solid wastes and excavation wastes are also examined under this title. Each of the process management related to special wastes is planned with separate legislation such as Waste Oil Management Regulation (Government gazette 30.07.2008, no 26952), Waste Batteries and Accumulators Control Regulation (Government gazette 31.08.2004, no 25569).

The increasing amount of waste creates enormous pressure on the implementation of a sustainable waste management, creating opportunities for the implementation of new approaches and strategies. The term "Zero Waste" was first used in the chemical industry in 1973 in connection with the recovery of usable components from chemical compounds. [9].

Zero waste is a whole system approach that aims to eliminate waste instead of "managing" it. In addition to encouraging waste diversion from landfill and incineration, it is a guiding design philosophy to eliminate waste at its source and at all points in the supply chain [10].

Zero Waste International Alliance's Zero Waste concept, which was made in 2004, is "a source of recyclable materials and other products by encouraging human beings to have a sustainable natural life cycle and change their way of life in this direction with a purpose that is suitable for ethical rules, economic structure, and has a vision. It guides to be designed so that it can be used. With Zero Waste Management, it is aimed to systematically design and

manage products and processes in order to reduce and prevent the toxicity of wastes and products in their structure, to protect and preserve all resources, to prevent waste incineration and burial. With the zero waste application, the threats to the earth, human, animal or plant life can be eliminated by discharges to the soil, water or air" [11].

Therefore, zero waste management systems include product design, consumption and resource recovery stages. Zero waste products based on cradle-to-cradle design principles are essential. These types of products will ultimately not generate any waste during the production stages. The service life of the product designed in this way should be easily extended with repair and thus it should be ready for use again [12].

Reducing wastes to zero and ensuring their sustainability at the same time is expressed as "zero waste management". The main purpose of this management system is to reduce the pollution caused by environmental problems during production at the source with the most appropriate method, and to minimize these wastes with the directions to be made in the next stage [7].

When it is aimed to have zero waste, a holistic approach is required, such as zero energy, human and material resources, zero emissions in air, soil and water, zero waste in management and production activities, zero waste in product life and zero use of toxic substances [13].

In Turkey, companies, institutions or organizations, there are 7 steps that need to apply to be included in the Zero Waste System.

Zero Waste System Application Stages;

4.2. Determination of focal points

To ensure zero waste management, the people who will lead the team should be determined. These are the persons who will be responsible for the establishment, effective and efficient implementation, monitoring, information flow and reporting of the zero waste management system in the organization.

4.3. Determination of the current situation

While implementing the Zero Waste Management System in your organization, first of all, it will help you to determine how you are in terms of wastes and analyze your current situation.

4.4. Planning

At this stage, a deadline plan specific to the institution is prepared based on the current situation.

4.5. Determination of Needs and Supply

While applying the Zero Waste System in the institution, all the equipment that will be needed is determined, listed and supplied before the

implementation, by considering each unit in the institution (such as offices, dining hall, infirmary).

4.6. Education

After the supply of the equipment is completed, practical training and information activities are carried out for the target audiences before starting the application.

4.7. Application

The accumulation equipment provided is placed at points easily accessible by personnel, at appropriate intervals. Information posters designed according to the equipment are hung on the equipment in an easily visible way. Attention should be paid to the color scale in spooling equipment and promotional materials.

4.8. Reporting

At this stage, monitoring is carried out by the working team in order to evaluate the effectiveness of the application, and if any, the deficiencies, deficiencies or the parties to be developed are determined and measures are taken.

5. CONCLUDED REMARKS FOR TURKEY

With the "Zero Waste Summit" held on November 1, 2018; With the Zero Waste project, the goal of increasing a livable environment and a stronger economy has been determined by separating wastes at their source and ensuring recycling. According to the summit realized, the Zero Waste Project is a savings and efficiency project [14]. It is seen as a resource to be converted into waste raw materials and new products with the recent studies on the environment. During the approximately one year period the project is in operation; 58,000 tons of waste electrical and electronic equipment, 2.2 million tons of packaging waste, 38,000 tons of vegetable and 184,000 tons of end of life tires were collected separately in 80,000 tons of mineral waste oil sources and recycled (Zero Waste Summit, 2018). The main goal is to spread this practice to the whole country with the published Zero Waste Regulation.

REFERENCES

- [1]. BP Statistical Review of World Energy, 68th edition, June 2019. Available: <https://www.bp.com/content/dam/bp/business-sites/en/global/corporate/pdfs/energy-economics/statistical-review/bp-stats-review-2019-full-report.pdf>, (accessed 15 December 2020).
- [2]. A. U. Zaman, S. Lehmann, "The zero waste index: a performance measurement tool for waste management systems in a 'zero waste city,'" *Journal of Cleaner Production*, Vol. 50, pp. 123-132, 2013.

- [3]. Zero Waste International Alliance, <http://zwia.org/>, [Online], Available: (2020).
- [4]. Zero Waste Sonoma. Extended Producer Responsibility (EPR) or Product Stewardship and Take-back. Available: <https://zerowastesonoma.gov/produce/residents/extended-producer-responsibility>, (accessed 15 December 2020).
- [5]. Solid Waste Management, "Total Domestic Waste Disposed Per Capita", available: https://data.gov.sg/dataset/solid-waste-management-total-domestic-waste-disposed-per-capita?view_id=e7298947-e719-49a4-96a5-81d6c4a64154&resource_id=21727d9f-dc4f-4992-a354-4375a3a766c4 (accessed 15 December 2020).
- [6]. Singapore Zero Waste Plan, "Singapore's zero-waste plan aims to raise domestic recycling rate from 22 to 30 per cent by 2030", available: <https://www.ecobusiness.com/news/singapores-zero-waste-plan-aims-to-raise-domestic-recyclingrate-from-22-to-30-per-cent-by-2030/>, (accessed 15 December 2020).
- [7]. F.F. Kavak, "Sıfır Atık Yönetimi: Marmara Üniversitesi Anadoluhisarı Kampüsü Örneği," *MSc thesis*, İstanbul, 2020.
- [8]. <http://www.no-burn.org/meetourmembers-yppbb> [Online]. Available: (2020).
- [9]. P. Palmer, "Getting to Zero Waste," *Sebastopol: Purple Sky Press*, 2004.
- [10]. T. Curran, I.D. Williams, "A zero waste vision for industrial networks in Europe," *Journal of Hazardous Materials*, pp. 207-208, 3-7, 2012.
- [11]. <http://zwia.org/zero-waste-community-principles/> (accessed 15 December 2020).
- [12]. A. U. Zaman, "Roadmap towards Zero Waste Cities", *International Journal of Waste Resources*, Vol. 4 (2), 2014.
- [13]. B. Kopacek, Literature Review, "Approaches to zero waste," *Deliverable 1.1, Towards Zero Waste in Industrial Network*, Tech. Rep., Available: www.zerowin.eu, 2010.
- [14]. <https://sifiratik.gov.tr/> [Online], Available: (2020).



RESEARCH ARTICLE

Effectiveness of fly ash in boron removal from Tuzla (Çanakkale) geothermal fluid

M. Oğuzhan Şahin¹ , Tijen E. Bektaş^{2,*} , Deniz Ş. Yücel³

¹Çanakkale Onsekiz Mart University, School of Graduate Studies, Department of Energy Resources and Management, Çanakkale, TURKEY

²Çanakkale Onsekiz Mart University, Faculty of Engineering, Department of Chemical Engineering, Çanakkale, TURKEY

³Çanakkale Onsekiz Mart University, Faculty of Engineering, Department of Mining Engineering, Çanakkale, TURKEY

ABSTRACT

The heat accumulated in the inner parts of the earth's crust is transmitted to the fluid in the geothermal aquifer by means of transportation. The geothermal fluid is transported to the surface either by wells or naturally. In this study, the geothermal fluid in Tuzla geothermal field in Çanakkale city was examined due to its high boron content (10.3 mg L⁻¹). It was aimed to remove boron from geothermal fluid by adsorption in order to prevent possible negative effects on the environment. Fly ash was obtained from Çan thermal power plant. The specific surface area of the fly ash was 14.6 m² g⁻¹ and the particle size was between 1.45 and 186 µm. According to ASTM C618 standard, fly ash was classified as Class C. Fly ash was composed of anhydrite, lime, hematite, cristobalite, quartz, calcite and feldspar. Various parameters such as initial pH, adsorbent dosage, contact time, and temperature were studied experimentally for the removal of boron from the geothermal fluid. The suitability of pseudo-first-order, pseudo-second-order, and intraparticle kinetic models to experimental data was examined. The data obtained from the isotherm studies were applied to the Langmuir, Freundlich and Dubinin-Radushkevich models.

Keywords: Adsorption, boron, fly ash, geothermal fluid

1. INTRODUCTION

Water contaminated with boron is handled as an environmental problem because the small amounts of boron in irrigation water cause plant growth to stop and can be toxic to organisms [1]. According to the boron sensitivity of the plants, irrigation water safe boron content is in the range of 0.3-4 mg L⁻¹ [2]. For this reason, the excess boron in the water must be removed by a suitable method.

Different methods are used to remove boron from wastewater, including ion exchange, adsorption, chemical precipitation, reverse osmosis, solvent extraction, and membrane filtration [1-5]. Among these methods, adsorption is the most widely used [6]. Fly ash is a good adsorbent and, also cheap and plentiful [7, 8]. Worldwide, waste materials from thermal power plants are estimated to be around 700 million tonnes, of which at least 70% is fly ash [9]. During the electricity generation in thermal power

plants in Turkey annually approximately 14.26 million tons of fly ash are emerging and it's only a small amount is used [10, 11].

Within Turkey, 227 geothermal fields with a temperature range of 20-287 °C have been discovered and almost 2000 hot and mineral springs have been determined [12]. Geothermal fluid is used for electricity generation, residential, spa and greenhouse heating, CO₂ extraction, balneological uses and tourism in Turkey. Geothermal fluids of Turkey are highly mineralized with elevated levels of As, B, Cd, and Pb [13]. The high element content of geothermal fluid has certain detrimental environmental consequences, such as pollution of surface water, groundwater, and soil [14]. Tuzla geothermal field located in northwestern Turkey, approximately 70 km southwest of the Çanakkale city. Tuzla is one of the major high-enthalpy geothermal field of Turkey and the boron concentration in geothermal fluid is high [15].

Corresponding Author: ennilb@gmail.com (Tijen E. Bektaş)

Received 17 December 2020; Received in revised form 2 February 2021; Accepted 7 February 2021

Available Online 22 February 2021

Doi: <https://doi.org/10.35208/ert.842192>

© Yildiz Technical University, Environmental Engineering Department. All rights reserved.

This paper has been presented at EurAsia Waste Management Symposium 2020, Istanbul, Turkey

In this study, boron removal from Tuzla geothermal fluid by batch adsorption experiments was investigated using fly ash. Optimum conditions were determined by examining the effects of various parameters for the removal of boron from geothermal fluid.

2. MATERIALS AND METHODS

2.1. The study area

Fly ash was provided as a waste material from fluidized bed combustion Çan thermal power plant, Çanakkale, northwestern Turkey. Thermal power plant works 2*160 MW electric power and produces approximately 450.000 tons of ash waste per year. The characterization of fly ash was determined by BET, SEM-EDX, XRD and XRF analysis.

Physicochemical parameters (pH, temperature, electrical conductivity and salinity) of the Tuzla geothermal fluid were measured by using a WTW 340i multiparameter (Table 1). Geothermal fluid was sampled in 500-mL*20 polyethylene bottles and stored at 4 °C until further analysis.

Table 1. Physicochemical parameters of the geothermal fluid

Electrical conductivity (mS/cm)	Salinity (‰)	pH	Temperature (°C)
76.1	56	8.07	92.2

A series of batch adsorption experiments were performed to evaluate the effects of certain parameters, such as initial pH, adsorbent dosage, contact time, and temperature. A certain amount of fly ash and 50 mL of geothermal fluid was contacted with a shaking water bath at 140 rpm for a certain period of time. After all samples were filtered, the boron in the filtrate was analyzed according to the Carmine Method and measured using spectrophotometer (Hach DR 5000). The boron concentration of Tuzla geothermal fluid was determined as 10.3 mg L⁻¹.

The amount of boron adsorbed from the geothermal fluid to the fly ash surface was calculated by the following equation:

$$q = \frac{(C_0 - C_e)V}{m} \quad (1)$$

where q is the amount of boron adsorbed (mg g⁻¹); C_0 and C_e (mg L⁻¹) are the boron concentration at initial

and equilibrium, respectively; V is the geothermal fluid volume (L) and m is the amount of fly ash (g).

3. RESULTS AND DISCUSSION

3.1. Characterization of fly ash

The particle size of fly ash was between 1.45 and 186 µm, with surface area of 14.6 m² g⁻¹. The main components of the fly ash were SiO₂ (32.16%), CaO (29.05%), Al₂O₃ (19.22%) and Fe₂O₃ (7.03%), and the loss on ignition value was 4.7%. According to ASTM C618 standard [16], fly ash was classified as Class C. The total sulfur and carbon contents of fly ash were 5.88% and 1.43%, respectively. The metal concentrations contained in the fly ash was identified as Al > Fe > Mn > Zn > Cr > Cu > Pb > Co > Ni. The Al and Mn concentrations of the fly ash were identified to be above the average for continental crust determined by Krauskopf and Bird [17]. The mineralogical composition of the fly ash comprises anhydrite, lime, hematite, cristobalite, quartz, calcite and feldspar. The shape of the fly ash particles showed an irregular morphology in the SEM images (Fig 1). The EDX analysis of fly ash indicated that the ash was mainly composed of O, C, Si, Al, Fe, Ca, S, Na and Ti. The pH and EC of fly ash leachate was measured as 12.19 and 4.83 mS cm⁻¹, respectively.

3.2. Effect of initial pH on boron removal

The pH effect on boron adsorption was investigated at different pH values. The range of pH was 2–12. The pH of the geothermal fluid were adjusted with NaOH and HCl solutions. Then, 0.5 g of fly ash was added to 50 ml of the samples and it was kept in a shaking water bath at 25 °C for 24 h. The results were given in Fig 2. Fig 2 showed that boron removal was affected by the change in pH. It was observed that the maximum boron removal efficiency was obtained at pH 4. The main components of fly ash were Si, Ca and Al oxides. The reaction Si, Ca and Al-rich fly ash with geothermal fluid causes co-precipitation of metal hydroxides. The interaction of borate anions with positively charged hydroxylated oxide surfaces is more favorable. Also, under low pH condition this metal compounds were leached to the solution. We suggested that boron was co-precipitated and accumulated with Si, Ca and Al hydroxides. Similar result was found by Öztürk and Kavak [6].

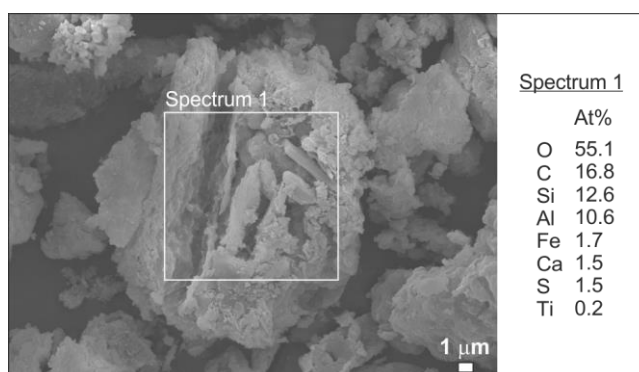


Fig 1. SEM image and EDX result of fly ash

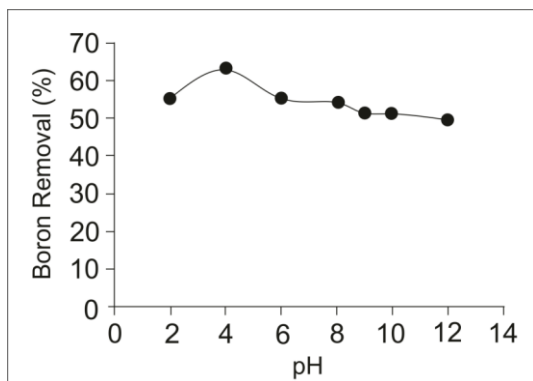


Fig 2. Effect of initial pH on boron removal

3.3. Effect of adsorbent dosage on boron removal

The effect of the amount of adsorbent was investigated by adding different amounts of fly ash (0.25-2.5 g 50 mL⁻¹) to the geothermal fluid at pH 4 and contacting it in a shaking water bath at 25 °C for 24 hours. The effect of fly ash content on boron removal was given in Fig 3. The boron removal efficiency of the fly ash was varied approximately from 64 to 88% at adsorbent amount of 0.25 and 2.5 g 50 mL⁻¹, respectively. Boron removal percentage increased as the surface area increased with the increase in the amount of fly ash.

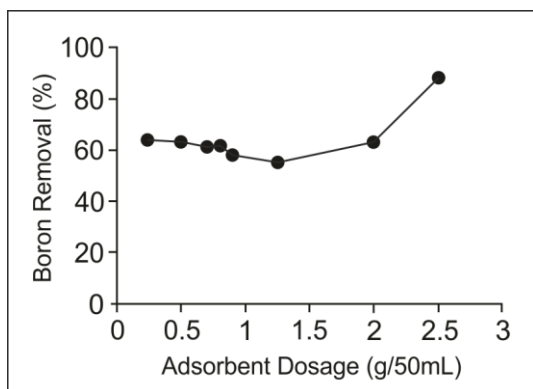


Fig 3. Effect of adsorbent dosage on boron removal

3.4. Adsorption isotherms

The Langmuir, Freundlich and Dubinin-Radushkevich (DR) isotherm equations were discussed. The Langmuir equation is given below [18]:

$$\frac{C_e}{q_e} = \frac{1}{Q_o b} + \frac{C_e}{Q_o} \tag{2}$$

Table 2. Constants of different isotherm models

	Q_o (mg g ⁻¹)	b (L mg ⁻¹)	R^2
Langmuir Isotherm	0.058	-0.286	0.95
	K (mg g ⁻¹) (L mg ⁻¹) ^{1/n}	n	R^2
Freundlich Isotherm	4365	-0.15	0.78
	q_s (mg g ⁻¹)	B (mol ² k ⁻¹ J ⁻²)	R^2
D-R Isotherm	1.7×10^{-8}	-2×10^{-6}	0.80

where C_e (mg L⁻¹) and q_e (mg g⁻¹) are the solution concentration in the equilibrium and the amount of boron adsorbed by fly ash in the equilibrium, respectively. Q_o and b indicate the monolayer capacity and absorption energy constant, respectively.

Freundlich equation is given by the following equation [18];

$$\log q_e = \log K + \frac{1}{n} \log C_e \tag{3}$$

Here, Freundlich capacity constant is K ((mg g⁻¹)(L mg⁻¹)^{1/n}), and Freundlich intensity constant is n .

Dubinin-Radushkevich (D-R) isotherm equation is given by Equation (4) [19]

$$\ln q_e = \ln q_s + B \epsilon^2 \tag{4}$$

where q_s is the D-R constant and ϵ can be correlated as

$$\epsilon = RT \ln \left[1 + \frac{1}{C_e} \right] \tag{5}$$

where R represents the ideal gas constant (8.314 J mol⁻¹ K⁻¹) and T represents the absolute temperature. The constant B gives the mean free energy. The constants of all isotherm equations were given in Table 2. The results showed that the experimental data fitted well with the Langmuir isotherm ($R^2=0.95$) (Fig 4). It can be said that monolayer adsorption occurs on surface.

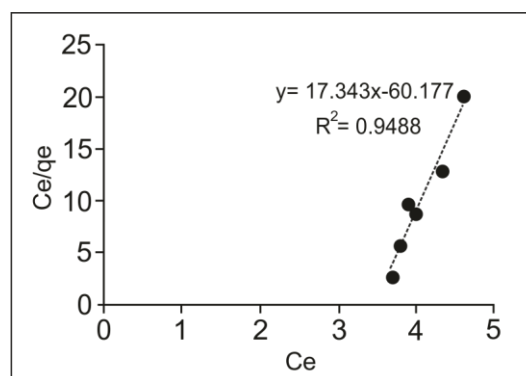


Fig 4. Langmuir isotherm plots for boron removal

3.5. Effect of contact time on boron removal

Inadequate contact time of the fluid and adsorbent may not provide good removal. Therefore, optimal contact time was determined. For this purpose, geothermal fluid at pH of 4 was shaken with 2.5 g fly ash at 25 °C for different periods. The results were shown in Fig 5. The boron removal was not determined until the 400th mins. Boron removal increased gradually after this period and 88% boron removal was obtained in 24 h.

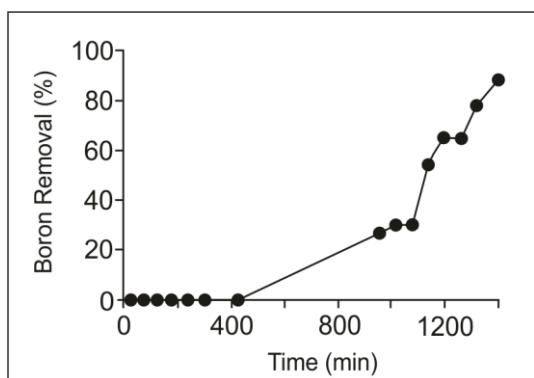


Fig 5. Effect of contact time on boron removal

3.6. Kinetic models

In order to explain the mechanism of adsorption process, pseudo-first-order, pseudo-second-order and intraparticle kinetic models were examined. The Lagergren equation was used to find the rate constant of the pseudo-first-order adsorption [20, 21]:

$$\log(q_e - q_t) = \log q_e - \frac{k_1 t}{2.303} \quad (6)$$

q_t is the amount of boron adsorbed (mg g^{-1}) at time t (min). k_1 (min^{-1}) is the rate constant.

The equation for the pseudo-second-order kinetic model is used as follows [22, 23]:

$$\frac{t}{q_t} = \frac{1}{k_2 q_e^2} + \frac{t}{q_e} \quad (7)$$

Here, k_2 ($\text{g mg}^{-1} \text{min}^{-1}$) is the rate constant.

The adsorption process takes place in a few steps that involves the transport of solute molecules from the solution to the solid particle surface, followed by diffusion of these molecules into the pores of the particle. The intraparticle diffusion equation can be given as [18],

$$q = kt^{1/2} \quad (8)$$

where k_i is the intraparticle diffusion rate constant ($\text{mg g}^{-1} \text{min}^{-1/2}$). The k_i is the slope of straight line portions of the plot of q_t vs. $t^{1/2}$ (Fig 6).

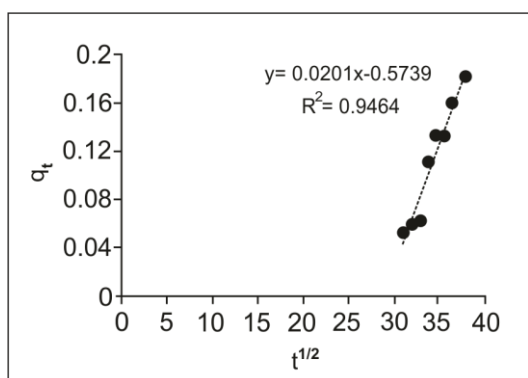


Fig 6. Intraparticle model for boron adsorption onto fly ash

The kinetic constants were shown in Table 3. According to the results, it could be said that the kinetic data were more compatible with the pseudo-first order and intra-particle kinetic models. These results showed that the adsorption of boron was physical and was controlled by diffusion mechanism. Halim et al. [24] obtained similar results.

3.7. Effect of temperature on boron removal

The data obtained showed that the boron removal decreased as the temperature increased (Table 4). The standard free energy change (ΔG°), enthalpy change (ΔH°) and entropy change (ΔS°) of adsorption can be expressed with the following equations:

$$\Delta G^\circ = -RT \ln K \quad (9)$$

where K is the equilibrium constant and T is the temperature. Equilibrium constant (K) is calculated according to the equation below;

$$K = \frac{C_s}{C_e} \quad (10)$$

C_s indicates the concentration of adsorbent (mg L^{-1}), while C_e indicates the equilibrium concentration of solution (mg L^{-1}).

Van't Hoff equation is represented by Eq. (11);

$$\ln K = \frac{\Delta S^\circ}{R} - \frac{\Delta H^\circ}{RT} \quad (11)$$

Fig 7 showed the plot of $\ln K$ versus $1/T$. The enthalpy change values from the slope of this graph and ΔS° ($\text{J mol}^{-1} \text{K}^{-1}$) from the intercept point were found (Table 4). The negative free energy change at various temperatures showed that the adsorption process occurred spontaneously. A negative enthalpy change value indicated that adsorption was exothermic. The negative entropy change suggested the system exhibits random behavior.

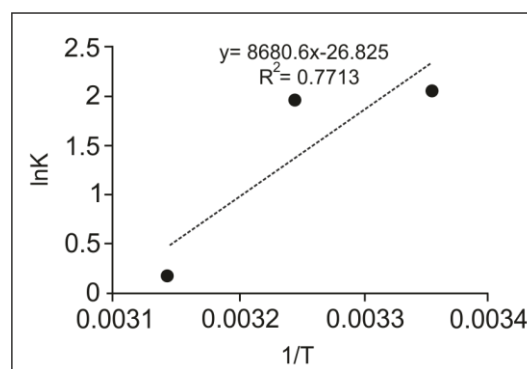


Fig 7. Van't Hoff plot

Table 3. Different kinetic parameters for boron removal

Pseudo-first-order			Pseudo-second-order			Intraparticle model	
k_1	q_e	R^2	k_2	q_e	R^2	k_i	R^2
(min^{-1})	(mg g^{-1})		($\text{g mg}^{-1} \text{min}^{-1}$)	(mg g^{-1})		($\text{mg g}^{-1} \text{min}^{-1/2}$)	
0.0048	3.24	0.90	0.8902	9.9701	0.78	0.02	0.95

Table 4. Thermodynamic parameters

T(°C)	C_e (mg L ⁻¹)	K	ΔG° (kJ mol ⁻¹)	ΔH° (kJ mol ⁻¹)	ΔS° (J mol ⁻¹ K ⁻¹)
25	1.2	7.58	-5.019	-72.17	-223.02
35	1.3	6.92	-4.954		
45	4.7	1.19	-0.463		

4. CONCLUSIONS

In this study, fly ash as a waste material from fluidized bed combustion Çan thermal power plant was used as an adsorbent for boron removal from Tuzla geothermal fluid. This process seems economical as fly ash is available in large quantities and inexpensively. The maximum amount of boron adsorption from the geothermal fluid onto fly ash was obtained at the initial pH of 4. The boron removal efficiency was determined 88% at 25 °C, initial pH 4 and 2.5 g of fly ash per 50 mL solution. According to the experimental results, the Langmuir isotherm model was the most suitable for this process. Among these kinetic models considered for the removal of boron with fly ash, the intra-particle model best fitted the experimental data. Parameters from thermodynamic studies (ΔG° and ΔH°) indicated that the boron adsorption onto fly ash was spontaneous and exothermic process.

ACKNOWLEDGEMENTS

This study was supported by the Scientific Research Projects Coordination Unit of Çanakkale Onsekiz Mart University under FYL-2019-3086 numbered project. This paper was presented in 5th EurAsia Waste Management Symposium.

REFERENCES

- [1]. İ. Yilmaz, N. Kabay, M. Brjyak, M. Yuksel, J. Wolska and A. Koltuniewicz, "A submerged membrane-ion-exchange hybrid process for boron removal," *Desalination*, Vol. 198, pp. 310–315, 2006.
- [2]. R.O. Nable, G.S. Banuelos and J.G. Paull, *Plant and Soil*, Kluwer Academic Publishers, Netherlands, pp. 181–198, 1997.
- [3]. H. Polat, A. Vengosh, I. Pankratov and M. Polat, "A new methodology for removal of boron from water by coal and fly ash," *Desalination*, Vol. 164, pp. 173–188, 2004.
- [4]. M. Yurdakoc, M. Y. Seki, S. Karahan and K. Yurdakoc, "Kinetic and thermodynamic studies of boron removal by Siral 5, Siral 40, and Siral 80," *Journal of Colloid and Interface Science*, Vol. 286, pp. 440–446, 2005.
- [5]. N. Kabay, I. Yilmaz Ipek, I. Soroko, M. Makowski, O., Kirmizisakal, S. Yag, M. Bryjak and M. Yuksel, "Removal of boron from Balçova geothermal water by ion exchange–microfiltration hybrid process," *Desalination*, Vol. 241(1-3), pp. 167–173, 2009.
- [6]. N. Ozturk and D. Kavak, "Boron removal from aqueous solutions by adsorption on waste sepiolite and activated waste sepiolite using full factorial design," *Adsorption*, Vol. 10, pp. 245–257, 2005.
- [7]. C. H. Weng and C. P. Huang, "Adsorption characteristics of Zn(II) from dilute aqueous solution by fly ash," *Colloids and Surfaces A: Physicochemical and Engineering Aspects*, Vol. 247, pp. 137–143, 2004.
- [8]. D. Sanliyuksel Yucel, "Removal of heavy metals from aqueous solution using fly ash: Can Thermal Power Plant, NW Turkey as a case study," *Karalmas Science and Engineering Journal*, Vol. 7(1), pp. 291–298, 2017.
- [9]. M. Ondova, N. Stevulova and A. Estokova, "The study of the properties of fly ash based concrete composites with various chemical admixtures," *Procedia Engineering*, Vol. 42, pp. 1863–1872, 2012.
- [10]. E. Sayilgan and K. Kurklu, "Uçucu kül örneğinden demir ve alüminyum gideriminde Taguchi yaklaşımı," *Uludağ Üniversitesi Mühendislik Fakültesi Dergisi*, Vol. 23(3), pp. 133–142, 2018.
- [11]. D. Sanliyuksel Yucel and B. Ileri, "Mitigation of Environmental Effects of Anthropogenic Metal Contamination Using Fly Ash," *Geological Bulletin of Turkey*, Vol. 63, pp. 43–56, 2020.
- [12]. O. Mertoglu, S. Simsek and N. Basarir, "Geothermal country update report of Turkey (2010–2015)", Proceedings of World Geothermal Congress 2015, Melbourne, Australia, 19-24 April 2015, International Geothermal Association, Bonn, pp. 1–7, 2015.
- [13]. A. Baba and H. Armannsson, "Environmental impact of the utilization of a geothermal area in

- Turkey," *Energy Source*, Vol. 1(3), pp. 267–278, 2006.
- [14]. H. Marmara, D., Sanliyüksel Yucel, S., Ozden and M.A., Yucel, "Kestanol Jeotermal Akışkanının Hidrokimyasını ve Çevresel Etkilerinin Belirlenmesi," *Türkiye Jeoloji Bülteni*, Vol 63, pp. 97–116, 2020.
- [15]. T. Yalcin, "Geochemical characterization of the Biga Peninsula thermal waters (NW Turkey)," *Aquatic Geochemistry*, Vol. 13(1), pp. 75–93, 2007.
- [16]. American Society for Testing and Materials (ASTM). Standard C618–15 standard specification for coal fly ash and raw or calcined natural pozzolan for use in concrete. West Conshohocken, PA: ASTM International, 2015.
- [17]. K. B. Krauskopf and D. K. Bird, Introduction to Geochemistry, 3rd ed., McGraw-Hill, New York, 1995.
- [18]. W.J. Weber, Physicochemical Processes for Water Quality Control, John Wiley and Sons Inc., New York, 1972.
- [19]. M.M. Dubinin, "The potential theory of adsorption of gases and vapors for adsorbents with energetically non-uniform surface," *Chemical Reviews*, Vol. 60, pp. 235, 1960.
- [20]. S. Lagergren, "About the theory of so called adsorption of soluble substances", K. Sven. Vetenskapsakad. *Kungliga Svenska Vetenskapsakademiens Handlingar*, Vol. 24 (4), pp. 1–39, 1898.
- [21]. Y.S. Ho, "Citation review of Lagergren kinetic rate equation on adsorption reaction," *Scientometrics*, Vol. 59 (1), pp. 171–177, 2004.
- [22]. Y.S. Ho, "Removal of metal ions from sodium arsenate solution using tree fern," *Process Safety and Environmental Protection*, Vol. 81, pp. 352–356, 2003.
- [23]. Y.S. Ho, "Review of second-order models for adsorption systems," *Journal of Hazardous Materials*, Vol. 136, pp. 681–689, 2006.
- [24]. A.A. Halim, N.A. Roslan, N.S. Yaacob and M.T. Latif, "Boron removal from aqueous solution using Curcumin-impregnated activated carbon," *Sains Malaysiana*, Vol. 42(9), pp. 1293–1300, 2013.



RESEARCH ARTICLE

Investigation of electricity generation performance of grape marc in membrane-less microbial fuel cell

Banu Taskan^{1,*} 

¹Department of Environmental Engineering, Firat University, Elazig, TURKEY

ABSTRACT

Grapes are among the most widely grown fruits globally, with a third of the overall production used in winemaking. Both red and white winemaking processes generate significant amounts of solid organic waste such as grape marc that requires proper disposal. Grape marc, a natural plant product containing abundantly lignocellulosic compounds, is a promising raw material for production of renewable energy. In this study, the grape marc was used as an anode nutrient in the membrane-less microbial fuel cell (ML-MFC) system, and the electricity generation capacity of the grape marc as an environmentally friendly energy source was investigated in detail. The maximum power density produced in the ML-MFC reactor was determined as 274.9 mW m⁻², and the total internal resistance was 309.5 Ω. Cyclic voltammetry results showed the presence of electroactive microorganisms on the surface of the anode electrode provided a high biological activity. The presence of elliptical and round-shaped microorganisms on the anode electrode surface was observed. Quantitative polymerase chain reaction (qPCR) analyzes have shown that grape marc supports bacterial growth on the electrode surface.

Keywords: Grape marc, membrane-less microbial fuel cell (ML-MFC), electricity generation, microbial analysis

1. INTRODUCTION

Bioenergy is one of the most important alternatives for sustainable energy production. In addition to sustainable energy production, using organic pollutants as a bioenergy source is a powerful way to prevent environmental pollution [1, 2]. Energy generation using biomass is a sustainable process considering CO₂ emissions and the limitation in fossil fuels globally. Agricultural wastes are substantial natural resources because of their abundance and in the environment for energy production [1]. Various organic wastes such as rice husk, corn waste, palm waste, sugar cane, and grape marc can be used as renewable energy sources [3]. Grape marc, a typical form of waste biomass with organic residues produced from the process of wine production, has high lignocellulosic content resistant to biologic degradation in the environment [4].

In the world, millions of tons of grape marc are produced every year [5]. For this reason, it has a significant risk potential for the environment when

discharged without proper treatment. If the grape marc is discharged without stabilization, it causes many environmental problems such as surface and groundwater pollution, malodor, flies, and insect infestation [6, 7]. In addition to the grape marc, the wine production process produces winery wastewater containing high nutrient concentrations such as nitrates, phosphates, and different organic compounds [8, 9]. The contamination of these pollutants to the surface water sources causes eutrophication, which has an adverse effect on biotic components in the environment. Many previous studies reported that the grape marc causes many environmental problems such as soil pollution, surface water pollution, damage of plants, and odor [10]. For this reason, the wastes generated in the winery production process cannot be discharged without treatment [11]. This creates a considerable annihilation problem for wineries [4, 12, 13]. Various treatment strategies were used to remove pollutants in wastes produced by the winery production process to prevent these environmental problems. These treatment strategies include the extraction of

Corresponding Author: btaskan@firat.edu.tr (Banu Taskan)

Received 16 February 2021; Received in revised form 28 February 2021; Accepted 12 March 2021

Available Online 23 March 2021

Doi: <https://doi.org/10.35208/ert.881517>

© Yildiz Technical University, Environmental Engineering Department. All rights reserved.

commercial chemicals such as tannin, ethanol, and phenol from the grape marc and their use in technologies of energy conversion, including pyrolysis, combustion, and gasification [5, 14, 15]. The previous studies showed that the organic content and specifications of grape marc are suitable for thermochemical energy conversion [5, 16-18]. In previous studies, the energy generation potential of grape marc in the anaerobic digestion was investigated by Makadia, et al. [7] and Da Ros, et al. [19]. These studies demonstrated that the grape marc has sufficient bioenergy generation potential and would be promising biomass in the renewable energy generation process. However, the occurrence of highly endergonic reactions in energy recovery from grape marc by any of the thermal transformation (i.e., gasification) processes causes environmental pollution [4, 5]. To overcome the harmful effect of the classical energy production process, it is necessary to focus on a more environmentally friendly process that does not create any pollution during energy generation. Thus, bioenergy production can provide higher energy recovery efficiency and be a more environmentally friendly approach [7]. ML-MFC reactor is one of these processes and is among the promising electrochemical systems in energy storage and conversion.

ML-MFC is a promising technology among the electrochemical systems in terms of the direct electricity generation from organic wastes and environmentally friendly nature. ML-MFC does not need the proton exchange membranes (PEM) to physically separate anode and cathode compartments and transfer hydrogen ions between them [20, 21]. In MFC systems, bacteria produce electrons by oxidizing organic pollutants and transfer them to the anode electrode surface without producing any secondary pollutants [22-25]. Despite the lower bioelectricity generation of ML-MFC than MFC having PEM, they do not need expensive PEM during the operation. The current ML-MFC studies have focused on improving the electricity generation capacity by using novel electrode materials and substrate sources [26-28].

This study concentrated on using grape marc in the anode compartment of ML-MFC as a substrate source to produce electricity. For this purpose, the grape marc was added to the anode compartment of ML-MFC, and ML-MFC electricity generation performance was investigated in detail using electrochemical impedance spectroscopy (EIS), linear sweep voltammetry (LSV), and cyclic voltammetry (CV). The biofilm morphology and viability were examined using microscopic techniques. Additionally, the anode biofilm microbiome was analyzed by using the quantitative polymerase chain reaction (qPCR) method.

2. MATERIALS AND METHOD

2.1. ML-MFC setup and operation

In this study, a mixture of the anaerobic digester (Elazig municipal wastewater treatment plant) sludge and sediment sludge obtained from the golden horn

(Istanbul, Turkey) was used as an inoculum source. The physical properties of grape marc containing C, H, N, O, and S; moisture 68.71%, volatile matter 75.83%, ash 6.52%. The grape marc was dried at room temperature (21 ± 2 °C), grounded, and then used as an organic substrate source for electroactive bacteria in the anode of ML-MFC (Fig 1a and Fig 1b). The inoculum was mixed with grape marc at the ratio of 1/5 and then added to the anode compartment of ML-MFC. A cylindrical plastic bottle with a height of 24 cm and a diameter of 8 cm was used as an ML-MFC reactor (Fig 2a). The cathode compartment was filled with tap water. A sand layer with a height of 2 cm was formed to physically separate anode and cathode compartments (the average diameter of sand particles is 1 mm). The height of the anode compartment was 11 cm. The anode electrode was set 7 cm below the anode surface. The ML-MFC was covered with aluminum foil to protect the growth of photosynthetic microorganisms and operated at room temperature. The cathode compartment of ML-MFC was continuously aerated by using an aquarium pump to provide oxygen for the cathodic reactions. The dissolved oxygen concentration of the cathode compartment was kept at between 5.5-6 mg L⁻¹.



Fig 1. Wet grape marc (a), dried-ground grape marc (b)

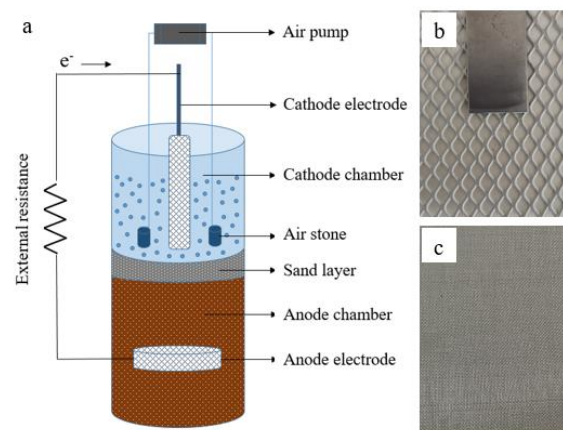


Fig 2. Schematic view of ML-MFC reactor (a), Platinum-coated titanium electrode (b), Stainless-steel electrode (c)

2.2. Anode and cathode electrodes

The stainless-steel and platinized titanium mesh were purchased from the Fuel cell store (www.fuelcellstore.com) and used as anode and cathode electrodes in ML-MFC. The electrodes were placed in ethanol for 15 min to remove micro and nano-scale particles and then washed with pure water. The 1000Ω resistance was used to fix anode

and cathode electrodes. The anode and cathode electrodes are shown in Fig 2b and Fig 2c.

2.3. Analysis

Electrochemical analysis

The voltages generated in the ML-MFC were measured by using an Agilent 34970a digital multimeter every 3 min (Data Acquisition/Switch Unit) and recorded to the computer using Agilent Benchlink Data Logger 3 V4.3 software. The electrochemical analysis was performed by using a Gamry interface 1000 potentiostat (Gamry, Warminster, PA). The EIS analysis was carried out in a frequency range of 100 kHz to 0.1 Hz with an amplitude value of 5 mV. The primary components of internal resistance of ML-MFC were determined using Gamry Echem Analyst V6.25 software according to the equivalent circuit model given by Abazarian, et al. [29]. The max power density of ML-MFC was measured using LSV analysis at the scanning rate of 2.5 mV s⁻¹. The CV analysis was carried out at the scanning rate of 5 mV s⁻¹ from 1.0 to -1.0 V.

The amount of current and power generated in the reactor was calculated based on the equations below [20]:

$$V = I \times R \quad (1)$$

$$P = I \times V = I^2 \times R \quad (2)$$

Table 1. Primers used for qPCR amplification

Target microorganism	Primer names	Sequences
Bacteria	907R	5'-CCGTCAATTCMTTGTAGTTT-3'
Bacteria	BacV2f	5'-CCTACGGGAGGCAG CAG-3'
Eukaryote	Euk1A	5'-CTGGTTGATCCTGCCAG-3'
Eukaryote	Euk516r	5'-ACCAGACTTGCCCTCC-3'
Archaea	517F	5'-GCYTAAAGSRNCCGTAGC-3'
Archaea	909R	5'-TTTCAGYCTTGCGRCCGTAC-3'

The genomic DNA of biofilm samples was isolated by using PowerSoil DNA isolation kit (Mo Bio Laboratories, USA) according to the manufacturer protocol. The primer sets given in Table 1 were used to amplification of genomic DNA. Roche-Fast Start SYBR Green Master (Roche, Nutley, NJ, USA) was used in the Roche LightCycler® 96 real-time PCR system (Roche Applied Science) to perform the qPCR analysis in triplicates for each sample. The copy numbers of each gene were calculated using cycle threshold (CT) values based on the standard curve.

3. RESULTS AND DISCUSSION

3.1. Power generation in ML-MFC

The power generation capacity of MFCs depends on the organic content and degradation of substrate used

Where; V is the voltage in volts (V), I is the current in ampere (A), and R is the known value of the external load resistor in ohms (Ω).

Microscopic observations and microbial analysis

The biofilm samples on the anode electrode surface were obtained at the end of the operation period to perform microscopic analysis. The scanning electron microscopy (SEM) observations were performed using Zeiss electron microscopy (Carl Zeiss AG, Oberkochen, Germany) according to the protocol given by Taşkan, et al. [30]. According to the manufacturer protocol, the viability of anode biofilm was analyzed using the LIVE/DEAD® BacLight™ bacterial viability kit (Thermo Fisher Scientific, USA). Eclipse Ni-U microscope (Nikon, Japan) was used to perform viability analysis. The red color represents dead cells in the images, and the green color represents living cells [31].

The genomic DNA of biofilm samples was isolated by using PowerSoil DNA isolation kit (Mo Bio Laboratories, USA) according to the manufacturer protocol. The primer sets given in Table 1 were used to amplification of genomic DNA. Roche-Fast Start SYBR Green Master (Roche, Nutley, NJ, USA) was used in the Roche LightCycler® 96 real-time PCR system (Roche Applied Science) to perform the qPCR analysis in triplicates for each sample. The copy numbers of each gene were calculated using cycle threshold (CT) values based on the standard curve.

in the anode compartment. In this study, the electricity generation capacity of grape marc was determined by LSV analysis by plotting the power curve of ML-MFC (Fig 3). A maximum power density of 274.9 mW m⁻² and a maximum current density of 0.44 A m⁻² was achieved by ML-MFC fueled by grape marc. The obtained maximum power density of ML-MFC is higher compared with many similar previous studies. In a previous study, the treatment and electricity generation capacity of copper contained wastewater using a membrane-less double compartment MFC was investigated, and a maximum power density of 31.3 mW m⁻² was reported by Liu, et al. [32]. Morris and Jin [33] reported a maximum power density of 7 mW m⁻² with petroleum hydrocarbon at the concentration of 16 g k⁻¹ g by using an ML-MFC. In a study, the bioelectricity generation capacity of different electrode materials

(stainless-steel, aluminum, and titanium mesh) and sediment sludges having different sediment and salt ratio were investigated by Bartolome, et al. [34]. It was reported that the maximum power density of titanium mesh, aluminum, and stainless-steel electrodes were 400, 140, and 90 mW m⁻², respectively. In another study, the electricity generation capacity of ML-MFC reactor using sewage sludge as the substrate source was investigated, and it was reported that the maximum power density reached was 187 mW m⁻² [35]. Compared with previous studies, the maximum power density obtained by this study is higher than many previous studies. It seems possible that the high power density of ML-MFC is due to the high organic content of grape marc.

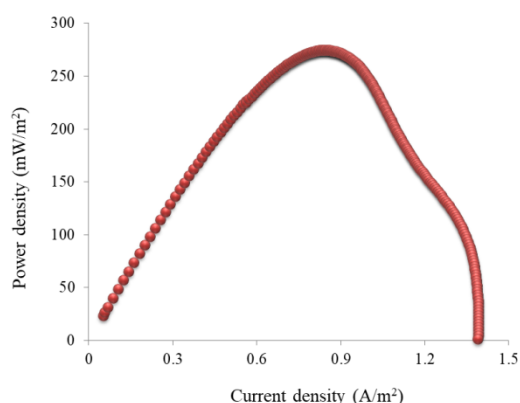


Fig 3. The power density produced in the ML-MFC reactor

3.2. Electrochemical performance of ML-MFC

In the current study, CV and EIS analysis were performed to evaluate the electrochemical performance of ML-MFC. EIS is one of the most powerful analyses that inform the ohmic resistance (R_{Ω}), mass transfer resistance (R_{mt}), and charge transfer resistance (R_{ct}) of ML-MFC. The internal resistance of MFC significantly affects the electricity generation performance. The equivalent circuit model given by Abazarian, et al. [29] was used to analyze the internal resistance of ML-MFC. The Nyquist plot and equivalent circuit model are shown in Fig 4. The equivalent circuit model includes solution resistance (R_s), mass transfer resistance (R_{mt}), cathode charge transfer resistance (R_{ct}), and other resistances (R_o) present at the cathode. Additionally, constant phase elements (CPEs) representing the capacitance of electrical double layer are also available in the model to consider for the structure and porosity of the electrode [41]. The CPE_{ct} , CPE_{mt} , and CPE_o are related to mass transfer, charge transfer, and other processes contained in the cathode. The R_s , R_{ct} , R_{mt} , and R_o are 24.1, 206.5, 70.3 and 8.6 Ω , respectively. The total internal resistance of the ML-MFC reactor was calculated as 309.5 Ω from the formula $R_t = R_s + R_{ct} + R_{mt} + R_o$. Hou, et al. [36] investigated the effect of two different anode electrode materials (carbon cloth and stainless-steel fiber felt) modified and unmodified with graphene on MFC performance. It was reported that the total internal resistance of MFCs with unmodified carbon cloth and stainless-steel fiber felt

were 235.4 and 974.5 Ω , respectively. In another study, a total internal resistance of 437.7 Ω was reported by Taşkan, et al. [20] with a graphene-coated nickel-titanium (NiTi) alloy electrode. Another study reported that the total internal resistance of a double chamber MFC with graphite plate and tin-coated copper mesh electrodes were 408 and 477 Ω , respectively [37]. In another study, a tubular separating electrode assembly with graphite granule bed anode and simple carbon-fabric cathode was investigated as nylon fabric, J-fabric, and glass fiber separators in MFCs. It has been reported that the internal resistance of these three different MFCs is in the range of 614.71–1711.59 Ω . [38].

CV analysis is used to measure the catalytic processes, and redox reaction that occur in the anode and cathode electrodes of MFC [39]. Additionally, the CV helps to profoundly understand the biological activity of the anode biofilm, which converts organic matter in the grape marc into bioelectricity. Fig 5 shows the CV curves at the beginning (red) and at the end of the operating period (blue). Due to the insufficient of electroactive microorganism colonization on the surface of anode, no clear oxidation/reduction peak was detected in the CV curve obtained in the initial phase of the reactor. The CV results at the end of the operation showed that an oxidation peak of 0.55 mA was detected at -0.070 V, while two cathodic reduction peaks of -0.61 mA and -0.42 mA at -0.50 V and 0.01 V, respectively. The anodic peak confirms the presence of electroactive bacteria and electrogenic activity on the anode electrode. The cathodic peaks show that effective hydrogen (H^+) transfer from anode to cathode and the reduction of oxygen cathode electrode surface. Nimje, et al. [39] investigated simultaneous nitrate reduction and electricity generation by *Bacillus subtilis* under anaerobic conditions, using glucose and nitrate as the carbon source in a single chamber MFC. They reported two cathodic reduction peaks at about 0.1 V and -0.4 V and two anodic oxidation peaks at 0.05 V and 0.25 V. In another study, an anodic peak of 0.6 mA at -0.05 V was detected in MFC with modified polyaniline-coated carbon fabric anode, while a reduction peak of -1.28 mA at -0.5 V was observed by Hou, et al. [40].

3.3. Microscopic and molecular analysis

The SEM and viability images of anode biofilm are given in Fig 6. The biofilm structure and bacterial morphology are shown in the SEM image of anode biofilm in Fig 6a. It is observed from the SEM image that the presence of abundant round and elliptical bacteria on the anode surface, while rod-shaped bacteria were rarely found. The SEM image demonstrated that the anode surface provides a suitable environment for attachment and colonization of anode microorganisms. The bacterial viability image showed live (green) and dead (red) bacteria in anode biofilm. It can be concluded that the stainless-steel mesh anode has good biocompatibility with electrogenic bacteria, and provide relatively high viability of biofilm (Fig 6b).

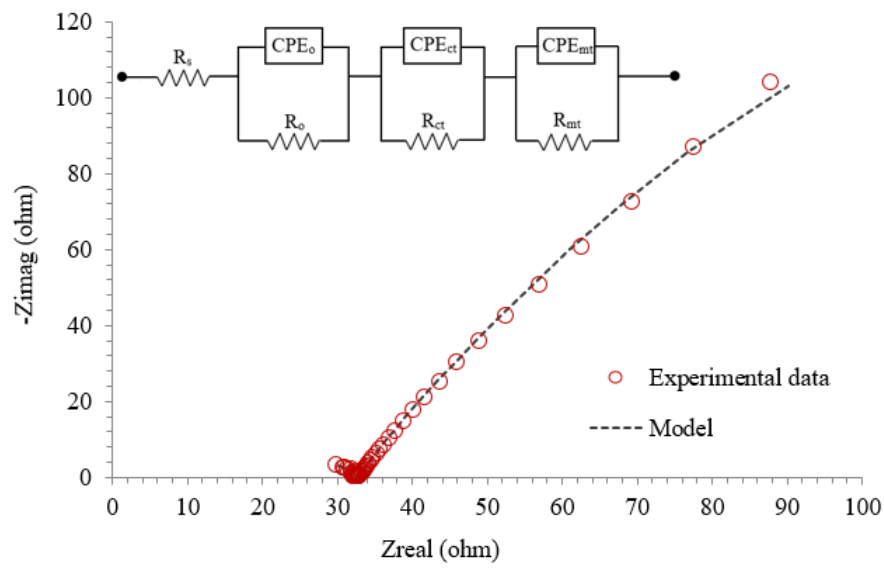


Fig 4. EIS diagram of anode electrode in ML-MFC reactor

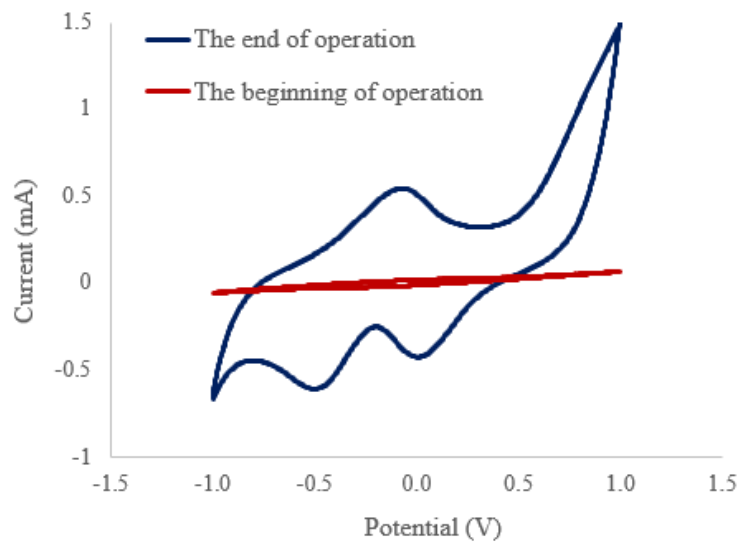


Fig 5. CV curves obtained at the beginning and end of the operation in the ML-MFC reactor

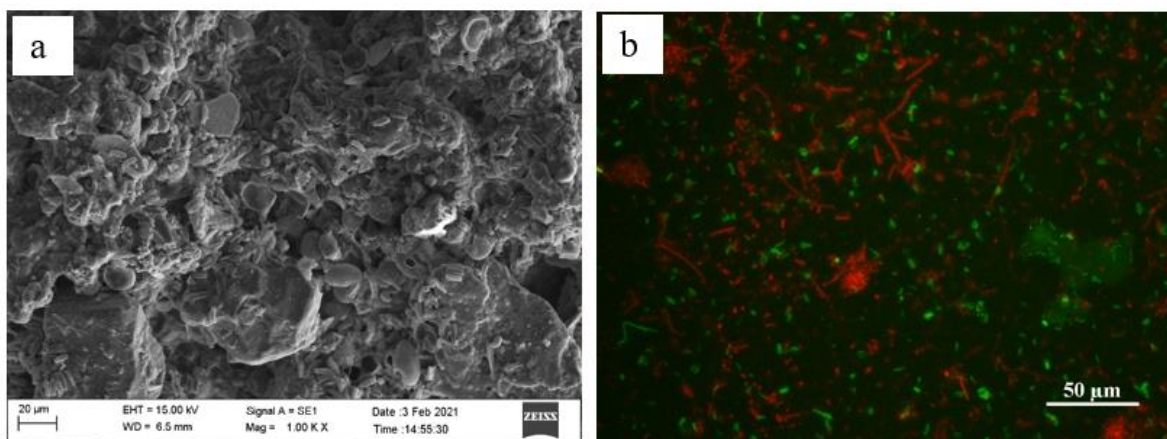


Fig 6. SEM image (a) and fluorescence microscopy image (b) of the biofilm on the anode electrode surface at the end of the operation

In addition to the microscopic observations, the gene copy numbers of bacteria, eukaryotes, and archaea were determined by qPCR analysis. The qPCR analysis was effectively used to determine the cell concentration by previous researchers [41, 42]. The gene copy numbers of bacteria (16S rRNA) in anode medium at the beginning of the operation period were 1.26×10^{10} copies μL^{-1} while it was 3.19×10^{10} copies μL^{-1} anode biofilm at the end of the operation period. The number of bacteria in the anode electrode surface increased approximately 2.5 times from the beginning to the end of the operation period (Fig 7). This finding suggests that grape marc contributes to the growth of bacteria and accordingly supports electricity generation. The copy numbers of eukaryotic genes (18S rRNA) were 3.84×10^6 copies μL^{-1} at the beginning of the operation, while it was 1.72×10^5 copies μL^{-1} at the end of the operation period of ML-MFC on the anode electrode surface. The number of eukaryotic

microorganisms in the anode compartment of ML-MFC was significantly decreased during the operation period of ML-MFC. The decrease in the number of eukaryotic microorganisms might be insufficient light and inorganic carbon sources for photosynthetic eukaryotes. In addition to the bacteria and eukaryotes, the number of archaea was investigated in anode biofilm. While the gene copy number of archaea in ML-MFC anode was 4.66×10^7 copies μL^{-1} at the beginning of the operation period, it increased to 6.19×10^7 copies μL^{-1} (1.3 times more) in the anode biofilm at the end of the operation period. This result confirms that the anode compartment of the ML-MFC was suitable for the growth of archaea. However, the environmental operation conditions relatively limited the growth of archaea such as low operation temperature (21 ± 2 °C) of ML-MFC for archaeal microorganisms.

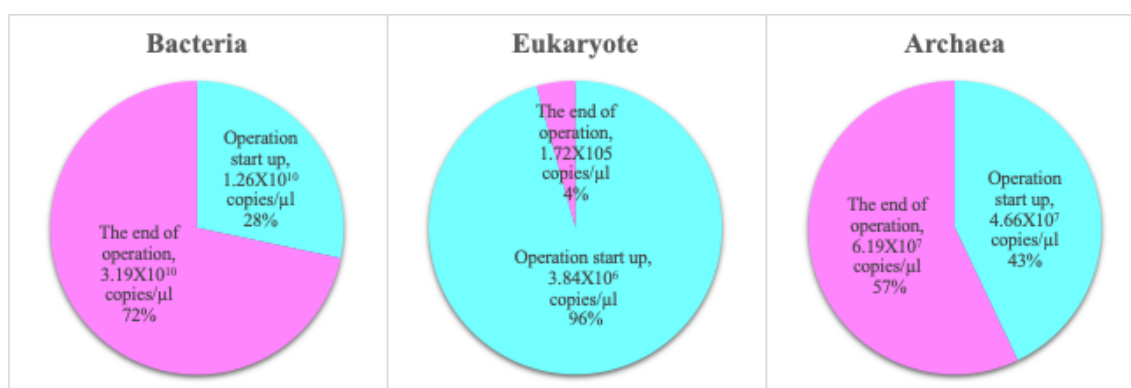


Fig 7. Quantification of bacteria, eukaryote, and archaea cells in the anode compartment at the beginning and end of the operation period by qPCR analysis

4. CONCLUSIONS

In this study, the grape marc was used as a substrate source for anode microorganism in ML-MFC for the first time, and the electricity generation capacity was investigated in detail. The maximum power density of ML-MFC was 274.9 mW m^{-2} , which is comparable to the literature studies. The CV results showed that the microbial colonization on anode biofilm did not occur at the beginning of the operation period, while the electroactive biofilm occurred during the operation period. The qPCR results proved that the number of bacteria on the anode surface increased approximately 2.5 times from the beginning to the end of the ML-MFC operation period. The microscopic observations of anode biofilm confirmed the presence of viable bacterial colonization on the anode electrode surface. As a result, the power generation performance of ML-MFC fueled with grape marc is relatively high compared to some literature studies, and this study has the potential to shed light on future MFC studies for the use of grape marc as a substrate source.

REFERENCES

- [1]. J. Kassongo, E. Shahsavari and A.S. Ball, "Renewable energy from the solid-state anaerobic digestion of grape marc and cheese

wey at high treatment capacity," *Biomass and Bioenergy*, Vol. 143, 105880, 2020.

- [2]. M. Bustamante, R. Moral, C. Paredes, A. Pérez-Espinosa, J. Moreno-Caselles and M. Pérez-Murcia, "Agrochemical characterisation of the solid by-products and residues from the winery and distillery industry," *Waste Management*, Vol. 28 (2), pp. 372-380, 2008.
- [3]. C. Schönnenbeck, G. Trouvé, M. Valente, P. Garra and J. Brillhac, "Combustion tests of grape marc in a multi-fuel domestic boiler," *Fuel*, Vol. 180, pp. 324-331, 2016.
- [4]. J. Kassongo, E. Shahsavari and A.S. Ball, "Co-Digestion of Grape Marc and Cheese Whey at High Total Solids Holds Potential for Sustained Bioenergy Generation," *Molecules*, Vol. 25 (23), pp. 5754, 2020.
- [5]. R.A. Muhlack, R. Potumarthi and D.W. Jeffery, "Sustainable wineries through waste valorisation: A review of grape marc utilisation for value-added products," *Waste Management*, Vol. 72, pp. 99-118, 2018.
- [6]. D. Ying, C. Chuanyu, H. Bin, X. Yuen, Z. Xuejuan, C. Yingxu and W. Weixiang, "Characterization and control of odorous gases at a landfill site: A case study in Hangzhou, China," *Waste Management*, Vol. 32 (2), pp. 317-326, 2012.

- [7]. T.H. Makadia, E. Shahsavari, E.M. Adetutu, P.J. Sheppard and A.S. Ball, "Effect of anaerobic co-digestion of grape marc and winery wastewater on energy production," *Australian Journal of Crop Science*, Vol. 10 (1), 57, 2016.
- [8]. M. Bustamante, C. Paredes, R. Moral, J. Moreno-Caselles, A. Pérez-Espinosa and M. Pérez-Murcia, "Uses of winery and distillery effluents in agriculture: characterisation of nutrient and hazardous components," *Water Science and Technology*, Vol. 51 (1), 145-151, 2005.
- [9]. K.P. Mosse, A.F. Patti, E.W. Christen, T.R. Cavagnaro, "Winery wastewater inhibits seed germination and vegetative growth of common crop species," *Journal of Hazardous Materials*, Vol. 180 (1-3), pp. 63-70, 2010.
- [10]. H. Javier, S.J. Ángel, G. Aida, G.M. del Carmen and M.M. de los Ángeles, "Revalorization of grape marc waste from liqueur wine: biomethanization," *Journal of Chemical Technology & Biotechnology*, Vol. 94 (5), pp. 1499-1508, 2019.
- [11]. X. Melamane, R. Tandlich and J. Burgess, "Anaerobic digestion of fungally pre-treated wine distillery wastewater," *African Journal of Biotechnology*, Vol. 6(17), 2007.
- [12]. K.R. Corbin, Y.S. Hsieh, N.S. Betts, C.S. Byrt, M. Henderson, J. Stork, S. DeBolt, G.B. Fincher and R.A. Burton, "Grape marc as a source of carbohydrates for bioethanol: Chemical composition, pre-treatment and saccharification," *Bioresource Technology*, Vol. 193, pp. 76-83, 2015.
- [13]. F.-M. Pelleria and E. Gidaracos, "Chemical pretreatment of lignocellulosic agroindustrial waste for methane production," *Waste Management*, Vol. 71, pp. 689-703, 2018.
- [14]. Y. Chen, J.J. Cheng and K.S. Creamer, "Inhibition of anaerobic digestion process: a review," *Bioresource Technology*, Vol. 99(10), pp. 4044-4064, 2008.
- [15]. J. Mata-Alvarez, J. Dosta, S. Macé and S. Astals, "Codigestion of solid wastes: a review of its uses and perspectives including modeling," *Critical Reviews in Biotechnology*, Vol. 31 (2), pp. 99-111, 2011.
- [16]. P. Guo, W.L. Saw, P.J. Van Eyk, E.B. Stechel, R. De Nys, P.J. Ashman and G.J. Nathan, "Gasification reactivity and physicochemical properties of the chars from raw and torrefied wood, grape marc, and macroalgae," *Energy & Fuels*, Vol. 31(3), pp. 2246-2259, 2017.
- [17]. M. Miranda, J. Arranz, S. Román, S. Rojas, I. Montero, M. López and J. Cruz, "Characterization of grape pomace and pyrenean oak pellets," *Fuel Processing Technology*, Vol. 92 (2), pp. 278-283, 2011.
- [18]. C. Marculescu and S. Ciuta, "Wine industry waste thermal processing for derived fuel properties improvement," *Renewable Energy*, Vol. 57, pp. 645-652, 2013.
- [19]. C. Da Ros, C. Cavinato, D. Bolzonella and P. Pavan, "Renewable energy from thermophilic anaerobic digestion of winery residue: Preliminary evidence from batch and continuous lab-scale trials," *Biomass and Bioenergy*, Vol. 91, pp. 150-159, 2016.
- [20]. E. Taşkan, S. Bulak, B. Taşkan, M. Şaşmaz, E. Gürtekin and A. Bayri, "Mikrobiyal Yakıt Hücresinde Grafen Kaplı Nikel-Titanyum (NiTi) Alaşımının Anot Elektrotu Olarak Kullanılması," *Fırat Üniversitesi Mühendislik Bilimleri Dergisi*, Vol. 31(2), pp. 319-326, 2019.
- [21]. C.E. Reimers, L.M. Tender, S. Fertig and W. Wang, "Harvesting energy from the marine sediment-water interface," *Environmental Science & Technology*, Vol. 35(1), pp. 192-195, 2001.
- [22]. J. Prasad and R.K. Tripathi, "Scale-up and control the voltage of sediment microbial fuel cell for charging a cell phone," *Biosensors and Bioelectronics*, Vol. 172, 112767, 2020.
- [23]. R.M. Allen and H.P. Bennetto, "Microbial fuel-cells," *Applied Biochemistry and Biotechnology*, Vol. 39(1), pp. 27-40, 1993.
- [24]. B.E. Logan, B. Hamelers, R. Rozendal, U. Schröder, J. Keller, S. Freguia, P. Aelterman, W. Verstraete and K. Rabaey, "Microbial fuel cells: methodology and technology," *Environmental Science & Technology*, Vol. 40(17), pp. 5181-5192, 2006.
- [25]. Y. Liang, H. Zhai, B. Liu, M. Ji and J. Li, "Carbon nanomaterial-modified graphite felt as an anode enhanced the power production and polycyclic aromatic hydrocarbon removal in sediment microbial fuel cells," *Science of the Total Environment*, Vol. 713, 136483, 2020.
- [26]. X. Yang and S. Chen, "Microorganisms in Sediment Microbial Fuel Cells: Ecological Niche, Microbial Response, and Environmental Function," *Science of the Total Environment*, Vol. 756, 144145, 2020.
- [27]. X. Cao, H.-l. Song, C.-y. Yu and X.-n. Li, "Simultaneous degradation of toxic refractory organic pesticide and bioelectricity generation using a soil microbial fuel cell," *Bioresource Technology*, Vol. 189, pp. 87-93, 2015.
- [28]. P. Xu, E. Xiao, D. Xu, J. Li, Y. Zhang, Z. Dai, Q. Zhou and Z. Wu, "Enhanced phosphorus reduction in simulated eutrophic water: a comparative study of submerged macrophytes, sediment microbial fuel cells, and their combination," *Environmental Technology*, Vol. 39(9), pp. 1144-1157, 2018.
- [29]. E. Abazarian, R. Gheshlaghi and M.A. Mahdavi, "Impact of light/dark cycle on electrical and electrochemical characteristics of algal cathode sediment microbial fuel cells," *Journal of Power Sources*, Vol. 475, 228686, 2020.
- [30]. E. Taşkan, S. Bulak, B. Taşkan, M. Şaşmaz, S. El Abed and A. El Abed, "Nitinol as a suitable anode material for electricity generation in microbial fuel cells," *Bioelectrochemistry*, Vol. 128, pp. 118-125, 2019.
- [31]. Ş. Topcu and E. Taşkan, "Effect of the tetracycline antibiotics on performance and microbial community of microbial fuel cell,"

- Bioprocess and Biosystems Engineering*, Vol. 44, pp. 595-605, 2020.
- [32]. W.P. Liu, X.F. Yin, J.J. Lu, G.B. Liang and Y.M. Chen, "Copper recovery from copper-containing wastewater through treating membraneless microbial fuel cell and its electricity production," *Zhongguo Youse Jinshu Xuebao/Chinese Journal of Nonferrous Metals*, Vol. 27(3), pp. 648-654, 2017.
- [33]. J.M. Morris and S. Jin, "Enhanced biodegradation of hydrocarbon-contaminated sediments using microbial fuel cells," *Journal of Hazardous Materials*, Vol. 213-214, pp. 474-477, 2012.
- [34]. G.J.C. Bartolome, B.E. Piojo, A.P.L. Palugod and R.L. Patata, "Design and Performance of a Single-Chamber Membraneless Sediment Microbial Fuel Cell for Bioenergy Generation," *2019 IEEE 11th International Conference on Humanoid, Nanotechnology, Information Technology, Communication and Control, Environment, and Management (HNICEM)*, pp. 1-6, 2019.
- [35]. B. Taşkan, E. Taşkan and H. Hasar, "Electricity generation potential of sewage sludge in sediment microbial fuel cell using Ti-TiO₂ electrode," *Environmental Progress and Sustainable Energy*, Vol. 39(5), pp. 1-8, 2020.
- [36]. J. Hou, Z. Liu, Y. Li, S. Yang and Y. Zhou, "A comparative study of graphene-coated stainless steel fiber felt and carbon cloth as anodes in MFCs," *Bioprocess and Biosystems Engineering*, Vol. 38 (5), pp. 881-888, 2015.
- [37]. E. Taskan, H. Hasar, "Comprehensive comparison of a new tin-coated copper mesh and a graphite plate electrode as an anode material in microbial fuel cell," *Applied Biochemistry and Biotechnology*, Vol. 175 (4), pp. 2300-2308, 2015.
- [38]. V. Yousefi, D. Mohebbi-Kalhari, A. Samimi and M. Salari, "Effect of separator electrode assembly (SEA) design and mode of operation on the performance of continuous tubular microbial fuel cells (MFCs) ," *International Journal of Hydrogen Energy*, Vol. 41(1), pp. 597-606, 2016.
- [39]. V.R. Nimje, C.-C. Chen, H.-R. Chen, C.-Y. Chen, M.-J. Tseng, K.-C. Cheng, R.-C. Shih and Y.-F. Chang, "A single-chamber microbial fuel cell without an air cathode," *International Journal of Molecular Sciences*, Vol. 13(3), pp. 3933-3948, 2012.
- [40]. J. Hou, Z. Liu and P. Zhang, "A new method for fabrication of graphene/polyaniline nanocomplex modified microbial fuel cell anodes," *Journal of Power Sources*, Vol. 224, pp. 139-144, 2013.
- [41]. M. Siegert, M.D. Yates, A.M. Spormann and B.E. Logan, "Methanobacterium dominates biocathodic archaeal communities in methanogenic microbial electrolysis cells," *ACS Sustainable Chemistry & Engineering*, Vol. 3(7), pp. 1668-1676, 2015.
- [42]. J. Chen, X. Liu, J. Zheng, B. Zhang, H. Lu, Z. Chi, G. Pan, L. Li, J. Zheng, X. Zhang, J. Wang and X. Yu, "Biochar soil amendment increased bacterial but decreased fungal gene abundance with shifts in community structure in a slightly acid rice paddy from Southwest China," *Applied Soil Ecology*, Vol. 71, pp. 33-44, 2013.